# The American Mineralogist

## *Journal of the Mineralogical Society of America*

Vol. 40 JULY-AUGUST, 1955 Nos. 7 and 8

## *Contents*

### I. Contributions to Canadian Mineralogy

Volume 5, Part 7
*Sponsored by the* Walker Mineralogical Club
*Editor:* L. G. Berry, *Kingston, Ontario*

Hawleyite, isometric cadmium sulphide, a new mineral........ R. J. Traill & R. W. Boyle 555
Cerianite, $CeO_2$: a new rare-earth oxide mineral........ A. R. Graham 560
Kimberlite at Bachelor Lake, Quebec........ K. D. Watson 565
The structures of the minerals of the descloizite and adelite groups: II—Pyrobelonite........ D. M. Donaldson & W. H. Barnes 580
The structures of the minerals of the descloizite and adelite groups: III—Brackebuschite........ D. M. Donaldson & W. H. Barnes 597
Determination of the mode of a metamorphic rock........ D. M. Shaw & W. D. Harrison 614
Uraninite and thorianite from Ontario and Quebec........ S. C. Robinson & A. P. Sabina 624
Studies of radioactive compounds: VIII—Uranophane and beta-uranophane........ D. H. Gorman & E. W. Nuffield 634
Synthesis, structures and properties of platinum metal tellurides........ W. O. J. Groeneveld Meijer 646
Structure of zinc sulphide minerals........ F. G. Smith 658
The mineralogy and genesis of the bauxite deposits of Jamaica, B.W.I........ V. G. Hill 676
Notes and news: "Hewettite" and "metahewettite"........ W. H. Barnes 689
  Heazlewoodite from Miles Ridge, Yukon Territory... Vladimir S. Papezik 692
  Niggliite, a monotelluride of platinum?...... W. O. J. Groeneveld Meijer 693
  Lattice dimensions of cadmium sulphide........ F. G. Smith 696
  A new centrifuge tube for mineral separation........ E. H. Nickel 697
  The distribution of major and minor elements among some co-existing ferromagnesian silicates........ E. H. Nickel 699

(*continued on cover 2*)

EDITOR: WALTER F. HUNT
ASSISTANT EDITOR: LEWIS S. RAMSDELL

BOARD OF ASSOCIATE EDITORS:

ELBURT F. OSBORN
IAN CAMPBELL
WILLIAM F. BRADLEY

ADOLF PABST (1955)
BRIAN MASON (1955–56)
FRANCIS J. TURNER (1955–57)

Published bi-monthly by the Society

*(contents continued)*

Walker Mineralogical Club .......... 704
Peacock Memorial Prize .......... 705

## II. Other Contributions

*Editor:* **W. F. Hunt,** *Ann Arbor, Michigan*

The alkali feldspars: I. orthoclase-microperthites .......... W. S. MacKenzie and J. V. Smith 707
The alkali feldspars: II. A simple *X*-ray technique for the study of alkali feldspars .......... J. V. Smith and W. S. MacKenzie 733
Kutnahorite: a manganese dolomite, $CaMn(CO_3)_2$ .......... Clifford Frondel and L. H. Bauer 748
Notes and news: A new method for mounting samples for powder *X*-ray spectrometry. H. D. Holland, W. B. Head III, G. G. Witter, Jr., and G. B. Hess 761
Beyrichtite, a discredited species. Charles Milton and Joseph M. Axelrod 767
Llama bones with lead-copper mineralization from Bolivia. Charles Milton 770
Mineralogical Society (London) .......... 773
Book Reviews .......... 781
New mineral names .......... 787

---

## Mineralogical Society of America

Associated with the Geological Society of America

*President:* Harry H. Hess, Princeton University, Princeton, New Jersey.
*Vice-President:* Clifford Frondel, Harvard University, Cambridge 38, Massachusetts.
*Secretary:* C. S. Hurlbut, Jr., Harvard University, Cambridge 38, Massachusetts.
*Treasurer:* Earl Ingerson, U. S. Geological Survey, Washington 25, D. C.
*Editor:* Walter F. Hunt, University of Michigan, Ann Arbor, Michigan.
*Councillors:* Victor T. Allen, Institute of Geophysical Technology, St. Louis, Missouri.
C. Osborne Hutton, Stanford University, Palo Alto, California.
Felix Chayes, Geophysical Laboratory, Washington, D. C.
Leonard G. Berry, Queen's University, Kingston, Ontario, Canada.
Sterling B. Hendricks, U. S. Department of Agriculture, Beltsville, Maryland.

---

The enlarged issues of this journal for 1955 are made possible by a grant from the Penrose Fund of the Geological Society of America.

## The American Mineralogist—Journal of the Mineralogical Society of America

A journal containing articles on mineralogy, crystallography, petrography, and allied sciences, is issued every two months. Contributions are invited from everyone.
Office of Publication, Mineralogical Laboratory, Ann Arbor, Michigan.

The general conduct of the journal is in the hands of the editor, **Walter F. Hunt,** Ann Arbor, Michigan, to whom all manuscripts should be submitted. To assist the editor the council of the Mineralogical Society has appointed **Lewis S. Ramsdell,** Ann Arbor, Michigan, assistant editor, and the following board of associate editors:

**William F. Bradley,** Illinois State Geological Survey, Urbana, Illinois.
**Ian Campbell,** California Institute of Technology, Pasadena 4, California.
**Brian H. Mason,** American Museum of Natural History, New York, N. Y.
**Elburt F. Osborn,** Pennsylvania State University, University Park, Pennsylvania.
**Adolf Pabst,** University of California, Berkeley 4, California.
**Francis J. Turner,** University of California, Berkeley 4, California.

It will expedite publication if two copies of each manuscript are submitted to the editor.

Sent to all members and fellows of the Mineralogical Society of America. Membership dues $4.00 annually, fellowship dues $5.00 annually. Subscriptions for libraries, colleges, institutions, companies and similar organizations $6.00 annually.

Entered as second class matter at the post office at Menasha, Wis., under Act of March 3, 1879. Acceptance for mailing at the special rate of postage provided for in section 1103, Act of Oct. 3, 1917, paragraph 4 section 429 P. L. & R. authorized March 13, 1922.

Notice of change of address, orders, and remittances should be sent to Dr. Earl Ingerson, U. S. Geological Survey, Washington 25, D. C.

Printed by the George Banta Publishing Company, Menasha, Wisconsin
Printed in the United States of America

THE AMERICAN MINERALOGIST

JOURNAL OF THE MINERALOGICAL SOCIETY OF AMERICA

Vol. 40 JULY–AUGUST, 1955 Nos. 7 and 8

# HAWLEYITE, ISOMETRIC CADMIUM SULPHIDE, A NEW MINERAL*

R. J. TRAILL AND R. W. BOYLE,
*Geological Survey of Canada, Ottawa.*

## ABSTRACT

A new mineral identical with isometric cadmium sulphide has been found in the Hector-Calumet mine, Galena Hill, Yukon Territory. The mineral occurs as a fine-grained, bright yellow, earthy coating on sphalerite and siderite, in vugs and along late fractures. Geochemical and mineralogical evidence, together with laboratory studies, suggest that the mineral has been deposited from meteoric waters. The name hawleyite is given to this new mineral in honor of J. E. Hawley, Miller Research Professor, Queen's University, Kingston; Ontario.

Hawleyite is isometric, with space group $F\bar{4}3m$, $a = 5.818 \pm 0.005$ Å, and a sphalerite-type structure. Assuming a cell content of 4[CdS], the calculated specific gravity is 4.87.

## INTRODUCTION

In 1954, while investigating the lead-zinc-silver deposits in the Keno-Galena Hill area of the Yukon one of the authors (R.W.B.) collected a specimen of sphalerite richly coated with a bright yellow mineral. The specimen was submitted to the *X*-ray Laboratory, Geological Survey of Canada, for identification of the yellow mineral.

The *x*-ray powder pattern of the mineral was found to match the pattern of $\beta$-CdS, the isometric polymorph of cadmium sulphide. A survey of the literature revealed that this compound has not been reported as occurring in nature.

The new mineral is named hawleyite in honor of Professor J. E. Hawley of Queen's University, Kingston, Ontario, who has contributed greatly to Canadian mineralogy as a mineralogist and teacher.

## IDENTIFICATION (R.J.T.)

The specimen consists of a mixture of massive siderite and coarsely-crystalline sphalerite, with a bright yellow coating. A microscopic examination revealed that the coating was composed of a bright yellow mineral, now named hawleyite, admixed with lesser amounts of fine-grained sphalerite and siderite. The grain-size of the hawleyite was so small that individual grains could not be discerned.

---

* Published by permission of the Deputy Minister, Department of Mines and Technical Surveys, Ottawa.

Some of the admixed sphalerite and siderite was removed by brushing the coating through a 325-mesh screen, but a sample of hawleyite suitable for quantitative chemical analysis and specific-gravity determination could not be obtained. A partly purified sample was analyzed semi-quantitatively by *x*-ray spectrography and found to contain 50–70 per cent cadmium, 5–10 per cent zinc, and less than 5 per cent iron. Selenium could not be detected, indicating that less than 0.05 per cent is present.

Several *x*-ray powder photographs of hawleyite were taken using a camera with a diameter of 57.54 mm., and nickel-filtered copper radiation. The observed intensities and measured spacings of the hawleyite pattern are listed in Table 1, together with the spacings calculated from a lattice constant of 5.818 Å. The observed intensities and measured spacings of the *x*-ray patterns of artificial β-CdS published by Milligan (1934) and Ulrich & Zachariasen (1925) are reproduced in Table 2. The close agreement between the patterns of Tables 1 and 2 clearly establishes the identity of the natural and artificial materials.

TABLE 1. HAWLEYITE, β-CdS; *X*-RAY POWDER PATTERN
Isometric $F\bar{4}3m$; $a=5.818$ Å, $Z=4$

| *I* (Cu) | *d* (meas) | *hkl* | *d* (calc) | *I* (Cu) | *d* (meas) | *hkl* | *d* (calc) |
|---|---|---|---|---|---|---|---|
| 10 | 3.36 Å | 111 | 3.36 Å | 1 | 1.298 Å | 420 | 1.301 Å |
| 4 | 2.90 | 200 | 2.91 | 3 | 1.186 | 422 | 1.188 |
| 8 | 2.058 | 220 | 2.057 | 3 | 1.120 | 333, 511 | 1.120 |
| 6 | 1.753 | 311 | 1.754 | ½ | 1.028 | 440 | 1.028 |
| 1 | 1.680 | 222 | 1.680 | 2 | 0.985 | 531 | 0.983 |
| 2 | 1.453 | 400 | 1.454 | ½ | 0.918 | 620 | 0.920 |
| 3 | 1.338 | 331 | 1.335 | ½ | 0.887 | 533 | 0.887 |

Hawleyite has a sphalerite-type structure with space group $F\bar{4}3m$. The lattice constant, $a=5.818\pm0.005$ Å, was calculated from the powder pattern. Assuming a cell content of 4[CdS], the calculated specific gravity of the mineral is 4.87.

## OCCURRENCE (R.W.B.)

The Hector-Calumet mine, from which the hawleyite was obtained, is the largest and most productive of the lead-zinc-silver mines in the Keno-Galena Hill area, Yukon Territory. This mineral district is in the central Yukon 35 miles northeast of Mayo and some 220 miles due north

Table 2. Artificial β-CdS; *X*-Ray Powder Pattern
Isometric $F\bar{4}3m$; $a=5.820$ Å, $Z=4$

| Ulrich & Zachariasen (1925) | | *hkl* | (Milligan 1934) | |
|---|---|---|---|---|
| *I* (Cu) | *d* (meas)[1] | | *I* (Cu) | *d* (meas) |
| 5 | 3.35 Å | 111 | 10 | 3.36 Å |
| 1 | 2.93 | 200 | 3 | 2.90 |
| 5 | 2.062 | 220 | 10 | 2.06 |
| 5 | 1.758 | 311 | 9 | 1.756 |
| ½–1 | 1.683 | 222 | 1 | 1.683 |
| 1 | 1.452 | 400 | 1 | 1.456 |
| 2–2½ | 1.337 | 331 | 2 | 1.335 |
| 1½ | 1.303 | 420 | 1 | 1.302 |
| 2½ | 1.191 | 422 | 3 | 1.189 |
| 2½ | 1.122 | 333, 511 | 3 | 1.121 |
| 2 | 1.033 | 440 | 2 | 1.026 |
| 3½ | 0.985 | 531 | 2 | 0.982 |
| 1 | 0.971 | 442, 600 | | |
| 2½ | 0.922 | 620 | | |
| 1½ | 0.888 | 533 | | |
| 1 | 0.879 | 622 | | |

[1] Spacings calculated from the $\theta$ values of Ulrich & Zachariasen.

of Whitehorse. The district is served by an all weather road from Whitehorse and by Canadian Pacific Airlines.

The consolidated rocks underlying the area are mainly sediments belonging to the Yukon group of Precambrian or Paleozoic age. They consist of sericitic, chloritic, and graphitic schists, phyllites, and quartzites. Conformable sills and lenses of greenstone occur throughout the sediments.

The lead-zinc-silver vein deposits of Keno and Galena Hills occur in brecciated fault zones and sheeted zones. Two types of veins are recognized; an early vein type consisting of quartz, pyrite, and arsenopyrite, and a late vein type mineralized with siderite, galena, sphalerite, and argentian tetrahedrite. Both types may occur separately. The early type, however, may be fractured and contain minerals of the second type.

The veins near the surface are highly oxidized. The depth of oxidation varies but is seldom less than 50 feet. The minerals found in the oxidized zone include limonite, various manganese oxides, calcite, gypsum, smithsonite, cerussite, anglesite, quartz, azurite, malachite, and oxides of arsenic and antimony.

A marked feature of the veins in both the primary and oxidized parts, is the presence of numerous vugs and open spaces in which excellent crystals of galena, sphalerite, siderite, calcite, gypsum, and quartz abound.

The specimen of hawleyite was obtained from a vuggy part of the primary zone of the Hector-Calumet mine. Similar occurrences of cadmium sulphide have been noted in other veins, but at the time of writing the examination of the ores is not complete, and it is not known whether or not all of the cadmium sulphide is hawleyite. Some may be greenockite.

## ORIGIN

The geochemistry of the veins has not been worked out in detail but the mode of occurrence of the hawleyite suggests that it is a secondary mineral which has been deposited from meteoric waters in vugs and along late fractures.

Geochemical work shows that the sphalerite in the veins contains up to 1 per cent cadmium which undoubtedly replaces zinc in the sphalerite structure. Analyses of the meteoric waters show that zinc is present in amounts up to 2 parts per million. Cadmium was not detected, probably owing to its very low concentration in the waters. The waters are acid with a pH between 4 and 6. Sulphate ($SO_4$) is the principal anion, and some $H_2SO_4$ is present, accounting in part for the acid pH.

Analyses of the vein material show that the concentrations of zinc and cadmium in the oxidized parts are as much as 5 per cent lower than in the primary parts. These chemical facts in conjunction with mineralogical studies indicate that during the oxidation process the sphalerite is altered to limonite by the meteoric waters with consequent solution and transport of the zinc and probably the cadmium as sulphates.

Laboratory studies on the precipitation of cadmium sulphide from solutions of cadmium salts have been made by several investigators, and their results have a direct bearing on the origin of the hawleyite. Thus, Böhm & Niclassen (1924) first showed by *x*-ray diffraction that $\beta$-CdS is precipitated by $H_2S$ from cadmium sulphate solutions. Their findings were confirmed by Ulrich & Zachariasen (1925) who prepared $\beta$-CdS for *x*-ray study by passing $H_2S$ into a saturated solution of cadmium sulphate. Dana (1944, p. 230) reports incorrectly that Ulrich & Zachariasen prepared isometric CdS by heating CdS in sulphur vapor for two hours at 700–800°. Actually, Ulrich & Zachariasen prepared the hexagonal polymorph, $\alpha$-CdS, by heating $\beta$-CdS in sulphur vapor. Milligan (1934) showed that $\beta$-CdS is formed at 30° C. when $H_2S$ is passed through a 0.1 N solution of cadmium sulphate made acid by the addition of 1 c. c. of concentrated $H_2SO_4$ to 50 c. c. of solution. Milligan also found that

$\alpha$-CdS is produced from 0.1 N solutions of cadmium nitrate, chloride, bromide, and iodide when treated in the same manner. These laboratory studies indicate clearly that hawleyite is the polymorph of cadmium sulphide which will be precipitated under reducing conditions from acidic sulphate solutions.

Considering the field facts and the knowledge that cadmium follows zinc closely in its geochemistry, it is logical to assume that in the zone of oxidation cadmium would be taken into solution by the meteoric waters which contain $H_2SO_4$, and be transported downward into the zone of reduction. $H_2S$, generated by the action of $H_2SO_4$ on primary sphalerite and other sulphides, would reduce the cadmium sulphate and precipitate hawleyite ($\beta$-CdS) as shown by the laboratory studies.

Acidic sulphate solutions, from which the hawleyite polymorph of cadmium sulphide precipitates, are common in sulphide deposits, and it seems probable that hawleyite is more common than its very recent discovery would indicate. Much material, previously identified as greenockite by casual hand-specimen examination, may prove to be hawleyite when identified by *x*-ray diffraction.

## REFERENCES

Böhm, J. & Niclassen, H. (1924): Über amorphe Niederschläge und Sole, *Zeits, anorg. Chem.*, **132,** 7.

Dana, J. D. & E. S. (1944): *System of Mineralogy,* **1,** ed. 7, by C. Palache, H. Berman and C. Frondel, New York.

Milligan, W. O. (1934): The color and crystal structure of precipitated cadmium sulphide, *J. Phys. Chem.*, **38,** 797–800.

Ulrich, F. & Zachariasen, W. (1925): Über die Kristallstruktur des $\alpha$- und $\beta$-CdS sowie des Wurtzits, *Zeits. Krist.*, **62,** 260–273.

# CERIANITE $CeO_2$: A NEW RARE-EARTH OXIDE MINERAL

A. R. Graham, *Dominion Gulf Company, Toronto, Ontario, Canada.*

## Abstract

The discovery of a cubic (*Fm3m*) mineral with cell-edge 5.42 ± 0.01 Å and composition $(Ce, Th)O_2$ with Ce:Th about 16:1 indicates a three-way isomorphous series among cerium, thorium and uranium dioxide minerals.

## Introduction

Late in August 1954, the author observed a few minute translucent dark greenish-amber radioactive octahedrons in a mineral separate from a sample of carbonate rock. The sample had been submitted for study from mineral claims of the Dominion Gulf Company in Lackner Township, Sudbury Mining District, Ontario, by Dr. E. G. Robinson of our Company. A group mounted directly as a powder sample in an *x*-ray powder camera gave a diffraction pattern sufficiently well-populated with spots to define a cubic (*Fm3m*) lattice with cell-edge 5.42 ± 0.01 Å. As this cell-edge lies within the range 5.40–5.47 Å quoted for pitchblende-uraninite (Brooker & Nuffield, 1952), either fluorite or mineral uranium dioxide or both were at first suspected. However, the clear translucency of the crystals as opposed to the usual opacity of uraninites, and their radioactivity, demanded more conclusive evidence for such an identification.

Immediate information available included qualitative optical emission and fluorescent *x*-ray spectrographic analyses on rock and mineral bulk samples from the immediate area. In general, thorium, cerium and other rare-earths predominated quantitatively over uranium. Search of the cubic cell-edge tables of Frevel (1942) published in Parrish, Ekstein & Irwin (1953), showed that artificial cerium dioxide had the nearest cell-edge (5.40 Å) among the required fluorite structure types. Fluorite itself had to be discarded as a possibility because of the radioactivity, and because its specific gravity, 3.18 is below that of the heavy liquid used in the original separation. Mineral cerium dioxide with some thorium or uranium in solid solution was the remaining possibility. The name "cerianite" was therefore tentatively assigned to the mineral by analogy with thorianite and uraninite. More crystals were immediately sought for confirmatory element analysis.

## Description of Locality

Additional samples and information on the occurrence were kindly supplied by Dr. Robinson and by Mr. G. E. Parsons, Dominion Gulf Company, who had also collected in the area. Their attention had been drawn by an increase in radioactivity over a partly-exposed narrow dike-form zone of impure sugary carbonate rock in a nephelinized hybrid gneiss. This increased radioactivity appeared to be related to brownish, silicate-rich, pod-shaped inclusions a foot or so in long dimension scattered throughout the carbonate rock. These may represent partly absorbed inclusions of wallrock. The latter is described as a medium to dark gray crudely banded gneissic rock, locally comprising a nepheline syenite intrusive facies, and a nephelinized granulitic facies of more mafic constitution. The granulitic rocks seem to represent a highly metamorphosed and metasomatized mixed volcanic and sedimentary series. The carbonate rock may be either a rheomorphic derivative of the sedimentary series, or a sövite dike similar to those of Alnö area, Sweden (von Eckerman, 1948).

The original sample in which the first crystals of cerianite were discovered was taken across the contact of one of the silicate-rich inclusions with the carbonate rock, and included portions of both rock types. A well-defined contact, discernible within a few millimetres, was evident between a light gray crystalline carbonate rock with grain-size up to 2–3 millimetres, and a slightly coarser, dark gray to brownish gray more silicate-rich phase. The latter material, a hybrid of carbonate, nepheline and feldspar, owed its brownish tinge to 10%–20% by volume of a translucent brown tremolitic amphibole in fine to coarse prisms, occasionally reaching about one centimetre in length. Both phases contained approximately 10% total by volume of magnetite and ilmenite as subhedral to euhedral crystals up to 1 or 2 millimetres in size. Accessory transparent white prisms of apatite up to 200 microns in length were more numerous in the carbonate-rich phase.

## ISOLATION OF CERIANITE

A further sample, weighing about one pound, of the material submitted by Mr. Parsons was selected for separation. More silicate-rich than the original, it showed a deeper brown colour, and apparently represented an inclusion nearly completely absorbed in the carbonate rock. The sample was carefully crushed to $-\frac{1}{4}$ inch, and leached overnight in a large volume of cold 1:10 HCl, to remove soluble carbonate. The residue, amounting to about 40% of the original sample, was further crushed with frequent screening to secure a large volume of material in the size-range of the original crystals recovered, $-80+150$ mesh. This fraction was then separated into heavy and light portions using diiodomethane of gravity 3.21. The heavy portion was passed through the Franz isodynamic separator at the highest magnetic flux available. The final non-magnetic residue contained about half a gram of translucent white apatite, minor gray nepheline, and pinkish albite and microcline, as well as about one milligram of dark greenish-amber octahedral crystals similar to the original material isolated and described.

Hand-picking yielded slightly under a milligram of apparently pure crystals. Twice this amount had been recovered in the first operation on about half the weight of original sample. Thus, three milligrams represented the total material available for analysis and further study. Two milligrams approximately were submitted to Mr. D. A. Moddle, the Provincial Assayer for Ontario. Through his courtesy, a special quantitative spectrochemical analysis was carried out by Mr. Wiley O. Taylor of the Provincial Assay Laboratory. The method used was a variation of that employed by K. J. Murata of the U. S. Geological Survey, involving controlled dilutions of the sample. The results of this analysis appear in Table 1.

TABLE 1. SPECTROCHEMICAL ANALYSIS

| Oxide | Weight per cent |
|---|---|
| $CeO_2$ | 80 ±20 |
| $ThO_2$ | 5.1± 0.5 |
| $Nb_2O_5$ | 1.8± 0.2 |
| $La_2O_3$ | 1.5± 0.2 |
| $Y_2O_3$ | 1.2± 0.2 |
| $Yb_2O_3$ | 1.1± 0.1 |
| $Ta_2O_5$ | 0.6± 0.05 |
| $ZrO_2$ | 0.6± 0.05 |
| $U_3O_8$ | N.D. |

## DISCUSSION OF RESULTS

Although the accuracy of the analysis for the major constituent is not high, the great excess of Ce over the other elements found, and the position of its range bracketing the theoretical content of Ce in $CeO_2$ (81%), are confirmatory evidence for the identity of the mineral. The presence of 5% Th accounts for the radioactivity as well as the slight increase in cell-edge from 5.40 to 5.42 Å. As cerium also forms an oxyfluoride with similar crystallography and cell-size, a spot test for fluorine was performed. The result was negative.

During the literature search for possible previous mention of a cerium dioxide mineral, several analyses of thorianites and uraninites were noted in which cerium figures as a minor or trace constituent. Three of these quoted in Dana's Seventh Edition are from localities where more cerium-rich minerals are also reported. It is probable that close study of these and other similar localities will result in the establishment of a three-way isomorphous series among uranium, thorium and cerium oxide minerals. Elsewhere in this issue appears evidence for at least a part of the uraninite-thorianite series; the appreciable thorium in the analysis above is an indication of a thorianite-cerianite series.

The metallogenetic implications of the occurrence are interesting because of the presence of fluorine and chlorine in apatite and minor fluorite in the region. Magnetite-apatite-ilmenite-pyrochlore deposits are associated with the complex nepheline syenite intrusive. A hypothesis of origin of similar deposits, advanced by several geologists in various forms (e.g., von Eckerman, 1948), postulates transfer in, and deposition from, a high-temperature halide-rich fluid, with localization control by both structure and change of chemical environment.

A possible analogous origin for the cerianite suggests itself. Removal of chlorine, fluorine and phosphorous from such a halide-rich fluid by reaction with calcareous sediments to form apatite and fluorite may have allowed crystallization of cerium as oxide instead of the more usual monazite, perovskite (knopite), complex carbonate, or cerian pyrochlore. The process is visualized as taking place at temperatures and pressures comparable to those of the granulitic facies developed in the surrounding rocks. An alternative explanation, also attractive, is formation of cerianite as a skarn mineral from pre-existing bastnaesite, or other rare-earth carbonate, under contact metamorphic conditions induced by the neighbouring intrusive syenite plug.

## Summary and Conclusions

On the evidence adduced above, the existence in nature of a cerium dioxide mineral isostructural (and at least in part isomorphous) with thorianite and uraninite, is proposed. By analogy with the latter two minerals, the name "cerianite" should be appropriate for the pure end member. Application of compositional nomenclature to the mineral described above would place it as a thorian cerianite.

Characterization of minerals in this oxide group by cell-edge relationships alone appears fallacious. At least qualitative information on chemical composition should be available. The state of oxidation, i.e., incidence of "defect structures" in the uranian and cerian members of the group is a further complication which would appreciably affect cell-size.

## References

Brooker, E. J., & Nuffield, E. W. (1952): Studies of radioactive compounds: IV-Pitchblende from Lake Athabaska, Canada. *Contrib. to Can. Mineral.* **5**, Pt. 4, 363–385. *Am. Mineral.*, **37**, 363–385.

Courtel, R., & Loriers, J. (1950): Sur la formation de $Ce_2O_3$ cubique dans l'oxydation du cerium, et sa mise en evidence par diffraction electronique. *C.R. acad. sci. Paris,* **230,** 735–7. *Struct. Reports for* 1950, **13**.

Frevel, L. K. (1942): Tabulated diffraction data for cubic isomorphs. *Ind. Eng. Chem. & Analyt. Ed.* **14,** 687–693.

Parrish, W., Ekstein, M. G., & Irwin, B. W. (1953): *Data for X-Ray Analysis* **2,** *Philips Tech. Lib.*

von Eckerman, Harry (1948): The alkaline district of Alnö Island. *Sver. Geol. Under.*, Ser. Ca, no. **36,** 163 pp.

# KIMBERLITE AT BACHELOR LAKE, QUEBEC

K. D. Watson, *University of California, Los Angeles.*

## Abstract

Kimberlite forms small bodies intruding Keewatin-type rocks near Bachelor Lake in Lesueur Township, Abitibi-East County, Quebec. Most of it has porphyritic and panidiomorphic textures and consists of olivine and altered olivine, phlogopite, calcite, augite, perovskite, magnetite, ilmenite, apatite, and chlorite. Some of the calcite, which composes as much as 45 per cent of certain specimens, forms medium to fine anhedral grains sharply molded against or completely enclosing euhedral crystals of olivine, phlogopite, augite, perovskite, magnetite, and apatite in a manner strongly suggesting that it is a late-crystallizing primary mineral. The Bachelor Lake kimberlite is similar chemically, mineralogically, and texturally to some ultrabasic rocks of Paleozoic or younger age that occur at several localities in eastern North America. The recognition of this rock-type in northern Quebec has interest in respect to the problem of the provenance of some of the diamonds found in glacial drift south of the Great Lakes.

## Introduction

Bachelor Lake is in Lesueur Township, Abitibi-East County, Quebec (Fig. 1) and may be reached most conveniently at present by means of aircraft based at Senneterre and Amos. The kimberlite occurs about three miles southwest of the Lake, near a zinc-lead-silver deposit owned by Dome Exploration (Quebec) Limited.

The geology of the area has been described briefly by Longley (1951) and by Graham (1950). The rocks exposed on the Dome property are mainly regionally metamorphosed Keewatin-type andesitic lavas, andesitic pyroclastics, and rhyolitic pyroclastics, which generally strike northeast and dip very steeply. These are intruded by a large body of olivine gabbro and gabbro and by many narrow, northwesterly-striking, vertical dikes of spessartite.

The kimberlite is in an area largely covered by glacial drift and it does not crop out. During the course of investigation of the zinc-lead-silver deposit, however, it was intersected by nine inclined diamond drill holes which were directed southeastward across a northeasterly-trending belt 1,800 feet long. It intrudes andesite and rhyolite-lapilli-tuff, which are carbonatized, but otherwise unaltered, immediately at the contacts. The relative positions of the intersections and of the outcrops of other rocks between drill holes and the orientation of contacts with respect to the drill core show that the kimberlite is not a continuous regular body and suggest, as a simple interpretation, that it, like the spessartite exposed nearby, forms northwesterly-striking steeply-dipping dikes a few feet wide.

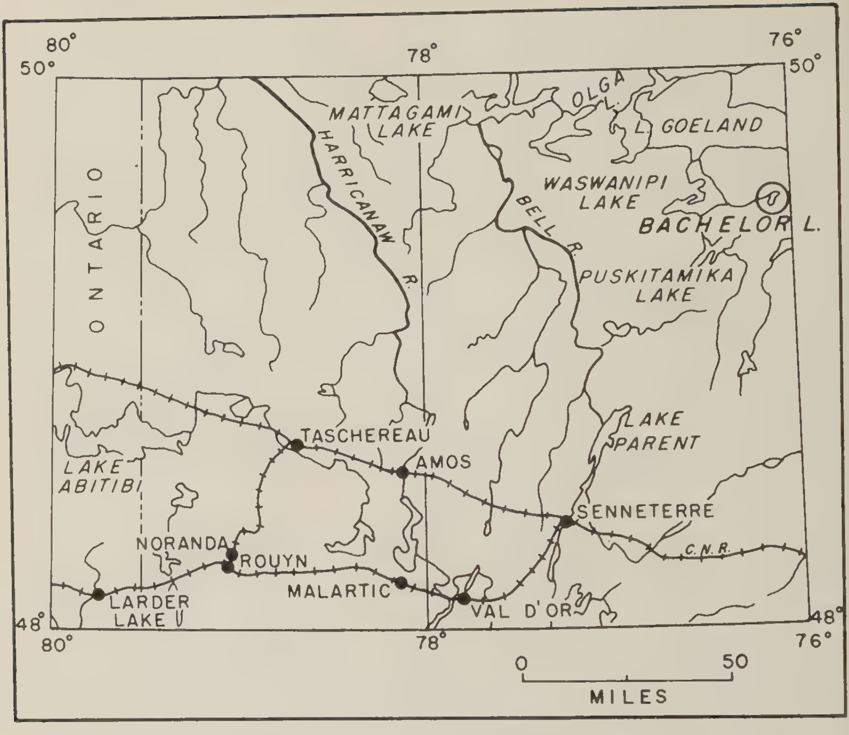

Fig. 1. Index map of northwestern Quebec showing location of Bachelor Lake.

## PETROGRAPHY

The kimberlite[1] is a medium to dark gray massive rock in which olivine and its pseudomorphs, phlogopite, calcite, and, in a few specimens, ilmenite are clearly visible megascopically. The olivine and its pseudomorphs, which are generally almost black, and the phlogopite, which is generally bronzy brown, tend to be euhedral. In some specimens they form abundant medium- to fine-grained phenocrysts in a dark gray, very fine-grained to aphanitic groundmass; in others, they are contained in a matrix rich in medium- to fine-grained white calcite; and in others, they show a complete gradation from medium to aphanitic thereby producing a seriate texture. The texture of the rock and the proportions of the various minerals discernible megascopically vary not only from one dike to another but also to some extent within individual dikes. The variations within individual dikes are erratic; reductions in grain size or in amount of phenocrysts are not evident megascopically along contacts or in narrow apophyses except within a millimeter or two of the contact. Veinlets of white calcite are common locally in several dikes.

---

[1] The name *kimberlite* was proposed by Lewis (1888, pp. 129–131) for a porphyritic peridotite composed of olivine and its alteration products, as well as bronzite, chrome diallage, smaragdite, biotite, perovskite, pyrope, ilmenite, chromite, and other minerals. The name *mica-peridotite* was proposed by Diller (1892, pp. 286-289) for a rock composed essentially of biotite, serpentine pseudomorphous after olivine, and perovskite with minor amounts of apatite, muscovite, magnetite, chlorite, calcite, and some undetermined secondary material. Through subsequent use, these names have gradually acquired somewhat broader meanings and at present they are regarded by some as synonymous (*e.g.* Williams, *et al.*, 1954, pp. 79–80). Others, however, have preferred to separate the kimberlites, which are porphyritic, from the plutonic periodtites (*e.g.* Martens, 1924, p. 313; Tröger, 1935, p. 297). In this paper, the rocks from Bachelor Lake are called kimberlite because their texture is dominantly porphyritic and their chemical and mineralogical compositions closely resemble those of some well-known kimberlites; rocks from other localities are called either mica peridotite or kimberlite depending on whichever one was used in the publication dealing with a particular locality.

Microscopically, panidiomorphic texture is conspicuous, for euhedral crystals are predominant not only among the large grains of olivine and phlogopite but also among the small ones and those of the minor constituents—augite, perovskite, magnetite, and apatite. Thus, according to the usage recommended by Knopf (1936, pp. 1748–1749) and followed by others, the kimberlite may be considered a lamprophyre. Poikilitic texture is also very noticeable in some thin sections. The host-crystals in most of these sections are calcite but in a few they are phlogopite. The calcite forms either anhedral grains up to a few millimeters across that completely enclose smaller euhedral crystals of other minerals, or optically continuous webs between closely spaced euhedral crystals. A few sections clearly show glomeroporphyritic texture caused by the arrangement of olivine crystals and, to a lesser degree, phlogopite in clusters. Microscopic study reveals that near the contacts of a dike, many of the phlogopite crystals are oriented with their major dimensions parallel to the dike margin. Elsewhere in the dikes, however, the structure is massive except for the subparallel orientation of flakes of phlogopite and laths of antigorite between some large crystals of olivine and phlogopite.

The mineralogical compositions of five representative specimens of the kimberlite determined by micrometric analyses of four thin sections of each specimen, are recorded in Table 1 in percentage by volume. The total amount of magnetite and ilmenite, exclusive of magnetite derived from olivine and of fine-grained ilmenite in perovskite, was measured in thin sections and the ratio of this ilmenite to magnetite was measured roughly in polished sections.

*Olivine* and pseudomorphs after olivine range in amount from 54 per cent by volume in one measured thin section to 24 per cent in another.

It forms euhedral and subhedral crystals ranging from about .05 to 10 mm. and lying mainly between .5 and 2 mm. in diameter. The composition of the olivine, based on measurements of $nY$ and $2V$, is $Fo_{85}Fa_{15}$. Unaltered olivine was seen in only nine of the 53 thin sections examined and none was seen in specimens 1, 4, and 5 (Table 1). No relationship is evident between degree of alteration of olivine and amount of calcite present, for specimens 2 and 3 contain approximately the same proportion of fresh to altered olivine although they contain respectively the least and greatest amount of calcite. A transition from practically unaltered to completely altered olivine may occur in the width of a single thin section. In specimens 1 and 2 and several others, the altered olivine crystals consist of fine-grained aggregates of fibrolamellar and fibrous serpentine containing magnetite dust; in specimens 3, 4 and 5 and several others, they consist of aggregates of fine flakes and laths of yellow strongly birefringent bowlingite. A few specimens contain pseudomorphs after olivine that are composed of rims of bowlingite and cores of randomly oriented minute flakes of talc. One thin section, which contains some olivine crystals partly replaced by bowlingite, contains others completely pseudomorphed by fine-grained calcite and bowlingite. The distribution of the calcite in these pseudomorphs suggests that it has replaced olivine relics in grains that previously had been partly altered to bowlingite.

Table 1. Mineralogical Composition of Kimberlite

| | 1 | 2 | 3 | 4 | 5 |
|---|---|---|---|---|---|
| Olivine and altered olivine | 48 | 45 | 29 | 38 | 41 |
| Phlogopite | 9 | 21 | 24 | 20 | 26 |
| Calcite | 18 | 13 | 39 | 20 | 17 |
| Augite | — | 0.2 | 0.1 | 6 | 1 |
| Perovskite | 3 | 7 | 1 | 1 | 3 |
| Apatite | 0.1 | 0.2 | 0.1 | 2 | 4 |
| Magnetite | 12 | 6 | 6 | 5 | 4 |
| Ilmenite | 7 | 4 | 1 | — | 3 |
| Antigorite and calcite | — | — | — | 7 | — |
| Chlorite | 3 | 4 | — | — | 1 |
| Bowlingite (?), etc. | — | — | — | 1 | — |

*Phlogopite* ranges in amount from 29 per cent by volume in one measured thin section to 6 per cent in another, but it constutes 20 to 25 per cent in most. Its crystals are euhedral and subhedral and are mainly .25 to 2 mm. in diameter although they range from about .01 to 10 mm.

Some optical properties of the phlogopite in the specimens of Table 1 are as follows:

| | 1 | 2 | 3 | 4 | 5 |
|---|---|---|---|---|---|
| $nY$ (±.005) | 1.600 | 1.595 | 1.620 | 1.620 | 1.620 |
| $2V$ (estimated) | 5–10° | 5–10° | 15–20° | 15–20° | 15–20° |
| Dispersion | weak | weak | $v>r$ (strong) | $v>r$ (strong) | $v>r$ (strong) |

These refractive indices show, according to the data of Winchell (1951, p. 374), that the phlogopites of specimens 1 and 2 have higher ratios of Mg to Fe than those of specimens 3, 4, and 5. The olivine in specimens 2 and 3, however, has properties that reveal no difference in the MgFe ratio. The phlogopite crystals in many specimens are distinctly zoned. They have parts in which the absorption and birefringence—$Y$ and $Z$ = medium brown, $B$ = .045—indicate a lower ratio of Mg to Fe than in other parts in which the absorption and birefringence are lower—$Y$ and $Z$ = pale yellow, $B$ = .030 (Winchell, 1951, pp. 374–375). In some specimens the zoning is normal, that is, the ratio of Mg to Fe decreases from core to rim; in others, it is reversed and commonly oscillatory.

The phlogopite crystals in most specimens have rims, partial rims, and irregular patches within them composed of a micaceous mineral that differs markedly from the phlogopite by having the following reversed pleochroism and absorption—$X$ = deep orange brown, $Y$ and $Z$ = very pale yellow, almost colorless, $X > Y = Z$. These rims and patches have their cleavage traces and extinction positions parallel to those of the phlogopite crystal. The other optical properties nearly match those of phlogopite except for the birefringence which is about .010 higher in phlogopite. In most specimens the amount of this mineral is much less than one per cent but in one containing 20–25 per cent phlogopite, it constitutes almost 5 per cent of the rock. Reversed absorption and somewhat similar colors have been recorded for a highly manganiferous mica (Jakob, 1924, pp. 157–158), for the manganiferous mineral—ganophyllite—which is related to stilpnomelane (Winchell, 1951, p. 391), and for the mica-like mineral—astrophyllite (Winchell, 1951, p. 481). The other optical properties of the manganiferous mica and ganophyllite, however, are only approximately like those of the mineral in the kimberlite and those of astrophyllite are quite different. Mica with this abnormal absorption has been observed by others in kimberlite elsewhere and in the closely allied rocks, mica peridotite and alnöite (du Toit, 1907, p. 169;

Miser & Ross, 1923*a*, pp. 315–316; Miser & Ross 1923*b*, p. 277; Holmes, 1936, p. 383; Wagner, 1914, pp. 58 and 108; Martens, 1924, p. 311; Ross, 1926, p. 219; Singewald & Milton, 1930, p. 56). Wagner's book contains excellent photomicrographs (Plate XII) of lamprophyric kimberlite from South Africa which show rims of mica with abnormal absorption of cores of normal phlogopite in a relationship identical to that in the kimberlite from Bachelor Lake.

*Calcite*, which ranges from 12 to 45 per cent by volume in the measured thin sections, forms anhedral grains. Some of these are as much as 5 mm. across, others are only a few microns, but many are between .1 and 1 mm. Where calcite is abundant, it appears as a matrix in which dominantly euhedral and subhedral crystals of other minerals are embedded. In some specimens it is poikilitic and forms either anhedral grains completely enclosing smaller euhedral crystals of other minerals, or optically continuous webs a few millimeters across, between closely spaced euhedral crystals. In several specimens calcite appears to have slightly replaced phlogopite and, less commonly, olivine and clinopyroxene. In specimen 4, fine-grained calcite has partly pseudomorphed some of the antigorite laths. Some of the calcite in the kimberlite, however, shows no evidence of having originated by replacement of other minerals.

*Clinopyroxene* occurs in less than half of the thin sections, although it constitutes nine per cent by volume in one. It forms stubby euhedral or subhedral prisms and irregular granules which are visible only microscopically and are generally less than .1 mm. long. The clinopyroxene crystals tend to be clustered around the edges of olivine phenocrysts; some are partly included within the margins of the phenocrysts and others are enclosed within phlogopite. Most of the clinopyroxene is a pale brownish gray variety having the properties $Z \wedge c$ *ca* 45°, (+) $2V$ *ca* 60°, and $r > v$ (distinct). This may be augite. In one specimen, a small proportion of the clinopyroxene is pale green but otherwise similar to the brownish gray variety. One section contains a small prism having the distinctive strong pleochroism, almost parallel extinction, and negative elongation of aegirine.

*Perovskite*[2] is a minor accessory in all specimens and reaches a maximum of seven per cent by volume in one measured thin section. It is included within phlogopite and calcite and in a few places, is molded on olivine. It forms equant grains that are mainly between .02 and .1 mm. in diameter. Many of these are euhedral to subhedral and rectangular or octagonal in cross section. The perovskite crystals are pale purplish brown or yellow; some are isotropic and others are weakly birefringent.

---

[2] Optical identification confirmed by $x$-ray diffractometer.

The rims and cores of many grains are rendered almost opaque by an abundance of fine-grained ilmenite.

*Apatite* is also present in minor amounts in all specimens and reaches a maximum of five per cent by volume in one measured thin section. Most of its crystals are slender euhedral prisms .01 to .1 mm. long although a few are stout and attain lengths up to 5 mm. Some of the apatite prisms form groups that radiate into calcite from points of attachment on olivine crystals but most are entirely enclosed in calcite. A few small crystals show a zonal structure which may be similar to that of the skeletal crystals in South African kimberlite (Wagner, 1909, p. 551).

*Magnetite* occurs in all specimens and, excluding that formed by alteration of olivine, ranges in amount from about four to twelve per cent by volume. Nearly all specimens because of their abundant magnetite, are very noticeably magnetic. Most of the magnetite forms subhedral equant crystals which are mainly between .01 and .1 mm. in diameter. Many of these are included in phlogopite and calcite and a few are molded on olivine.

*Ilmenite* is present in most specimens and, exclusive of that at the margins of perovskite crystals, reaches a maximum content of seven per cent by volume. Most of it occurs as highly irregular anhedra, mainly .2 to 1 mm. in diameter, which contrast markedly in shape and size with the crystals of magnetite. Much of the ilmenite occurs interstitially among olivine crystals and some of it has phlogopite molded on it. Many of the anhedra are surrounded by wide irregular discontinuous rims of magnetite which apparently crystallized later than ilmenite. The large ilmenite grains contain widely spaced, thin yet persistent, lamellae of exsolved magnetite parallel to (0001). Some sections of specimen 3 contain no ilmenite but they show small areas apparently composed of very fine-grained leucoxene, talc, and bowlingite, surrounded by magnetite. These aggregates, which are roughly circular to hexagonal in outline might possibly be pseudomorphs after magnesian ilmenite or geikielite.

*Antigorite*, other than that obviously formed by alteration of olivine, is present in only a few samples. In specimen 4, in which it makes up seven per cent by volume, it forms laths mainly .1 to .3 mm. long which compose part of the groundmass and which commonly are partly or completely enclosed in phlogopite. Most of these are partly replaced by fine-grained calcite and some are completely pseudomorphed by it. Some of the laths consist of a single crystal of antigorite; others are composite and are composed in part of many small laths oriented with their long axes perpendicular to a median cleavage trace running the length of the large lath. Some laths composed largely of calcite show a similar composite structure.

The origin of this antigorite is unknown. It may be a late primary mineral which has undergone partial carbonatization or it may be an alteration product of some pre-existing mineral. In the latter possibility, the original mineral may have been melilite for its composition would enable it to yield antigorite and calcite, its habit is commonly lath-like, and it commonly shows a combination of peg structure and a median cleavage trace reminiscent of the structure of the composite laths described above. Furthermore, melilite has been observed in kimberlite and mica peridotite elsewhere and is an essential constituent of the closely related rock, alnöite.

*Chlorite* forms rims only a few microns wide on phlogopite and mica with abnormal absorption in some thin sections. In addition, it is present as aggregates of minute ill-defined grains in the groundmass of several specimens and in one analyzed micrometrically (No. 2), it composes four per cent by volume.

Besides the minerals described above, pyrite and pyrrhotite were seen in small amounts in several polished sections and clusters of radiating fibers, which may be bowlingite and possibly some zeolite, are present in the groundmass of a few specimens and constitute about one per cent of specimen 4. In one drill hole, the rhyolitic rocks intruded by the kimberlite are cut by many narrow veinlets of fine-grained riebeckite, and a few groups of riebeckite fibers form small inclusions in the kimberlite within a millimeter or two of the contact.

## CHEMICAL COMPOSTION

Chemical analyses and norms of three samples of kimberlite from Bachelor Lake are given in Table 2 and compositions of other kimberlites and a mica peridotite are included for comparison. Relative to other kinds of ultrabasic rocks, those in Table 2 are rich in $TiO_2$ and $P_2O_5$ owing to their high content of ilmenite and perovskite and of apatite. Although Nos. 1 and 2 contain more $TiO_2$ than the others in the table, they are not greatly abnormal, for the average mica peridotite of Daly (1933, p. 20) has 4.95 per cent $TiO_2$ and illustrations of some kimberlites show ilmenite and perovskite in great abundance (Williams, 1939, plate III). The $CO_2$ content of most of the rocks in Table 2 is extremely high.[3] Although No. 3 has a higher content than the rest, it is by no means unique, and, for example, it is surpassed in $CO_2$ content by a similar rock

---

[3] Kimberlites very rich in $CO_2$, which are common, were apparently excluded in compiling the averages (7 and 8).

TABLE 2. KIMBERLITE

| | 1 | 2 | 3 | 4 | 5 | 6 | 7 | 8 |
|---|---|---|---|---|---|---|---|---|
| CHEMICAL ANALYSES | | | | | | | | |
| $SiO_2$ | 22.74 | 24.15 | 22.86 | 26.16 | 26.20 | 28.83 | 35.02 | 36.33 |
| $TiO_2$ | 5.86 | 6.46 | 2.98 | 2.50 | 3.60 | 5.67 | 1.22 | 1.89 |
| $Al_2O_3$ | 3.09 | 2.58 | 3.78 | 3.79 | 11.34 | 2.94 | 3.90 | 5.09 |
| $Fe_2O_3$ | 8.47 | 7.67 | 4.79 | 7.88 | 3.97 | 3.60 | 5.15 | 7.43 |
| $Cr_2O_3$ | 0.09 | trace | 0.06 | 0.17 | n.d. | n.d. | n.d. | n.d. |
| FeO | 7.54 | 8.36 | 5.32 | 2.63 | 13.89 | 5.13 | 4.14 | 3.40 |
| MnO | 0.21 | 0.16 | 0.17 | 0.30 | 0.22 | n.d. | 0.06 | 0.10 |
| NiO | trace | 0.02 | — | 0.12 | n.d. | n.d. | n.d. | n.d. |
| MgO | 23.83 | 24.03 | 14.58 | 23.40 | 9.33 | 24.31 | 31.29 | 26.63 |
| CaO | 11.82 | 10.27 | 22.24 | 14.70 | 12.36 | 11.24 | 6.80 | 6.78 |
| $Na_2O$ | 0.27 | 0.25 | 0.33 | trace | 0.67 | 0.75 | 0.34 | 0.37 |
| $K_2O$ | 0.94 | 1.02 | 1.52 | 0.78 | 1.46 | 1.31 | 1.05 | 2.43 |
| $H_2O+$ | 6.22 | 4.98 | 3.42 | 6.75 | 7.19 | 3.96 | 7.43 | 7.25 |
| $H_2O-$ | 0.76 | 0.90 | 1.65 | 0.16 | 2.22 | 0.83 | — | — |
| $P_2O_5$ | 0.68 | 0.23 | 1.32 | 0.86 | 1.40 | 0.77 | 0.87 | 0.66 |
| $CO_2$ | 7.24 | 9.02 | 14.84 | 9.94 | 6.42 | 11.64 | 2.73 | 1.64 |
| S | n.d. | n.d. | n.d. | — | 0.48 | n.d. | n.d. | n.d. |
| Total | 99.76 | 100.10 | 99.86 | 100.14 | 100.51* | 100.98 | 100.00 | 100.00 |
| NORMS | | | | | | | | |
| C | — | 0.71 | — | 1.12 | 4.39 | 0.20 | — | — |
| or | — | 7.78 | 9.45 | 5.00 | 8.90 | 7.78 | 6.67 | 13.07 |
| ab | — | 2.10 | 2.62 | — | 5.76 | 6.29 | 2.62 | — |
| an | 4.17 | — | 4.45 | 4.73 | 11.95 | — | 5.84 | 5.00 |
| lc | 3.27 | — | — | — | — | — | — | 1.09 |
| ne | 1.14 | — | — | — | — | — | — | 1.70 |
| kp | 1.11 | — | — | — | — | — | — | — |
| $CaSiO_3$ | — | — | 1.63 | — | — | — | 2.09 | 5.68 |
| $MgSiO_3$ | — | 1.54 | 4.00 | 11.10 | 1.35 | 12.47 | 5.03 | 4.90 |
| $FeSiO_3$ | — | — | 0.11 | — | 0.99 | — | 0.10 | — |
| $Mg_2SiO_4$ | 42.07 | 39.51 | 23.17 | 33.18 | 15.61 | 27.86 | 51.22 | 43.19 |
| $Fe_2SiO_4$ | — | — | 0.71 | — | 12.75 | — | 1.05 | — |
| cs | 1.29 | — | — | — | — | — | — | — |
| mt | 7.89 | 8.82 | 7.19 | 2.32 | 4.87 | — | 7.42 | 5.57 |
| cm | 0.22 | — | — | 0.22 | – | — | — | — |
| hm | 3.04 | 1.60 | — | 6.24 | — | 3.60 | — | 3.52 |
| il | 11.25 | 12.31 | 5.78 | 4.71 | 6.99 | 10.79 | 2.28 | 3.65 |
| ap | 1.68 | 0.34 | 3.02 | 2.02 | 3.36 | 2.02 | 2.02 | 1.68 |
| pr | — | — | — | — | 0.96 | — | — | — |
| cc | 16.60 | 18.20 | 34.40 | 22.60 | 14.80 | 18.00 | 6.20 | 3.70 |
| $MgCO_3$ | — | 2.10 | — | — | — | 7.05 | — | — |
| $H_2O+$ | 6.28 | 5.03 | 3.48 | 6.75 | 7.31 | 3.95 | 7.43 | 7.25 |
| Total | 100.01 | 100.04 | 100.01 | 99.99 | 99.99 | 100.01 | 99.97 | 100.00 |

1, 2, 3. Kimberlite, Bachelor Lake, Quebec; specimens 1, 2, and 3 in Table 1; W. H. Herdsman, analyst.

4. Kimberlite, Jagersfontein, Orange Free State (Williams, 1932, p. 246).

5. Kimberlite, Alnö area, Sweden; mode: pseudomorphs after olivine (serpentine, chlorite, and talc) 45.8%, biotite 28.4%, calcite 14.9%, perovskite 5.4%, apatite 3.4%, titanomagnetite 1.1%, pyrite 1.0% (von Eckermann, 1948, p. 102).

6. Mica peridotite, Fayette County, Pennsylvania (Kemp & Ross, 1907, p. 517).

7. Average of ten "basaltic" kimberlites (Nockolds, 1954, p. 1023).

8. Average of four "micaceous" kimberlites (Nockolds, 1954, p. 1023).

* Corrected for O equivalent of S (von Eckermann, 1948, p. 102).

from Pennsylvania that contains 17.5 per cent (Honess & Graeber, 1926, p. 6). Specimens 2 and 6 contain $CO_2$ in excess of CaO and thus it was necessary to calculate some of it as $MgCO_3$ in their norms.

## CONCLUSIONS

An important problem posed by the kimberlite of Bachelor Lake is the origin of its plentiful calcite. This question is not peculiar to the Bachelor Lake rocks, however, for among kimberlites elsewhere, and mica peridotites and alnöites, carbonate-rich ones are very common indeed.[4] It is clear that the calcite in the kimberlite at Bachelor Lake is not a product of weathering, as was assumed to be the case in some similar rocks elsewhere, for the bedrock has been well scoured glacially and the drill cores are from depths of a few hundred feet or more below surface. It is unlikely, moreover, that the calcite is a product of hydrothermal alteration by fluids derived from a source distinctly younger than the kimberlite for carbonate is either absent or virtually so in thin sections of all the other rocks and the ores from the area. Thus, the conclusion seems inescapable that the calcite is a product of the kimberlite magma itself. Since carbonate rocks are unknown in the Precambrian section in this part of Quebec, no sound basis exists for postulating that the magma obtained its carbonate by reaction with limestone or dolomite.

Some of the calcite in the kimberlite at Bachelor Lake has undoubtedly formed by partial replacement of other minerals and that which occurs with antigorite as well-defined laths in specimen 4 may possibly have been derived from melilite. Some of it, however, shows no evidence of a secondary origin and it occurs as medium to fine anhedral grains sharply molded against or completely enclosing euhedral crystals of olivine, phlogopite, augite, perovskite, magnetite, and apatite in a manner strongly suggesting that it is a late-crystallizing primary mineral. It might be argued that such textural relationships could originate by selective replacement of a very fine-grained groundmass in preference to coarser phenocrysts by virtue of the greater reactivity of the finer material. If this were the case, however, one would expect that the resulting aggregate would inherit a fine-grained texture since this has happened where fine-grained andesite and rhyolite-lapilli-tuff have been carbonatized immediately adjacent to the dikes. The possibilities remain that the calcite originated by selective replacement of a glass groundmass or of medium- to fine-grained *anhedra* of an unstable mineral such as melilite. However, since no evidence of these was seen in the 53 thin sections examined, these possibilities must be considered remote.

---

[4] It is worth mentioning here that Sosman's experimental evidence on the low intrusion-temperature of peridotites, now widely considered in petrogenetic studies of ultrabasic rocks in general, is derived from a mica peridotite in Pennsylvania that contains a considerable proportion of carbonate (1938, p. 358).

The tentative conclusion that some of the calcite in the kimberlite at Bachelor Lake is a late-crystallizing primary mineral differs with the conclusion of Shand (1947, pp. 444–445), Taljaard (1936, pp. 312–315), and Tröger (1935, p. 297) that the abundant calcite of South African kimberlite was derived from melilite formerly present in the rock. The suggestion made by Shand and Taljaard that South African kimberlites are highly altered melilite basalts (olivine melilitites), may be applicable to the Bachelor Lake kimberlite, however, for chemically it resembles olivine melilitite in its high content of $TiO_2$ and $P_2O_5$ and in several other respects (*cf.* Nockolds, 1954, p. 1029) and it contains possible pseudomorphs after melilite in some specimens.

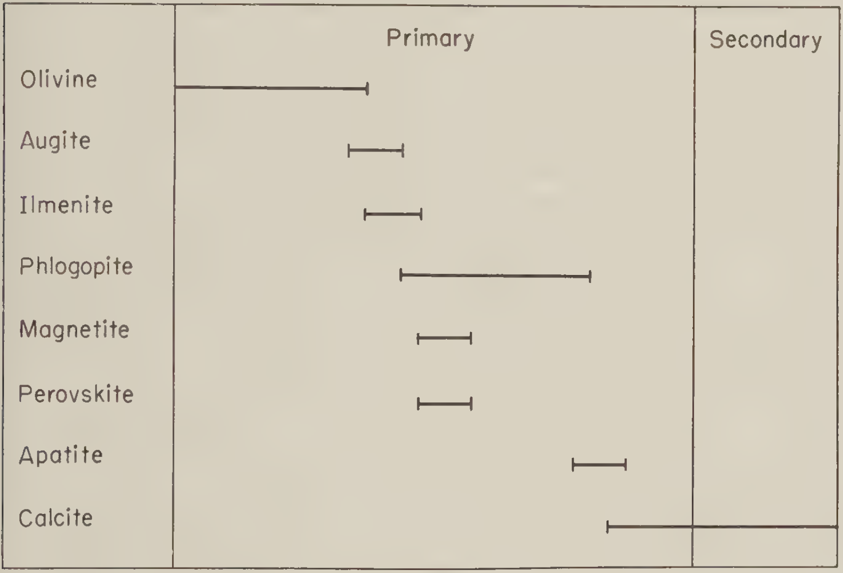

Fig. 2. Diagram showing paragenesis of primary minerals of kimberlite, Bachelor Lake.

The sequence of crystallization of the primary minerals, inferred from their textural relationships, is given in Figure 2. The well-defined laths in specimen 4, now consisting of antigorite and calcite but perhaps originally consisting of melilite, formed before crystallization of phlogopite was completed.

This study of the kimberlite at Bachelor Lake has led to two geological speculations. The first is concerned with the age of the intrusives. Figure 3 shows the distribution of mica peridotite, kimberlite, and alnöite in eastern North America. That it is legitimate to regard these rock-types as closely related is emphasized by the facts that the alnöites at some of these localities grade into mica peridotites or kimberlites by loss of melilite (Bowen, 1922, p. 6, p. 34; Harvie, 1909, p. 261, p. 275; Martens, 1924, pp. 310–314) and that the mica peridotite or kimberlite at other of these localities contains melilite (Smyth, 1902, pp. 26–30; Williams, *et al.*, 1954, pp. 79–80). In all the places shown in Figure 3 with the exception of Bachelor Lake and Pike County, southwestern Arkansas, the ultrabasic rocks cut sedimentary rocks of Paleozoic age, the youngest rocks with which they are in contact. The mica peridotite of Pike County is early Upper Cretaceous for it cuts Lower Cretaceous sediments and has furnished material to the lower part of an Upper Cretaceous formation

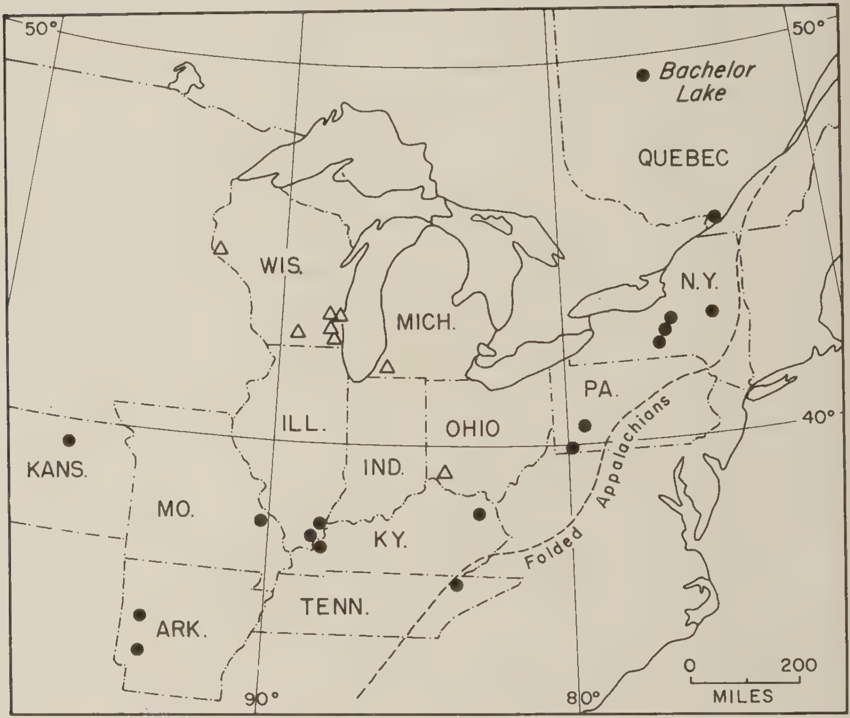

FIG. 3. Map of part of eastern North America showing locations of mica peridotite, kimberlite, and alnöite occurrences (black circles) and of some of the diamond discoveries in glacial drift (triangles). Data from Martens (1924), Tolman & Landes (1939), Hobbs (1899), and several other sources.

(Ross, *et al.*, 1929, p. 189); the Monteregian intrusives of southern Quebec, to which the alnöites and mica peridotite plotted in Figure 3 belong, have recently been assigned by Clark (1952, pp. 109-110, p. 123) to the Cretaceous or early Tertiary. Although flat-lying limestone of Ordovician age crops out at Waswanipi Lake (Blake, 1953, pp. 16–18) shown in Figure 1, it does not extend eastward to Bachelor Lake, and hence its relationship to the kimberlite in unknown. The kimberlite at Bachelor Lake contains altered olivine and abundant calcite but it has not been metamorphosed either thermally or regionally. In view of this and particularly of the occurrence of similar rocks in eastern North America which are Paleozoic or later in age, the speculation that the kimberlite of Bachelor Lake may be younger than Precambrian merits consideration.

The second speculation deals with the provenance of the diamonds that have been found from time to time in glacial drift in Wisconsin, Illinois, Michigan, Indiana, and Ohio (the localities of some of these discoveries are shown in Figure 3). Interest in this problem has been displayed in Canada on various occasions and recently led Chubb to investigate a large crater in Ungava which now bears his name. In connection with this problem, it may be significant that more than 10,000 diamonds have been found in mica peridotite at Murfreesboro, Arkansas, one diamond has been reported in kimberlite near Syracuse, New York (Kraus & Slawson, 1947, p. 191), and diamonds have been recovered from alluvial gravels a short distance downstream from outcrops of mica peridotite in Union County, Tennessee (Hall & Amick, 1944, p. 429). Data plotted on the Glacial Map of North America (1945) suggest the possibility—proposed long ago by Hobbs (1899, pp. 386–388)—that some of the diamonds found in glacial drift south of the Great Lakes might have been moved from somewhere in northern Quebec. For this reason the recognition of a rock-type in northern Quebec, which is known to contain diamonds elsewhere in eastern North America, may be of some geologic interest.

## ACKNOWLEDGMENTS

The writer is grateful to Mr. J. B. Redpath, Executive Vice-President of Dome Mines Limited, for permission to publish this article and to the University of California for funds for chemical analyses. It is a pleasure to thank Dr. C. Durrell for his help in the microscopic study and in the preparation of the manuscript.

## REFERENCES

BLAKE, D. A. W. (1953): Waswanipi Lake area (East half), *Quebec Dept. Mines*, Geol. Rept. **59**, 1–23.

Bowen, N. L. (1922): Genetic features of alnoitic rocks at Isle Cadieux, Quebec, *Am. J. Sci.*, **3,** 5th ser., 1–34.

Clark, T. H. (1952): Montreal area, Laval and Lachine map-areas, *Quebec Dept. Mines,* Geol.Rept. **46,** 1–159.

Daly, R. A. (1933): *Igneous rocks and the depths of the earth,* McGraw-Hill, New York.

Diller, J. S. (1892): Mica-peridotite from Kentucky, *Am. J. Sci.*, **44,** 3rd ser., 286–289.

Du Toit, A. L. (1907): Geological survey of the eastern part of Griqualand West, 11th *Ann. Rept. Geol. Comm. Cape of Good Hope,* 87–176.

Flint, R. F. (1945): Glacial map of North America, *Geol. Soc. America, Spec. Pap.*, **60.**

Graham, R. B. (1950): Southwest part of Lesueur Township, Abitibi-East County, *Quebec Dept. Mines,* Prelim. Rept. **243,** 1–15.

Hall, G. M. & Amick, H. C. (1944): Igneous rock areas in the Norris region, Tennessee, *Jour. Geol.*, **52,** 424–430.

Harvie, R. (1909): On the origin and relations of the Palaeozoic breccia of the vicinity of Montreal, *Roy. Soc. Canada, Trans.*, **3,** 3rd ser., 249–299.

Hobbs, W. H. (1899): The diamond field of the Great Lakes, *Jour. Geol.*, **7,** 375–388.

Holmes, A. (1936): A contribution to the petrology of kimberlite and its inclusions, *Geol. Soc. S. Africa, Trans.*, **39,** 379–428.

Honess, A. P., & Graeber, C. K. (1926): Petrography of the mica peridotite dike at Dixonville, Pennsylvania, *Penn. State Coll, Min. Met. Expt. Sta.*, Bull., **2,** 1–16.

Jakob, J. (1925): Beiträge zur chemischen Konstitution der Glimmer I Mitteilung: Die Schwedischen Manganophylle, *Zeits. Krist.*, **61,** 155–163.

Kemp. J. F., & Ross, J. G. (1907): A peridotite dike in the Coal Measures of southwestern Pennsylvania, *Annals. N.Y. Acad. Sci.*, **17,** 509–518.

Knopf, A. (1936): Igneous geology of the Spanish Peaks region, Colorado, *Geol. Soc. America, Bull.*, **47,** 1727–1784.

Kraus, E. H. & Slawson, C. B. (1947): *Gems and gem materials,* ed. 5, McGraw-Hill, New York.

Lewis, C. (1888): The matrix of the diamond, *Geol. Mag.*, **5,** 129–131.

Longley, W. W. (1951): Bachelor Lake area, *Quebec Dept. Mines,* Geol. Rept. **47,** 1–38.

Martens, J. H. C. (1924): Igneous rocks of Ithaca, New York, and vicinity, *Geol. Soc. America,* Bull. **35,** 305–320.

Miser, H. D., & Ross, C. S. (1923*a*): Diamond-bearing peridotite in Pike County, Arkansas, *U. S. Geol. Surv.*, Bull. **735,** 279–322.

——— (1923*b*): Peridotite dikes in Scott County, Arkansas, *U. S. Geol. Surv.*, Bull. **735,** 271–278.

Nockolds, S. R. (1954): Average chemical compositions of some igneous rocks, *Geol. Soc. America,* Bull., **65,** 1007–1032.

Ross, C. S. (1926): Nephelite-hauynite alnöite from Winnett, Montana, *Am. J. Sci.*, **11,** 5th ser., 218–227.

Ross, C. S., Miser, H. D., & Stephenson, L. W. (1929): Water-laid volcanic rocks of early Upper Cretaceous age in southwestern Arkansas, southeastern Oklahoma, and northeastern Texas, *U. S. Geol. Surv., P. P.*, **154,** 175–202.

Shand, S. J. (1947): *Eruptive Rocks,* ed. 3, Wiley, New York.

Singewald, J. T. & Milton, C. (1930): An alnoite pipe, its contact phenomena, and ore deposition near Avon, Missouri, *Jour. Geol.*, **38,** 54–66.

Smyth, C. H. (1902): Petrography of recently discovered dikes in Syracuse, N. Y.; with note on the presence of melilite in the Green Street dike, *Am. J. Sci.*, **14,** 4th ser., 26–30.

SOSMAN, R. B. (1938): Evidence on the intrusion-temperature of peridotites, *Am. J. Sci.*, **35,** 5th ser., 353–359.

TALJAARD, M. S. (1936): South African melilite basalts and their relations, *Geol. Soc., S. Africa, Trans.*, **39,** 281–316.

TOLMAN, C., & LANDES, K. K. (1939): Igneous rocks of the Mississippi Valley lead-zinc districts, *in* Contributions to a knowledge of the lead and zinc deposits of the Mississippi Valley region, *Geol. Soc. America, Spec. Paper*, **24,** 71–103.

TRÖGER, W. E. (1935): *Spezielle Petrographie der Eruptivgesteine—ein Nomenklature—Kompendium*, Deutschen Mineralogischen Gesellschaft, Berlin.

VON ECKERMANN, H. (1948): The alkaline district of Alnö Island, *Sveriges Geol. Undersök.*, **36,** Ser. Ca., 1–176.

WAGNER, P. A. (1914): *The diamond fields of southern Africa.* Transvaal Leader, Johannesburg.

——— (1909): Ueber skelettförmigen Apatit aus dem Kimberlit der De Beers-Grube, Kimberley, Südafrika, und die Anwendung einer Kochsalschmelze zum Nachweis desselben, *Centralbl. Mineralogie,* 550–552.

WILLIAMS, A. F. (1932): *The Genesis of the diamond* I, Benn, London.

WILLIAMS, G. J. (1939): The kimberlite province and associated diamond deposits of Tanganyika Territory, *Tanganyika Dept. Lands and Mines, Geol. Div.*, Bull. **12,** 1–38.

WILLIAMS, H., TURNER, F. J., & GILBERT, C. M. (1954): *Petrography*, Freeman, San Francisco.

WINCHELL, A. N. & WINCHELL, H. (1951): *Elements of optical mineralogy*, Part II—*Descriptions of minerals*, Wiley, New York.

# THE STRUCTURES OF THE MINERALS OF THE DESCLOIZITE AND ADELITE GROUPS:
# II—PYROBELONITE

D. M. Donaldson[1] and W. H. Barnes, *Division of Physics, National Research Council, Ottawa, Canada.*

## Abstract

The structure of pyrobelonite, $PbMn(VO_4)(OH)$, has been established by two-dimensional Patterson, Fourier, and difference methods applied independently to each of the three principal zones. The coordination of oxygen around vanadium is tetrahedral; it is octahedral around manganese, and sevenfold around lead. Interatomic distances are given. The accuracy of the results is discussed in terms of the standard deviations of atomic positions and of interatomic distances. The close structural relationship of pyrobelonite to descloizite is confirmed.

## Introduction

In continuation of a series of studies of the minerals of the descloizite and adelite groups (Barnes & Qurashi, 1952; Qurashi & Barnes, 1954), the structure of pyrobelonite, $PbMn(VO_4)(OH)$, has now been determined.

Both Strunz (1939) and Richmond (1940) are in agreement on the close structural relationship that must exist between pyrobelonite and descloizite, which is strikingly demonstrated by precession photographs of the three principal zones of each (see Qurashi & Barnes, 1954, Fig. 1). Interpretation of the original analytical results of Mauzelius (see Flink, 1919), however, has given rise to slight variations in the formula proposed for pyrobelonite, depending on the significance attached to the reported Mn:Pb ratio of 35:22. Thus Strunz (1939) gives it as $MnPb(VO_4)(OH)$ in his *Abstract* (p. 496) and *Summary* (p. 505), and as $Mn(Pb, Mn)(VO_4)(OH)$, to indicate replacement of some of the lead by manganese, in that section of his paper devoted especially to pyrobelonite (p. 502). On the other hand, Richmond expresses it as $(Mn, Pb)_2(VO_4)(OH)$, rounding off the Mn:Pb ratio to 5:3 in one place (p. 460) and 3:2 (perhaps a typographical error) in another (p. 477). In the latest edition of Dana's *System of Mineralogy* (1951) it is acknowledged that, if the observed Mn:Pb ratio (Flink, 1919) is real, "Mn may in part be in substitution for Pb, the formula then being $Mn(Pb, Mn)(VO_4)(OH)$," but the conclusion is reached that "the departure from the 1:1 ratio of Mn:Pb probably is due to analytical error" and the formula accepted, therefore is $MnPb(VO_4)(OH)$.* This has been employed successfully throughout the present structure investigation.

---

[1] National Research Laboratories Postdoctorate Fellow, now I.C.I. Fellow, The University, Edinburgh, Scotland.

### *Experimental, and Crystal Data*

The experimental data were obtained by means of Weissenberg and precession photographs ($MoK_\alpha$ radiation, $\lambda = 0.7107$ Å) of two crystals from Långban, Sweden (Harvard No. 94831) having dimensions $200 \times 50 \times 40\mu$ and $88 \times 50 \times 50\mu$, respectively.

Pyrobelonite is orthorhombic, space group $Pnma$ ($D_{2h}^{16}$) or $Pn2a$ ($C_{2v}^{9}$), with $a = 7.66_3$, $b = 6.19_1$, $c = 9.52_2$ Å (see Barnes & Qurashi, 1952). There are $4[PbMn(VO_4)(OH)]$ per cell and the calculated density is 5.79 gm. per ml. The observed density given by Hintze (1933), quoting Flink (1919), however, is only 5.377, and, if a Mn:Pb ratio of 5:3 were correct, the calculated value would be 5.23 gm. per ml. (although Richmond, 1940, gives it as 5.39). Apart from the two small crystals employed for the diffraction photographs, only one other from the Harvard 94831 specimen was available for the present investigation, but it had a mass of ~6 mg. Although this is too small for very accurate measurements with the Berman balance (Berman, 1939; Fairbairn & Sheppard, 1945), a value of 5.58 gm. per ml. (mean of ten determinations) was obtained for the density at 23° C., using carbon tetrachloride as the displacement liquid. The surface of the crystal was irregular, there were a few firmly-attached small fragments of other materials, and, owing to the virtual opacity it was not possible to estimate the degree of homogeneity of the crystal, so that the observed density probably is low rather than high. Crystals from another Långban specimen (U. S. National Museum No. 94601), freed from adhering matrix, were too small, and not sufficiently numerous, for a direct density determination, nor could any useful results be obtained by means of Cargille "heavy liquids." The question of the significance, if any, to be attached to the difference between the calculated and observed densities in relation to the possible substitution of managanese for lead will be mentioned later in the discussion.

Intensities were estimated visually from the precession and Weissenberg photographs using multiple exposure and multiple film techniques, respectively. The usual corrections for Lorentz and polarization factors were applied. For ease in the calculation of absorption corrections, the first crystal ($200 \times 50 \times 40\mu$), from which the $h0l$ reflection intensities were obtained, was treated as a cylinder, and the second, which was employed for the $\{hk0\}$ and $\{0kl\}$ zones, was considered as a sphere of volume $88 \times 50 \times 50 \mu^3$. This has the advantage of making the absorption corrections, in all three zones, functions of sin $\theta$ (Bradley, 1935; Evans & Ekstein, 1952). The deviations from the true values should be small because of the comparative regularity of shape of the crystals and of their small size. The absorption coefficient for Mo$K_\alpha$ ($\lambda = 0.7107$ Å) is 474 per cm.

---

* $PbMn(VO_4)(OH)$ is preferred for uniformity with descloizite, $Pb(Zn, Cu)(VO_4)(OH)$, and conichalcite, $CaCu(AsO_4)(OH)$ because the Pb in pyrobelonite and in descloizite, and the Ca in conichalcite, occupy corresponding sites in the structures of the three minerals.

## ANALYSIS OF THE STRUCTURE

Because of the close similarity between corresponding reciprocal lattice nets of pyrobelonite and descloizite (Barnes & Qurashi, 1952; Qurashi & Barnes, 1954), the Pb, Mn and V atoms of pyrobelonite could justifiably have been assigned the parameters established for Pb, Zn, and V, respectively, in descloizite as a prelude to refinement of the pyrobelonite structure. It was decided, however, to carry out the present study as independently as possible of the descloizite results. Furthermore, one of the principal objects was to determine the coordinates of the oxygen atoms with the highest accuracy warranted by two-dimensional analysis of the data. Hence the three principal zones of pyrobelonite have been analysed separately and each has been refined without averaging the coordinates or correction factors (such as the temperature factor) among the three zones. This method provides a means for direct comparison of coordinates obtained independently for each of two separate zones.

### *The* {*h*0*l*} *Zone*

Of 130 possible reflections in the range sin $\theta/\lambda \leqq 0.75$, 92 were observed, together with 8 outside this range. The (010) Patterson map was computed using all these observed reflections, and is reproduced in Fig. 1A. From an analysis of the peaks due to Pb-Pb, Pb-Mn, and Pb-V vectors, $x$ and $z$ coordinates for the metal atoms were obtained. Since the atomic numbers of Mn and V differ so slightly, it was impossible to distinguish between the positions occupied by the manganese and by the vanadium atoms. In this one instance, therefore, the descloizite structure was taken as a guide and the vanadium atoms in pyrobelonite were placed in the positions which corresponded most closely with those occupied by vanadium in descloizite. Structure factors were calculated* with these metal-atom coordinates and a Fourier synthesis was carried out. The (010) Fourier map is shown in Fig. 1B where it will be seen that the metal atoms are clearly resolved but only slight indications of the oxygen-atom positions appear.

---

* No choice between the alternative space groups (*Pnma* and *Pn*2*a*) was necessary at this stage because the equivalent positions and structure factor equations are the same for the {*h*0*l*} zone.

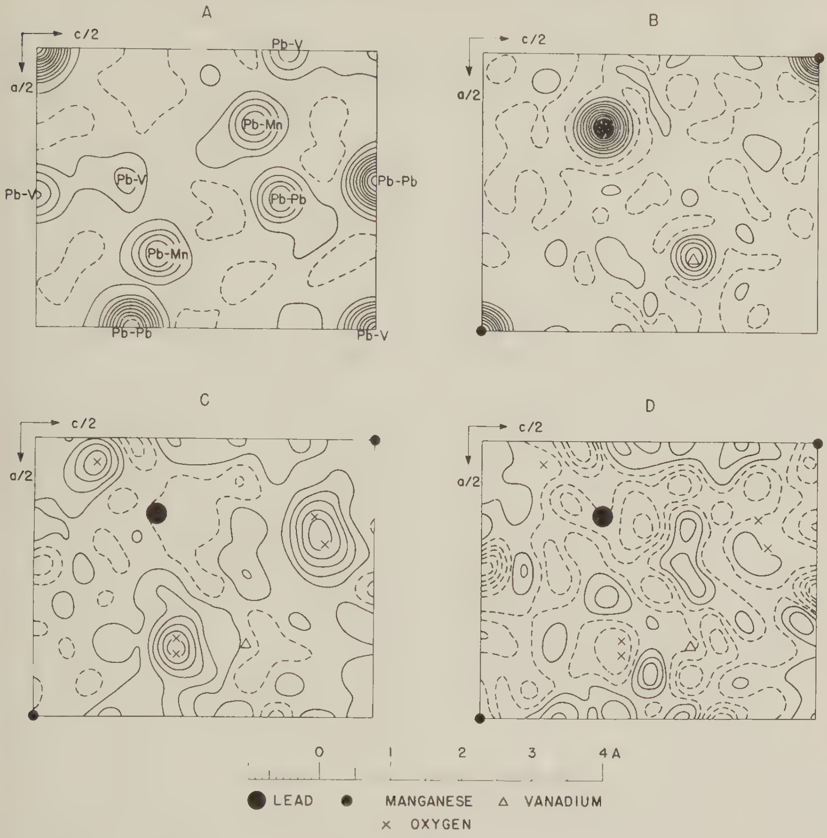

FIG. 1. The {$h0l$} zone of pyrobelonite; (A) Patterson map with contours at regular, but arbitrary, intervals (doubled at origin); (B) Fourier map with contours at intervals of $\sim 5e.\text{Å}^{-2}$ ($10e.\text{Å}^{-2}$ around Pb), zero contour broken; (C) $(F_o - F_{c(m)})$ map with contours at intervals of $\sim 2e.\text{Å}^{-2}$, zero and negative contours broken; (D) final $(F_o - F_c)$ map with contours at intervals of $\sim 1e.\text{Å}^{-2}$, zero and negative contours broken.

The coordinates of the oxygen atoms were obtained, the positions of all the atoms were refined, appropriate temperature factors were determined, and termination-of-series errors were corrected by means of the difference-synthesis technique (Cochran, 1951). Since the accuracy of the results, especially in the location of the oxygen atoms, is dependent on the difference syntheses, it was necessary to exercise care in the selection of values for the atomic scattering factors. The scattering curves for the different atoms were obtained as follows.

*Lead*. It was assumed that lead is present as the divalent ion. The *atomic* scattering curve for Pb in the *International Tables* (1935), therefore, was adjusted to that of $Pb^{+2}$ by reducing the value at $\sin \theta/\lambda = 0$ from 82 to 80, leaving those at $\sin \theta/\lambda \geqq 0.4$ unchanged, and drawing a smooth curve from 80 at $\sin \theta/\lambda = 0$ to join that representing these higher values.

*Manganese.* The assumption was made that manganese also is present as the divalent ion. The scattering curve for $Mn^{+2}$ was derived from that of Mn by comparison with those for Ca and $Ca^{+2}$ (*International Tables*, 1935).

*Vanadium.* It is probable that the vanadium-oxygen bonds have some covalent character and, hence, that vanadium is not present as $V^{+5}$. Consequently $V^{+2.5}$ was chosen as a compromise between the unionized and fully ionized metalloid atom. The corresponding scattering curve was calculated from recent atomic scattering data for vanadium (Qurashi, 1954) by deducting the contributions of one 4*s* and one and one-half 3*d* electrons, utilizing the screening parameters and individual electron contributions given by Viervoll & Ögrim (1949).

*Oxygen.* In order to balance the ionic charges present, it was necessary to consider each oxygen atom to have gained $1\frac{1}{2}$ electrons. The scattering curve for $O^{-1.5}$ was obtained by interpolation between the data for O and $O^{-2}$ (*International Tables*, 1935), and was employed for all the oxygen atoms including that of the OH group.

With the foregoing scattering factors for $Pb^{+2}$, $Mn^{+2}$, $V^{+2.5}$, corrected for thermal motion, $(F_o - F_{c(m)})$ syntheses were performed, where $F_{c(m)}$ is the structure factor calculated for the metal atoms alone. The map representing the final synthesis of this type is shown in Fig. 1C, where it will be observed that the oxygen atoms appear clearly, although only one of the five in the asymmetric unit is resolved. Nevertheless, $x$ and $z$ coordinates for the oxygen atoms, and some alterations of the metal-atom positions, were obtained from this synthesis.

Refinement of all positions (metal and oxygen atoms), and of the temperature factor corrections, was completed through successive $(F_o-F_c)$ syntheses, where $F_c$ is the structure factor calculated for the metal atoms and the oxygen atoms. The last difference map is reproduced in Fig. 1D, from which it can be seen that the gradients at all the atomic positions are small enough to be neglected. The background density varies from $-4e.\text{Å}^{-2}$ to $+4e.\text{Å}^{-2}$. The final $x$, $z$ coordinates obtained for this zone are presented later in Table 4.

The temperature factor corrections, of the usual form $\exp[-B(\sin \theta/\lambda)^2]$, applied to the scattering curves were obtained qualitatively from the difference syntheses by attempting to reduce the background density around the atoms to zero. The final values of $B$ for the $\{h0l\}$ zone are presented later, with those for the other two zones, in Table 5. The structure factor data, derived from the $x$, $z$ coordinates of Table 4 (see under $\{h0l\}$), the scattering curves defined previously, and these temperature factors, are given in Table 1. The value of the reliability index $R$ is 0.15 when the metal atoms only are considered, but drops to 0.09 when the contributions of the oxygen atoms are included.

TABLE 1. STRUCTURE FACTOR DATA FOR THE $\{h0l\}$ ZONE ($F_o$, OBSERVED; $F_{c(m)}$, CALCULATED FOR METAL ATOMS ONLY; $F_c$, CALCULATED FOR METAL ATOMS AND OXYGEN ATOMS)

| *hkl* | $F_{c(m)}$ | $F_o$ | $F_c$ | *hkl* | $F_{c(m)}$ | $F_o$ | $F_c$ |
|---|---|---|---|---|---|---|---|
| 000 | +520 | — | +684 | 2.0.10 | +29 | 39 | +36 |
| 200 | +44 | 51 | +43 | 2.0.11 | +43 | 67 | +63 |
| 400 | −218 | 225 | −257 | 2.0.12 | +20 | <33 | +22 |
| 600 | +112 | 139 | +125 | 2.0.13 | −83 | 89 | −99 |
| 800 | +188 | 184 | +194 | 2.0.14 | +33 | <36 | +29 |
| 10.0.0 | −38 | 35 | −43 | 301 | −179 | 127 | −125 |
| 002 | −146 | 148 | −151 | 302 | −91 | 121 | −116 |
| 004 | +5 | <17 | −4 | 303 | +166 | 151 | +150 |
| 006 | +281 | 234 | +243 | 304 | +99 | 106 | +109 |
| 008 | −146 | 186 | −172 | 305 | −214 | 215 | −222 |
| 0.0.10 | +76 | 103 | +99 | 306 | −30 | 49 | −48 |
| 0.0.12 | +107 | 101 | +109 | 307 | −38 | 83 | −72 |
| 0.0.14 | −80 | 76 | −65 | 308 | −44 | 27 | −30 |
| 0.0.16 | +74 | 69 | +65 | 309 | +69 | 84 | +75 |
| 101 | +21 | <11 | +6 | 3.0.10 | +64 | 63 | +63 |
| 102 | −133 | 115 | −121 | 3.0.11 | −141 | 125 | −131 |
| 103 | −291 | 231 | −271 | 3.0.12 | −34 | 43 | −33 |
| 104 | +138 | 185 | +190 | 3.0.13 | +17 | <35 | +24 |
| 105 | +88 | 76 | +63 | 401 | +31 | 37 | +33 |
| 106 | −40 | 48 | −53 | 402 | +228 | 226 | +251 |
| 107 | −50 | 36 | −32 | 403 | −4 | <21 | +2 |
| 108 | −59 | 62 | −54 | 404 | +100 | 86 | +91 |
| 109 | −130 | 130 | −134 | 405 | −21 | <24 | −13 |
| 1.0.10 | +85 | 81 | +71 | 406 | −142 | 136 | −139 |
| 1.0.11 | +65 | 77 | +69 | 407 | +25 | 27 | +31 |
| 1.0.12 | −44 | 39 | −50 | 408 | +193 | 186 | +203 |
| 1.0.13 | −62 | 57 | −60 | 409 | −10 | <30 | −12 |
| 1.0.14 | −15 | <36 | −9 | 4.0.10 | −5 | <31 | −20 |
| 201 | −189 | 152 | −167 | 4.0.11 | −9 | <32 | −16 |
| 202 | +96 | 95 | +91 | 4.0.12 | −42 | 41 | −33 |
| 203 | +30 | 59 | −45 | 4.0.13 | +15 | <35 | +8 |
| 204 | +68 | 77 | +62 | 4.0.14 | +112 | 105 | +103 |
| 205 | +123 | 118 | +112 | 501 | −105 | 123 | −105 |
| 206 | +28 | <23 | +27 | 502 | +111 | 92 | +93 |
| 207 | +145 | 148 | −128 | 503 | +66 | 59 | +50 |
| 208 | +59 | 85 | +64 | 504 | −121 | 147 | −154 |
| 209 | +57 | 73 | +60 | 505 | −123 | 114 | −111 |

TABLE 1—(*continued*)

| *hkl* | $F_{c(m)}$ | $F_o$ | $F_c$ |
|---|---|---|---|
| 506 | +36 | 32 | +50 |
| 507 | −34 | 33 | −40 |
| 508 | +56 | 70 | +63 |
| 509 | +25 | 31 | +38 |
| 5.0.10 | −84 | 70 | −70 |
| 5.0.11 | −87 | 87 | −85 |
| 5.0.12 | +43 | 35 | +41 |
| 601 | +123 | 98 | +101 |
| 602 | +2 | <25 | +8 |
| 603 | −22 | <26 | −19 |
| 604 | +27 | <26 | +23 |
| 605 | −84 | 100 | −93 |
| 606 | +84 | 75 | +75 |
| 607 | +104 | 116 | +100 |
| 608 | −11 | <31 | −17 |
| 609 | −44 | <32 | −31 |
| 6.0.10 | +38 | 56 | +38 |
| 6.0.11 | −33 | <35 | −39 |
| 6.0.12 | +42 | <36 | +46 |
| 701 | +37 | <27 | +28 |
| 702 | +43 | 49 | +44 |
| 703 | −198 | 175 | −189 |
| 704 | −47 | 51 | −55 |
| 705 | +85 | 101 | +84 |
| 706 | +16 | <30 | +30 |
| 707 | −35 | <31 | −24 |
| 708 | +23 | <32 | +23 |
| 709 | −115 | 121 | −124 |
| 7.0.10 | −35 | 35 | −33 |
| 7.0.11 | +71 | 70 | +65 |
| 801 | −38 | 48 | −44 |
| 802 | −60 | 80 | −74 |
| 803 | +6 | <30 | −5 |
| 804 | +3 | <30 | +8 |
| 805 | +28 | <31 | +25 |
| 806 | +145 | 147 | +149 |
| 807 | −35 | <32 | −28 |
| 808 | −76 | 94 | −76 |
| 809 | +14 | <35 | +22 |
| 8.0.10 | +48 | 70 | +59 |
| 901 | −11 | 31 | −16 |
| 902 | −74 | 79 | −81 |
| 903 | −73 | 72 | −67 |
| 904 | +84 | 73 | +85 |
| 905 | +4 | <33 | +2 |
| 906 | −26 | <34 | −35 |
| 907 | −26 | <34 | −19 |
| 908 | −42 | <35 | −37 |
| 909 | −47 | 65 | −53 |
| 9.0.10 | +64 | 56 | +65 |
| 10.0.1 | −68 | 69 | −63 |
| 10.0.2 | +68 | 69 | +66 |
| 10.0.3 | +12 | <34 | +4 |
| 10.0.4 | +38 | 51 | +44 |
| 10.0.5 | +48 | <35 | +50 |
| 10.0.6 | −25 | <35 | −19 |
| 10.0.7 | −62 | 47 | −55 |
| 10.0.8 | +66 | 66 | +64 |
| 11.0.1 | −71 | 72 | −75 |
| 11.0.2 | −14 | <35 | −16 |
| 11.0.3 | +80 | 77 | +76 |
| 11.0.4 | +16 | <36 | +20 |
| 11.0.5 | −101 | 88 | −94 |
| 12.0.2 | +70 | 74 | +70 |
| 13.0.2 | +45 | 46 | +44 |

### *The {0kl} Zone*

Of 37 possible reflections in the range $\sin\theta/\lambda \leqq 0.6$, 33 were observed. The (100) Patterson map, computed with these terms, is reproduced in Fig. 2A. Examination of this map shows that the peak distributions for the Pb-Pb, Pb-V, and Pb-Mn vectors can be explained satisfactorily if the Pb and V atoms are lying along $y = \pm\frac{1}{4}$ (special positions (c) of *Pnma*) and the Mn atoms are in special positions (b) of *Pnma*. On this basis the space group *Pnma* was adopted provisionally and refinement proceeded by means of Fourier and difference-synthesis techniques as for the {*h*0*l*} zone.

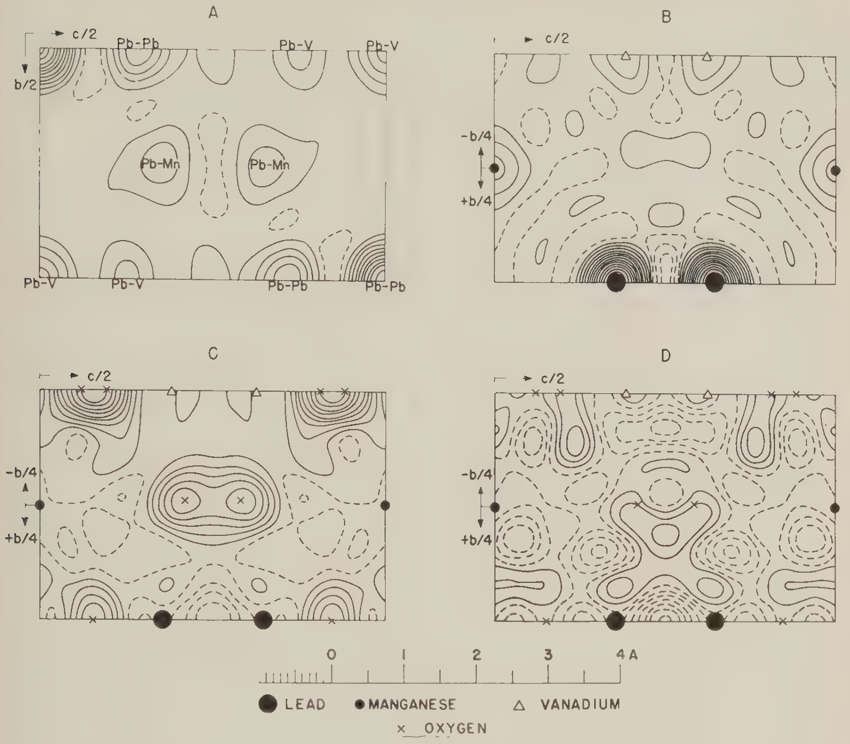

FIG. 2. The {0*kl*} zone of pyrobelonite; (A) Patterson map with contours at regular, but arbitrary, intervals; (B) Fourier map with contours at intervals of $\sim 7e.\text{Å}^{-2}$, zero contour broken; (C) $(F_o - F_{c(m)})$ map with contours at intervals of $\sim 2e.\text{Å}^{-2}$, zero and negative contours broken; (D) final $(F_o - F_c)$ map with contours at intervals of $\sim 1e.\text{Å}^{-2}$, zero and negative contours broken.

The (100) Fourier map is shown in Fig. 2B where, again, the metal atoms are clearly resolved but the positions of the oxygen atoms are only vaguely indicated. Fig. 2C shows the results of the $(F_o - F_{c(m)})$ synthesis from which the coordinates of the oxygen atoms were obtained; only one pair of oxygen atoms is not resolved. The final $(F_o - F_c)$ synthesis is reproduced in Fig. 2D. In this map the gradients at the atomic positions are negligible and the general background density varies from $-3.5e.\text{Å}^{-2}$ to $+3.5e.\text{Å}^{-2}$ with the exception of a trough of $-6e.\text{Å}^{-2}$ between two lead atoms. Examination of the electron density in the immediate vicinity of these lead atoms indicates that they may have a slight degree of asymmetric thermal motion, the effect being multiplied at the trough. No correction for this was applied, however, because the individual effects, if real, are no larger than the random peaks. The final $y$, $z$ coordinates obtained for the {0*kl*} zone are collected in Table 4.

The final values of the temperature factor constant ($B$) for this zone are given in Table 5. The structure factor data, based on the $y$, $z$ coordinates of Table 4 (see under $\{0kl\}$) are presented in Table 2. The reliability index $R$ is 0.16 for the metal atoms alone, and 0.10 for all the atoms. The values of $F_o$ for the planes (020) and (040) are very much smaller than the corresponding values of $F_c$ (see Table 2). This is probably due to extinction and the contributions from these two planes were omitted from the difference syntheses. If they are given zero discrepancy, $R$ for all the atoms becomes 0.06.

Table 2. Structure Factor Data for the $\{0kl\}$ Zone ($F_o$, Observed; $F_{c(m)}$, Calculated for Metal Atoms Only; $F_c$, Calculated for Metal Atoms and Oxygen Atoms)

| $hkl$ | $F_{c(m)}$ | $F_o$ | $F_c$ | $hkl$ | $F_{c(m)}$ | $F_o$ | $F_c$ |
|---|---|---|---|---|---|---|---|
| 000 | +520 | — | +684 | 0.2.10 | −7 | <38 | +3 |
| 020 | −262 | 216 | −287 | 031 | +165 | 158 | +164 |
| 040 | +307 | 276 | +376 | 033 | −27 | 39 | −45 |
| 060 | −146 | 142 | −156 | 035 | −111 | 122 | −115 |
| 002 | −147 | 149 | −150 | 037 | +132 | 142 | +133 |
| 004 | +6 | <34 | +7 | 039 | −53 | 53 | −55 |
| 006 | +281 | 239 | +244 | 042 | −105 | 104 | −106 |
| 008 | −146 | 170 | −172 | 044 | −1 | <42 | −1 |
| 0.0.10 | +77 | 109 | +92 | 046 | +212 | 192 | +187 |
| 011 | −201 | 152 | −183 | 048 | −115 | 145 | −134 |
| 013 | +31 | 56 | +50 | 051 | −124 | 105 | −113 |
| 015 | +128 | 145 | +137 | 053 | +21 | <43 | +25 |
| 017 | −151 | 161 | −151 | 055 | +85 | 102 | +91 |
| 019 | +58 | 65 | +58 | 057 | −107 | 94 | −106 |
| 0.1.11 | +46 | 57 | +49 | 062 | +148 | 124 | +119 |
| 022 | +274 | 182 | +200 | 064 | +69 | 82 | +85 |
| 024 | +119 | 166 | +154 | 066 | −102 | 77 | −84 |
| 026 | −162 | 139 | −132 | 071 | +90 | 76 | +93 |
| 028 | +215 | 223 | +223 | 073 | −16 | 25 | −26 |

### *The* $\{hk0\}$ *Zone*

All 28 possible reflections in the range $\sin\theta/\lambda \leqq 0.06$ were observed. The (001) Patterson map is reproduced in Fig. 3A. The coordinates obtained from an analysis of this map in terms of the Pb-Pb, Pb-Mn, and Pb-V vectors required no departure from the space group *Pnma*. Refinement, therefore, was carried out as for the previous two zones.

The (001) electron-density map is shown in Fig. 3B. In this zone the lead and vanadium atoms are not resolved and thus were assumed to be exactly superimposed. Good resolution of the manganese atom is apparent but there are no indications of the oxygen atoms. The latter, however, emerge clearly in the $(F_o - F_{c(m)})$ map reproduced in Fig. 3C, with the exception of the OH group. The final $(F_o - F_c)$ synthesis is repre-

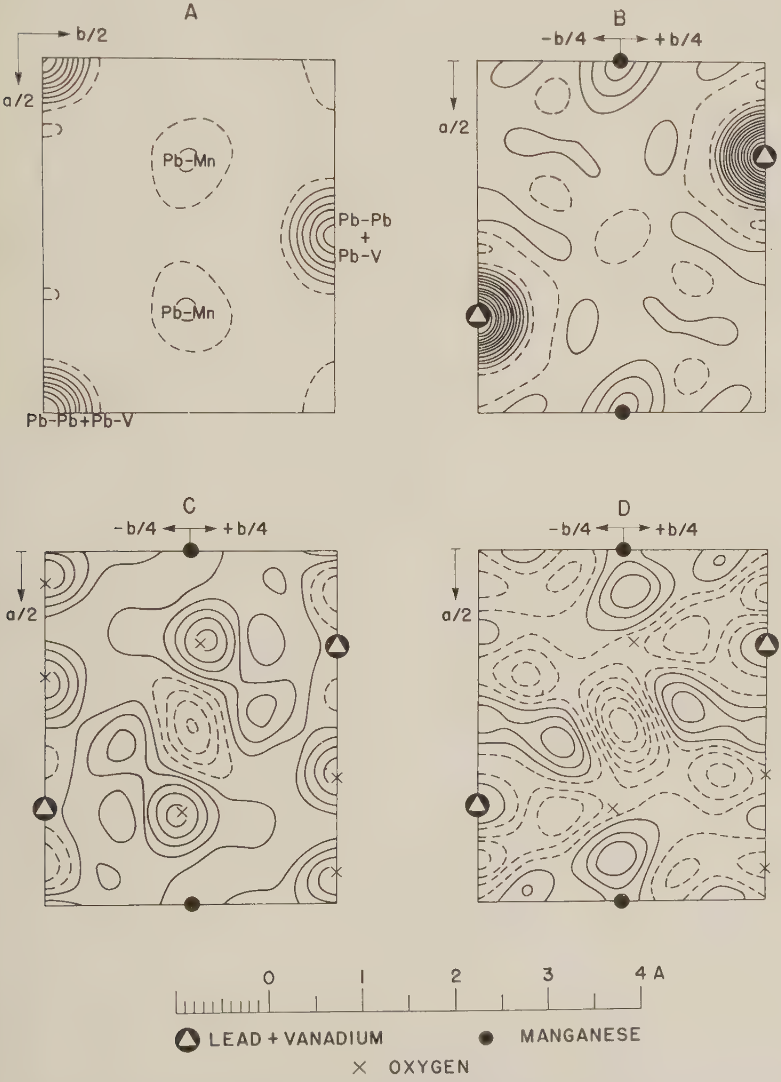

FIG. 3. The $\{hk0\}$ zone of pyrobelonite; (A) Patterson map with contours at regular, but arbitrary, intervals; (B) Fourier map with contours at intervals of $\sim 7e.\text{Å}^{-2}$, zero contour broken; (C) $(F_o - F_{c(m)})$ map with contours at intervals of $\sim 2e.\text{Å}^{-2}$, zero and negative contours broken; (D) final $(F_o - F_c)$ map with contours at intervals of $\sim 1e.\text{Å}^{-2}$, zero and negative contours broken.

sented in Fig. 3D, where the gradients at the atomic positions are negligibly small and, apart from a trough of $-6e.\text{Å}^{-2}$ at $(\frac{1}{4},0)$, the general background density varies from $-3.5e.\text{Å}^{-2}$ to $+3.5e.\text{Å}^{-2}$. Although there are indications in this case of possible asymmetric thermal motion of the manganese atoms no corrections for this were applied because the variation in electron density around the manganese atoms is of the same order of magnitude as the general background.

In the projection of this zone, the lead and vanadium atoms appear to be exactly superimposed; if they are not, the separation can only be very slight because no shifts from the superimposed positions were indicated by the difference syntheses (Fig. 3D). The reason for the apparent absence of the hydroxyl group can be found by reference to the $x$, $y$ coordinates obtained for the $\{h0l\}$ and $\{0kl\}$ zones (Table 4); the OH is present in the large peak representing the lead and vanadium atoms. With this information, an adjustment of the temperature factor corrections could have been applied to the scattering curves for these two atoms in order to produce a peak for the OH group in the difference syntheses of the $\{hk0\}$ zone. This would have vitiated the complete independence of treatment of this zone, however, and therefore no allowance for the OH group was made during the refinement procedure.

The final $x$, $y$ coordinates obtained for the $\{hk0\}$ zone are given in Table 4.

The final values of the temperature factor constant ($B$) for this zone are listed in Table 5. The structure factor data, calculated with the $x$ $y$, coordinates of Table 4 (see under $\{hk0\}$) are given in Table 3. The reliability index $R$ is 0.12 for the metal atoms only and 0.08 when the oxygen atom contributions are included. The values of $F_o$ for (020), (040), and (210) are very much smaller than the corresponding values of $F_c$ (see Table 3). This again is probably due to extinction and the contributions from these three planes were omitted from the difference syntheses. If they are given zero discrepancy, $R$ for all the atoms becomes 0.04.

### *Correlation of the Results from the Three Zones*

Although the reflection intensities for each zone were placed on an approximately absolute scale independently of the data for the other two zones, the differences in scale from zone to zone are very small as may be seen by a comparison of $F_o$'s for the axial reflections common to pairs of zones (Tables 1, 2, 3). In fact the difference in scale of the $00l$ reflections (common to the $\{h0l\}$ and $\{0kl\}$ zones), calculated from

$$\frac{\Sigma F_{00l}(\text{ for } \{h0l\}) - \Sigma F_{00l}(\text{for } \{0kl\})}{\frac{1}{2}[\Sigma F_{00l}(\text{for } \{h0l\}) + \Sigma F_{00l}(\text{for } \{0kl\})]}$$

Table 3. Structure Factor Data for the {*hk*0} Zone ($F_o$, Observed; $F_{c(m)}$, Calculated for Metal Atoms Only; $F_c$, Calculated for Metal and Oxygen Atoms)

| *hkl* | $F_{c(m)}$ | $F_o$ | $F_c$ |
|---|---|---|---|
| 000 | +520 | — | +684 |
| 200 | +36 | 45 | +38 |
| 400 | −208 | 225 | −236 |
| 600 | +124 | 136 | +142 |
| 800 | +172 | 183 | +177 |
| 020 | −259 | 220 | −260 |
| 040 | +301 | 296 | +355 |
| 060 | −132 | 137 | −135 |
| 210 | −337 | 254 | −309 |
| 220 | +109 | 118 | +99 |
| 230 | +270 | 240 | +240 |
| 240 | +22 | 35 | +23 |
| 250 | −195 | 191 | −191 |
| 260 | +58 | 69 | +55 |
| 270 | +136 | 115 | +118 |
| 410 | +68 | 74 | +66 |
| 420 | +304 | 264 | +270 |
| 430 | −57 | 53 | −54 |
| 440 | −151 | 180 | −166 |
| 450 | +43 | 43 | +43 |
| 460 | +176 | 161 | +161 |
| 610 | +193 | 201 | +211 |
| 620 | −30 | 36 | −34 |
| 630 | −167 | 190 | −176 |
| 640 | +97 | 112 | +110 |
| 650 | +132 | 150 | +149 |
| 810 | −74 | 66 | −62 |
| 820 | −94 | 85 | −70 |
| 830 | +67 | 61 | +58 |

is less than 1%; it is 2% for the *h*00 reflections (common to the {*h*0*l*} and {*hk*0} zones), and it is 3% for the 0*k*0 reflections (common to the {*hk*0} and {0*kl*} zones). Furthermore, the discrepancies between the $F_o$'s for the set of axial reflections common to a pair of zones, calculated from expressions of the form

$$\frac{\Sigma|F_{00l}(\text{for }\{h0l\})-F_{00l}(\text{for }\{0kl\})|}{\frac{1}{2}[\Sigma F_{00l}(\text{for }\{h0l\})+\Sigma F_{00l}(\text{for }\{0kl\})]}$$

lie between 2% and 5% for the three pairs of principal zones. Since this is the order of accuracy to be expected of $F_o$'s obtained from visually estimated intensities, the errors in the absorption corrections, as anticipated, must be small.

The atomic coordinates obtained independently for each zone together with the mean values are listed in Table 4. In all cases, the average is the arithmetic mean except for O(3) and O(4).

The maximum difference between two values of the same coordinate for the lead atoms occurs for $x$ (see Table 4) and corresponds to 0.014 Å. The discrepancy probably is attributable to the value for the {*hk*0} zone because V is superimposed on Pb in the (001) maps (Fig. 3). Because the discrepancy is so small, however, the values were not weighted in calculating the mean. No similar assessment of the manganese coordinates is possible because of their special positions. The largest difference in the vanadium coordinates ($x$) corresponds to 0.006 Å.

The differences between values for the same oxygen coordinates vary

TABLE 4. FRACTIONAL COORDINATES OF THE ATOMS (DERIVED INDEPENDENTLY FOR EACH ZONE AND THEN AVERAGED)

| Atom | *x* | | | *y* | | | *z* | | |
|---|---|---|---|---|---|---|---|---|---|
| | {*hk*0} | {*h*0*l*} | Mean | {*hk*0} | {0*kl*} | Mean | {*h*0*l*} | {0*kl*} | Mean |
| Pb | 0.1350 | 0.1332 | 0.1341 | 1/4 | 1/4 | 1/4 | 0.1776 | 0.1775 | 0.1776 |
| Mn | 0 | 0 | 0 | 0 | 0 | 0 | 1/2 | 1/2 | 1/2 |
| V | 0.3650 | 0.3658 | 0.3654 | 3/4 | 3/4 | 3/4 | 0.3130 | 0.3125 | 0.3128 |
| O(1) | 0.178 | 0.190 | 0.184 | 3/4 | 3/4 | 3/4 | 0.432 | 0.442 | 0.437 |
| O(2) | 0.538 | 0.542 | 0.540 | 3/4 | 3/4 | 3/4 | 0.410 | 0.405 | 0.408 |
| O(3) | 0.367 | 0.360 | 0.371 | 0.515 | 0.510 | 0.513 | 0.207 | 0.210 | 0.209 |
| O(4) | 0.367 | 0.390 | 0.371 | 0.985 | 0.990 | 0.987 | 0.207 | 0.210 | 0.209 |
| OH | — | 0.139 | 0.139 | — | 1/4 | 1/4 | 0.412 | 0.422 | 0.417 |

from 0.029 to 0.095 Å with the exception of one of 0.176 Å (see fractional coordinates $x$ for O(4), Table 4), but, even with the inclusion of this one, the r.m.s. difference is only 0.078 Å. If the space group is *Pnma* (and not *Pn2a*), O(3) and O(4) must be superimposed exactly in the (010) projection by virtue of the mirror plane perpendicular to *b*. In Fig. 1C, O(3) and O(4) are not separately resolved, but, in the final difference map (Fig. 1D) there is some evidence that they may not have precisely the same $x$ coordinate; this is recognized by the inclusion of $x = 0.360$ for O(3) and $x = 0.390$ for O(4) in the appropriate {*h*0*l*}-column of Table 4. In view of the fact that this is the sole indication that *Pnma* might not be the correct choice of space group, and that it depends on a single coordinate of an unresolved oxygen atom, it cannot be given very much weight. It is still possible, of course, that some deviations from the special positions of *Pnma* have not been found (and hence that the space group is really *Pn2a*) but they would have to be very small in the case of the metal atoms, although they could be larger for the atoms of oxygen (see the standard deviations of atom-positions given later). Therefore, the space group *Pnma* has been retained and the final (mean) values of the coordinates of O(3) and O(4) are the averages of those for *both* atoms (see Table 4).

The corrections applied to the atomic scattering curves for isotropic thermal motion of the atoms are collected in Table 5. The variation

TABLE 5. VALUES OF THE TEMPERATURE FACTOR CONSTANT, *B*, FOR EACH OF THE THREE ZONES

| Atom | {*hk*0} | {0*kl*} | {*h*0*l*} |
|---|---|---|---|
| Pb | 1.2 | 0.9 | 0.9 |
| Mn | 0.5 | 0.7 | 0.7 |
| V | 1.0 | 0.7 | 0.8 |
| O | 0 | 0 | 0 |

among the factors for the same atom in each of the three zones is small, thus indicating very little, if any, asymmetric component. This is borne out by the final difference maps (see Figs. 1D, 2D, 3D).

## ACCURACY OF RESULTS

Standard deviations of peak positions were calculated from $\sigma(x) = \sigma(A_h)/A_{hh}$, where

$$\sigma(A_h) = \frac{2\pi}{aA}(\sum_3 h^2\Delta F^2)^{1/2}$$

and $A_{hh}$ is the curvature at these points on the electron-density maps (Cruickshank, 1949). If the curve at the peak position of a resolved atom is represented by the expression $\rho = \mathrm{a} + \mathrm{b}r + \mathrm{c}r^2$, then $A_{hh} = \delta^2\rho/\delta r^2) = 2\mathrm{c}$. Assuming the peaks to be spherically symmetrical (reasonably justified by Figs. 1D, 2D, 3D), and hence that $\sigma(x) \simeq \sigma(y) \simeq \sigma(z) = \sigma$, the standard deviations ($\sigma$) in their positions are 0.01 Å for lead, 0.04 Å for vanadium, 0.05 Å for manganese, and 0.11 Å for oxygen, the curvatures at the oxygen positions, of necessity, being obtained from the partial difference maps (Figs. 1C, 2C, 3C), while those for the metal atoms were taken from the Fourier maps (Figs. 1B, 2B, 3B). The values for these standard deviations are supported by the good agreement between the same coordinates measured separately in two zones (see Table 4), for which the r.m.s. deviations are 0.01 Å for lead, 0.006 Å for vanadium, and 0.078 Å for oxygen. It thus appears, on the basis of $\sigma = 0.11$ Å for the oxygen positions, that the relatively large difference of 0.176 Å for the $x$-coordinate of O(4), obtained from the data for the $\{hk0\}$ and $\{h0l\}$ zones (Table 4), should not be considered as significant (Cruickshank, 1949, p. 67).

TABLE 6. STANDARD DEVIATIONS (IN Å) OF INTERATOMIC DISTANCES

| | | | | | |
|---|---|---|---|---|---|
| Pb-O, | 0.11 | Pb-Pb, | 0.014 | Mn-Mn, | 0.07 |
| Mn-O, | 0.12 | Pb-Mn, | 0.05 | Mn-V, | 0.06 |
| V-O, | 0.12 | Pb-V, | 0.04 | V-V, | 0.06 |
| O-O, | 0.16 | | | | |

Standard deviations of interatomic distances were calculated with expressions of the form $\sigma_{\mathrm{Pb-V}} = [\sigma_{\mathrm{Pb}}{}^2 + \sigma_{\mathrm{V}}{}^2]^{\frac{1}{2}}$ and are collected in Table 6.

## DESCRIPTION OF THE STRUCTURE AND INTERATOMIC DISTANCES

The coordination of oxygen atoms around the atoms of vanadium is tetrahedral, with V at distances of 1.83 Å from O(1), 1.62 Å from O(2), and 1.77 Å from O(3) and from O(4). The six closest oxygen-oxygen distances in this tetrahedron lie in the range 2.72–2.99 Å. On the basis of the standard deviations of interatomic distances, the $VO_4$ tetrahedron is regular within the limits of experimental error.

There is a tetragonal bipyramidal arrangement of oxygen atoms around the atoms of manganese, with Mn-O distances of 2.04, 2.18, and 2.22 Å (three values only, because Mn is at a centre of symmetry). The twelve closest oxygen-oxygen distances in this polyhedron vary from 3.09 to 3.14 Å, and thus, on the basis of the standard deviations for Mn-O and O-O (see Table 4), the oxygen atoms form a regular octahedron with Mn at the centre, within the limits of experimental error.

The coordination of oxygen atoms around Pb is less regular. Each atom of lead has seven nearest oxygen neighbours, the Pb-O distances varying from 2.28 to 2.89 Å. There must, therefore, be real differences among the Pb-O distances because some of these differences are greater than three times the standard deviation of 0.11 Å (Cruickshank, 1949, p. 67).

The closest approach of lead atoms is 4.07 Å (between Pb at $x, \frac{1}{4}, z$ and Pb at $\frac{1}{2}+x, \frac{1}{4}, \frac{1}{2}-z$), that of manganese atoms is 3.10 Å ($=b/2$), and that of vanadium atoms is 4.11 Å (between V at $x, \frac{3}{4}, z$ and V at $\frac{1}{2}+x, \frac{3}{4}, \frac{1}{2}-z$). The shortest Pb-Mn distances are 3.59 Å between Pb at $x, y, z$ and Mn at $0, 0, \frac{1}{2}$, and 3.62 Å between Pb at $x, y, z$ and Mn at $\frac{1}{2}, 0, 0$. Between lead and vanadium, the closest approach is 3.47 Å (between Pb at $\frac{1}{2}-x, \frac{3}{4}, \frac{1}{2}+z$ and V at $x, \frac{3}{4}, z$), with the next nearest lead atoms at distances of 3.72 Å (for Pb at $\frac{1}{2}+x, \frac{1}{4}, \frac{1}{2}-z$) and 3.79 Å (for Pb at $x,y,z$), respectively, from the same vanadium atom. The shortest distance between manganese and vanadium is 3.51 Å (Mn at $0, 0, \frac{1}{2}$; V at $\frac{1}{2}-x, \frac{1}{4}, \frac{1}{2}+z$).

## DISCUSSION

The structure of pyrobelonite is almost identical with that of descloizite (Qurashi & Barnes, 1954), as was anticipated from the close correspondence, both in relative intensities and in Bragg angles, of reflections from the three principal zones of each. The main differences are in the locations of the oxygen atoms which, in pyrobelonite, deviate appreciably from the idealized positions assigned provisionally to them in the descloizite structure (cf. Figs. 1C, 2C, 3C with Fig. 3 of Qurashi & Barnes, 1954). No special significance should be attached to this, however, until refinement of the descloizite structure is complete. A better comparison is afforded between the present Figs. 1C, 2C, 3C and the corresponding partial difference maps for conichalcite (Qurashi & Barnes, 1954, Fig. 8), from which it will be observed that agreement between corresponding oxygen-atom positions is very good.

The difference between the density (5.79 gm. per ml.) calculated on the basis of $4[PbMn(VO_4)(OH)]$ per unit cell and the measured values of 5.377 (Flink, 1919) and 5.58 (this paper), both for Långban material, is somewhat puzzling. The lower value (5.377) implies a Mn:Pb ratio of ∼32:22 (close to that of the Mauzelius analysis; Flink, 1919), but, assuming random substitution of Mn for Pb throughout the lattice this would reduce the observed peak heights for Pb by almost 20%. There was no evidence of any such effect in the present structure analysis. It seems probable, therefore, that the earlier density measurement is much too low. The present value of 5.58 gm. per ml. (obtained with the only suitable crystal available and, as mentioned previously, also probably low) corresponds to a Mn:Pb ratio of ∼27:22. It is, of course, possible that substitution may exist to varying degrees in different specimens even from the same locality, but, certainly in the two crystals employed for the present structure investigation, any substitution of part of the lead by manganese could only be negligibly small. It is highly desirable that the density of pyrobelonite should be redetermined if suitable specimens can be found.

## ACKNOWLEDGMENTS

Grateful acknowledgement is made to Professor Clifford Frondel for the crystals of pyrobelonite employed for the structure determination and the density measurement, to Dr. George Switzer for crystals from a U. S. National Museum specimen which it was hoped could be ground into spheres for more precise absorption corrections, and to Mrs. M. E. Pippy for assistance with the calculations.

## REFERENCES

BARNES, W. H. & QURASHI, M. M. (1952): Unit cell and space group data for certain vanadium minerals, *Am. Mineral.*, **37**, 407–422.

BERMAN, H. (1939): A torsion microbalance for the determination of specific gravities of minerals, *Am. Mineral.*, **24**, 434–440.

BRADLEY, A. J. (1935): The absorption factor for the powder and rotating-crystal methods of $x$-ray crystal analysis, *Proc. Phys. Soc.*, **47**, 879–899.

COCHRAN, W. (1951): The structures of pyrimidines and purines. V. The electron distribution in adenine hydrochloride, *Acta Cryst.*, **4**, 81–92; Some properties of the $(F_o - F_c)$-synthesis, *Acta Cryst.*, **4**, 408–411.

CRUICKSHANK, D. W. J. (1949): The accuracy of electron-density maps in $x$-ray analysis with special reference to dibenzyl, *Acta Cryst.*, **2**, 65–82.

DANA, J. D. & E. S. (1951): *System of Mineralogy*, **2**, ed. 7, by C. Palache, H. Berman and C. Frondel, New York, p. 816.

EVANS, H. T., & EKSTEIN, M. G. (1952): Tables of absorption factors for spherical crystals, *Acta Cryst.*, **5**, 540–542.

FAIRBAIRN, H. W., & SHEPPARD, C. W. (1945): Maximum error in some mineralogic computations, *Am. Mineral.*, **30**, 673–703.

FLINK, G. (1919): *Geol. Fören. Förh.*, **41**, 433, reference obtained from Hintze (1933), Strunz (1939), Richmond (1940), Dana (1951), *loc. cit.*

Hintze, C. (1933): *Handbuch der Mineralogie*, Bd. 1, Abt. 4, Berlin, pp. 673–675.

*International Tables for the Determination of Crystal Structures* (1935), Berlin.

Qurashi, M. M. (1954): On the completion and extension of the table of atomic scattering factors published by Viervoll and Ögrim, *Acta Cryst.*, **7**, 310–312.

Qurashi, M. M., & Barnes, W. H. (1954): The structures of the minerals of the descloizite and adelite groups: I—descloizite and conichalcite (part 1), *Am. Mineral.*, **39**, 416–435.

Richmond, W. E. (1940): Crystal chemistry of the phosphates, arsenates, and vanadates of the type $A_2XO_4(Z)$, *Am. Mineral.*, **25**, 441–479.

Strunz, H. (1939): Mineralien der Descloizitgruppe, *Zeit. Krist.*, (A) **101**, 496–506.

Viervoll, H., & Ögrim, O. (1949): An extended table of atomic scattering factors, *Acta Cryst.*, **2**, 277–279.

# THE STRUCTURES OF THE MINERALS OF THE DESCLOIZITE AND ADELITE GROUPS: III—BRACKEBUSCHITE

D. M. DONALDSON[1] AND W. H. BARNES, *Division of Physics, National Research Council, Ottawa, Canada.*

## ABSTRACT

The structure of brackebuschite, $Pb_2(Mn, Fe)(VO_4)_2 \cdot H_2O$, has been determined, although there is still some uncertainty about the location of the water molecule (if it is indeed present). Atoms of Pb, Mn and Fe, and V are in special positions. The coordination of oxygen with vanadium is tetrahedral; it is fourfold or sixfold with manganese depending on the $H_2O$-sites, and it is eightfold with one lead atom and tenfold with the other. Metal-to-oxygen distances are given and the accuracy of the results is discussed. By comparison with the structure of pyrobelonite it is shown that brackebuschite should not be classified with the minerals of the descloizite and adelite groups.

## INTRODUCTION

Several attempts have been made to classify brackebuschite according to the chemical composition deduced from the analyses of Doering (1883) which are the only ones available in the literature. Thus Dana (1892) suggested that the formula is "perhaps $A_3V_2O_8+H_2O$* with $A=Pb$ chiefly, also Fe, Mn", but observed that Damour regarded Mn, Fe, (and Cu) as impurities; these data are repeated by Mellor (1947). Dana also credits Groth with the suggestion that brackebuschite might be the monoclinic equivalent of descloizite.

Strunz (1939) referred brackebuschite to a type $A_2(XO_4)(OH)$,* and, on the basis of *x*-ray diffraction powder photographs, concluded that it must be completely different structurally from the minerals of the descloizite group. On the other hand, Richmond (1940), without examination of brackebuschite by *x*-ray methods, assigned it the formula $(Pb, Mn)_2VO_4(OH)$ with $Pb:Mn=2:1$ and suggested that it forms a series with pyrobelonite, which he formulated $(Mn, Pb)_2VO_4(OH)$ (see, Donaldson & Barnes, 1955). He, therefore, placed brackebuschite "tentatively" in the *orthorhombic* section of family $ABXO_4(Z)$ with pyrobelonite, descloizite, higginsite (i.e., conichalcite; Berry, 1951), etc. (Richmond, 1940, pp. 444, 476, 477).

After a careful examination of Doering's analytical results in the light of original specific gravity, unit cell, space group ($P2_1/m$), and indexed powder data, Berry & Graham (1948) came to the conclusions that the ideal structural formula of brackebuschite is $2[Pb_2(Mn, Fe)(VO_4)_2 \cdot H_2O]$, that the mineral belongs to the chemical type $A_3(XO_4)_2 \cdot nH_2O$ with $n=1$, and that their investigation had failed to show any relationship with pyrobelonite. These results have been incorporated in the Seventh Edition of Dana's *System of Mineralogy* (1951). The formula of Berry & Graham (1948) is in complete agreement with that suggested by Doering in 1883 and Dana in 1892.

---

[1] National Research Laboratories Postdoctorate Fellow, now I.C.I. Fellow, The University, Edinburgh, Scotland.

* The letter *R* is used by Dana (1892) for the cation whereas it is employed by Strunz (1939) for the metalloid of the anion; in this paper it has been changed to *A* for the former and *X* for the latter in conformity with later formulae (Richmond, 1940; Berry & Graham, 1948; Dana, 1951).

During a recent survey of unit cell and space group data for a number of vanadium minerals in this laboratory (Barnes & Qurashi, 1952), several interesting similarities and differences were observed between precession photographs of brackebuschite on the one hand and those of members of the descloizite and adelite groups on the other (see, Qurashi & Barnes, 1954, Fig. 1). With the information now available on the structures of descloizite and conichalcite (Qurashi & Barnes, 1954) and pyrobelonite (Donaldson & Barnes, 1955) it is of particular interest to compare the atomic arrangement in brackebuschite with that characteristic of the minerals of the descloizite and adelite groups.

## EXPERIMENTAL, AND CRYSTAL DATA

The experimental work was carried out with two crystals from the same (Sierra de Cordoba) specimen (Harvard Museum, 96255) as those examined by Berry & Graham (1948); the crystals had the dimensions $45 \times 30 \times 180\mu$ and $50 \times 35 \times 80\mu$. Intensities were estimated visually from precession and Weissenberg photographs (Mo$K_\alpha$ radiation) using multiple exposure technique for the former and multiple film technique for the latter, and were corrected for the Lorentz and polarization factors. The absorption coefficient for Mo$K_\alpha$ ($\lambda = 0.7107$ Å) is 535 per cm. and approximate absorption corrections were applied, assuming cylindrical crystals.

Brackebuschite is monoclinic, space group $P2_1/m(C_{2h}^2)$ or $P2_1(C_2^2)$, with $a = 7.68_1$, $b = 6.15_5$, $c = 8.88_0$ Å, and $\beta = 111°50'$ (Barnes & Qurashi, 1952). There are $2[Pb_2(Mn, Fe)(VO_4)_2 \cdot H_2O]$ per cell. The calculated density is 6.11 gm. per ml.; observed specific gravity (Berry & Graham, 1948), 6.05 (Doering, 1883, found 5.85 which he acknowledged must be low because the specimen employed contained up to 4 per cent of quartz and ferruginous matter).

In order to facilitate direct comparison with descloizite and pyrobelonite it is convenient to refer brackebuschite to a $B$-centered cell (see, Barnes & Qurashi, 1952; Qurashi & Barnes, 1954) given by the transformation matrix $\bar{1}00/0\bar{1}0/102$. The dimensions of the new cell are $a' =$

$7.68_1$, $b'=6.15_5$, $c'=2\times 8.26_2$ Å, $\beta=93°45'$, and the space group is $B2_1/m$ or $B2_1$; coordinates, diagrams, and discussion throughout this paper are in terms of this *B*-centered cell.

## ANALYSIS OF THE STRUCTURE

Direct comparison of corresponding zero-level precession photographs of brackebuschite, pyrobelonite, and descloizite (see, Qurashi & Barnes, 1954, Fig. 1) shows that corresponding *hk*0 reflections from the three minerals are almost identical in relative intensities and Bragg angles, corresponding 0*kl* reflections are very similar, but there are important differences between the *h*0*l* reflections from brackebuschite and corresponding ones from pyrobelonite and descloizite. Although it would thus have been feasible to assume that the *x* and *y* coordinates of the lead atoms in brackebuschite probably are virtually the same as those in descloizite (Qurashi & Barnes, 1954) and in pyrobelonite (Donaldson & Barnes, 1955) it was decided to start the structure analysis of brackebuschite by computing the (100) Patterson map. The result is shown in Fig. 1 from which it is apparent that the majority of the peaks lie along $y=0$ and $\frac{1}{2}$. These must represent most of the metal-metal vectors. It follows, therefore, that the lead together with some of the lighter metal atoms must lie on, or close to, the same planes which are separated by $b/2$. The positions of the other peaks in Fig. 1 suggest that the remainder of the lighter

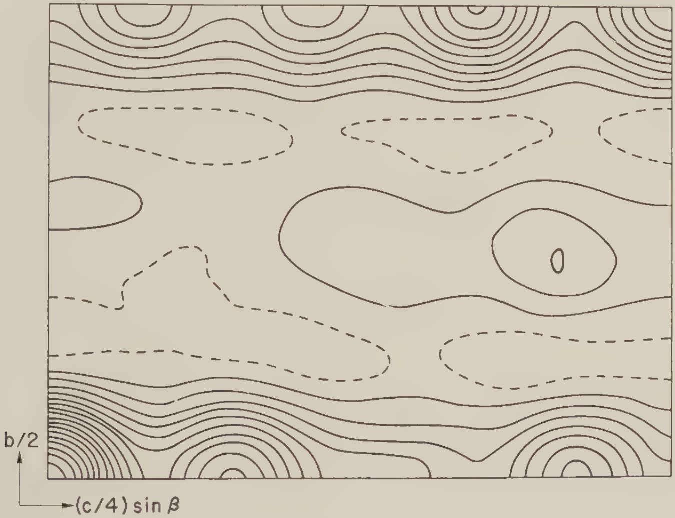

FIG. 1. Patterson map for the {0*kl*} zone of brackebuschite. Contours are regular, but arbitrary, intervals; zero contour broken.

metal atoms must be situated on, or near, planes midway between these. If all the metal-atom sites are exactly in the planes specified, they are consistent with space group $B2_1/m$ for the metal atoms, and hence this space group was adopted provisionally as the basis for the structure analysis.

The equivalent positions of $B2_1/m$ are

(*a*) $0,0,0;\ 0,\frac{1}{2},0;\ \frac{1}{2},0,\frac{1}{2};\ \frac{1}{2},\frac{1}{2},\frac{1}{2}$
(*b*) $\frac{1}{2},0,0;\ \frac{1}{2},\frac{1}{2},0;\ 0,0,\frac{1}{2};\ 0,\frac{1}{2},\frac{1}{2}$
(*c*) $x,\frac{1}{4},z;\ \bar{x},\frac{3}{4},\bar{z};\ \frac{1}{2}+x,\frac{1}{4},\frac{1}{2}+z;\ \frac{1}{2}-x,\frac{3}{4},\frac{1}{2}-z$
(*d*) $x, y, z;\ x, \frac{1}{2}-y, z;\ \frac{1}{2}+x, y, \frac{1}{2}+z;\ \frac{1}{2}+x, \frac{1}{2}-y, \frac{1}{2}+z;$
$\bar{x}, \bar{y}, \bar{z};\ \bar{x}, \frac{1}{2}+y, \bar{z};\ \frac{1}{2}-x, \bar{y}, \frac{1}{2}-z;\ \frac{1}{2}-x, \frac{1}{2}+y, \frac{1}{2}-z.$

From a detailed interpretation of the (100) Patterson map $y$, $z$ coordinates were obtained for lead, manganese*, and vanadium, with lead and vanadium at $y=\pm\frac{1}{4}$ (special positions (*c*)) and with manganese in special positions (*a*) or (*b*). In view of the small difference between the atomic numbers of manganese and vanadium, the choice of which should be placed in the available positions was governed by the sites occupied by zinc and vanadium in descloizite. The structure was not prejudged by this selection because an "average" atom $X$ of $f=\frac{1}{2}(f_{\mathrm{Mn}}+f_{\mathrm{V}})$ could equally well have been placed in each of the positions at this stage.

A (100) Fourier synthesis with metal-atom coordinates obtained from the analysis of the Patterson map was then carried out (see Fig. 2). The positions of Pb, Mn, and V were refined and termination-of-series errors were corrected by successive difference syntheses (Cochran, 1951) using coordinates for these atoms alone until those for the oxygen atoms had been determined. After inclusion of the latter only minor shifts in the positions of the metal atoms were required in succeeding difference syntheses.

Examination of the $hk0$ intensities showed that, in addition to the absences characteristic of the $B$-centering, all reflections for which $h=4n+2$, $k=2n$ and for which $h=4n$, $k=2n+1$ were either unobservable or very weak. On the assumption that this effect must be caused by the positions of the lead atoms, it follows that the $x$, $y$ coordinates of Pb are $x=\frac{1}{8}$, $y=\frac{1}{4}$, etc. (special positions (c)). Because the lead atoms determine the phases of most reflections, it was possible to carry out a Fourier synthesis for this zone immediately (see Fig. 2) and then to proceed with refinement by successive difference syntheses as in the case of the $\{0kl\}$ zone.

Finally the $\{h0l\}$ zone was refined by the same procedure, commencing

---

* Since the atoms of Fe in brackebuschite must be occupying some of the Mn-sites, "manganese" refers to both Fe and Mn unless otherwise noted in the text.

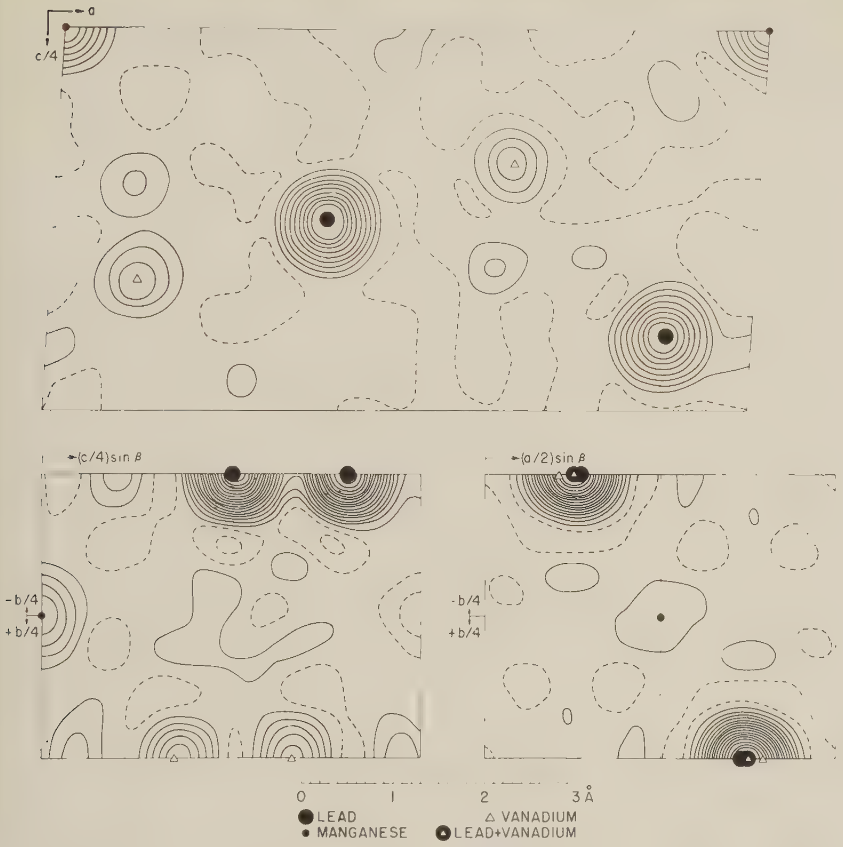

FIG. 2. Fourier maps of the brackebuschite structure. Contours at intervals of $\sim 8e.\text{Å}^{-2}$ for (010), $\sim 5e.\text{Å}^{-2}$ for (100), $\sim 12e.\text{Å}^{-2}$ for (001); zero and negative contours broken.

with metal-atom coordinates derived from the (100) and (001) electron-density maps.

The atomic scattering factors employed for lead and for vanadium were those used in the structure investigation of pyrobelonite (Donaldson & Barnes, 1955).

According to Doering's analyses (1883), manganese and iron are present in approximately equal atomic proportions. The scattering curve for "manganese," therefore, was obtained as the mean of those for the divalent ions, $Mn^{2+}$ and $Fe^{2+}$, which in turn were derived from the *atomic* scattering curves in the *International Tables* (1935), taking those for Ca and $Ca^{2+}$ as a guide (*International Tables*, 1935).

The three scattering curves were corrected for the temperature factor, $\exp(-B(\sin\theta/\lambda)^2)$, with $B=1.9$ for lead, 0.5 for vanadium, and 1.5 for

TABLE 1. METAL ATOM POSITIONS IN FRACTIONAL COORDINATES

| Atom | $x$ | $y$ | $z$ |
|---|---|---|---|
| Pb(1) | 0.1149 | 0.250 | 0.3745 |
| Pb(2) | 0.6233 | 0.250 | 0.2989 |
| V(1) | 0.6462 | 0.250 | 0.0865 |
| V(2) | 0.1233 | 0.250 | 0.1644 |
| Mn | 0 | 0 | 0 |

manganese. These values were obtained qualitatively from the difference syntheses by attempting to reduce the background density around the different atoms to as near zero as possible. It should be noted that the same corrections were applied to the scattering curves for Pb, V, and Mn, respectively, in all three zones, even for non-equivalent atoms.

The final coordinates of the metal atoms are given in Table 1. Values of the structure factors calculated for these atoms alone, $F_{c(m)}$, are listed in Table 3.

## POSITIONS OF THE OXYGEN ATOMS, AND THE WATER MOLECULE

There are some indications of the presence of oxygen atoms in the Fourier maps (see Fig. 2), particularly in that on (010), but they are not sufficiently clear for a reliable estimate of the atomic coordinates. The difference syntheses reproduced in Fig. 3 were calculated with the coefficients $(F_o - F_{c(m)})$; they show a set of peaks which, by correlation among the maps for the three zones, were identified as representing the oxygen atoms. The best mean coordinates obtained from these maps are given in Table 2. In view of the poor resolution of the oxygen peaks in the difference syntheses it was not considered profitable to attempt refinement of these values.

Difference syntheses were then computed after subtracting the contributions of all the metal *and* the oxygen atoms. The same scattering curve for the latter ($O^{-1.5}$) was employed as in the case of pyrobelonite

TABLE 2. OXYGEN ATOM POSITIONS IN FRACTIONAL COORDINATES

| Atom | $x$ | $y$ | $z$ |
|---|---|---|---|
| O(1) | 0.114 | 0.023 | 0.104 |
| O(2) | 0.114 | 0.477 | 0.104 |
| O(3) | 0.941 | 0.250 | 0.230 |
| O(4) | 0.299 | 0.250 | 0.247 |
| O(5) | 0.632 | 0.023 | 0.145 |
| O(6) | 0.632 | 0.477 | 0.145 |
| O(7) | 0.455 | 0.250 | 0.017 |
| O(8) | 0.846 | 0.250 | 0.024 |

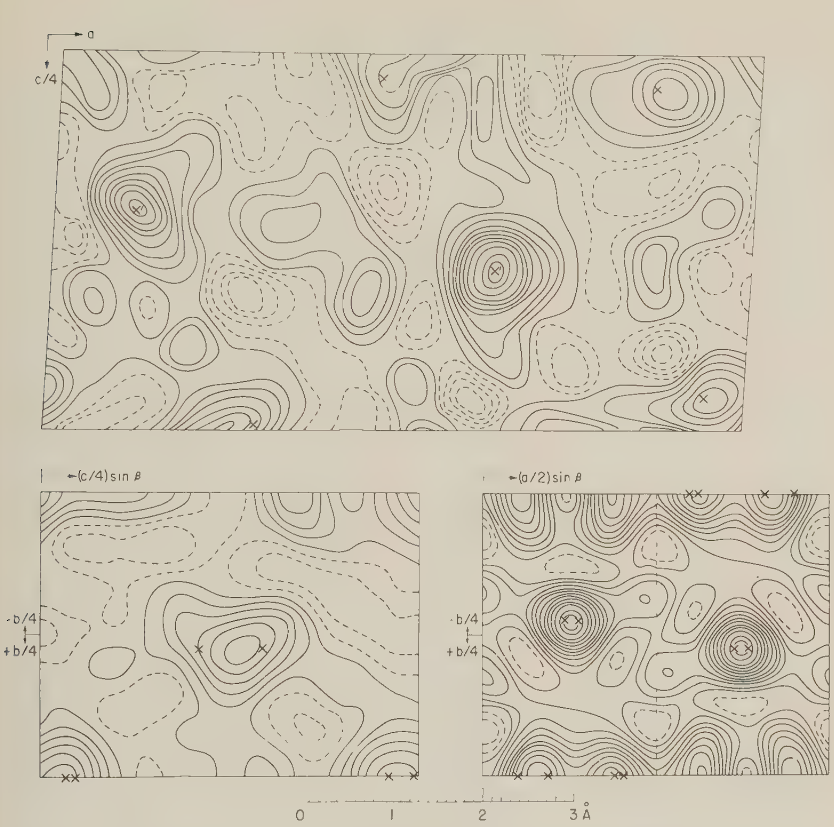

FIG. 3. $(F_o - F_{c(m)})$ maps of the brackebuschite structure. Contours at intervals of $\sim 2e.\text{Å}^{-2}$; zero and negative contours broken. Positions of single oxygen atoms indicated by X, and those of two pairs of superimposed oxygen atoms by X′.

(Donaldson & Barnes, 1955). The maps are reproduced in Fig. 4 and it was hoped that some clear indication of the positions of the water molecules might be obtained at this stage. There are a few relatively large peaks in the final difference maps (Fig. 4), generally of 6 to 8 $e.\text{Å}^{-2}$ but with two of 14 and 16 $e.\text{Å}^{-2}$, respectively, in the (001) map, but none could be correlated through all three zones. On this basis, therefore, it was not possible to fix the position of the water molecule, although a possible site will be discussed later. It should be mentioned that there was originally a peak of approximately 200 $e.\text{Å}^{-2}$, representing two lead and two vanadium atoms (see Fig. 2), between the two large peaks (14 and 16 $e.\text{Å}^{-2}$) in the (001) map. Thus, although part of either of these residual peaks might be due to the water molecule, both could be accounted for by asymmetric thermal motion of one or both of the crystallographically distinct lead atoms.

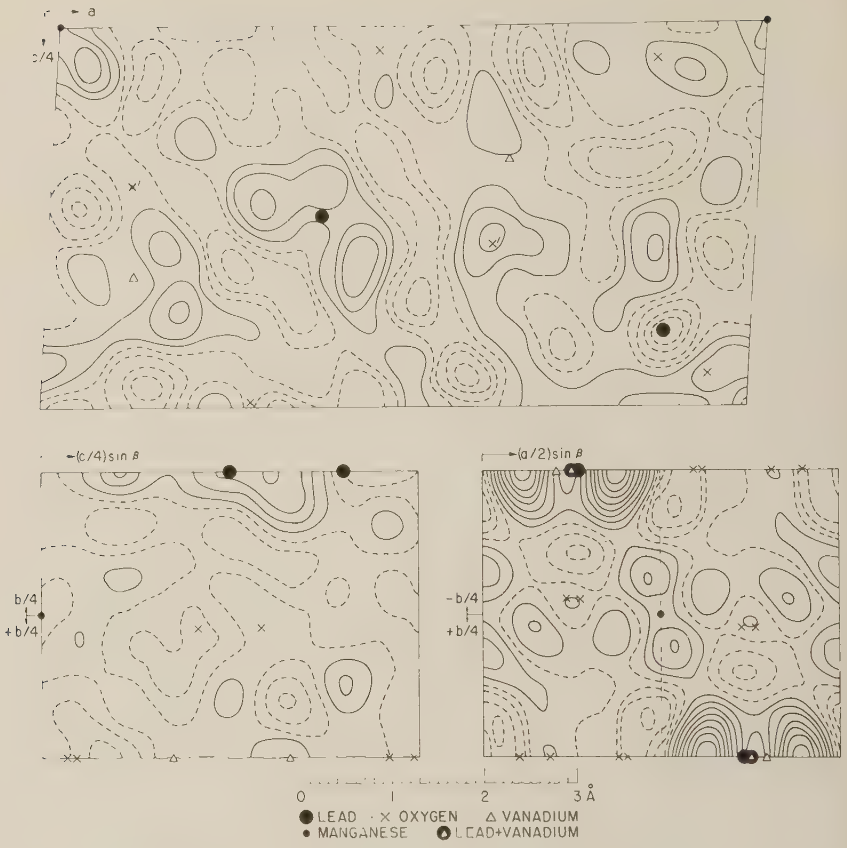

FIG. 4. Final difference $(F_o - F_c)$ maps of the brackebuschite structure. Contours at intervals of $\sim 2e.\text{Å}^{-2}$; zero and negative contours broken. Positions of two pairs of superimposed oxygen atoms indicated by X′.

## ACCURACY OF RESULTS

Values of $F_c$, $F_{c(m)}$, and $F_o$ are given in Table 3. The reliability index, $R$, is 0.09 for the $\{hk0\}$ zone, 0.12 for the $\{0kl\}$ zone, and 0.18 for the $\{h0l\}$ zone when the contributions of *the metal atoms only* are included; it is 0.06 for the $\{hk0\}$ zone, 0.08 for the $\{0kl\}$ zone, and 0.12 for the $\{h0l\}$ zone (overall value, 0.10) when the contributions of *the metal and the oxygen atoms* are included.

Standard deviations in the distances between metal atoms were calculated, assuming that the atoms may be considered as symmetrical and independent (Cruickshank, 1949), despite the fact that the criterion of complete refinement has not been met rigidly in the present case.

TABLE 3. STRUCTURE FACTOR DATA ($F_o$, OBSERVED; $F_{c(m)}$, CALCULATED FOR METAL ATOMS ONLY; $F_c$, CALCULATED FOR ALL METAL AND OXYGEN ATOMS WITH EXCEPTION OF $H_2O$)

| hkl | $F_o$ | $F_c$ | $F_{c(m)}$ |
|---|---|---|---|
| 000 | — | +1196 | +940 |
| 200 | 117 | +118 | +104 |
| 400 | 524 | −525 | −467 |
| 600 | <46 | +1 | −1 |
| 800 | 261 | +279 | +274 |
| 210 | 652 | −614 | −667 |
| 220 | 43 | +42 | +48 |
| 230 | 486 | +460 | +522 |
| 240 | 73 | +66 | +61 |
| 250 | 376 | −355 | −355 |
| 260 | <45 | +21 | +22 |
| 270 | 196 | +208 | +230 |
| 410 | 47 | −34 | −38 |
| 420 | 511 | +480 | +527 |
| 430 | <44 | +27 | +31 |
| 440 | 349 | −343 | −319 |
| 450 | <46 | −18 | −19 |
| 460 | 237 | +261 | +272 |
| 610 | 345 | +385 | +362 |
| 620 | 67 | +67 | +76 |
| 630 | 293 | −310 | −305 |
| 640 | <45 | +4 | +3 |
| 650 | 231 | +247 | +228 |
| 810 | 43 | +42 | +36 |
| 820 | 138 | −176 | −200 |
| 830 | 43 | −34 | −30 |
| 020 | 617 | −589 | −585 |
| 040 | 618 | +600 | +516 |
| 060 | 294 | −277 | −270 |
| 012 | 312 | +295 | +336 |
| 022 | 312 | +291 | +290 |
| 032 | 294 | −270 | −257 |
| 042 | 95 | −104 | −104 |
| 052 | 162 | +140 | +166 |
| 062 | 112 | +128 | +128 |
| 072 | 100 | −103 | −94 |
| 014 | 269 | −272 | −261 |
| 024 | 190 | +163 | +301 |
| 034 | 223 | +209 | +203 |
| 044 | 145 | −114 | −121 |
| 054 | 108 | −139 | −136 |
| 064 | 114 | +112 | +142 |
| 074 | 65 | +86 | +85 |
| 016 | <72 | −32 | +4 |
| 026 | <81 | +2 | −2 |
| 036 | <90 | +41 | −3 |
| 046 | 106 | +88 | +91 |
| 056 | <99 | +1 | +3 |
| 066 | <94 | 0 | −1 |
| 018 | 123 | −144 | −133 |
| 028 | <87 | +36 | +44 |
| 038 | 94 | +115 | +108 |
| 048 | <99 | +81 | +45 |
| 058 | <99 | −78 | −74 |
| 068 | <88 | +21 | +27 |
| 0.1.10 | 229 | +243 | +282 |
| 0.2.10 | <93 | −119 | −128 |
| 0.3.10 | 221 | −210 | −231 |
| 0.4.10 | 145 | +163 | +168 |
| 0.5.10 | 154 | +150 | +168 |
| 0.6.10 | <75 | −61 | −64 |
| 0.1.12 | <96 | +70 | +77 |
| 0.2.12 | 228 | +240 | +249 |
| 0.3.12 | <100 | −59 | −64 |
| 0.4.12 | 106 | −116 | −122 |
| 0.5.12 | <90 | +42 | +46 |
| 0.1.14 | 341 | −362 | −339 |
| 0.2.14 | <100 | −11 | −20 |
| 0.3.14 | 306 | +301 | +287 |
| 0.4.14 | <93 | +65 | +71 |
| 0.5.14 | 199 | −233 | −219 |
| 0.1.16 | 107 | +119 | +122 |
| 0.2.16 | <99 | −64 | −56 |
| 0.3.16 | 97 | −103 | −105 |
| 0.4.16 | 78 | +83 | +90 |
| 0.1.18 | <90 | +38 | +48 |
| 0.2.18 | 92 | +103 | +97 |
| 002 | 181 | −165 | −164 |
| 004 | 204 | −182 | −186 |
| 006 | 163 | +139 | +146 |
| 008 | 144 | +148 | +73 |
| 0.0.10 | 234 | +237 | +246 |
| 0.0.12 | 186 | −178 | −187 |
| 0.0.14 | 98 | +90 | +98 |
| 0.0.16 | <81 | +112 | +126 |
| 0.0.18 | <73 | −57 | −49 |
| 101 | <37 | +28 | +30 |
| 103 | 152 | −170 | −176 |
| 105 | 637 | +588 | +652 |
| 107 | <64 | −12 | −12 |
| 109 | 217 | −263 | −318 |
| 1.0.11 | 210 | +230 | +226 |
| 1.0.13 | <81 | +9 | +43 |
| 1.0.15 | 101 | +124 | +124 |
| 1.0.17 | <78 | +24 | +9 |
| 1.0.19 | <58 | +3 | 0 |
| 202 | 326 | +313 | +379 |
| 204 | 145 | −178 | −190 |
| 206 | 182 | +176 | +89 |
| 208 | <70 | −34 | −44 |
| 2.0.10 | 344 | +302 | +276 |
| 2.0.12 | <80 | +86 | +84 |
| 2.0.14 | 253 | −276 | −289 |
| 2.0.16 | 180 | +244 | +248 |
| 2.0.18 | 121 | +101 | +78 |
| 301 | <60 | +145 | +146 |
| 303 | 169 | −186 | −86 |
| 305 | <67 | +60 | +60 |
| 307 | 322 | +364 | +356 |
| 309 | 110 | −136 | −144 |
| 3.0.11 | <80 | −31 | +23 |
| 3.0.13 | <82 | +73 | +69 |

TABLE 3—(*continued*)

| *hkl* | $F_o$ | $F_c$ | $F_{c(m)}$ | *hkl* | $F_o$ | $F_c$ | $F_{c(m)}$ |
|---|---|---|---|---|---|---|---|
| 3.0.15 | 81 | +106 | +93 | $2.0.\overline{10}$ | 242 | −198 | −202 |
| 3.0.17 | <71 | +93 | +86 | $2.0.\overline{12}$ | <80 | −74 | −64 |
| 402 | 311 | +309 | +320 | $2.0.\overline{14}$ | 356 | +358 | +361 |
| 404 | 322 | +287 | +250 | $2.0.\overline{16}$ | <80 | −72 | −68 |
| 406 | 78 | −51 | −54 | $2.0.\overline{18}$ | <69 | −27 | −14 |
| 408 | <78 | +1 | +16 | $30\bar{1}$ | 98 | +87 | +144 |
| 4.0.10 | <81 | −75 | −81 | $30\bar{3}$ | 352 | +363 | +365 |
| 4.0.12 | 215 | +214 | +219 | $30\bar{5}$ | 467 | −429 | −426 |
| 4.0.14 | <80 | −27 | −33 | $30\bar{7}$ | <72 | −71 | −71 |
| 4.0.16 | <71 | −16 | −31 | $30\bar{9}$ | 366 | +323 | +365 |
| 501 | <76 | +43 | +55 | $3.0.\overline{11}$ | <80 | −65 | −69 |
| 503 | <77 | +142 | +161 | $3.0.\overline{13}$ | 92 | +89 | +57 |
| 505 | 255 | −286 | −309 | $3.0.\overline{15}$ | <81 | −60 | −66 |
| 507 | 115 | +147 | +160 | $3.0.\overline{17}$ | 76 | +89 | +95 |
| 509 | 214 | +247 | +289 | $40\bar{2}$ | 117 | +148 | +159 |
| 5.0.11 | 122 | −141 | −129 | $40\bar{4}$ | 356 | +282 | +223 |
| 5.0.13 | <79 | +24 | +17 | $40\bar{6}$ | <75 | +16 | +31 |
| 602 | <80 | −68 | −108 | $40\bar{8}$ | <78 | +50 | +68 |
| 604 | 205 | +211 | +208 | $4.0.\overline{10}$ | 107 | −137 | −129 |
| 606 | <82 | −8 | −6 | $4.0.\overline{12}$ | 225 | +222 | +208 |
| 608 | <82 | +69 | +71 | $4.0.\overline{14}$ | <80 | −15 | +3 |
| 6.0.10 | <82 | −108 | −114 | $4.0.\overline{16}$ | <71 | −58 | −64 |
| 6.0.12 | <76 | +38 | +42 | $50\bar{1}$ | 198 | +161 | +169 |
| 6.0.14 | 245 | +247 | +236 | $50\bar{3}$ | <77 | −1 | −16 |
| 701 | <82 | +36 | +30 | $50\bar{5}$ | <78 | −91 | −93 |
| 703 | 111 | +150 | +125 | $50\bar{7}$ | 352 | +321 | +282 |
| 705 | <81 | +77 | +73 | $50\bar{9}$ | <81 | −54 | −60 |
| 707 | 150 | −135 | −122 | $5.0.\overline{11}$ | <82 | −25 | −17 |
| 709 | 121 | +140 | +146 | $5.0.\overline{13}$ | <80 | +15 | +7 |
| 7.0.11 | <66 | +34 | +12 | $5.0.\overline{15}$ | 133 | +121 | +98 |
| 802 | 111 | −133 | −142 | $60\bar{2}$ | 183 | +211 | +238 |
| 804 | <76 | −84 | −66 | $60\bar{4}$ | <81 | +34 | +26 |
| 806 | 117 | +120 | +111 | $60\bar{6}$ | <82 | +42 | +16 |
| 808 | 75 | +47 | +47 | $60\bar{8}$ | <82 | −100 | −104 |
| 901 | 48 | +54 | +42 | $6.0.\overline{10}$ | 178 | +181 | +201 |
| $10\bar{1}$ | <37 | −57 | −64 | $6.0.\overline{12}$ | 111 | +144 | +141 |
| $10\bar{3}$ | 258 | +219 | +229 | $6.0.\overline{14}$ | 131 | −193 | −186 |
| $10\bar{5}$ | 299 | +274 | +266 | $70\bar{1}$ | <82 | −5 | −6 |
| $10\bar{7}$ | 397 | −387 | −290 | $70\bar{3}$ | 143 | −161 | −169 |
| $10\bar{9}$ | 211 | +249 | +242 | $70\bar{5}$ | 269 | +283 | +284 |
| $1.0.\overline{11}$ | 130 | +116 | +103 | $70\bar{7}$ | 169 | +89 | +82 |
| $1.0.\overline{13}$ | <81 | +41 | +32 | $70\bar{9}$ | 91 | −123 | −138 |
| $1.0.\overline{15}$ | 109 | −90 | −52 | $7.0.\overline{11}$ | <66 | +75 | +72 |
| $1.0.\overline{17}$ | <78 | −69 | −75 | $80\bar{2}$ | <78 | +16 | +14 |
| $1.0.\overline{19}$ | 237 | +258 | +254 | $80\bar{4}$ | <76 | −73 | −37 |
| $20\bar{2}$ | 133 | −148 | −249 | $80\bar{6}$ | <72 | −2 | −2 |
| $20\bar{4}$ | 302 | +293 | +296 | $80\bar{8}$ | <60 | −10 | −11 |
| $20\bar{6}$ | <64 | +6 | +79 | $90\bar{1}$ | 63 | −36 | −32 |
| $20\bar{8}$ | 204 | +205 | +213 | $90\bar{3}$ | 27 | +33 | +31 |

Thus the final difference maps (Fig. 4) demonstrate that some systematic errors remain. These are due in part to the fact mentioned previously that the same corrections were applied to the scattering curve for a metal atom of a given atomic number regardless of the zone under investigation, even when atoms of that atomic number were crystallographically non-equivalent. Others arise from the use of final coordinates which are *averages* of the measurements obtained separately from the three zones, thus leaving gradients at some atomic positions in the final difference maps. The calculations, however, should be valid for lead because the peaks in the electron-density maps arising from such very heavy atoms should not be affected appreciably by the presence of the smaller peaks and their associated diffraction ripples. The standard deviation obtained from the Pb-Pb distances was 0.02 Å.

The standard deviation for the Mn-Mn, V-V and Mn-V distances is 0.05 Å, and for the Pb-Mn and Pb-V distances it is 0.04 Å. These values may be low because the precise location of Mn and V will be affected to a greater extent than that of Pb by the incomplete refinement and by the fact that the unresolved oxygen peaks are of comparable size.

The method was useless in the case of oxygen because of the poor resolution and the presence of spurious peaks of similar height (see Fig. 3). Comparison of coordinates from the three zones suggest that errors in the oxygen atom positions may be as high as 0.25 Å. The sites finally adopted, however, are reasonable on chemical grounds and, as stated in connection with Table 3, there is a marked improvement in the reliability index for each zone when the contributions of oxygen atoms in these positions are included.

## DESCRIPTION OF THE STRUCTURE, AND DISCUSSION

The structure of brackebuschite projected on (100) and on (010) is shown in Fig. 5. The tetrahedral arrangment of oxygen atoms around each of the crystallographically distinct vanadium atoms is the same within the limited accuracy with which the parameters of the oxygen atoms are known, but no definite conclusions can be drawn regarding the regularity of the oxygen tetrahedra. The closest O-O distances in the two non-equivalent $VO_4$ groups are 2.75 to 3.02 Å in one and 2.79 to 3.01 Å in the other. The V-O distances are given in Table 4.

This tetrahedral coordination of oxygen around vanadium is found also in pucherite (Qurashi & Barnes, 1953), in descloizite (Qurashi & Barnes, 1954), in pyrobelonite (Donaldson & Barnes, 1955), and in $V_2O_5$(Ketelaar, 1936). In a more recent structure for $V_2O_5$ proposed by Byström, Wilhelmi & Brotzen (1950) and in the structure of $KVO_3 \cdot H_2O$ (Christ,

TABLE 4. VANADIUM-OXYGEN DISTANCES (IN Å)

| | |
|---|---|
| V(2)–O(1), 1.72 | V(1)–O(5), 1.71 |
| V(2)–O(2), 1.72 | V(1)–O(6), 1.71 |
| V(2)–O(3), 1.83 | V(1)–O(7), 1.80 |
| V(2)–O(4), 1.86 | V(1)–O(8), 1.90 |

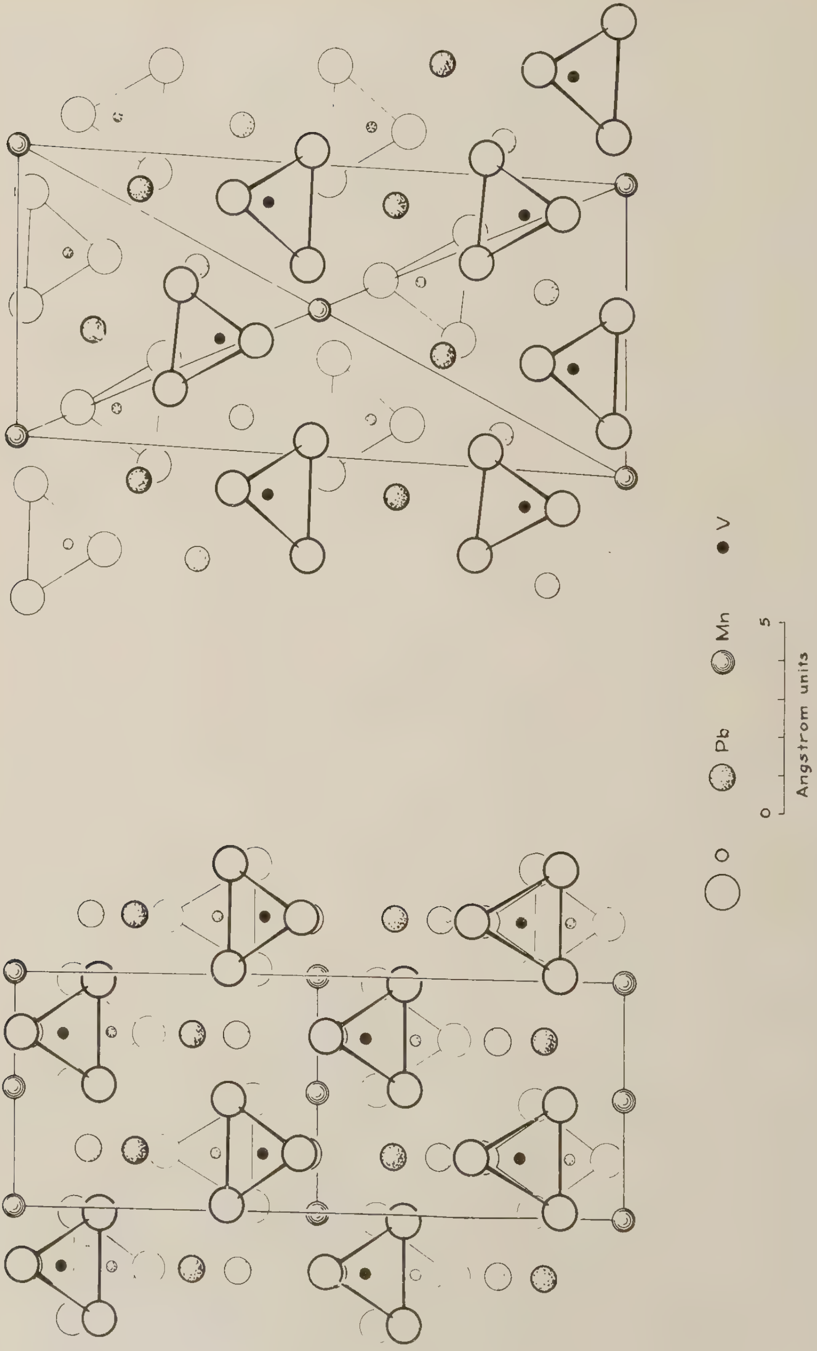

FIG. 5. Projection of the structure of brackebuschite (left) on (100), and (right) on (010); *c* vertical in each case.

Clark & Evans, 1953) there is fivefold coordination of oxygen around vanadium, the oxygen atoms forming a system of linked distorted trigonal bipyramids. This arrangment, however, also may be considered as made up of distorted tetrahedral $VO_4$ building units (see Fig. 3*a* of Byström, Wilhelmi & Brotzen, 1950, and $O_I$, $O_{II}$, $O'_{III}$ in Fig. 2 of Christ, Clark & Evans, 1953).

The coordination of oxygen with manganese is square within the limits of experimental error. The Mn-O distances are 1.88 Å and 2.00 Å (the manganese atoms are at centres of symmetry) and the distances between oxygen atoms are 2.73 Å and 2.75 Å, respectively. The plane of the square is tilted at an angle of 50° to (010) about one of the diagonals, and the structure around manganese consists of these square arrays of oxygen atoms, sharing a corner, and running in a zig-zag along the *b*-axis with the manganese atoms at the centres of the squares.

The initial distinction between the vanadium and manganese positions is thus confirmed by the coordination of the oxygen atoms around these sites. Interchanging the manganese atom and one of the vanadium atoms would result in a most improbable configuration for the $VO_4$ group.

Although no coordinates have been assigned to the water molecules, the most reasonable positions for them on spatial grounds are above and below the centre of the plane of the four oxygen atoms around the manganese atom. This would not affect the coordination around any of the other metal atoms but would make the oxygen coordination sixfold around manganese with tetragonal bipyramidal polyhedra of oxygen atoms sharing edges. The environment of the manganese atoms would then resemble that of the metal atoms in the structures of MnO and FeO (Wells, 1945, p. 312). One of the extraneous peaks on each of the (100) and (001) electron-density maps is consistent with such a position for the water molecule, but no confirmation is obtained from the (010) map. It is possible, of course, that the chemical analysis (Doering, 1883) may be in error. Unfortunately, brackebuschite is a rare mineral but, if sufficient pure material could be collected, a new analysis would be highly desirable. No clear indication of whether the $H_2O$ should be included or not can be obtained from comparison of the observed and calculated densities although it may be noted that the value calculated on the basis of $Pb_4MnFe(VO_4)_4 \cdot 2H_2O$ is slightly higher than that observed by Berry & Graham (1948). It is interesting to note that the oxygen coordination around each Mn in pyrobelonite (Donaldson & Barnes, 1955) is sixfold, and it may be significant that the positions of the OH groups in that structure correspond to those now suggested for the $H_2O$ molecules in brackebuschite.

Different arrangments of oxygen atoms occur around each of the two non-equivalent lead atoms. One of these, Pb(1) has eight nearest oxygen neighbours at distances of 2.54 to 2.95 Å. Within this octahedron, the closest O-O distances vary from 2.58 to 3.36 Å. The other lead atom, Pb(2), has ten nearest oxygen neighbours at distances of 2.58 to 3.02 Å, and the closest approach of oxygen atoms within this polyhedron is 2.75 Å. There appears to be no resemblance between either of these polyhedra and the arrangment of the seven nearest oxygen atoms around the lead in pyrobelonite (Donaldson & Barnes, 1955).

The two lead atoms, Pb(1) and Pb(2), are 4.18 Å apart, but the shortest Pb-Pb distance is between Pb(2) and its equivalent through the centre of symmetry at $\frac{3}{4}$, $\frac{1}{2}$, $\frac{1}{4}$ where the distance is 4.04 Å. The nearest Mn is 3.82 Å from Pb(1) and 3.84 Å from Pb(2). The closest approach of vanadium and lead is 3.48 Å between Pb(1) and V(2); other Pb-V distances are 3.53, 3.75, and 3.97 Å. The manganese atoms are separated by 3.08 Å, and they are at distances of 3.21 and 3.51 Å respectively, from the nearest two cystallographically distinct vanadium atoms. V(1) and V(2) are 4.30 Å apart.

Throughout the structure investigation it has been assumed that the space group of brackebuschite is $B2_1/m$ and not $B2_1$. The primary object of the present study has been to establish the features of the brackebuschite structure in sufficient detail to determine its relationship to that characteristic of the minerals of the descloizite and adelite groups. No attempt has been made to attain very high accuracy in the determination of interatomic distances which would have required three-dimensional treatment of the observed data because of the overlapping of oxygen atoms. The accuracy attained, however, is sufficient to show that if the space group is in fact $B2_1$, only minor displacements of the metal atoms from the special positions of $B2_1/m$ could be involved, although the sites of the oxygen atoms and of the water molecules (if present) are somewhat more flexible.

## Relationship between Brackebuschite and the Minerals of the Descloizite and Adelite Groups

In assessing the structural relationship of brackebuschite to the minerals of the descloizite and adelite groups, it is appropriate to select pyrobelonite as a typical example of the latter. Its structure, which is essentially the same as those of descloizite and conichalcite, has been refined with satisfactory accuracy (Donaldson & Barnes, 1955), and the suggestion has been made (Richmond, 1940) that pyrobelonite actually forms a chemical series with brackebuschite.

The three principal projections of the structures of both minerals are shown schematically in Fig. 6. In the study of pyrobelonite (Donaldson

& Barnes, 1955) the origin chosen was not the most suitable for such direct comparison but this has now been adjusted. It should also be noted that $c/2$ in brackebuschite corresponds to $c$ in pyrobelonite.

The major differences between the structures of the two minerals appear to be due to the presence of the additional manganese atoms in pyrobelonite, the accommodation of which requires some alteration in the lattice of the lead and vanadium atoms from brackebuschite to pyrobelonite (see particularly the projections on (010)). The changes are primarily along the direction of the $c$-axis, which increases from 8.26 Å for $c/2$ in brackebuschite to 9.52 Å for $c$ in pyrobelonite.

The reasons for the interesting similarities and differences between corresponding precession photographs of brackebuschite and pyrobelonite (Barnes & Qurashi, 1952; Qurashi & Barnes, 1953, Fig. 1) are now evident from Fig. 6. The projections on (001) are almost identical except for very slight displacements of lead, vanadium, and oxygen atoms in brackebuschite which are superimposed in pyrobelonite, thus accounting for the almost identical precession photographs of the $\{hk0\}$ zones. Additional manganese atoms in pyrobelonite, and changes in the $z$-coordinates, are the principal differences between the projections on (100), but the similarity is still sufficiently close to explain why corresponding $0kl$ reflections are so much alike. Because of different symmetry elements, in addition to the presence of additional manganese atoms and different positions for the lead atoms in pyrobelonite, the projections on (010) are quite different, and thus very little resemblance would be expected between corresponding $h0l$ reflections, as is indeed found to be the case.

It is clear from Fig. 6 that, although the structures of brackebuschite and pyrobelonite are similar in some respects, the relationship is not of the type suggested by Richmond (1940), who implied that the two minerals were isostructural, differing only in the Pb:Mn ratio. The present results are in complete agreement with the contents of the unit cell derived from chemical analysis (Doering, 1883) except perhaps for the water-content, and with the observed specific gravity (Berry & Graham, 1948). They substantiate the conclusion of Berry & Graham (1948) that brackebuschite probably belongs to a chemical type $A_3(XO_4)_2 \cdot n\mathrm{H_2O}$, and they demonstrate clearly that brackebuschite should not be classified with the minerals of the descloizite and adelite groups.

## ACKNOWLEDGMENTS

Grateful acknowledgment is made to Professor Clifford Frondel for the crystals of brackebuschite, and to Mrs. M. E. Pippy for assistance

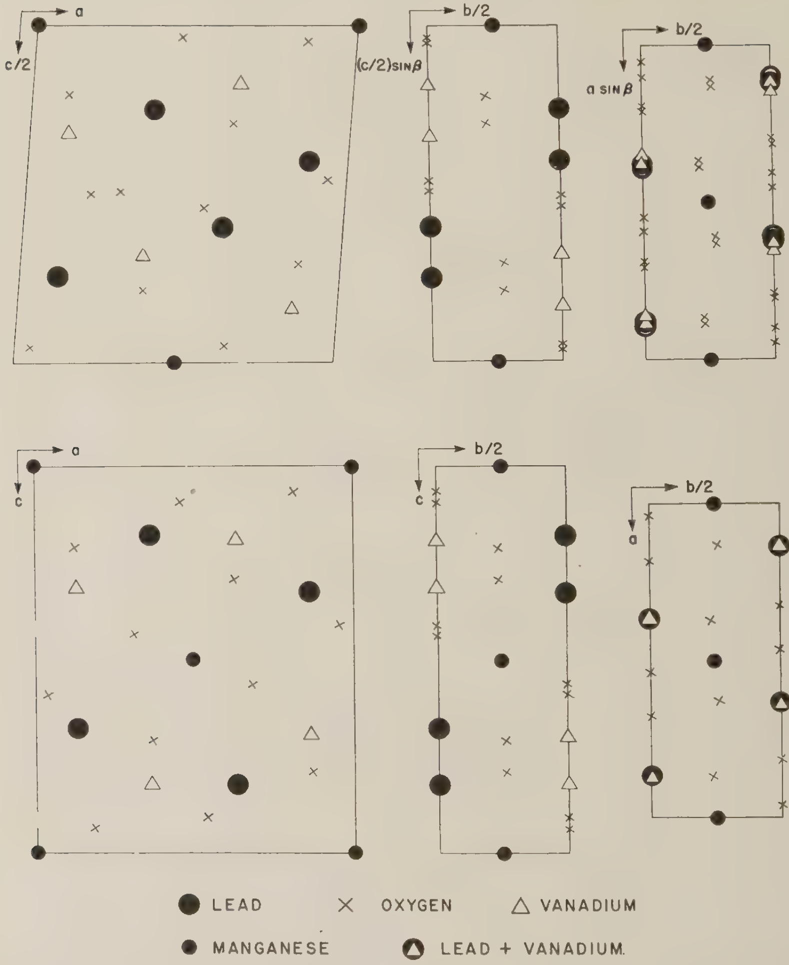

FIG. 6. Projections on (010), (100), and (001) of (top) brackebuschite and (bottom) pyrobelonite (possible $H_2O$ sites not shown in former; OH sites not shown in latter).

with the structure factor and Fourier calculations. We are indebted especially to Dr. Howard T. Evans for his kindness in preparing Fig. 5.

## REFERENCES

BARNES, W. H., & QURASHI, M. M. (1952): Unit cell and space group data for certain vanadium minerals, *Am. Mineral.*, **37**, 407–422.

BERRY, L. G. (1951): Observations on conichalcite, cornwallite, euchroite, liroconite, and olivenite, *Am. Mineral.*, **36**, 484–503.

Berry, L. G., & Graham, A. R. (1948): *X*-ray measurements on brackebuschite and hematolite, *Am. Mineral.*, **33,** 489–495.

Byström, A., Wilhelmi, K. A., & Brotzen, O. (1950): Vanadium pentoxide —A compound with five-coordinated vanadium atoms, *Acta Chem. Scand.*, **4,** 1119.

Christ, C. L., Clark, J. R., & Evans, H. T. (1953): The crystal structure of $KVO_3 \cdot H_2O$, *J. Chem. Phys.*, **61,** 1114.

Cochran, W. (1951): The structures of pyrimidines and purines. V. The electron distribution in adenine hydrochloride, *Acta Cryst.*, **4,** 81–92; Some properties of the $(F_o - F_c)$-synthesis, *Acta Cryst.*, **4,** 408–411.

Cruickshank, D. W. J. (1949): The accuracy of electron-density maps in *x*-ray analysis with special reference to dibenzyl, *Acta Cryst.*, **2,** 65.

Dana, J. D. (1892): *System of Mineralogy*, ed. 6, by E. S. Dana, p. 791, New York. (The copy consulted was a 1929 reprint, with Appendices I and II.)

Dana, J. D., & E. S. (1951): *System of Mineralogy*, **2,** ed. 7, by C. Palache, H. Berman and C. Frondel, New York.

Donaldson, D. M., & Barnes, W. H. (1955): The structures of the minerals of the descloizite and adelite groups: II—pyrobelonite, *Am. Mineral.*, **40,** 580–596.

Doering, A. (1883): There is some confusion in the literature about the references to Doering's analyses (compare Hintze, C. (1933): *Handbuch der Mineralogie*, Bd. 1, Abt. 4, Berlin, pp. 670, 671, where they are cited correctly, with Strunz, 1939, *loc. cit.*, and Richmond, 1940, *loc. cit.*). The results of one of two preliminary analyses made by Döring (sic) are quoted by Rammelsberg, C. (1880): Ueber die Vanadinerze aus dem Staat Córdoba in Argentinien, *Zeit. d. Deutsch. Geol. Ges.*, **32,** 708–713, on p. 711 from a letter he received from Doering. Doering himself contributed a section (III. Brackebuschita. *A*. Descripcion Química, pp. 501–505), among several others, to a long paper by Brackebusch, L., Rammelsberg, C., Doering, A. & Websky, M. (1883): Sobre los Vanadatos Naturales de las Provincias de Córdoba y de San Luis (República Argentina), *Bol. Acad. Nac. Cienc. Córdoba*, **5,** 441–524, in which the results of two later analyses (both slightly different from the one quoted by Rammelsberg, 1880, *loc cit.*) appear on pp. 503, 504, and the specific gravity (5.85) is given on p. 504. All three. published analyses (Döring, quoted by Rammelsberg, 1880, *loc. cit.;* Doering, in Brackebusch, Rammelsberg, Doering & Websky, 1883, *loc. cit.*) appear in Dana (1892), but only the first in Berry & Graham (1948) and in Dana (1951).

*International Tables for the Determination of Crystal Structures* (1935), Berlin.

Ketelaar, J. A. A. (1936): Die Kristallstruktur des Vanadinpentoxyds, *Zeit Krist.*, (A) **95,** 9.

Mellor, J. W. (1947): *A comprehensive treatise on inorganic and theoretical chemistry*, **9,** As, Sb, Bi, V, Cb, Ta, p. 778, London.

Qurashi, M. M., & Barnes, W. H. (1953): The structure of pucherite, $BiVO_4$, *Am. Mineral.*, **38,** 489.

Qurashi, M. M., & Barnes, W. H. (1954): The structures of the minerals of the descloizite and adelite groups: I-descloizite and conichalcite (part 1), *Am. Mineral.*, **39,** 416–435.

Richmond, W. E. (1940): Crystal chemistry of the phosphates, arsenates, and vanadates of the type $A_2XO_4(Z)$, *Am. Mineral.*, **25,** 441–479.

Strunz, H. (1939): Mineralien der Descloizitgruppe, *Zeit. Krist.*, (A) **101,** 496–506.

Wells, A. F. (1945): *Structural Inorganic Chemistry*, Oxford.

# DETERMINATION OF THE MODE OF A METAMORPHIC ROCK

Denis M. Shaw and W. D. Harrison*
*Hamilton College, McMaster University, Hamilton, Ontario.*

## Abstract

An outcrop of a sillimanite gneiss was sampled and its mode estimated by the point-counter. Statistical analysis shows that foliation does not bias the results, which are independent of the orientation of the slides to a reasonable probability. Considerable lack of homogeneity in the rock sampled is indicated by the muscovite and quartz figures, stressing the need for careful sampling of metamorphic rocks where any geochemical work is anticipated.

## Introduction

In studies of metasomatism too little attention is usually given to the material which has been metasomatized. In particular it does not seem to be realized that it is necessary to know the range of composition of the original rock before metasomatism can be proved, unless there are very far-reaching changes in composition. This is especially necessary when the rocks are sedimentary and when the metasomatism does not involve wholesale replacement by minerals of the heavy metals.

The first author has been investigating the effects of metamorphism on the composition of the Littleton pelitic rocks of New Hampshire, which can be traced from fossiliferous (Devonian) shales to sillimanite gneisses. The results on trace elements are now complete (Shaw, 1954) and work on the major elements is under preparation. To supplement chemical analyses it was decided to investigate the variation in mode, which would at the same time cast light on the problem of mode determination in foliated rocks.

The point-counter analyses were carried out by the second author (Harrison, 1954). Since the work was initiated Chayes has published a theoretical study of thin-section analysis (Chayes, 1954) in which it is shown that it is immaterial whether thin sections are cut parallel or perpendicular (or at any other angle) to the foliation. One of the purposes of this paper is to present experimental evidence bearing on the subject.

The first author is indebted to the Penrose Bequest Fund of the Geological Society of America and the Geological Survey of Canada for grants which aided this research. The advice and assistance of Professor J. D. Bankier, Department of Mathematics, Hamilton College, McMaster University is gratefully acknowledged.

---

* Now at Queen's University, Kingston, Ontario.

### *The Problem*

To calculate the composition of a rock unit it is first necessary to estimate the mineralogical mode and reliability of the estimate. Apart from difficulties in identification the chief sources of variation are as follows:

(a) variability of hand specimens
(b) variability of thin sections from any hand specimen
(c) operator and mechanical error in the point-counter method

One outcrop was studied in detail, taking several hand specimens. From each of three rocks three sections were cut, parallel to three perpendicular planes, one of which was parallel to the foliation. The operator and mechanical error was estimated by replicate analyses, sixfold for one rock and twofold for the others.

The rock chosen was a sillimanite gneiss located 1 mile south-east of West Rumney, P.O., N.H. Major constituents are muscovite, biotite, quartz and sillimanite, with garnet, opaques, chlorite, tourmaline, apatite and plagioclase in minor amounts. All the major and most of the minor constituents are present in each slide, so the outcrop shows no major inhomogeneities in composition. The grain-size averages about 0.5 mm., but sillimanite and the minor constituents (except garnet) are frequently much smaller. Much of the sillimanite occurs as fine needles embedded in quartz and muscovite grains. Some is also present as dark masses of fibrolite. Garnet is present as sporadic porphyroblasts. The rock has a well-developed schistosity and foliation,[1] the latter due to bands alternately rich and poor in muscovite or sillimanite. The combination of these textural features illustrates well the difficulties likely to be encountered in the estimation of homogeneity in metamorphic rocks, and is illustrated in Figures 1, 2 and 3.

### *Inhomogeneity in a Single Thin Section*

Before presenting the results of the experiment it is necessary to indicate the effect of two textural features on the results for a single thin section.

Porphyroblasts will always be a problem in modal determinations. Table 1 (left half) shows the result of analyzing the two halves of a slide separately.[2] Garnet occurs as porphyroblasts and in this section one garnet crystal was located in one half and none in the other half. It is evident that the abundance of porphyroblasts cannot be estimated with any precision. Probably the only satisfactory solution of this

---

[1] Foliation is used in Harker's sense, referring to segregational banding.

[2] Spacing of microtraverses was 0.50 mm, except for analyses of about 4000 points, where the spacing was 0.25 mm.

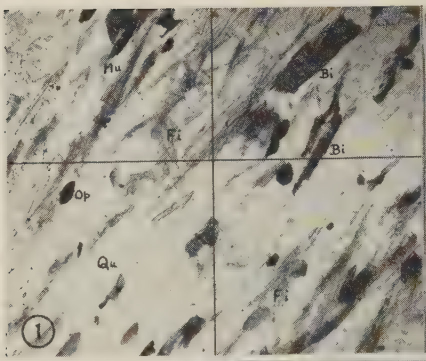

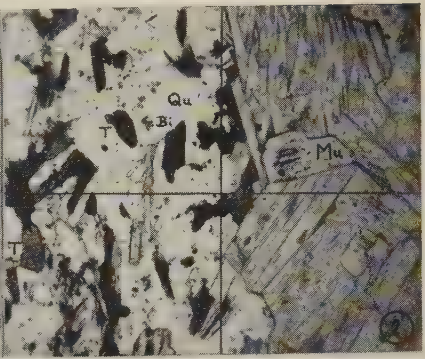

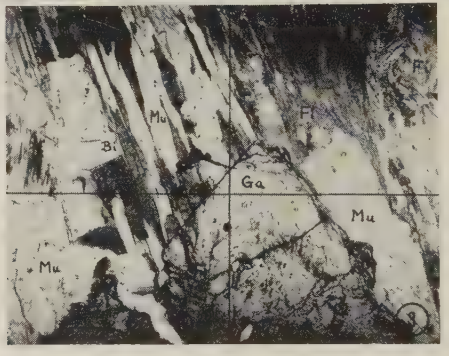

FIGS. 1–3. Photomicrographs of slides analyzed. Magnification 50×. Abbreviations as follows: Mu, muscovite; Bi, biotite; Qu, quartz; Fi, fibrolite; Ga, garnet; Op opaques; T, tourmaline.

FIG. 1. L29A3. The schistosity and weak foliation are shown by the subparallel crystals of fibrolite, biotite and muscovite.

FIG. 2. L29C3. Well-developed foliation is apparent, with muscovite in a segregated band.

FIG. 3. L29A1. A garnet porphyroblast in a foliated rock consisting of alternate bands of muscovite-biotite and fibrolite-muscovite. Fractures have developed in the garnet, perpendicular to the schistosity.

problem would be to estimate these crystals separately on large polished sections.

Secondly, foliation banding affects the estimate in the same manner. Table 1 (right) shows the effect of varying the count length on a single foliated section. In column A are the results for about a quarter of the slide area and in column B the results for the whole slide (including A). Foliation in this case was parallel to the traverse direction. The variation is most noticeable for quartz and muscovite, and could obviously be avoided by traversing at right angles to the foliation. No specific attempt was made to do this, in order to avoid a favorable orientation and to emphasize possible variability.

Table 1. Inhomogeneities

| *Inhomogeneity due to porphyroblasts* | | | *Inhomogeneity due to foliation* | | |
|---|---|---|---|---|---|
| Mineral | Slide L29B3 | | Mineral | Slide L29C3 | |
| | First half | Second half | | A | B |
| Muscovite | 21.5 | 18.6 | Muscovite | 45.6 | 21.4 |
| Sillimanite | 3.4 | 3.4 | Sillimanite | 7.0 | 5.0 |
| Biotite | 11.8 | 22.5 | Biotite | 25.3 | 15.2 |
| Quartz | 52.9 | 51.3 | Quartz | 18.3 | 56.7 |
| Garnet | 5.2 | nil | Opaques | 2.6 | 1.2 |
| Opaques | 1.5 | 1.1 | Tourmaline | 1.1 | .5 |
| Chlorite | .9 | .2 | Plagioclase | .2 | .1 |
| Tourmaline | 2.2 | 2.8 | | | |
| Apatite | .2 | nil | | | |
| Plagioclase | .6 | .1 | | | |
| Total | 100.2 | 100.0 | Total | 100.1 | 100.1 |
| Points tallied | 2000 | 2022 | Points tallied | 1124 | 3484 |

### *Results and Discussion*

Table 2 gives the results of the 30 analyses of 9 thin sections of 3 hand specimens of the rock (L29). The orientations are indicated by letters A, B and C where B indicates the foliation plane and A and C the planes mutually perpendicular to each other and to B. The hand specimens are numbered 1, 2 and 3 in the final figure of the slide symbol.

It is evident that reproducibility is satisfactory, and in few cases is there much disagreement among replicate analyses of the same slide (e.g., sillimanite, L29B3). However there are notable differences between different slides. This may arise in several ways: (a) variation in estimates of one hand specimen but without any foliation bias, (b) variation in estimates of one hand specimen due to bias caused by the foliation, (c) variation in composition between hand specimens irrespective of foliation bias. Any separate estimates of a population (in this case the composition of the outcrop) will differ, and the differences will reflect the homogeneity of the population. We require to find however the relative importance of (a), (b) and (c), i.e., whether it matters in what direction the slides are cut and whether we take one or more hand specimens. These factors can be assessed, together with reproducibility, by variance analysis. For the reader unfamiliar with this procedure the methods and symbols of Dixon & Massey (1951,

TABLE 2. ANALYSES OF HAND-SPECIMENS

| Mineral | *Specimen* 1—L29A1 | | | | | | *Specimen* 1—L29B1 | | | | | |
|---|---|---|---|---|---|---|---|---|---|---|---|---|
| Muscovite | 39.5 | 39.8 | 44.6 | 44.1 | 44.3 | 41.8 | 30.4 | 34.1 | 33.1 | 31.2 | 29.5 | 33.2 |
| Sillimanite | 19.3 | 19.8 | 16.0 | 17.9 | 18.0 | 17.1 | 8.5 | 5.7 | 4.7 | 7.3 | 8.1 | 7.4 |
| Biotite | 15.6 | 14.9 | 14.5 | 14.9 | 14.3 | 15.3 | 23.6 | 22.0 | 22.6 | 23.8 | 23.5 | 23.2 |
| Quartz | 17.3 | 17.3 | 16.1 | 14.3 | 15.6 | 16.7 | 30.5 | 31.6 | 34.1 | 30.3 | 32.0 | 29.5 |
| Garnet | 5.3 | 5.4 | 5.3 | 6.0 | 5.5 | 5.5 | 3.4 | 3.5 | 2.6 | 3.3 | 3.2 | 3.6 |
| Opaques | 1.5 | 1.0 | 1.5 | 1.2 | .9 | 1.7 | 1.8 | 1.5 | 1.2 | 1.8 | 1.3 | 1.4 |
| Chlorite | .9 | 1.0 | 1.3 | 1.0 | .9 | 1.0 | .7 | .9 | 1.0 | 1.3 | 1.4 | .9 |
| Plagioclase | .1 | .4 | .4 | .2 | .2 | .3 | .9 | .6 | .5 | .6 | .7 | .7 |
| Tourmaline | .5 | .5 | .3 | .4 | .2 | .5 | .2 | .1 | .2 | .3 | .2 | .1 |
| Total | 100.0 | 100.1 | 100.0 | 100.0 | 99.9 | 99.9 | 100.0 | 100.0 | 100.0 | 99.9 | 99.9 | 100.0 |
| Points Tallied | 1946 | 1870 | 1951 | 1656 | 1771 | 1917 | 2100 | 3558 | 2500 | 2500 | 2200 | 2200 |

| | *Specimen* 1—L29C1 | | | | | |
|---|---|---|---|---|---|---|
| Muscovite | 38.8 | 38.5 | 36.0 | 37.2 | 37.6 | 37.2 |
| Sillimanite | 10.6 | 10.4 | 10.9 | 11.0 | 11.1 | 11.2 |
| Biotite | 19.0 | 18.1 | 19.4 | 19.6 | 18.8 | 19.2 |
| Quartz | 23.1 | 24.8 | 24.6 | 24.4 | 23.9 | 24.9 |
| Garnet | 5.0 | 5.3 | 5.2 | 5.0 | 5.0 | 4.6 |
| Opaques | 1.4 | 1.2 | 1.6 | 1.2 | 1.3 | 1.1 |
| Chlorite | 1.5 | 1.0 | 1.7 | 1.1 | 1.8 | 1.3 |
| Plagioclase | .3 | .2 | .3 | .2 | .3 | .5 |
| Tourmaline | .4 | .6 | .4 | .4 | .3 | .1 |
| Total | 100.1 | 100.1 | 100.1 | 100.1 | 100.1 | 100.1 |
| Points Tallied | 2010 | 1900 | 1896 | 2079 | 2046 | 1941 |

| | *Specimen* 2 | | | | | | *Specimen* 3 | | | | | |
|---|---|---|---|---|---|---|---|---|---|---|---|---|
| | L29A2 | | L29B2 | | L29C2 | | L29A3 | | L29B3 | | L29C3 | |
| Muscovite | 22.5 | 24.0 | 33.5 | 31.5 | 32.2 | 28.4 | 13.0 | 11.1 | 20.1 | 20.1 | 21.4 | 21.7 |
| Sillimanite | 11.6 | 11.8 | 14.8 | 15.2 | 16.8 | 18.5 | 8.2 | 11.0 | 3.4 | 11.5 | 5.0 | 4.3 |
| Biotite | 28.1 | 26.3 | 23.9 | 24.2 | 23.6 | 23.7 | 17.0 | 16.5 | 17.1 | 15.5 | 15.2 | 13.6 |
| Quartz | 30.4 | 29.1 | 14.4 | 16.4 | 21.8 | 23.2 | 60.6 | 60.4 | 52.1 | 42.6 | 56.7 | 59.0 |
| Garnet | 3.1 | 3.6 | 6.6 | 7.1 | 3.0 | 2.9 | nil | nil | 2.6 | 2.7 | nil | nil |
| Opaques | 3.1 | 3.6 | 4.6 | 3.5 | 1.6 | 2.2 | 1.2 | 1.0 | 1.3 | 3.7 | 1.1 | 1.0 |
| Chlorite | 1.1 | 1.6 | 1.4 | 1.2 | .7 | .7 | nil | nil | .5 | 1.4 | nil | .1 |
| Plagioclase | .1 | .1 | .1 | .1 | nil | .1 | nil | nil | .4 | nil | .1 | .1 |
| Tourmaline | nil | .1 | .7 | .8 | .2 | .2 | .1 | .1 | 2.5 | 2.2 | .5 | .4 |
| etc. | nil | nil | nil | nil | nil | nil | nil | .1 | .1 | .4 | nil | nil |
| Total | 100.0 | 100.2 | 100.0 | 100.0 | 99.9 | 99.9 | 100.1 | 100.2 | 100.1 | 100.1 | 100.0 | 100.2 |
| Points Tallied | 2213 | 2000 | 2034 | 2062 | 1799 | 1736 | 2000 | 2000 | 4022 | 1933 | 3484 | 2000 |

pp. 134–138) are used in the following, where variance analysis is carried out for each of the major constituents muscovite, sillimanite, biotite and quartz. The procedure for muscovite will be outlined first.

The muscovite measurements are set out in Table 3, together with the sums of the individual measurements from each category ($T_{ij}$), and the

TABLE 3. MUSCOVITE IN L29

| | | Orientations | | | Totals | | | | |
|---|---|---|---|---|---|---|---|---|---|
| | | A | B | C | A | B | C | $T_{i.}$ | $n_{i.}$ |
| Rocks | 1 | 39.5 | 30.4 | 38.8 | 254.1 | 191.5 | 225.3 | 670.9 | 18 |
| | | 39.8 | 34.1 | 38.5 | | | | | |
| | | 44.6 | 33.1 | 36.0 | | | | | |
| | | 44.1 | 31.2 | 37.2 | | | | | |
| | | 44.3 | 29.5 | 37.6 | | | | | |
| | | 41.8 | 33.2 | 37.2 | | | | | |
| | 2 | 22.5 | 33.5 | 32.2 | 46.5 | 65.0 | 60.6 | 172.1 | 6 |
| | | 24.0 | 31.5 | 28.4 | | | | | |
| | 3 | 13.0 | 20.1 | 21.4 | 24.1 | 40.2 | 43.1 | 107.4 | 6 |
| | | 11.1 | 20.1 | 21.7 | | | | | |
| | | | | $T_{.j}$ | 324.7 | 296.7 | 329.0 | 950.4 | |
| | | | | $n_{.j}$ | 10 | 10 | 10 | | 30 |

sums of all the measurements on a particular hand specimen ($T_{i.}$) and the number of measurements ($n_{i.}$), and similar quantities for each orientation ($T_{.j}$ and $n_{.j}$). The bottom figure in column 9 is $T_{..}$, the sum of all the muscovite measurements, and the bottom figure in column 10 is $n$, the total number of measurements. The steps in computing the variance figures are as follows:

(1) $C = \dfrac{T_{..}^2}{n}$

(2) Total sum of squares: $\sum X^2 - C$ ($X$ is an individual measurement in Table 5).

(3) Subclasses: $\sum_{ij} \dfrac{T_{ij}^2}{n_{ij}} - C$ ($T_{ij}$ is an individual total from Table 3, comprising $n_{ij}$ measurements.)

(4) Residual: (2)–(3)

(5) Orientations: $\sum_{j} \dfrac{T_{.j}^2}{n_{.j}} - C = \dfrac{1}{10} \sum_{j} T_{.j}^2 - C$

(6) Rocks: $\sum_{i} \dfrac{T_{i.}^2}{n_{i.}} - C$

(7) Interactions: (3)–(5)–(6)

The variance figures are listed in Table 4, together with the appropriate degrees of freedom (*d.f.*), the quotients giving the mean squares in column 4. Following the usual procedure the ratio of interactions and residual mean squares is computed first (column 5). This is found to exceed the value of the $F$-distribution for 99% probability and the

Table 4. Analysis of Variance of Muscovite

| Source | Sum of Squares | $d.f.$ | Mean square | $s_3^2/s_4^2$ | $s^2/s_3^2$ |
|---|---|---|---|---|---|
| Orientations | 61.526 | 2 | $30.763 = s_1^2$ | | .27 |
| Rocks | 1756.124 | 2 | $878.062 = s_2^2$ | | 7.57 |
| Interactions | 463.905 | 4 | $115.976 = s_3^2$ | 40.2 | |
| Residual | 60.633 | 21 | $2.887 = s_4^2$ | | |
| Total | 2342.188 | 29 | 80.765 | | |

$F_{.99}\ (4,\ 21) = 4.37$
$F_{.95}\ (2,\ 4) = 6.94$
$F_{.99}\ (2,\ 4) = 18.0$

Mean $\overline{X} = T_{..}^{2}/n = 31.68$

Table 5. Analysis of Variance for Quartz, Biotite, Sillimanite

| | Source | Sum of Squares | $d.f.$ | Mean Square | $s_3^2/s_4^2$ | $s^2/s_3^2$ |
|---|---|---|---|---|---|---|
| Quartz | Orientations | 71.429 | 2 | 35.715 | | .14 |
| | Rocks | 4813.222 | 2 | 2406.611 | | 9.49 |
| | Interactions | 1014.538 | 4 | 253.635 | 72.1 | |
| | Residual | 73.865 | 21 | 3.517 | | |
| | Total | 5973.054 | 29 | 205.967 | | |

$\overline{X} = 29.92$

| | | | | | | |
|---|---|---|---|---|---|---|
| Biotite | Orientations | 92.683 | 2 | 46.342 | | 1.42 |
| | Rocks | 264.780 | 2 | 132.390 | | 4.06 |
| | Interactions | 130.384 | 4 | 32.596 | 73.6 | |
| | Residual | 9.300 | 21 | .443 | | |
| | Total | 497.147 | 29 | 17.143 | | |

$\overline{X} = 19.57$

| | | | | | | |
|---|---|---|---|---|---|---|
| Sillimanite | Orientations | 210.662 | 2 | 105.331 | | 1.85 |
| | Rocks | 177.317 | 2 | 88.659 | | 1.56 |
| | Interactions | 227.392 | 4 | 56.848 | | |
| | Residual | 59.412 | 21 | 2.829 | 20.1 | |
| | Total | 674.783 | 29 | 23.268 | | |

$\overline{X} = 11.57$

appropriate number of degrees of freedom (4,21) as given in Table 4 (from Dixon & Massey, 1951, Appendix, Table 7). The significance of this is difficult to assess and its discussion is relegated to the Appendix. In the last column of Table 4 are found the ratios of orientations-to-interactions and rocks-to-interactions mean squares. These are compared with the values of the *F*-distribution for 95% and 99% probability (2, 4 *d.f.*) as given in Table 4. From this it is concluded that there is no significant difference between means for different orientations. For rocks there is a significant difference at the 95% level only. In other words, any of the slides from a given rock gives an equally valuable estimate of the composition of the rock, regardless of its orientation.

Table 6. Significance Tests

| Mineral | Interactions—Residual | Orientations—Interactions | | Rocks—Interactions | |
|---|---|---|---|---|---|
| | 99% | 99% | 95% | 99% | 95% |
| Muscovite | HS | — | — | — | S |
| Quartz | HS | — | — | — | S |
| Biotite | HS | — | — | — | — |
| Sillimanite | HS | — | — | — | — |

HS = Highly significant.
S = Significant.
— = Not significant.

However it seems unlikely that a single rock is a good estimate of the composition of the outcrop.

Results for quartz, biotite and sillimanite are set out in Table 5, omitting the computations and omitting the *F*-values which are the same as in Table 4. The significance tests are summarized in Table 6. It is seen that the interactions term is highly significant in every case, but otherwise the means are only significantly different for rocks when the muscovite and quartz figures are tested at the 95% level.

In every case the variance components may be interpreted as follows. The residual mean square ($s_4^2$) measures the experimental error and its square root expresses this as a standard deviation. By subtracting the residual sum of squares from the total sum of squares (or by adding the orientations, rocks and interactions sums of squares) a figure is obtained which estimates the variability of the outcrop and which has 29 minus 21 or 8 degrees of freedom. The mean square ($s_o^2$) is calculated and $s_o$ is

TABLE 7. AVERAGE COMPOSITION OF ALL SLIDES

| Mineral | % | $s_e$ | $s_o$ |
|---|---|---|---|
| Muscovite | 31.7 | 1.7 | 16.9 |
| Quartz | 29.9 | 1.9 | 27.2 |
| Biotite | 19.6 | 0.7 | 7.8 |
| Sillimanite | 11.6 | 1.7 | 8.8 |
| Garnet | 3.8 | | |
| Opaques | 1.8 | | |
| Chlorite | 1.0 | | |
| Tourmaline | 0.5 | | |
| Plagioclase | 0.3 | | |
| Total | 100.2 | | |

then the standard variation. Table 7 contains the values of $s_4$ ($=s_e$) and $s_o$, together with the estimated average composition of the outcrop.

## CONCLUSIONS

The results of the experiment may be summarized as follows. If it is desired to measure the modal composition of a metamorphic formation numerous slides should be analyzed. The orientation of the slides with respect to any foliation planes is irrelevant, but to get a good estimate several rocks should be used. Whereas the latter is intuitively obvious to any geologist, the former is not and the writers have come across considerable criticism along the lines that it is "wrong" to use a section cut parallel to foliation.

The large figures in Table 12 for $s_o$ in the case of muscovite and quartz suggest that the original sedimentary formation consisted of beds rich in sand and beds rich in aluminous material, or alternatively that metamorphic differentiation has simulated this state of affairs. The much lower experimental errors ($s_e$) for all four minerals studied indicate again the value of the point counter as an analytical tool.

## APPENDIX

### *Significance of the Interactions Mean Square*

In Table 7 and successive Tables it is seen that the interactions-to-residual mean squares exceeds the appropriate $F$-value. In other words the interactions term is significant. The implication of this is discussed by Dixon & Massey (1951, p. 137) who say:

> "Several factors may cause the interaction to be significant.
>
> 1. There is no interaction, but we have obtained a value which we declare significant. This will occur 5 per cent of the time if we use a 5 per cent level of significance.

2. The two variables of classification are interacting, i.e., producing effects together which would not be produced separately.
3. Another uncontrolled factor is of sufficient importance to include in the experiments.
4. The items in the subgroups are not randomly drawn."

In view of the fact that four minerals all show an interactions term which appears highly significant, it seems improbable that this is due to chance. Of the remaining three factors the writers can make no choice. An uncontrolled factor which may possibly be important is lineation, but this is very weak in these rocks and might be expected to affect sillimanite more than quartz, whereas the reverse seems the case. A true interaction might be produced by the confusion of basal muscovite with quartz in the foliation plane. This was detected early in the work however, and in any case should not affect sillimanite and biotite.

## REFERENCES

CHAYES, F. (1954): The Theory of Thin-Section Analysis. *Jour. Geol*, **62,** 92–101.

DIXON, W. J., & MASSEY, F. J. (1951): *Introduction to Statistical Analysis.* New York.

HARRISON, W. D. (1954): Determination of the Composition of Metamorphic Rocks by Use of the Point Counter. *M.Sc. thesis, McMaster University.*

SHAW, D. M. (1954): Trace Elements in Pelitic Rocks: Part I, Variations During Metamorphism. *Geol. Soc. Am., Bull.* **65,** 1151–1166.

# URANINITE AND THORIANITE FROM ONTARIO AND QUEBEC[1]

S. C. Robinson[2] and A. P. Sabina,[3]
*Geological Survey of Canada, Ottawa.*

## Abstract

The occurrence and mineral associations of 20 specimens of uraninite and thorianite are described. All the deposits occur in the Grenville Sub-province of the Canadian Shield.

The range in composition of these 20 specimens as determined by *x*-ray spectrography is $U_3O_8$ 25–73%, $ThO_2$ 7-55% and PbO 7–14%. Lattice constants ($a_0$) generally increase with increasing thorium content and range from 5.449 to 5.564 angstroms. After heating in air at 1000° C. for ten minutes the lattice constants are all reduced and more closely approach a lineal relation to the composition. The fact that none of the specimens oxidized to $U_3O_8$ on heating, indicates that they belong to the $\alpha$ group of Wasserstein.

The 20 specimens are readily subdivided into three distinct groups within each of which composition, lattice constants and type of deposits are distinctive.

An attempt to relate diffraction intensities of four different sets of planes to composition was inconclusive.

## *Introduction*

Uraninite has been recognized from many pegmatite deposits in Canada and particularly from those in the Grenville rocks of Ontario and Quebec. Analyses of uraninite from many localities were published by Ellsworth (1932). In none of these analyses does the thorium dioxide content exceed 15%. However, during the summer of 1954 many new deposits were found in a region extending from Monmouth township in Ontario, 100 miles northeastward to Huddersfield township in Quebec, and from several of these deposits high thorian uraninite or uranian thorianite was identified.

Preliminary studies of these minerals have shown that high thorian uraninites and some of the thorianites have compositions differing from any previously reported. Moreover, their occurrence is restricted to deposits that are singularly alike in geology and mineralogy.

This investigation is part of a continuing study of uranium minerals in Canada. Examinations of most of the deposits were made by one of the authors (S.C.R.) and *x*-ray data and computations were provided by the other (A.P.S.). We are indebted to J. Satterly and D. F. Hewitt of the Ontario Department of Mines for some of the specimens and for descriptions of two of the deposits. The co-operation of E. A. Brown and S. Kaiman of the Mines Branch, Ottawa, in supplying additional material is much appreciated. Officers of the various companies that are prospecting and mining in the region have greatly facilitated our work. To them, and to colleagues of the Geological Survey of Canada who have assisted us in many ways, we express our thanks.

---

[1] Published by permission of the Deputy Minister, Department of Mines and Technical Surveys, Ottawa, Canada.

[2] Geologist, Geological Survey of Canada.

[3] Technical Officer, Geological Survey of Canada.

### *Mineralogy and Location of Deposits*

The deposits are numbered and described in order of decreasing U:Th ratio of the uraninite or thorianite that they contain. The number of the deposit is the same as the number of the sample of uraninite or thorianite concentrated from it. Descriptions of deposits are taken from field notes except for that of Calumet Uranium Mines Ltd., whose description is based on specimens of the ore only.

Most of the accessory minerals of these deposits were identified by means of *x*-ray diffraction. Varietal names of feldspars, micas, pyroxenes and amphiboles are based on optical properties. Although uranothorite is reported from several of the deposits, its identification in all cases is tentative. It is metamict, and on heating in a vacuum to 1000° C. for five minutes, it yields a diffuse *x*-ray pattern equivalent to that of thorianite, as do other uranothorites. Continued heating of some specimens produced a product with a huttonite pattern. Many of the accessory minerals occur in small amounts. These were recognized in concentrates and middlings but were not seen in thin or polished sections.

In stating the location of the deposits, reference is given to province, township, concession or range, and lot in that order. Usually the concession (in Ontario) or range (in Quebec) is stated in roman numerals and the lot in arabic numerals but a letter is occasionally used for either concession or lot. Where work was known to have been in progress in the past year, the name of the company owning the deposit or holding it under option is given. Many of these deposits have been described more fully by Satterly & Hewitt (1955).

1. Ontario; Cardiff; XX; 7. Rounded masses of uraninite occur in a small concordant pegmatite, or migmatite band, in an area of hybrid granite gneiss. Accessory minerals include zircon, titanite and apatite.
2. Ontario; Faraday; XI; 16, 17. Faraday Uranium Mines Ltd., west drift in west adit. Small subhedral grains of uraninite occur in an ore shoot which consists of equal amounts of feldspar, magnetite and locally titanite. Quartz, zircon and fluorite are minor constituents. Uranothorite is also present in amounts slightly exceeding uraninite. The zircons exhibit sharply defined metamict and non-metamict multiple zoning. The ore shoot is a differentiate of granitic dyke rocks. These dykes are locally pegmatitic and are commonly radioactive. (*See* Satterly & Hewitt, 1955, p. 49.)
3. Quebec; Wakefield; III; 26. Uraninite crystals up to $\frac{1}{2}$ inch in diameter, occur at the contact between a zoned granite pegmatite and amphibolite. This border facies is a hornblende-rich syenite which contains accessory magnetite, pyrite, zircon and uranothorite.

4. Ontario; Cardiff; XI, XII; 27, 28. Centre Lake Uranium Mines Ltd., No. 4 dyke, 205′ level. This dyke has a banded migmatitic texture suggestive of metasomatic replacement. In it, uraninite occurs disseminated in a lens-shaped band which is made up of oligoclase and microcline in equal amounts, with minor diopside, titanite, biotite and fluorite. Traces of uranothorite are also present. (*See* Satterly & Hewitt, 1955, p. 24.)
5. Ontario; Cardiff; XV; 6. Uraninite occurs in bands in a small syenite dyke composed of relatively fine grained oligoclase and microcline with minor titanite evenly distributed through it. Diopside is also present in patches. Uraninite grains attain diameters of ¼ inch and are subhedral to anhedral. (*See* Satterly & Hewitt, 1955, p. 33.)
6. Ontario; Cardiff; XI, XII; 27, 28. Centre Lake Uranium Mines Ltd., No. 1. dyke, adit level. Uraninite occurs as subhedral grains up to ⅛ inch in diameter in a rather fine-grained footwall facies of the dyke. This rock is composed of equal amounts of microcline and albite (peristerite) with disseminated titanite and patches of diopside and hornblende. Some uranothorite and traces of pyrite and chalcopyrite are also present. (*See* Satterly & Hewitt, 1955, p. 28.)
7. Ontario; Cardiff; XXI; 9. This deposit is a very irregular pegmatite whose core is composed of a mixture of calcite and fluorite. Uraninite, in subhedral grains, occurs at the contact of the pegmatite with amphibolite, and in a tongue of fine grained syenite protruding from the main body of pegmatite. The syenite is composed of oligoclase and microcline with traces of diopside and titanite. Accessory minerals spatially associated with uraninite are hornblende, apatite, calcite, fluorite and traces of molybdenite and pyrite. Uraninite concentrates used in this investigation came wholly from the syenite differentiate. (*See* Satterly & Hewitt, 1955, p. 36.)
8. Ontario; Cardiff; XVII; A. Cardiff Uranium Mines Ltd., 125′ level south. Deposits of this mine are veins or dykes of calcite and fluorite that change transitionally along strike to pegmatite. They are composed dominantly of calcite with subordinate purple streaky fluorite, minor apatite, and locally, feldspar and diopside. Partly rounded cubes of uraninite up to 1½ inches in diameter are disseminated through the deposits. Accessory minerals include titanite, chondrodite, uranothorite, molybdenite and pyrite. (*See* Satterly & Hewitt, 1955, p. 17.)
9. Ontario; Cardiff; XIX; 2. Cardiff Uranium Mines Ltd., adit. This deposit was described by Wolfe & Hogg (1948); specimens collected by the writer were taken from the dump. Uraninite occurs in medium grained syenite and in calcite-diopside rock. Associated minerals are titanite, zircon, molybdenite and pyrrhotite. (*See* Satterly & Hewitt, 1955, p. 19.)
10. Ontario; Cardiff; XII; 29. Centre Lake Uranium Mines Ltd. Uraninite in cubes modified by octahedra, up to 1 inch in diameter, occurs in lenses of biotite-rich pyroxenite. These lenses together with bands rich in white calcite and leuco-granite occur in a series of amphibolites and crystalline limestone. Principal constituents of the radioactive lenses are biotite and diopside with minor hornblende, calcite and fluorite and accessory magnetite, titanite and apatite. No thorite or uranothorite were recognized in concentrates from this deposit. (*See* Satterly & Hewitt, 1955, p. 26.)
11. Ontario; Cardiff; XIX; 8. Anuwon Uranium Mines Ltd. Uraninite occurs in rounded to octahedral crystals in mica pyroxenite in which some pegmatite bands are emplaced. Associated minerals are apatite, salmon-coloured calcite, titanite, scapolite and fluorite. Crystals of uraninite occur in vugs in the rock. (*See* Satterly & Hewitt, 1955, p. 35.)
12. Ontario; Cardiff; XXI; 8. This well-defined lens-shaped pegmatite exhibits marked

differentiation from coarsely crystalline microcline and hornblende at the northeast end, to banded calcite-fluorite with an outer skin of hornblende and red apatite at the southwest end. Calcite-fluorite stringers and veins transect the coarse-grained facies in which feldspar and hornblende crystals attain lengths up to one foot and are partly oriented in comb texture normal to the walls. Uraninite in cubes modified by octahedra up to 1 inch in diameter occur in the 'skin' of hornblende and apatite with some accessory pyrite and molybdenite. (*See* Satterly & Hewitt, 1955, p.39.)

13. Ontario; Monmouth; VI; 5. Wadasa Gold Mines Ltd. The radioactive zones are composed dominantly of rounded diopside and phlogopite crystals in salmon-coloured calcite. Locally, tremolite is developed in crystals up to ½ inch in cross section. Uraninite occurs in cubes, rarely modified by the octahedron, up to ⅜ inch in diameter. Most of these cubes contain euhedral inclusions of diopside, Accessory minerals are pyrite and melanocerite. (*See* Satterly & Hewitt, 1955, p. 47.)
14. Ontario; Monmouth; XVII; 30. Homer Yellowknife Mines Ltd. Uraninite occurs as cubes up to ¼ inch in diameter in a skarn rock composed principally of calcite, diopside and phlogopite. Euhedral crystals of pyrite accompany the uraninite. This deposit was not visited by the authors. (*See* Satterly & Hewitt, 1955, p. 42.)
15. Ontario; Faraday; A; 29. Lockwood Farm. Rounded grains of uraninite and subhedral uranothorite occur in lenses of rock made up of coarse-grained tremolite and white calcite containing rounded grains of diopside. The presence of radioactive minerals is marked by a halo of hematite stain. Because the material tentatively identified as uranothorite occurs in and with uraninite, great care was taken in separation to use only the heaviest concentrate of a −200 mesh fraction. Examined under the microscope, the concentrate was found to be free from uranothorite. (*See* Satterly & Hewitt, 1955, p. 53.)
16. Quebec; Grand Calumet; VII; 29. Calumet Uranium Mines Ltd. This deposit was not visited. The crushed material which was studied, consists mainly of diopside, calcite, and mica with accessory uranian thorianite, monazite, rutile, and garnet.
17. Quebec; Huddersfield; V; 20. Yates Uranium Mines Ltd. Uranian thorianite in the form of small cubes, some of which are twinned, occurs in rock made up of salmon-coloured calcite, diopside and sparse phlogopite. Locally, actinolite and chondrodite are abundant. Veins of late white calcite with traces of fluorite transect all the above minerals. Thorite is present in about ¼ the amount of thorianite, and both are most abundant where phlogopite is plentiful. Lessingite, a silicate of thorium and rare earths is present in colourless grains.
18. Ontario; Dungannon; XVI; 14. Normingo Mines Ltd. Uranian thorianite occurs in zones marked by salmon-coloured calcite and phlogopite, in a country rock composed of impure micaceous marble and schist intruded by granite. The uranian thorianite is present as cubes up to ¼ inch in diameter, some of which are twinned. Accessory minerals in the thorianite zones are euhedral diopside, monazite, garnet, pyrite and pyrrhotite. (*See* Satterly & Hewitt, 1955, p. 48.)
19. Quebec; Huddersfield; V; 21, 22. Huddersfield Uranium and Minerals Ltd. Radioactive zones in impure crystalline limestone are composed of salmon-coloured calcite, euhedral diopside, and rounded subhedral phlogopite. Uranian thorianite occurs almost universally as interpenetration twins of the cube up to ½ inch in diameter, and contains inclusions of calcite, diopside, and phlogopite. Traces of titanite and thorite were identified in the middling concentrates.

    Acid pegmatites, worked for mica, occur within a few hundred feet of these deposits. Local weak areas of radioactivity were noted in the pegmatites but the minerals were not identified.

20. Quebec; Huddersfield; IV; 20. Yates Uranium Mines Ltd. This deposit is made up of salmon-coloured calcite, euhedral diopside and bands of phlogopite in an impure crystalline limestone host rock. Uranian thorianite is disseminated in the calcite but is slightly more concentrated in bands where diopside and phlogopite predominate. Accessory minerals are thorite and titanite with traces of chondrodite, allanite, and pyrite.

### *Laboratory Procedure*

Concentrates of uraninite and thorianite were made by Mr. P. Lavergne from sized material using the Haultain superpanner and the Franz isodynamic separator. To avoid contamination due to composite grains, all material was crushed to pass 100 mesh. In two samples in which uranothorite was intimately admixed with uraninite, the material was ground to pass 150 mesh. All concentrates were examined under the binocular microscope and where necessary, were reconcentrated. It is thought that concentrates were at least 99% pure in all cases.

Concentrates were then ground to pass 325 mesh in a power mortar and the resulting powders were analysed for U, Th and Pb by *x*-ray spectrography. Standards were prepared to conform as closely as possible to the composition of each concentrate and analyses were made by the internal standard method, using strontium as the internal standard. It is intended to make chemical analyses of these concentrates at a later date. However, checks indicate that errors in these *x*-ray analyses do not exceed ±5% of the amount present.

*X*-ray powder diffraction patterns were made of all concentrates using a standard 114.7 mm. diameter camera and lattice constants were calculated from the same 14 lines for each pattern. Checks of accuracy, using two specimens of fluorite, indicate that errors in the lattice constants do not exceed ±0.002 Å.

A few milligrams of each sample were heated in air over a Meker burner at approximately 1000° C. for 10 minutes. *X*-ray patterns of these heated samples were made on standard 57.3 mm. diameter cameras, and lattice constants were calculated from 10 lines in each pattern. These lattice constants are thought to be correct within limits of error of ±0.005 Å.

For ten of the samples, intensities of lines indexed as (220), (311), (222) and (400) were measured on the *x*-ray diffractometer. These four sets of planes were chosen both because they represent major crystal directions and because they occur in a range of 2 theta in which peaks are well-defined and background level varies only slightly. For each sample two mounts were measured and background counts were made at four positions. It was found that reproducibility of ratios was not better than ±5% of the figure given. There was an even greater variation in absolute values.

### *Composition, Lattice Parameter and Diffraction Intensities*

In the following table, twenty samples of uraninite and thorianite are listed in order of decreasing U:Th ratio. For each concentrate the percentage composition of $U_3O_8$, $ThO_2$ and PbO is given, together with the U:Th ratio and the lattice constant ($a_0$) of unheated and heated material in angstroms. For ten of the samples the following ratios of diffraction intensities are also given: $I(311):I(220)$, $I(222):I(220)$, $I(222):I(311)$, and $I(222):I(400)$.

In Figure 1 the uranium and thorium composition as a ratio is plotted as the ordinate of a graph in which the lattice constants of both unheated and heated uraninite or thorianite are plotted as the abscissae. Ratios of U:Th are plotted down to unity but where that ratio becomes less than one, the Th:U ratios are plotted.

Results tabulated in Table 1 and plotted in Figure 1 show that there is a broad general increase in lattice constants of uraninites and thorianites with decrease in U:Th ratio, and that this relation is better defined when the composition is compared with lattice constants of heated material. In terms of Wasserstein's (1954) proposed classification, all of the uraninites and thorianites described in this paper are gamma type because on heating in air they did not decompose but their lattice constants did shrink. Unfortunately Wasserstein did not give the temperature and period of heating, nor did he mention whether he had attempted to determine conditions under which the lattice constant is stabilized. Our decision to heat at approximately 1000° C., for 10 minutes is roughly in line with conditions reported by Heystek & Schmidt (1953).

It is possible that when optimum conditions of heating are known and when more precise analyses of the samples are available, it will be found that the relation of U:Th to lattice constant will more nearly approach the linear function reported by Slowinski & Elliott (1952) for the artificial uranium and thorium dioxide isomorphous series. However, Brooker & Nuffield (1952) have shown that the lattice constant decreases with increasing $UO_3:UO_2$ ratio and this may explain the greater spread of points in the high uranium end of the graph in Figure 1. It will be observed that this spread is reduced for heated material as would be expected.

The effect of radiogenic lead in varying amount on the lattice constant has not been evaluated. In heating uraninite at 1000° C. in evacuated tubes, a pronounced sublimate of lead forms on the walls of the tube; it may be assumed, therefore, that some lead is lost in heating to 1000° C. in air.

All uraninites and thorianites of the group here reported, contain varying but small amounts of rare earths. The recent recognition by

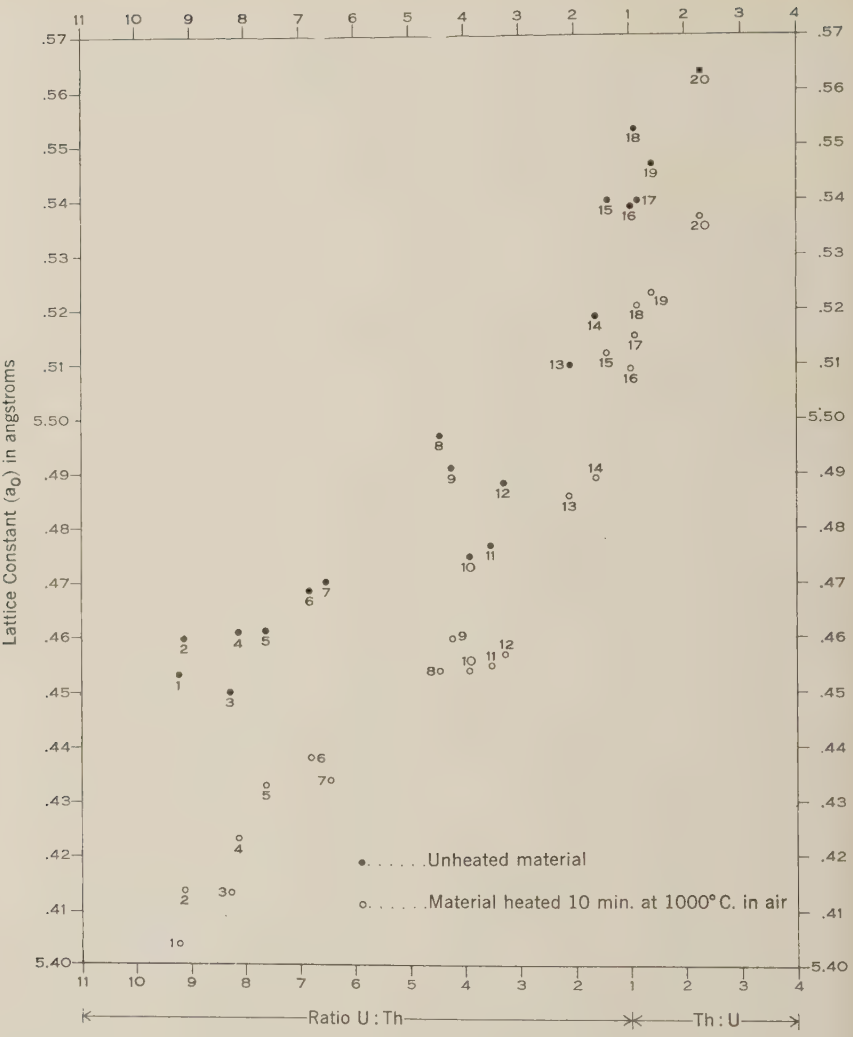

FIG. 1

Graham (1955) of a natural cerium dioxide, isostructural with uraninite and having a lattice constant within the range given for uraninite, suggests that cerianite must be considered as a third end member of the uraninite-thorianite series.

Attempts to use the lattice constant of uraninite or thorianite as an indicator of either composition or age must take account of all the above factors.

TABLE 1. COMPOSITION, LATTICE CONSTANT ($a_0$) AND RELATIVE DIFFRACTION INTENSITIES

| Sample No. | Location | U:Th | Unheated $a_0$(Å) | Heated $a_0$(Å) | Composition (%) | | | Diffraction Intensity | | | |
|---|---|---|---|---|---|---|---|---|---|---|---|
| | | | | | $U_3O_8$ | $ThO_2$ | PbO | $\frac{I(311)}{I(220)}$ | $\frac{I(222)}{I(220)}$ | $\frac{I(222)}{I(311)}$ | $\frac{I(222)}{I(400)}$ |
| 1 | Cardiff; XX; 7 | 9.2 | 5.454 | 5.404 | 73.0 | 7.7 | 10.75 | .82 | .21 | .26 | 1.8 |
| 2 | Faraday; XI; 16, 17 | 8.8 | 5.460 | 5.414 | 70.0 | 7.7 | 13.7 | .81 | .21 | .25 | 1.7 |
| 3 | Wakefield; III; 26 | 8.25 | 5.449 | 5.413 | 69.0 | 8.1 | 13.9 | | | | |
| 4 | Cardiff; XI, XII; 27, 28 | 8.1 | 5.461 | 5.423 | 65.0 | 7.7 | 11.9 | .84 | .20 | .24 | 1.6 |
| 5 | Cardiff; XV; 6 | 7.59 | 5.461 | 5.433 | 66.7 | 8.5 | 11.4 | | | | |
| 6 | Cardiff; XI, XII; 27, 28 | 6.79 | 5.468 | 5.438 | 64.5 | 9.2 | 11.9 | | | | |
| 7 | Cardiff; XXI; 9 | 6.43 | 5.469 | 5.434 | 66.7 | 10.0 | 8.4 | .79 | .20 | .25 | 1.9 |
| 8 | Cardiff; XVII; A | 4.44 | 5.497 | 5.454 | 62.8 | 13.6 | 12.8 | .75 | .22 | .29 | 2.2 |
| 9 | Cardiff; XIX; 2 | 4.24 | 5.491 | 5.460 | 62.7 | 14.3 | 10.7 | | | | |
| 10 | Cardiff; XII; 29 | 3.86 | 5.475 | 5.454 | 68.0 | 17.0 | 10.75 | | | | |
| 11 | Cardiff; XIX; 8 | 3.53 | 5.477 | 5.455 | 59.6 | 16.3 | 10.3 | | | | |
| 12 | Cardiff; XXI; 8 | 3.24 | 5.488 | 5.457 | 59.0 | 17.6 | 10.5 | | | | |
| 13 | Monmouth; VI; 5 | 1.89 | 5.510 | 5.486 | 53.0 | 27.0 | 10.0 | | | | |
| 14 | Monmouth; XVII; 30 | 1.61 | 5.519 | 5.489 | 48.0 | 28.8 | 9.4 | .78 | .21 | .27 | 1.9 |
| 15 | Faraday; A; 29 | 1.27 | 5.540 | 5.512 | 46.0 | 35.0 | 9.0 | .77 | .22 | .30 | 2.5 |
| 16 | Grand Calumet; VII; 29 | 0.94 | 5.539 | 5.509 | 39.8 | 41.0 | 8.4 | | | | |
| 17 | Huddersfield; V; 20 | 0.88 | 5.540 | 5.515 | 36.8 | 40.1 | 7.7 | | | | |
| 18 | Dungannon; XVI; 14 | 0.83 | 5.553 | 5.521 | 40.0 | 46.4 | 8.0 | .77 | .22 | .29 | 1.9 |
| 19 | Huddersfield; V; 21, 22 | 0.70 | 5.547 | 5.523 | 36.3 | 49.7 | 8.6 | .78 | .23 | .29 | 2.1 |
| 20 | Huddersfield; IV; 20 | 0.43 | 5.564 | 5.537 | 25.0 | 55.5 | 6.8 | .74 | .22 | .30 | 2.2 |

It is apparent that the twenty samples can be divided into three distinct groups:

1. Uraninites containing 10% $ThO_2$ or less, and having a lattice constant less than 5.470 Å.

2. Uraninites containing between 10% and 18% $ThO_2$ and having lattice constants between 5.47 Å and 5.50 Å.

3. High thorian uraninites containing more than 20% $ThO_2$ and all thorianites. Lattice constants for this group are 5.51 to 5.65 Å.

Uranium, thorium and lead contents of groups 1 and 2 fall within, or close to, ranges of those published in Dana (1944) for uraninite. The three high thorian uraninites of group 3, (samples 13, 14 and 15), have compositions that are intermediate between those of published uraninites and thorianites. Composition of some of the thorianites, notably samples 18 and 19, also fall in a range in which other published analyses are lacking. Th:U ratios of thorianites for which analyses are published in Dana (1944) are: 19.6, 6.4, 2.2 and 1.07. For the six thorianites of samples 16 to 20, Th:U ratios are 1.08, 1.13, 1.2, 1.4 and 2.3. It is evident that the high thorian uraninites and thorianites of samples Nos. 13–20 extend the range in composition of known natural minerals in the uraninite-thorianite series and so strengthen the evidence that this series is fully isomorphous.

There is an interesting similarity in the types of deposits and mineralogy within each of the three groups. Deposits of *group* 1 are pegmatite, granite, and syenite dykes which have well-defined walls but which in part, may be due to replacement. Dominant minerals are potash and soda feldspars with some quartz. Titanite is a consistent accessory mineral and zircon, apatite, and fluorite are also present in most deposits. In *group* 2 the deposits include calcite-fluorite-apatite veins that are transitional to pegmatites, and mica pyroxenites containing abundant calcite, fluorite, and minor apatite.

Deposits of *group* 3 are remarkably similar in essential characters and are quite unlike those of groups 1 and 2. They all occur in impure crystalline limestones as metasomatized zones which are apparently transitional to the country rock. In these zones, calcite is the dominant mineral and contains somewhat smaller proportions of subhedral diopside and phlogopite. In 7 of the 8 deposits the calcite is distinctively salmon-red in colour in contrast to the white and grey calcite in the impure limestone. Titanite, and less commonly, thorite, chondrodite and pyrite, are accessory minerals. It may be noted that Dana (1944) lists the one American deposit as occurring in serpentine at the contact of limestone and pegmatite.

Relative intensities of diffraction from the (220), (311), (222) and (400) planes in unheated material were measured to determine whether there was any systematic variation of relative intensity with U:Th ratio, which might indicate some ordered, rather than random substitution of Th for U in the lattice. The atomic scattering factor of uranium is roughly 2% greater than that of thorium, so that differences in diffraction intensities due to possible ordered substitution of Th for U would be slight. Moreover, possible ordered effects resulting from auto-oxidation of $UO_2$ to $UO_3$ might well overshadow the Th for U substitution. The four sets of ratios shown do exhibit some indication of a trend with the U:Th ratio but reversals and lack of consistency combined with the stated limits of experimental error require that these results be treated with reserve. In general the intensity of the (222) powder diffraction relative to (311) and (400) appears to increase with thorium content. Random substitution of thorium for uranium would result in a relative decrease in the (222) intensitites. Differences in the absorbtion of copper radiation by $UO_2$ due to oxidation of U, the presence of thorium, lead and rare earth elements such as cerium might also have a significant effect on the observed intensities. In this connection it may be significant that although the octahedron quite commonly modifies the cube in low thorian uraninites, it has not been observed in uraninite and thorianite crystals of group 3. It is also noteworthy that in 4 of the 5 deposits containing thorianite, twinned crystals were found with (111) as the twin axis. None of the uraninites exhibited this twinning.

## REFERENCES

BROOKER, E. J., & NUFFIELD, E. W. (1952): Studies of radioactive compounds: IV—Pitchblende from Lake Athabaska, *Am. Mineral.*, **37,** 363–385.

DANA, J. D., & E. S. (1944): *System of Mineralogy* **1,** ed. 7, by C. Palache, H. Berman and C. Frondel—New York.

DONNAY, J. D. H., & NOWACKI, W. (1954): Crystal Data, *Geol. Soc. Am., Mem.* **60.**

ELLSWORTH, H. V. (1932): Rare-element Minerals of Canada, *Geol. Surv., Canada, Ec. Geol. Ser.*, No. **11.**

GRAHAM, A. R. (1955): Cerianite $CeO_2$: A new rare earth oxide mineral, *Am. Mineral.*, **40,** 560–564.

HEYSTEK, H., & SCHMIDT, E. R. (1953): The technique of differential thermal analysis and its application to some South African minerals, *Trans. Geol. Soc. South Africa*, **56,** 149–176.

KERR, P. F. (1950): Mineralogical Studies of Uraninite and Uraninite-bearing Deposits, *Int. Tech. Rept., Raw Materials Division, U. S. Atomic Energy Commission.*

SATTERLY, J., & HEWITT, D. F. (1955): Some Radioactive Mineral Occurrences in the Bancroft Area, *Ont. Dept. Mines, Geol. Cir.* No. **2.**

SLOWINSKI, E., & ELLIOTT, N. (1952): Lattice constants and magnetic susceptibilities of solid solutions of uranium and thorium dioxides, *Acta Cryst.*, **5,** 768–770.

WASSERSTEIN, B.: Ages of uraninites by a new method, *Nature,* **174,** 1004–1005.

WOLFE, S. E., & HOGG, N. (1948): Report on some Radioactive Mineral Occurrences in Cardiff and Monmouth Townships, Haliburton County, Ontario, *Ontario Dept. Mines, P.R.* 1948–8.

# STUDIES OF RADIOACTIVE COMPOUNDS: VIII—URANOPHANE AND BETA-URANOPHANE[1]

D. H. Gorman and E. W. Nuffield,
*University of Toronto, Toronto, Canada.*

## Abstract

Uranophane and beta-uranophane are dimorphous with composition $CaO \cdot 2UO_3 \cdot 2SiO_2 \cdot 6H_2O$ as found by Nováček (1935). Uranophane: Monoclinic, $a=15.87$, $b=7.05$, $c=6.66$ Å, $\beta=97°\ 15'$; space group $P2_1/a$ or $P2/a$; $Z=2$; SG=3.83 (meas.), 3.85 (calc.); needle-like crystals elongated $b[010]$. Beta-uranophane: Monoclinic, $a=6.64$, $b=15.55$, $c=14.01$ Å, $\beta=91°$; space group $P2_1/c$; $Z=4$; SG=3.90 (meas.), 3.93 (calc.); needle-like crystals elongated $c[001]$.

## Uranophane

Uranophane $CaO \cdot 2UO_3 \cdot 2SiO_2 \cdot 6H_2O$, is by far the most common uranium silicate mineral. Billiet (1936) gives an account of the history of the species. It was first described by Websky in 1853 from Kupferberg, Silesia. Bořický described the same species from Wölsendorf in 1870 and called it uranotil. Since that time the two names have been synonymous, although in 1892, Pjatnitzky proposed uranotil for the well crystallized material, and uranophane for that material which could not be studied goniometrically. Subsequently uranophane, which occurs at practically every locality where pitchblende is found, was described by a number of investigators whose studies were concerned with the optics, chemistry and the goniometry of the species.

Billiet made the first *x*-ray study of the mineral. Powder photographs were taken, and unit cell dimensions determined from a series of single crystal rotation photographs. The chemical formula was then established from the *x*-ray data and existing chemical analyses. Since 1936 no further detailed work has been done, although uranophane has been reported from several localities not previously recorded.

In the course of a re-examination of all the uranium silicate minerals, the present authors, realizing the *x*-ray techniques employed by Billiet might have led to erroneous interpretation, undertook a more detailed *x*-ray examination of uranophane. Observations on physical properties and optics were also made, and are included in summary with those of previous investigators.

### *Physical properties*

Uranophane occurs as idiomorphic crystals which are prismatic or acicular, sometimes reticulate, but more often in divergent clusters or tufts. Crystals are found most frequently in small vugs, and rarely exceed 1 mm. in length. More commonly the mineral is compact, massive or powdery, and often is seen as scaly incrustations or films on primary minerals, and not infrequently as paper thin sheets in minute cracks.

---

[1] Extracted from Gorman's thesis for the Ph.D. degree, University of Toronto.

The color is rather variable, lemon yellow, canary yellow, orange yellow, and very often very pale yellow. The massive varieties exhibit the greatest variation in color. Various authors have described the luster of the crystals as pearly or greasy, probably an accurate assessment, although the material we studied was so minutely acicular as to appear silky. The massive varieties are earthy to resinous, or waxy for the more compact, scaly type.

Crystals have perfect pinacoidal cleavage, reasonably assumed to be (100) by analogy with that more precisely determined for beta-uranophane. The hardness, as far as can be ascertained, is 2–3 as expressed on Mohs' scale. The massive varieties can be scratched easily with a needle.

Billiet (1936) lists specific gravities of 2.6, 2.7, 3.81, 3.89, 3.96 and 4.17 recorded by various observers. He calculated a specific gravity of 3.81 and measured it as 3.809 using Clerici solution. We also found a variation in specific gravity for non-crystallized material, due in part we think, to the porosity of the material or admixed impurities. On clean, crystallized material from Wölsendorf, Bavaria, Gorman determined the gravity to be 3.83. It is interesting to note that this is the value used by Billiet in calculating his cell contents. The gravity calculated from our cell dimensions is 3.85.

As in a great many descriptions of secondary uranium minerals, those concerning uranophane are replete with "possibles" and "maybes" regarding fluorescence. On both massive and crystallized varieties previous determinations have been recorded as "some" and "faint green." The present authors found that under both long and short wave ultraviolet light the massive material showed no fluorescence, and the crystallized variety a faint green emission.

The optical properties of uranophane are well established. Table 1 is a summary of those properties compiled from data by Larsen, Hess & Schaller (1926) with our determinations shown in the second column. George (1949) states that for all the uranophane sent to him by field engineers the optical properties have always fallen within the limits recorded in the literature.

### *Crystallography*

Billiet (1936) made an $x$-ray examination of uranophane, obtaining a powder photograph of the material from Chinkolobwe, and unit cell dimensions from a series of rotational photographs—a remarkable feat

TABLE 1. THE OPTICAL PROPERTIES OF URANOPHANE

| | Larsen, Hess & Schaller (1926) | Gorman & Nuffield (1955) |
|---|---|---|
| $\alpha$ | 1.642–1.645 | 1.642 |
| $\beta$ | 1.665–1.667 | 1.666 |
| $\gamma$ | 1.667–1.672 | 1.668 |
| Sign | negative | negative |
| $2V$ | 32–45 (Na) | small |
| Dispersion | strong $r<v$ | marked |
| Opt. orient. | $Z$ = elongation | $Z$ = elongation |
| Pleochroism | $\alpha$ nearly colorless<br>$\beta$ pale canary yellow<br>$\gamma$ canary yellow | $\alpha$ nearly colorless<br>$\beta$ nearly colorless<br>$\gamma$ pale yellow |

considering the size of the crystals with which he worked. His cell dimensions were recorded as

$$a = 6.68\ \text{Å (probably kX)}, \qquad b = 15.28, \qquad c = 7.3 = \text{elongation}.$$

No powder data were given.

The present authors obtained *x*-ray powder patterns of several types of uranophane, powdery, waxy and crystallized. All patterns were identical except one of material from Mexico, which indicated a slightly smaller cell. The powdery or waxy material did not give such sharp patterns as the well crystallized type. A print of the powder photograph of well crystallized material from Nabburg, Bavaria is shown in Figure 1. Powder data for uranophane from Nabburg are given in Table 2.

Rotation and Weissenberg photographs were taken of a minute needle of uranophane from Nabburg. From these photographs the following data were obtained:

$$a = 15.87\ \text{Å}, \qquad b = 7.05 = \text{elongation}, \qquad c = 6.66, \qquad \beta = 97°15'$$

Some months later these constants were confirmed by Lipscomb.[1] The space group is $P2_1/a$ or $P2/a$.

Uranophane has always been described as orthorhombic, except by Pjatnitzky (1892, in Billiet, 1936) who reported it as triclinic. Billiet gives an exceedingly complete summary of the goniometry of this species, listing all the observed forms and angular measurements for an orientation $c$ = axis of elongation. In his conclusion he appears to make the majority of observations fit an orthorhombic symmetry. In reading his paper it is noticeable that he stresses over and over that most observers reported that goniometric measurements were poor. Because,

---

[1] Private communication, Prof. J. Gruner, University of Minnesota.

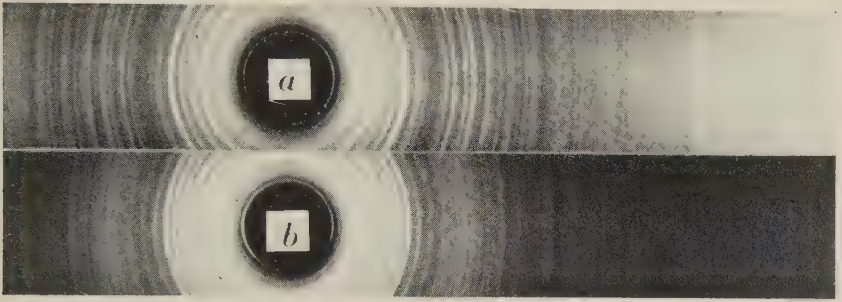

FIG. 1. (a) Uranophane, Nabburg, Bavaria; (b) beta-uranophane, Jachymov, Bohemia. *X*-ray powder photographs using Cu/Ni radiation ($\lambda = 1.5418$ Å); camera diameter 57.3 mm; actual size prints.

in his *x*-ray study, he used rotation photographs only, Billiet had no means of assessing properly the true symmetry, and merely conjectured it to be orthorhombic from previous goniometric measurements.

Uranophane is proved by the present authors to be monoclinic, $2/m$, with crystals elongated in the $b[010]$ direction.

$$a:b:c = 2.252:1:0.945, \qquad \beta = 97°15'$$
$$p:q:r = 0.448:1:1.067, \qquad \mu = 82°45'$$

The axial ratios were calculated from the cell dimensions.

It is interesting to note from Billiet's summary of goniometric studies,

TABLE 2. URANOPHANE, NABBURG, BAVARIA. *X*-RAY POWDER DATA

Cu/Ni radiation; $\lambda = 1.5418$ Å

| $I_{Cu}$ | $d$ | $I_{Cu}$ | $d$ | $I_{Cu}$ | $d$ | $I_{Cu}$ | $d$ |
|---|---|---|---|---|---|---|---|
| 10 | 7.55 | 8 | 2.08 | ½ | 1.364 | ½ | 0.956 |
| 3 | 6.41 | 5 | 1.947 | ½ | 1.326 | 4 | 0.951 |
| 4 | 5.21 | 5 | 1.901 | ½ | 1.288 | 1 | 0.935 |
| 6 | 4.67 | 5 | 1.859 | 3 | 1.256 | 1 | 0.918 |
| ½ | 4.23 | ½ | 1.816 | 5 | 1.226 | 2 | 0.909 |
| 9 | 3.83 | 5 | 1.764 | 3 | 1.171 | 2 | 0.897 |
| 4 | 3.48 | 5 | 1.733 | 3 | 1.151 | ½ | 0.886 |
| 5 | 3.17 | ½ | 1.708 | ½ | 1.133 | ½ | 0.877 |
| 9 | 2.94 | 3 | 1.646 | 1 | 1.109 | 3 | 0.870 |
| 5 | 2.86 | 4 | 1.589 | 1 | 1.099 | 3 | 0.837 |
| 4 | 2.64 | 4 | 1.564 | ½ | 1.041 | ½ | 0.825 |
| 3 | 2.57 | 2 | 1.531 | ½ | 1.024 | 2 | 0.811 |
| 2 | 2.49 | 4 | 1.491 | 1 | 1.016 | 1 | 0.805 |
| ½ | 2.24 | 1 | 1.454 | ½ | 1.001 | 2 | 0.798 |
| 7 | 2.17 | 3 | 1.434 | ½ | 0.986 | ½ | 0.790 |
|  |  |  |  |  |  | 2 | 0.786 |

that Zepharovich in his Mineralogisches Lexicon lists the angle between the largest pinacoidal faces as 82°, and that Schrauf in 1873 gave

$$(110)(\bar{1}10) = 97^\circ \quad \text{and} \quad (110)(1\bar{1}0) = 82\tfrac{1}{2}^\circ$$

All three of these goniometric measurements are in rigorous harmony with $\beta = 97^\circ 15'$ as determined by our *x*-ray analysis.

Owing to the size of the crystals available to us, their amenability to optical goniometry, and after a perusal of the existing literature on the measurements of uranophane crystals, we offer only this—that the crystals are elongated in the *b*[010] direction, there are basal and front pinacoids, and other smaller faces in the $\{h0l\}$ zone, with minute terminations of $\{0kl\}$ and possible $\{hkl\}$, all of simple indices.

### *Chemistry*

In Table 3 are listed 11 analyses of uranophane from various localities. The sources of these analyses are appended. In fairness it must be admitted that analyses were selected that were in close conformity with those published with the original description of the mineral. Other analyses showing appreciable amounts of Cu, Co, Ni, Fe exist and will be included in further papers on sklodowskite and cuprosklodowskite, when the isomorphism of these minerals with uranophane will be discussed.

Table 3. Chemical Analyses of Uranophane

| | 1 | 2 | 3 | 4 | 5 | 6 | 7 | 8 | 9 | 10 | 11 |
|---|---|---|---|---|---|---|---|---|---|---|---|
| $SiO_2$ | 17.08 | 13.78 | 13.02 | 14.48 | 13.72 | 13.24 | 13.47 | 13.24 | 14.23 | 13.9 | 13.3 |
| $UO_3$ | 53.33 | 66.75 | 63.93 | 62.84 | 66.67 | 65.87 | 64.36 | 65.96 | 69.32 | 67.2 | 61.0 |
| $Al_2O_3$ | 6.10 | 0.51 | trace | trace | trace | — | — | — | — | — | — |
| $Fe_2O_3$ | — | — | 3.03 | 2.88 | trace | 0.14 | 0.47 | trace | — | — | — |
| CaO | 5.07 | 5.27 | 5.13 | 5.49 | 6.67 | 7.05 | 7.49 | 7.00 | 2.86 | 6.5 | 10.3 |
| $H_2O$ | 15.11 | 12.67 | 14.55 | 13.79 | 12.02 | 13.11 | 13.33 | 13.17 | 12.28 | 12.6 | 13.9 |
| MgO | 1.46 | — | — | — | — | — | — | — | — | — | — |
| $K_2O$ | 1.85 | — | — | — | — | — | — | — | — | — | — |
| $P_2O_5$ | — | — | — | — | 0.29 | — | — | — | 1.10 | — | — |
| PbO | — | 0.45 | — | — | 0.60 | — | — | — | — | — | — |
| BaO | — | — | — | — | 0.28 | — | — | — | — | — | — |
| SrO | — | — | — | — | 0.13 | — | — | — | — | — | — |
| S.G. | — | 3.96 | — | 3.856 | 3.834 | — | — | — | 3.78 | — | — |
| Totals | 100.00 | 99.43 | 99.66 | 99.48 | 100.38 | 99.41 | 99.11 | 99.37 | 99.79 | 100.2 | 98.5 |

1. Uranophane, Kupferberg, Silesia; anal. Grundman (1859), recalc. Websky (1870) after deducting 7% impurities. 2. Uranotil, Wölsendorf, Bavaria; anal. Bořický (1870). 3, 4. Uranotil, Neustadtel, Saxony; anal. Winkler (1880). 5. Uranophane, Mitchell Co., N. C.; anal. Genth (1879). 6, 7, 8. Uranophane, Mitchell Co., N. C.; anal. von Foullon (1883). 9. Uranotil, Luiswishi, Katanga; anal. Schoep (1921). 10. Uranotil, Lusk, Wyoming; anal. Larsen, Hess & Schaller (1926). 11. Uranophane, Yancy, N. C.; anal. Sherwood (1952, priv. comm.). Note: analyses 1–7 taken from Dana (1892), analysis 8 from von Foullon (1885).

The analyses listed show a reasonable uniformity considering the nature of the material used, i.e. impure powdery or massive, and the small amounts available for analyses of the crystallized variety. Billiet (1936) lists all the formulae, in oxide form, that have been suggested, and in conclusion agrees with Nováček that the most reasonable choice is $CaO \cdot 2UO_3 \cdot 2SiO_2 \cdot 6H_2O$. There appeared some justification for a deviation from $6H_2O$ and Schoep (1927) maintained a water content of $7H_2O$. However, it will be shown in the following discussion of the calculation of the cell contents that $6H_2O$ is the better choice, and particularly so since unpublished data (Gorman) indicate that $6H_2O$ is the best choice for the water content of sklodowskite, the magnesium analogue of uranophane.

Billiet (1936) chose 4 representative analyses (5, 6, 7 & 8 of Table 3) and calculated the cell contents for his dimensions and a gravity of 3.834. His results are noted in the first 4 columns of Table 4. Column V shows the averages as calculated by the present authors. Thus Billiet justified the formula $2[CaO \cdot 2UO_3 \cdot 2SiO_2 \cdot 6H_2O]$.

TABLE 4. THE CELL CONTENTS OF URANOPHANE

| | I | II | III | IV | V | VI | VII |
|---|---|---|---|---|---|---|---|
| U | 4.04 | 3.98 | 4.00 | 3.90 | 3.98 | 3.91 | 4 |
| Si | 3.95 | 3.82 | 3.82 | 3.88 | 3.87 | 3.80 | 4 |
| Ca | 2.06 | 2.19 | 2.16 | 2.31 | 2.18 | 2.14 | 2 |
| O | 22.08 | 21.77 | 21.80 | 21.77 | 21.86 | 21.49 | 22 |
| $H_2O$ | 11.57 | 12.56 | 12.68 | 12.82 | 12.41 | 12.20 | 12 |
| Totals | 43.70 | 44.32 | 44.56 | 44.68 | 44.30 | 43.44 | 44 |

I–IV. Billiet's (1936) calculated cell contents for 4 analyses using his dimensions and SG 3.834. V. Aver. of I–IV. VI. Billiet's aver. recalc. using Gorman & Nuffield cell dimensions and SG 3.83. VII. Ideal cell contents for $2[CaO \cdot 2UO_3 \cdot 2SiO_2 \cdot 6H_2O]$.

The newly proposed cell dimensions with a measured specific gravity of 3.83 gave a cell content weight that is related to Billiet's by a factor of 0.983. It seemed superfluous to calculate the cell contents for each analysis, and consequently the conversion factor was applied to Billiet's calculated averages. The resultant atomic proportions are shown in Table 4, column VI with the ideal contents for $2[CaO \cdot 2UO_3 \cdot 2SiO_2 \cdot 6H_2O]$ given in column VII. The calculated specific gravity using this formula is 3.85, which is in close agreement with our measured value, 3.83.

### *Mode of occurrence*

Of the several uranium silicates, uranophane is the most abundant and has the widest geographical distribution. Moreover it is being identified from so many localities now that *x*-ray powder photography is used so extensively, that it appears to be one of the most common secondary uranium bearing minerals. It is found associated with other secondary uranium minerals, notably autunite, torbernite, beta-uranophane, kasolite, schoepite and sklodowskite and is an important constituent of gummite (as defined in Dana's System of Mineralogy, 1944).

There is no doubt that it is secondary after primary uranium minerals, but there is some disagreement as to whether it is of supergene or deuteric origin. Ross, Henderson & Posnjak (1931) favor a hydrothermal or deuteric origin for the occurrence at Spruce Pine, New Jersey where it is associated with fresh feldspar. George (1949) notes a similar type of occurrence at the Ruggles Mine, New Hamsphire. In several Ontario localities uranophane is invariably associated with feldspar, and could have had a deuteric origin.[1] George further states that a deuteric origin is not universal, and gives evidence for a supergene origin of uranophane in Portugal, in Stone Mountain, Virginia, and in Lusk, Wyoming. In the famed Chinkolobwe, Katanga deposits, where uranophane is abundant, Néve (1915) points out that it is the last radioactive mineral save the phosphates, and postulates a supergene origin. Hogarth (1951) describes a similar but smaller zone of uranophane at the Nicholson mine, Saskatchewan, placing this mineral very late in his paragenetic sequence.

In addition to the above mentioned localities, uranophane occurs at Wölsendorf and Nabburg, Bavaria; Kupferberg, Silesia; Schneeberg and Neustadtel, Saxony; Jachymov, Bohemia; Namaqualand, Africa; Yancy, North Carolina; Great Bear Lake, Wilberforce and Kenora districts, Canada. Uranophane from Villeneuve, Quebec (Hoffman, 1901) the earliest reference to Canadian material, is not uranophane, but is as yet unidentified.

## BETA-URANOPHANE

Nováček (1935) proposed the name beta-uranotile for greenish-yellow needle-like crystals from Jachymov, which gave by chemical analysis the same formula as uranophane, but distinctly higher indices of refraction. Billiet (1936) attempted single crystal *x*-ray studies of the Jachymov material but because of the quality of the crystals, only powder work was possible. This confirmed however, the distinction between uranophane and beta-uranotile. Steinocher & Nováček (1939) published the results of a detailed optical study of beta-uranotile. They showed that material labelled schroeckingerite from Bedford, New York and Mitchell county, North Carolina was in fact beta-uranotile and discovered the mineral in specimens from Wölsendorf. Precise goniometric measurements were not possible. Meixner (1949) observed the mineral on samarskite from Sankara, Nellore, India. Satterly (1955) found an occurrence in MacNicol township, Kenora district, Ontario.

---

[1] Private communication, Dr. J. Satterly, Ontario Dept. Mines.

We too found that the Jachymov beta-urantoile offered no opportunities for single crystal studies. Similarly a new occurrence from Quebec proved unsuitable. This material, sent to us by Mr. G. R. Forbes, an engineer with Yates Uranium Mines, was said to occur in lot 20, range 4, Huddersfield township, Pontiac county. It is found as tiny intergrown needles on orange-colored crystalline limestone which also contains uranoan thorianite. This study was finally made possible by another occurrence, in Faraday township, Hastings county, Ontario which was discovered by Dr. J. Satterly (Satterly & Hewitt, 1955) of the Ontario Department of Mines. Beta-uranotile occurs here sparingly in pegmatite dikes with other radioactive minerals such as uranothorite, uraninite, allanite and secondary uranophane. Our specimen consists of a piece of split drill core containing a 3 mm. cavity in plagioclase which is filled with radiating groups of well-crystallized needles.

### *Physical properties*

Beta-uranotile commonly occurs as minute acicular crystals in radial tufts, or as stubby, flattened prismatic crystals in reticulate groups. Unlike uranophane, the massive variety is less common, but it does occur as thin coatings and scales. The color varies from greenish yellow to orange yellow, unlike uranophane which is often a bright canary yellow. The highly acicular variety exhibits a silky luster, becoming more sub-adamantine to greasy for larger crystals, and waxy for the scaly type. The cleavage as recorded by Nováček (1935) and confirmed in this study is parallel to $b(010)$. The hardness is 2–3 on the Mohs' scale. Steinocher & Nováček (1939) list specific gravities of 3.953, 3.85 and 3.8. On clean, acicular crystals from Faraday township, Gorman determined the value 3.90. The calculated gravity, as shown below, is 3.93.

The degree of fluorescence has been reported as "questionable" or "none," yet all of the specimens examined by us show a definite though weak green emission under both short and long wave ultraviolet excitation. Satterly (1955) reports that a scaly beta-uranophane (identified by *x*-ray powder pattern) from the Kenora district, Ontario fluoresces bright green.

Steinocher & Nováček (1939) made an exceedingly detailed study of the optical properties. In summary they report for Na light: $\alpha$ 1.661–1.668, $\beta$ 1.682–1.695, $\gamma$ 1.689–1.702, negative, $2V$ small to 66°, $z \wedge c =$ 36–62°, $X$ colorless, $Y$ and $Z$ lemon yellow. Subsequent reports, including determinations made by the present authors confirmed their data. The "superbly crystalline" Urgeirica material of George (1949) which gave indices not in conformity with those of beta-uranotile was proved by Hogarth & Nuffield (1954) to be phosphuranylite.

### *Crystallography*

The Faraday crystals measure less than 1 mm. in length and closely resemble the Jachymov crystals described by Nováček (1935, Fig. 3). In Nováček's orientation they are elongated parallel to $c[001]$, somewhat flattened on $b(010)$ and also show $a(100)$. Two faces, $(h0l)$ and $(\bar{h}0l)$ terminate the crystals. The small face $c(001)$ noted by Nováček is not present and the (100) twinning which is common on Jachymov crystals, was not observed. The luster is vitreous, although sometimes pearly on the broad (010) cleavage faces.

A typical crystal mounted about the axis of elongation on a two-circle goniometer gave weak but distinct signals from $a(100)$ and $b(010)$ and a less distinct signal corresponding to a $\rho$ angle of $46 \pm 1°$ for one of the $(h0l)$ faces. Sharp rotation and Weissenberg films were obtained about $c[001]$ and zero and first level precession films about $a[100]$ and $b[010]$. The films showed monoclinic symmetry and gave the constants:

$a = 6.64$ Å, $b = 15.55$, $c = 14.01$ = elongation, $\beta = 91°$; space group $P2_1/c$

The rotation film about $c[001]$ showed alternate weak and strong layer lines indicating a pseudo-period with $c' = c/2$.

It is interesting to observe that Nováček detected the slight departure from orthorhombic geometry with two-circle measurements on imperfect crystals. He gave the $\rho$ angle of (001) as "no larger than 2°". Later Steinocher (Steinocher & Nováček, 1939) reported $\beta$ about 94° from measurements under the microscope.

Nováček obtained $\rho = 48° \ 36'$ (aver. of 7 from $49° \ 0'$ to $48° \ 19'$) from the one measurable $(h0l)$ face on his crystals. This compares with $46 \pm 1°$ measured on our material and corresponds to (102) or $(\bar{1}02)$ (calc. $47° \ 1'$ and $46° \ 5'$ respectively for our lattice constants). The $(h0l)$ termination which did not give a signal appears by inspection to have about the same $\rho$ angle and therefore it can be safely assumed that both (102) and $(\bar{1}02)$ are present on the Faraday crystals. The appearance of these faces in preference to (101) is compatible with the space group extinction condition: $(h0l)$ present only with $l$ even.

The usual $x$-ray powder print (Fig. 1) and powder data (Table 5) are presented to aid in the future identification of beta-uranophane.

### *Chemistry*

The only two complete analyses of beta-uranotile, both by Nováček, are presented in Table 6, together with the cell contents calculated for

TABLE 5. BETA-URANOPHANE, JACHYMOV, BOHEMIA. *X*-RAY POWDER DATA

Cu/Ni radiation; $\lambda = 1.5418$ Å

| $I_{Cu}$ | $d$ | $I_{Cu}$ | $d$ | $I_{Cu}$ | $d$ | $I_{Cu}$ | $d$ |
|---|---|---|---|---|---|---|---|
| 10 | 7.49 | 4 | 2.00 | 4 | 1.347 | 1 | 0.957 |
| 2 | 6.50 | 2 | 1.971 | 2 | 1.298* | 3 | 0.947 |
| 5 | 5.98 | 5 | 1.924 | 4 | 1.263* | 1 | 0.934 |
| 8 | 5.04 | 4 | 1.872 | 1 | 1.240 | 3 | 0.920 |
| 8 | 4.53 | 2 | 1.823 | 2 | 1.183 | 3 | 0.908 |
| 3 | 4.11 | 2 | 1.783 | 4 | 1.158 | 1 | 0.896 |
| 9 | 3.83 | 3 | 1.727 | 2 | 1.138 | 1 | 0.884 |
| 8 | 3.51 | 2 | 1.690 | 2 | 1.115 | 3 | 0.873 |
| 7 | 3.17 | 1 | 1.651 | 3 | 1.085 | 1 | 0.864 |
| 8 | 3.02 | 5 | 1.614 | 2 | 1.064 | 1 | 0.850 |
| 9 | 2.80 | ½ | 1.579 | 1 | 1.045* | 2 | 0.841 |
| 6 | 2.58 | 2 | 1.540 | 1 | 1.032* | 1 | 0.831 |
| 4 | 2.36 | 2 | 1.518 | 1 | 1.013* | 2 | 0.825 |
| ½ | 2.27 | 1 | 1.478 | 2 | 1.000* | 2 | 0.802 |
| 4 | 2.19 | ½ | 1.458 | 1 | 0.990 | | |
| 2 | 2.13 | ½ | 1.442 | 1 | 0.976 | | |
| 2 | 2.07 | ½ | 1.411 | 2 | 0.967 | | |

* Diffuse.

our lattice constants and the measured gravity, 3.90. The calculations suggest the cell contents $4[CaO \cdot 2UO_3 \cdot 2SiO_2 \cdot 6H_2O]$ which are compatible with the formula derived by Nováček. The departure of $SiO_2$ and CaO from the ideal may be attributed to the small quantity of material which was available for the analyses.

At this time there is insufficient data to propose structural formulae for uranophane and beta-uranophane. A determination of the character of the water would be helpful but unfortunately the problem of obtaining enough material for this purpose has not been overcome.

TABLE 6. CHEMICAL ANALYSES AND CELL CONTENTS OF BETA-URANOPHANE

| | 1 | 2 | 3 | 4 | 5 | 6 |
|---|---|---|---|---|---|---|
| $SiO_2$ | 13.11 | 12.9 | 14.02 | 7.5 | 7.3 | 8 |
| $UO_3$ | 66.29 | 66.9 | 66.8 | 7.9 | 8.0 | 8 |
| CaO | 7.32 | 7.1 | 6.55 | 4.5 | 4.3 | 4 |
| $H_2O$ | 12.87 | 12.6 | 12.62 | 24.4 | 23.9 | 24 |
| Totals | 99.59 | 99.5 | 100.00 | 44.3 | 43.5 | 44 |
| S.G. | 3.953 | 3.85 | | | | |

1. Jachymov, on 7.5 mgs.; anal. Nováček (1953) 2. Wölsendorf, Bavaria on 2 mgs.; anal. Nováček (1939) 3. Ideal composition based on $CaO \cdot 2UO_3 \cdot 2SiO_2 \cdot 6H_2O$. 4. Cell contents calculated for 1. 5. Cell contents calculated for 2. 6. Ideal cell contents.

### *Synonymy*

Although precedent has already been set for the use of varietal names in describing various forms of a single species, i.e. pitchblende and uraninite, brucite and nemalite, this is a practice that should be discouraged to the point of elimination. Uranophane has precedence over uranotile, and Nováček (1935) merely called his newly identified material beta-uranotile because specimens on which he worked were labelled uranotile. It is therefore proposed that the two species described in this paper be called uranophane and beta-uranophane.

## SUMMARY

This study has confirmed the dimorphic character of uranophane and beta-uranophane. The constants for the cell of uranophane and the pseudo-cell of beta-uranophane are compared in Table 7. The comparison shows the remarkable similarity of two of the cell edges, namely 7 Å and 6.6 Å, which it will be shown in a future paper, are a feature of several uranium silicate minerals. It was found that cleavage occurs in the plane of these two periods in beta-uranophane. Although the cleavage orientation could not be determined in our uranophane crystals, it may be assumed that uranophane cleaves in a similar, i.e. parallel to (100) as has already been proposed in various reports. Thus cleavage takes place in a plane which is normal or nearly normal to the longest and most variable of the three cell dimensions. It is further worth noting that the axis of crystal elongation is along the 7 Å period in both species.

TABLE 7. COMPARISON OF URANOPHANE AND BETA-URANOPHANE

| *Uranophane* | *Beta-uranophane* |
|---|---|
| $a=15.87$ Å | $b=15.55$ Å |
| $b=\ 7.05$ (elongation) | $c'=\ 7.005=c/2$ (elongation) |
| $c=\ 6.66$ | $a=\ 6.64$ |
| $\beta=97°15'$ | $\beta=91°$ |
| SG (calc.) = 3.85 | SG (calc.) = 3.90 |

## ACKNOWLEDGEMENTS

The authors wish to record their thanks to Professor C. Frondel, Harvard University, Professor V. B. Meen, Royal Ontario Museum, and Dr. J. Satterly of the Ontario Department of Mines for the loan of specimens and to Mr. L. Cowan who measured and projected some of the Weissenberg photographs. We wish further to acknowledge the assistance provided by a National Research Council of Canada Studentship (to D. H. G.) and a Research Council of Ontario grant (to E. W. N.).

## REFERENCES

BILLIET, V. (1936): Uranotiel en Sklodowskiet, *Natuur. Tijd. Gent* No. **8**, 284.

DANA, J. D., & E. S. (1892): *System of Mineralogy*, ed. 6, New York.

———. (1944): *System of Mineralogy*, **1**, ed. 7, by C. Palache, H. Berman & C. Frondel, New York.

GEORGE, D. (1949): Mineralogy of Uranium and Thorium bearing minerals, *U. S. Atomic Energy Commission Report*, *RMO*-**563**, 186.

HOFFMAN, G. (1899): *Geol. Surv. Canada, Annual Report*, **12**, 16R.

HOGARTH, D. (1951): Meta-zeunerite, uranophane, kasolite and cuprosklodowskite in Canada, *Amer. Min.*, **36**, 411.

HOGARTH, D., & NUFFIELD, E. W. (1954): Studies of radioactive compounds: VII—Phosphuranylite and dewindtite, *Amer. Min.*, **39**, 444.

LARSEN, E. S. (1921): Microscopic determination of the non-opaque minerals, *U. S. G. S.* Bull. **679**.

LARSEN, E. S., HESS, F., & SCHALLER, W. (1926): Uranium minerals from Lusk, Wyoming, *Amer. Min.*, **11**, 155.

MEIXNER, H. (1940): Notizen über neue Vorkommen einiger Uran minerale, *Zentr. Min.*, Abt. A, 145 (in *Min. Abs.* **10**, 544).

NÉVE, J. (1915): Uranium deposits of Chinkolobwe, Kasolo, Katanga, *private report*.

NOVÁČEK, R. (1935): Study of some secondary uranium minerals, *Vest. kral. Ces. Spol.* (*Mem. Soc. Roy. Sc. Boheme*), Cl 2, No. 7, 1.

ROSS, C., HENDERSON, E., & POSNJAK, E. (1931): Clarkeite, a new uranium mineral, *Amer. Min.*, **16**, 213.

SATTERLY, J. (1955): Radioactive mineral occurrences in the vicinity of Hawk and Richard Lakes, *Ontario Dept. Mines*, Geol. Circular No. **1**.

SATTERLY, J., & HEWITT, D. F. (1955): Some radioactive mineral occurrences in the Bancroft area, *Ontario Dept. Mines*, Geol. Circular No. **2**.

SCHOEP, A. (1921): Sur la presence du radium au Katanga, *Bull. soc. chim. Belg.*, **30**, 219.

STEINOCHER, V., & NOVÁČEK, R. (1939): On β-Uranotile, *Amer. Min.*, **24**, 324.

VON FOULLON, H. (1883): Ueber Verwitterungsproducte des Uranpecherzes und über die Trennung von Uran und Kalk, *Jahr. der k. k. geolog. Reich.*, 1 [Abstract in *Zeit. Kryst.* **10**, 423].

# SYNTHESIS, STRUCTURES, AND PROPERTIES OF PLATINUM METAL TELLURIDES[1]

W. O. J. Groeneveld Meijer,[2] *Queen's University,*
*Kingston, Ontario, Canada.*

## Abstract

Tellurides of all platinum metals have been synthesized and characterized by $x$-ray and optical methods. Ditellurides of ruthenium, osmium, rhodium, and iridium have pyrite type structures, ditellurides of platinum and palladium are of the cadmium iodide type, iridium and palladium monotellurides have nickel arsenide type structures.

## Introduction and Acknowledgements

Only one platinum metal mineral, sperrylite ($PtAs_2$) is known to occur with certainty in the Sudbury ores. Since tellurium is one of the products recovered from the ores and no tellurium-bearing platinum metal minerals have been reported, the synthesis of the tellurides of the platinum metals was undertaken in order to obtain data which might eventually be of mineralogical, and therefore of geochemical, interest. More specifically, their synthesis was performed so that optical and crystallographical observations derived from them would be of assistance in their possible ultimate detection in polished sections of the ores.

The work is limited to a description of the products obtained by dry fusion of the metals in various atomic proportions in a vacuum. Some observations are included on phase relationships, especially in the system palladium-tellurium.

The research program was carried out in the laboratories of the Department of Geological Sciences, Queen's University, Kingston, under the supervision of Dr. J. E. Hawley. The author is indebted to Dr. L. G. Berry for his suggestions during the preparation of the manuscript.

## Synthesis

In principle, two methods are available for the preparation of compounds of the platinum metals with metalloids such as tellurium:

(1) By a "wet" procedure; for instance through the reaction of hydrogen telluride ($H_2Te$) on a platinum metal salt in solution, and

(2) By a "dry" procedure; by direct fusion of the weighed constituents.

The latter method is the more favorable for our purposes. When homogeneous (one phase) products are obtained, it is not necessary to analyze the product since we may assume that it will have a composition equal to that of the charge which is weighed out in definite stochiometric proportions. Otherwise hindersome, secondary reactions such as hydrolysis, oxidation, and disproportionation can be avoided or controlled by heating the charges in evacuated and sealed tubes.

---

[1] Extracted from a portion of an unpublished Ph.D. thesis by the author: The Geochemistry of the Platinum Metals with Respect to Their Occurrence in Nickeliferous Sulphide Deposits—*Queen's University,* 1954. This work was carried out with the aid of a scholarship from the Research Council of Ontario (1953).

[2] Now with McPhar Geophysics Limited, 36 Cranfield Road, Toronto, Canada.

As the platinum metals melt at high to very high temperatures and tellurium melts at a relatively low temperature (452° C. at atmospheric pressure), the reactions take place in the heterogeneous systems solid-vapor or solid-liquid. It is thus of importance that the solid phase be present in a finely divided state. For that reason, the platinum metals were used in either their "sponge" or "black" form. The chemicals used for this work are listed in Table 1.

Charges of 1.2 to 0.5 gm. were prepared by weighing out the platinum metal and the powdered tellurium in proportions, corresponding to the expected formulae of the compounds to be prepared. The powders were mixed and inserted into Vycor or Vitreosil glass tubes 7–8 mm. bore, 25 cm long sealed at one end. The tubes were then attached to a vacuum pump by airtight rubber tubing and collapsed in the center by heating with an oxygen-hydrogen flame until only a small passageway remained. After evacuation and with the pump running, the narrow constriction was sealed with the flame. During the sealing operation, small amounts of tellurium sublimate from the charge, and condense immediately above the sealed join. For this reason a slight excess of the metalloid was generally added over the calculated amount.

TABLE 1. CHEMICALS USED FOR FUSIONS

Te, metallic, coarsely crystalline, Fisher, C. P.
Pd, sponge, Falconbridge .062% other PM's; .009% Fe, .026% $SiO_2$; traces of Ni and Ag.
Pt, sponge, Falconbridge .042% other PM's; .042% $SiO_2$; traces of Fe and Ni.
Ir, sponge, Falconbridge .14% other PM's; .12% Ni, .03% Fe, .13% Si.
Rh, sponge, Falconbridge .23% other PM's; .07% Ni, .07% Fe, trace of Ag.
Ru, sponge, Falconbridge .05% Rh, .13% Ni, .05% Fe; traces of Ag, Pt, Pd.
Os, black, Johnson, Matthey & Mallory, spectrographically pure.

As the reactions in question are exothermic in character, all mixed charges were first brought to reaction by inserting the sealed tubes in a steel shell and heating this slowly in a furnace from room temperature to approximately 850° C. They were left at this temperature for 2 hours and then allowed to cool over a period of 12 hours in the furnace.

With palladium and platinum compounds, the reaction product is compact and apparently homogeneous. In such cases the tubes were broken open and the nuggets were sawed in halves. One half was mounted in bakelite for polished section study, the other reserved for $x$-ray examination. With compounds of the other platinum metals the products were generally loosely sintered and very fine-grained. Good $x$-ray photographs were obtained from these powders. In order to increase the grain size, the sintered fusion products were reground and sealed anew in evacuated silica glass tubing with the addition of a small amount of tellurium. Since the reaction had clearly taken place, the tubes were now heated for 24 or more hours over the hottest gas flame obtainable with a Mecker burner. In some instances, the grain size did increase so that with repetition of the fusion and grinding processes, polished sections could be prepared. Since the products were still porous in those cases, they were impregnated with a solution of bakelite in acetone under reduced pressure.

All $x$-ray photographs were made by the Debye-Scherrer powder method using a camera with an internal diameter of 57.3 mm.[1] Full correction for film shrinkage was applied. The fusion products belonged either to cubic (pyrite type) or hexagonal (niccolite and cadmium iodide types) systems. After indexing the films by standard methods outlined in Henry, *et al.* (1951), unit cell dimensions were calculated from the more precise back reflections and the interplanar spacings calculated from these dimensions.

## INDIVIDUAL PRODUCTS

### *Ruthenium Ditelluride* ($RuTe_2$)

Ruthenium ditelluride has been synthesized by Thomassen (1929) by dry fusion in vacuum. The structure was determined as being that of pyrite with $a_0 = 6.360 \pm .002$ Å. Wöhler, *et al.* (1933) also synthesized and analyzed the compound by heating ruthenium trichloride with an excess of tellurium in a porcelain boat in a carbon dioxide stream at atmospheric pressure.

In this series of syntheses the compound was prepared by fusing the metals in their correct atomic proportion. The black sintered product showed no crystal forms under the binocular microscope. By refusion in vacuum, a coarser grained product was obtained. Thomassen (1929) reports that the compound melts at a temperature, estimated at between 400 and 600° C. At no time was a liquid phase observed here although much higher temperatures were applied.

Under the microscope, in polished section, the following properties were determined on the porous subhedral aggregate: It is isotropic, fine-grained and has a high ($F$) Talmage hardness. The color is white, the reflection is strong. Etch reactions performed after Short (1940) are negative with KOH, KCN, HCl, and $FeCl_3$. With $HgCl_2$ an iridescent, in part grey, stain is produced which is easily rubbed off. $HNO_3$ produces slight effervescence between grain boundaries; a brownish stain with some iridescent colors is produced. The effects are probably due to tellurium, which is found sparsely in the section.

---

[1] Using $CuK\alpha_1 = 1.54050$ Å. (Ni filter).

An excellent powder diagram (Table 2) was obtained from which all lines could be indexed. The unit cell edge with $a_0$-6.377 ± .001 Å is slightly larger than that obtained by Thomassen (1929).

TABLE 2. RUTHENIUM DITELLURIDE—$RuTe_2$: X-RAY POWDER DATA

Cubic, Pyrite Structure; $a_0 = 6.377 \pm .001$ Å

| I | d (meas) | hkl | d (calc) | I | d (meas) | hkl | d (calc) |
|---|---|---|---|---|---|---|---|
| ½ | 3.70 | 111 | 3.68 | 6 | 1.126 | 440 | 1.127 |
| 4 | 3.16 | 200 | 3.19 | 2 | 1.060 | 600 | 1.062 |
| 10 | 2.82 | 210 | 2.85 | 2 | 1.046 | 610 | 1.049 |
| 9 | 2.57 | 211 | 2.60 | 4 | 1.033 | 611 | 1.034 |
| 3 | 2.24 | 220 | 2.25 | 1 | 1.008 | 620 | 1.008 |
| ½ | 2.11 | 300 | 2.12 | 4 | .972 | 533 | .973 |
| 10 | 1.905 | 311 | 1.92 | 1½ | .961 | 622 | .962 |
| 2 | 1.823 | 222 | 1.84 | 4 | .951 | 630 | .951 |
| 4 | 1.752 | 320 | 1.77 | 3 | .940 | 631 | .940 |
| 7 | 1.694 | 321 | 1.70 | 1 | .921 | 444 | .921 |
| 2 | 1.582 | 400 | 1.593 | 1 | .884 | 640 | .884 |
| ½ | 1.466 | 331 | 1.463 | 4 | .877 | 720 | .877 |
| 2 | 1.418 | 420 | 1.426 | 5 | .8680 | 721 | .868 |
| 4 | 1.386 | 421 | 1.390 | 2 | .8530 | 642 | .853 |
| 2 | 1.355 | 332 | 1.359 | 10 | .8319 | 731 | .830 |
| 2 | 1.296 | 422 | 1.301 | 7 | .8181 | 650 | .817 |
| 6 | 1.223 | 333 | 1.227 | 8 | .8117 | 732 | .810 |
| 5 | 1.181 | 520 | 1.183 | 6 | .7989 | 800 | .798 |
| 5 | 1.161 | 521 | 1.163 | 2 | .7752 | 820 | .774 |

### *Osmium Ditelluride* ($OsTe_2$)

Osmium ditelluride has been synthesized by Thomassen (1929) by dry fusion of the elements in vacuum. The substance was found to have a cubic pyrite-type structure with $a_0 = 6.369 \pm .003$ Å.

In this work the compound was synthesized in the usual manner. It was not possible to obtain a polished section from the loosely textured and very fine-grained fusion product. Thomassen (1929) reports that the compound melts at a temperature estimated between 500 and 600° C. No such melting was observed in this work. At high temperatures, the compound dissociates and tellurium condenses at cooler portions of the evacuated tube.

The powder photograph could be readily indexed on the basis of a cubic unit cell with $a_0 = 6.398_5 \pm .001$ Å. The photograph shows one extra line (d = 2.07, Table 3) which corresponds to the strongest osmium line and whose presence is not unexpected, considering the observed dissociation of the compound. The intensities of the other lines are quite similar to the corresponding lines of ruthenium ditelluride.

TABLE 3. OSMIUM DITELLURITE $OsTe_2$: X-RAY POWDER DATA

Cubic, Pyrite Structure; $a_0 = 6.398_5 \pm .001$ Å

| *I* | *d* (meas) | *hkl* | *d* (calc) | *I* | *d* (meas) | *hkl* | *d* (calc) |
|---|---|---|---|---|---|---|---|
| 1 | 3.67 | 111 | 3.69 | 1 | 1.038 | 611 | 1.038 |
| 2 | 3.18 | 200 | 3.20 | 3 | 1.010 | 620 | 1.011 |
| 4 | 2.84 | 210 | 2.86 | 4 | .973 | 533 | .975 |
| 3 | 2.60 | 211 | 2.61 | 3 | .962 | 622 | .964 |
| 3 | 2.25 | 220 | 2.26 | 3 | .951 | 630 | .953 |
| 2 | 2.07 |  |  | 2 | .9414 | 631 | .943 |
| 10 | 1.909 | 311 | 1.93 | 2 | .8949 | 711 | .895 |
| 1 | 1.836 | 222 | 1.845 | 2 | .8859 | 640 | .886 |
| 1 | 1.770 | 320 | 1.773 | 3 | .8781 | 720 | .878 |
| 3 | 1.702 | 321 | 1.710 | 3 | .8707 | 721 | .870 |
| 1 | 1.426 | 420 | 1.430 | 3 | .8541 | 642 | .855 |
| 1 | 1.392 | 421 | 1.396 | ½ | .8465 | 722 | .847 |
| 2 | 1.360 | 332 | 1.362 | 10 | .8331 | 731 | .8328 |
| 2 | 1.304 | 422 | 1.306 | 4 | .8192 | 650 | .8194 |
| 5 | 1.229 | 333 | 1.230 | 6 | .8122 | 732 | .8125 |
| 2 | 1.184 | 520 | 1.187 | 6 | .7995 | 800 | .7997 |
| 1 | 1.167 | 521 | 1.168 | 1? | .7894 | 811 | .787 |
| 4 | 1.127 | 440 | 1.130 | ? | .7824 | 733 | .781 |
| 1 | 1.080 | 531 | 1.081 | 6 | .7759 | 820 | .776 |
| 2 | 1.067 | 442 | 1.067 |  |  |  |  |

### *Rhodium (Di?) Telluride* ($RhTe_{2+x}$)

Some controversy exists in the literature as to the composition of rhodium-tellurium compounds. Wöhler, *et al.* (1933) synthesized and analyzed a ditelluride. Strangely enough, the authors remark, no compound analogous in composition to $Rh_2Se_5$ is formed. Biltz (1937) re-analyzed the compound and found a formula $RhTe_{2.45}$. He reports that the substance has a pseudo-pyrite structure. This structure was reported for $RhSe_{2.48}$, where pyrite lines were split into several distinct lines.

However, Biltz (1937) only reports that "slight line splitting is likely" for $RhTe_{2.45}$, and no further *x*-ray data are given for the compound.

A telluride of rhodium was prepared from a charge of the elements, mixed in the atomic proportion of $RhTe_{2.5}$. After several heat treatments, a fine-grained product was obtained, which was rendered coherent by an excess of tellurium. The compound is isotropic, its color is white in reflected light and slightly darker than the tellurium with which it was intergrown. The Talmage hardness is high (*F*). Etch reactions are negative with KOH, KCN, $FeCl_3$, and HCl. With $HNO_3$ faint intergranular effervescence was observed which is likely due to the presence of tellurium.

TABLE 4. RHODIUM (DI?) TELLURIDE—$RhTe_{2+x}$ *X*-RAY POWDER DATA

Cubic, Pyrite Structure; $a_0=6.428\pm.001$ Å

| *I* | *d* (meas) | *hkl* | *d* (calc) | *I* | *d* (meas) | *hkl* | *d* (calc) |
|---|---|---|---|---|---|---|---|
| 2 | 3.17 | 200 | 3.22 | 2 | 1.052 | 610 | 1.058 |
| 10 | 2.83 | 210 | 2.87 | 5 | 1.039 | 611 | 1.043 |
| 9 | 2.58 | 211 | 2.53 | 1 | 1.006 | 620 | 1.017 |
| 2 | 2.24 | 220 | 2.27 | 3 | .978 | 533 | .980 |
| 10 | 2.91 | 311 | 1.940 | 1 | .966 | 622 | .969 |
| 1 | 1.83 | 222 | 1.857 | 4 | .958 | 630 | .958 |
| 3 | 1.76 | 320 | 1.782 | 4 | .9461 | 631 | .948 |
| 8 | 1.70 | 321 | 1.719 | 1 | .9264 | 444 | .928 |
| 2 | 1.59 | 400 | 1.608 | $\frac{1}{2}$ | .8898 | 640 | .891 |
| 2 | 1.43 | 420 | 1.438 | 6 | .8828 | 720 | .884 |
| 4 | 1.394 | 421 | 1.403 | 8 | .8744 | 721 | .875 |
| 2 | 1.360 | 332 | 1.370 | 3 | .8592 | 642 | .860 |
| 1 | 1.304 | 422 | 1.312 | 10 | .8368 | 731 | .837 |
| 6 | 1.231 | 333 | 1.238 | 8 | .8229 | 650 | .823 |
| 5 | 1.187 | 520 | 1.193 | 9 | .8161 | 732 | .816 |
| 4 | 1.166 | 521 | 1.173 | 6 | .8035 | 800 | .804 |
| 6 | 1.128 | 440 | 1.137 | 6 | .7797 | 820 | .780 |
| 1 | 1.068 | 600 | 1.071 | 5 | .7755 | 821 | .774 |

An excellent *x*-ray powder photograph was obtained with very clearly resolved $K\alpha_1$ and $K\alpha_2$ doublet in the back reflection region. No line splitting of any kind was observed and all lines could be indexed on the basis of a cubic unit cell with $a_0=6.428\pm.001$ Å (Table 4). The intensity distribution is very similar to that of ruthenium telluride and a pyrite structure is clearly indicated for this compound. There is thus no evidence to advance in favor of a so-called pseudo-pyrite structure although the lack of tellurium lines on the powder photograph, which was taken before the compound was prepared for polished section by refusing it with excess tellurium, does tend to corroborate the $RhTe_{2+x}$ formula.

### *Iridium (Di?) Telluride* ($IrTe_{2+x}$)

Wöhler, *et al.* (1933) report the existence of two iridium tellurides: $IrTe_2$ and $IrTe_3$. Biltz (1937) analyzed a compound, saturated with tellurium and found $IrTe_{2.89}$. He includes the substance in the pseudopyrite structural classification, although it is stated that a slight splitting of pyrite lines is only "likely." No further $x$-ray observations are mentioned.

In this work an iridium telluride was prepared from the charge $IrTe_{2.5}$. As with osmium, this compound loses tellurium at higher temperatures. A satisfactory polished section could not be prepared of the friable, sintered product.

The powder photograph of the product was easily indexed on the basis of a cubic unit cell with $a_0 = 6.411 \pm .002$ Å. No effects of line splitting could be observed in the very clear film. The intensities of the lines (Table 5) are very similar to those measured in the other compounds of the platinum metals already described with pyrite structures.

### *Iridium Monotelluride* (IrTe)

In the preparation of iridium ditelluride it was noticed that the product lost tellurium at higher temperatures. The $x$-ray powder photograph did not show iridium lines and as the diagram seemed amenable to indexing on a hexagonal lattice of the niccolite type, a fusion product was prepared of the composition IrTe.

Iridium monotelluride formed a friable fine-grained sintered product. It was impossible to prepare a polished section of the compound; attempts to fuse it in a hollow carbon electrode in the arc resulted in its dissociation to metallic iridium.

The powder photograph was indexed (Table 6) on the basis of an orthohexagonal unit cell with $a_0 = 3.930$ Å, $c_0 = 5.386$ Å, and $c = 1.370$. After a first trial indexing, more accurate interplanar spacings were obtained with the Philips $x$-ray diffractometer on a few planes with $00l$, $hk0$, and $hkl$ type indices.

### *Palladium Ditelluride* $PdTe_2$

Thomassen (1929) prepared palladium ditelluride and found for it a cadmium iodide type structure with $a_0 = 4.028 \pm .003$ Å, $c_0 = 5.118 \pm .004$ Å, and $c = 1.271$. Wöhler, *et al.* (1933) prepared the ditelluride as the only compound in the system Pd-Te.

Table 5. Iridium (Di?) Telluride—IrTe$_{2+x}$ *X*-ray Powder Data

Cubic, Pyrite Structure; $a_0=6.411\pm.002$ Å

| *I* | *d* (meas) | *hkl* | *d* (calc) |
|---|---|---|---|
| 2 | 3.14 | 200 | 3.21 |
| 5 | 2.81 | 210 | 2.87 |
| 5 | 2.57 | 211 | 2.62 |
| 2 | 2.23 | 220 | 2.27 |
| 7 | 1.91 | 311 | 1.934 |
| ½ | 1.82 | 222 | 1.851 |
| 1 | 1.755 | 320 | 1.780 |
| 3 | 1.692 | 321 | 1.715 |
| 1 | 1.422 | 420 | 1.433 |
| 2 | 1.383 | 421 | 1.400 |
| 1 | 1.350 | 332 | 1.368 |
| 2 | 1.299 | 422 | 1.310 |
| 4 | 1.223 | 333 | 1.235 |
| 3 | 1.181 | 520 | 1.191 |
| 2 | 1.161 | 521 | 1.171 |
| 4 | 1.126 | 440 | 1.134 |
| 1 | 1.063 | 600 | 1.070 |
| 1 | 1.048 | 610 | 1.055 |
| 3 | 1.036 | 611 | 1.041 |
| 2 | 1.009 | 620 | 1.014 |
| 4 | .975 | 533 | .979 |
| 1 | .964 | 622 | .967 |
| 4 | .954 | 630 | .956 |
| 3 | .9432 | 631 | .946 |
| 1 | .8872 | 640 | .889 |
| 3 | .8802 | 720 | .881 |
| 4 | .8715 | 721 | .873 |
| 3 | .8559 | 642 | .857 |
| 10 | .8340 | 731 | .835 |
| 5 | .8205 | 650 | .821 |
| 6 | .8141 | 732 | .815 |
| 5 | .8013 | 800 | .802 |
| 8 | .7776 | 820 | .778 |

Table 6. Iridium Monotelluride—IrTe: *X*-ray Powder Data

Hexagonal, niccolite structure; $a_0=3.930$ Å, $c_0=5.386$ Å, $c=1.370$

| *I* | *d* (meas) | *hk·l* | *d* (calc) |
|---|---|---|---|
| 3 | 5.29 | 00.1 | 5.40 |
| 1 | 3.34 | 10.0 | 3.40 |
| 10 | 2.83 | 10.1 | 2.88 |
| ½ | 2.64 | 00.2 | 2.69 |
| 6 | 2.09 | 10.2 | 2.11 |
| 6 | 1.94 | 11.0 | 1.96 |
| 2 | 1.824 | 11.1 | 1.847 |
| ½ | 1.779 | 00.3 | 1.796 |
| 3 | 1.606 | 20.1 | 1.625 |
| 3 | 1.576 | 11.2 | 1.588 |
| 4 | 1.428 | 20.2 | 1.437 |
| 1 | 1.339 | 00.4 | 1.346 |
| 1 | 1.317 | 11.3 | 1.326 |
| 3 | 1.244 | 21.1 | 1.251 |
| 2 | 1.229 | 20.3 | 1.235 |
| 4 | 1.156 | 21.2 | 1.160 |
| 2 | 1.131 | 30.0 | 1.134 |
| 4 | 1.107 | 30.1 | 1.111 |
| 3 | 1.044 | 21.3 | 1.045 |
| 2 | 1.026 | 10.5 | 1.027 |
| 3 | .9815 | 22.0 | .9828 |
| ½ | .9601 | 30.3 | .9594 |
| ½ | .9479 | 31.0 | .9438 |
| 3 | .9296 | 31.1 | .9302 |
| 2 | .9107 | 20.5 | .9102 |
| 4 | .8917 | 31.2 | .8912 |
| 6 | .8684 | 10.6 | .8684 |
| 2 | .8412 | 40.1 | .8406 |
| 4 | .8361 | 31.3 | .8353 |
| 5 | .8273 | 21.5 | .8262 |
| 3 | .8117 | 40.2 | .8113 |
| 8 | .7945 | 20.6 | .7938 |
| 1 | .7826 | 30.5 | .7820 |

In this work, palladium ditelluride was formed by fusing the elements in the correct atomic proportions. Metallic nuggets were obtained which were homogeneous in all respects. The compound is coarsely crystalline and shows the excellent platy cleavage, peculiar to compounds with the sheet-like cadmium iodide type structure.

In polished section, palladium ditelluride is homogeneous. The compound is white, lighter in color and more creamy than native tellurium. It is very easily scratched with a steel needle (Talmage hardness *B*). The cleavage plane (0001) is not well developed but shows up by application of a sharp object. The compound is quite strongly anisotropic: bluish and yellowish colors are observed. The etch reactions are negative for KOH, $HgCl_2$, KCN, and HCl. $FeCl_3$ forms a brown stain in two to five minutes. With $HNO_3$ faint effervescence was observed with rapid discoloration of the reagent droplet to orange brown; fumes stain slightly. In a fusion product of composition $PdTe_3$, the ditelluride is seen with native tellurium.

Interplanar spacings obtained from powder diffraction photographs check well with those calculated from data presented by Thomassen (1929).

### *Palladium Monotelluride* (PdTe)

Thomassen (1929) also prepared palladium monotelluride by dry fusion of the elements in evacuated tubes. For the compound a nickel arsenide structure was found with $a_0 = 4.127 \pm .004$ Å, $c_0 = 5.663 \pm .005$ Å, and $c = 1.372$.

The fusion product of palladium monotelluride forms a brassy compact product. In polished section it is very strongly anisotropic with colors ranging from deep blue to yellow. Its color is creamy white, the Talmage hardness is *C*; no cleavage was observed, either in hand specimen or polished section. The etch reactions are similar to those obtained with the ditelluride: negative with KOH, $HgCl_2$, KCN, and HCl; $FeCl_3$ leaves after five minutes an orange-brown stain. A reaction occurs with $HNO_3$ but no effervescence was observed, the reaction droplet turns deep red-brown but no precipitate forms within 30 seconds as with $PdTe_2$.

Interstitially between the larger monotelluride grains, a small amount of a myrmekitic intergrowth of monotelluride and an isotropic (?) compound appears. This fine-grained palladium monotelluride extinguished parallel with the larger bounding crystals, which show sutured contacts towards the intergrowth. This texture is not likely eutectic in origin, rather does it appear to be a product of a peritectic reaction, e.g.:

$$PdTe_{(\text{crystals})} + Pd_{1+x}Te_{(\text{melt})} = Pd_{1+y}Te_{(\text{crystals})}$$

A polished section was also prepared from a fusion product of composition $Pd_2Te_3$. Macroscopically it is very similar to the ditelluride but under the microscope, the product is seen to consist of two phases, one the ditelluride, the other an exsolution product, deposited along (0001) directions of the former. The latter is very fine-grained and differs from the monotelluride and the ditelluride by the absence of strong anisotropism. This exsolution product was too fine-grained to be isolated for powder diffraction work.

Thus, aside from PdTe and $PdTe_2$, two other phases are indicated: one isotropic phase, occurring as a myrmekitic intergrowth with palladium monotelluride and another fine-grained phase appearing as an exsolution product in $PdTe_2$.

Interplanar spacings calculated for palladium monotelluride are very similar to those calculated from Thomassen's data (1929).

### *Platinum Ditelluride* ($PtTe_2$)

Roessler (1897) prepared platinum ditelluride by heating platinum with an excess of tellurium in an open furnace. Wöhler, *et al.* (1933) also prepared and analyzed the compound. Thomassen (1929) synthesized it from the elements and determined the structure. It has a cadmium iodide type structure with $a_0 = 4.010 \pm .004$ Å, $c_0 = 5.201 \pm .005$ Å, and $c = 1.297$. No other tellurides are reported by Wöhler or Thomassen although the latter attempted to prepare the monotelluride. Roessler (1897) reports the existence of PtTe and $Pt_2Te$ which he obtained by melting the ditelluride in an oxidizing flame of a blowpipe on charcoal.

In this work the ditelluride was prepared in the usual manner. It formed a sintered product after fusion; refusion at higher temperatures yielded a product from which a satisfactory polished section could be prepared. No liquid phase was observed.

In polished section the aggregate of anhedral crystals takes on a good polish. The Talmage hardness is *B*. In reflected light $PtTe_2$ is white, with the same intensity of reflection as tellurium or slightly darker. It is moderately anisotropic. Etch reactions with $HgCl_2$, KCN, HCl, KOH and $FeCl_3$ are negative. $HNO_3$ produces locally slow intergranular effervescence. $HNO_3$ fumes tarnish the compound locally although some of these effects are possibly due to small amounts of tellurium.

The *x*-ray powder photograph of $PtTe_2$ is slightly diffuse. It is difficult to obtain a good mount of the compound due to its softness and flaky nature. Measured interplanar spacings agree well with those calculated from Thomassen's data (1929).

TABLE 7. SUMMARY OF PROPERTIES DETERMINED ON FUSION PRODUCTS

| Substance | Structure Type | Lattice Dimensions | Nature of Product | Anisotropism ×Nicols | Pleochroism 1 Nicol | Color | Brightness | Hardness | Cleavage Parting | Etch Reactions | | | |
|---|---|---|---|---|---|---|---|---|---|---|---|---|---|
| | | | | | | | | | | HCl, KOH, KCN | $HgCl_2$ | $FeCl_3$ | $HNO_3$ |
| $RuTe_2$ | $FeS_2$* | 6.377 | sintered aggregate | isotropic | none | white | strong | F | none | neg. | irides. stain? | neg. | sl. eff. intergranular |
| $OsTe_2$ | $FeS_2$* | 6.398 | loose powder | — | — | — | — | — | — | — | — | — | — |
| $RhTe_{2+x}$ | $FeS_2$* | 6.428 | sintered aggregate | isotropic | none | white | strong | F | none | neg. | fg'd ppte? | neg. | sl. eff. intergranular |
| $IrTe_{2+x}$ | $FeS_2$* | 6.411 | loose powder | — | — | — | — | — | — | — | — | — | — |
| IrTe | NiAs | $a_0=3.930$<br>$c_0=5.386$ | loose powder | — | — | — | — | — | — | — | — | — | — |
| $PdTe_2$ | $CdI_2$ | $a_0=4.028$<br>$c_0=5.118$ | c. gr'd nugget | moderately strong | none | creamy white | med. str. | B. | pinacoidal (0001) | neg. | neg. | brown stain | sl. eff. irid. st. |
| PdTe | NiAs | $a_0=4.127$<br>$c_0=5.663$ | med. gr'd nugget | strong | none | creamy white | med. str. | C | none | neg. | neg. | brown stain | no. eff. pos. stain |
| $PtTe_2$ | $CdI_2$ | $a_0=4.010$<br>$c_0=5.201$ | sintered aggregate | moderate | none | white | med. str. | B | pinacoidal (0001) | neg. | neg. | neg. | sl. eff. fumes stain |

* Pyrite type structure.

## CONCLUSIONS

The dry fusion procedure of synthesis has been found successful for preparing the following compounds:

$RuTe_2$, $OsTe_2$, $RhTe_{2+x}$, $IrTe_{2+x}$, IrTe, $PdTe_2$, PdTe, and $PtTe_2$.

Only palladium compounds form melts; other products do not melt in vacuum over the hottest gas flame available—in contrast to published accounts—indeed, they tend to dissociate at very high temperatures.

The platinum metal tellurides $RuTe_2$, $OsTe_2$, $RhTe_{2+x}$, and $IrTe_{2+x}$ all belong structurally to the pyrite group. Their interplanar spacings as well as the densities of their lines on *x*-ray powder photographs are consequently very similar; the unit cell edges are within the range $6.377 \leqq a_0 \leqq 6.428$ Å. The ditellurides of platinum and palladium are both hexagonal and belong to the cadmium iodide type which is characterized by a strong cleavage parallel (0001). IrTe and PdTe have niccolite structures. Properties determined on all products are shown in Table 7.

## REFERENCES

BILTZ, W. (1937): Notiz zu Selen- und Telleurverbindungen von Iridium and Rhodium. *Z. anorg. algem. Chem.*, **253,** 282–285.

HENRY, N. F. M., LIPSON, H., & WOOSTER, W. A. (1951): *The interpretation of x-ray diffraction photographs.* Macmillan & Co., London.

ROESSLER, C. (1897): Über Tellurverbindungen des Platins. *Z. anorg. Chem.*, **15,** 405–411.

SHORT, M. N. (1940): Microscopic determination of the ore minerals. 2nd ed., *U. S. Geol. Surv.*, Bull. **914.**

THOMASSEN, L. (1929): Über Kristallstrukfurtypen einiger binärer Verbindungen der Platinmetalle. *Z. phys. Chem.*, **48,** 277–287.

WÖHLER, L., EWALD, K., & KRALL, H. G. (1933): Die Sulfide, Selenide, und Telluride der sechs Platinmetalle. *Ber. Deu. Chem. Ges.*, **66,** part II, Section B, pp. 1638–1652 .

# STRUCTURE OF ZINC SULPHIDE MINERALS

F. G. Smith, *University of Toronto, Toronto, Canada.*

## Abstract

The topological relations between cubic and hexagonal tetrahedral structures are reviewed, emphasizing the occurrence of regular and random intergrowths of the two extreme types. An approximate method of measuring the ratio of cubic and hexagonal planes in mixed polytypic structures is derived from integrated intensities of the first two $x$-ray diffraction spectra. Application of the method to zinc sulphide minerals indicates a small but variable amount of hexagonal packing in sphalerite and a larger and also variable amount of cubic packing in wurtzite. No example of wurtzite with only hexagonal packing ($2H$ structure) was found.

## Introduction

The known structures of crystalline zinc sulphide are closely related: all have the same short range order but different long range order, analogous to the structures of silicon carbide. The bonding is dominantly homopolar and interatomic distances are very nearly the sum of the atomic radii (Aminoff, 1923; Evans, 1939, pp. 157–163; Wyckoff, 1951, p. 29). The tetrahedral coordination of both zinc and sulphur necessitates a rather open framework structure (Evans, 1939, pp. 157–163). The zinc atoms (also the sulphur) are related, one to the other, as are the centres of a close-packed lattice (W. L. Bragg, 1937; Ulrich & Zacharaisen, 1925; Fuller, 1929). In recent years it has been determined that the lattice may be other than cubic (three ZnS layers in the unit cell) or hexagonal (two ZnS layers in the unit cell), and that theoretically there are an infinite number of different packing methods, each with the same *a* unit cell dimension, but a unique *c* dimension and with a lattice which has partly cubic and partly hexagonal packing (Jagodzinski, 1949*a*, *b*, *c*, 1954*a*, *b;* Ramsdell, 1947; Ramsdell & Kohn, 1952; Zhdanov & Minervina, 1947). Five types of zinc sulphide minerals already have been described (Frondel & Palache, 1950), and at least 10 types have been synthesized by vapour reactions (Strock & Brophy, 1955); in the case of silicon carbide, which has a closely analogous structure, at least 19 types are known. The terminology which has become accepted designates the cubic ($3C$) and hexagonal ($2H$) end members of the series as two polymorphs (*beta* and *alpha*, respectively), and the intervening members as polytypes (Thibault, 1944). Since all of the polytypes have hexagonal or trigonal symmetry, they are said to be polytypes of the hexagonal end member. However it seems to be more consistent to consider all of the cubic, hexagonal, and rhombohedral [trigonal] structural varieties related in the above way to be polytypes of the one scheme of coordination. The term polymorph rather than polytype might be preferred by mineralogists, because each polytype may show a unique crystal morphology, but the general usage is such that we expect a significant density and entropy difference between any two polymorphs of a compound, but these are nearly immeasurably small in the case of polytypes. If mineral names were given to each of the various polytypes of a compound such as zinc sulphide, more than the usual confusion would result. However, if the net morphology is isometric, the mineral could be designated as sphalerite (even if it is a cyclic twin of four or eight rhombohedral or hexagonal individuals, occurrences of which have been described by Ramdohr & Websky (1943), and as wurtzite, if the morphology is rhombohedral or hexagonal. Additional information would be given if the number of ZnS layers per cell and the stacking sequences or ratio of cubic to hexagonal ZnS layers were also indicated in a simple way. The former is now given by a number, followed by *H* or *R* to indicate whether the symmetry is hexagonal or rhombohedral, but this scheme does not define the cubic and hexagonal sequences of ZnS layers. These may be given as Ramsdell-Zhdanov symbols which show the zig-zag sequence on the 11.0 plane, or perhaps preferably as a sequence of Jagodzinski symbols (*h* and *k* for hexagonal and cubic planes), but both are too cumbersome for complex and long *c*-period structures. A useful symbol would be one which would give explicitly the ratio of cubic to hexagonal packing. The derivation of this system and a practical method of determining it quantitatively from *x*-ray data, is described below.

In contrast to theoretical crystal structures, the ZnS minerals can be expected to be imperfect in many ways. In addition to substitution of Fe, Mn, Cd, and many other elements for Zn, and of Se, O, and other elements for S, and defect structures, dislocations, strain effects, lineage structure, inclusions, etc., there are many types of variations of the packing pattern possible, from small departures from the general stacking sequence to random stacking or to syntaxic intergrowth of two or more types of wurtzite or even of wurtzite and sphalerite (by analogy with the better known SiC polytypes). It will be apparent that the lower limit of determination of structure of the ZnS polytypes would be on atomic dimensions and thus impractical for mineralogical purposes. Probably if the main stacking periods and the ratio of cubic to hexagonal packing were designated for a macroscopic crystal, the structure of the mineral would be adequately described for most mineralogical purposes.

Although a considerable amount is known about cubic-hexagonal polytypic structures, there are no established relations between the conditions during crystallization and the stacking pattern. That temperature is one control follows from the following facts: 1) cubic SiC is the low temperature form (Humphrey *et al.*, 1952) and it is formed, if at all, in the outer, cooler, part of commercial SiC electric furnace "pigs," in which various hexagonal and trigonal polytypes (6*H*, 15*R*, 4*H*, 21*R*, etc.) are formed (Thibault, 1944, p. 272); 2) Fuller (1929) synthesized 2*H* ZnS at 1100° C. and substantially cubic ZnS has been synthesized at 940° C. (Swanson & Fuyat, 1953); Müller (1952) synthesized several polytypes of ZnS between 870 and 905° C. The composition of the solutions which deposit ZnS in veins has been said to be a control: the greater the acidity, the greater the probability of formation of wurtzite rather than sphalerite (Allen, Crenshaw, & Merwin, 1912, 1914). However, this relation has recently been seriously questioned, if not invalidated altogether (Corey, 1953) and a complete restudy with structural analysis of the ZnS products is desirable. The composition of (Zn, Cd)S has long been known (from synthesis of phosphors) to be a control over the crystalline form which deposits from water solutions: the greater the Cd/Zn ratio, the lower the probability of formation of the cubic form (Schleede, 1935; Randall, 1937). Allen & Crenshaw (1912) showed that the inversion temperature varies nearly linearly with the Fe/Zn ratio, from 1020° for ZnS to 880° when approximately 29 mol. per cent FeS is in solid solution. Manganese has been reported to have a similar effect (Kröger, 1939, 1940). The data in the literature allow the postulate that temperature is one control, but possibly the composition of the fluid phase from which the crystals are formed, and certainly the composition of the crystals, are modifying controls over the polytype structure. Pressure would have a negligible effect because the packing density of all of the polytypes of the same composition is very nearly a constant.

The identification of the simpler pure polytypes may be carried out by analysis of the crystal morphology (Thibault, 1944), and by *x*-ray and other diffraction methods such as Laue (Frondel & Palache, 1950; Mitchell, 1953), rotation (Frondel & Palache, 1950; Ramsdell, 1944, 1945, 1947; Ramsdell & Kohn, 1951*a*, *b;* Ramsdell & Mitchell, 1953; Jagodzinski & Laves, 1948), and also by the powder technique (Thibault, 1944, 1948; Ramsdell, 1947). When there is no regular stacking period or when a number of periods are present in one crystal, quantitative measurements by the above methods are complex. A number of mathematical analyses of the problem have been made (Wilson, 1942; Hendricks & Teller, 1942; Jagodzinski, 1949, 1954; Méring, 1949; Gevers, 1952, 1954; Paterson, 1952). These solutions predict the degree of broadening and/or displacement of certain reflections as a function of degree of defect of either the cubic or hexagonal limiting structure, but the facts are that if the defect is periodic, all reflections are sharp, and also some reflections occur which are not given by either of the limiting structures. What is needed is a simple method such as the relative intensity of a small number of *x*-ray diffractions which will give directly the ratio of cubic to hexagonal packing (and also the dominant stacking period) so that measurements may be made of natural and synthetic minerals. Data of this kind could be combined with temperature and composition data with the possibility that a thermometric relation might be established.

## STRUCTURE

The structure of all of the ZnS polytypes can be referred to common hexagonal axes, whether the symmetry is lower (rhombohedral) or higher (cubic). The conversion from cubic to hexagonal can be made because the fundamental tetrahedral coordination is almost exactly the same in all of the polytypes. In a regular tetrahedron, the trigonal ratio $c/a = \sqrt{2/3} = 0.81650$. The average value of three exact determinations of wurtzite by *x*-ray diffraction methods (Ulrich & Zacharaisen, 1925; Fuller, 1929; Swanson & Fuyat, 1953) is 0.8185. Dana (1944) gives 0.8179. These data suggest that the tetrahedron in the hexagonal and trigonal polymorphs is very slightly elongated parallel to *c*. Some of the tetrahedral distortion may be due to the temperature of synthesis. Pure ZnS crystallized in the presence of NaCl at 1100° C. has a value of 0.8179 (Fuller, 1929), and at 1200° C., 0.8194 (Swanson & Fuyat, 1953). The 3C type is measurably rhombohedral when formed above 850° C. (Buck & Strock, 1953). The data suggest that the higher the temperature, the more elongated is the structural tetrahedron parallel to the *c* axis. Some of the tetrahedral distortion may be due to solid solution and defect structure. Tucker & Senio (1954) found that when hexagonal boron carbide (BC) develops radiation damage from neutron bombardment, the volume increases due to defects, but while *a* increases 0.6%, *c* decreases 0.8%. Thus radiation damage in ZnS would be expected to flatten the structural tetrahedron. Large atoms such as Cd in Zn positions in general would be more easily polarized and the tetrahedral angles would be less strongly maintained. Other atoms such as Fe and Mn which have a weaker tendency than Zn to form the tetrahedral configuration of O and S, similarly would allow a larger change in the tetrahedral angles. Ulrich & Zacharaisen (1925) give cell dimensions of greenockite (CdS) which give a tetrahedral *c*/*a* ratio of 0.8115, indicating that the structural tetrahedron is flattened parallel to *c* when a larger and more easily polarized atom is in the wurtzite structure. However, since the departure from a regular tetrahedron is smaller than would be detected in most *x*-ray diffraction studies, it will be ignored in the following discussion.

Another simplification that can be made is to refer all of the hexagonal planes to a hypothetical one-layer ZnS cell. This gives fractional *l* values which, when multiplied by the real number of layers in the $c$-period, give rational planes when a whole number results. These "unit layer indices" will be used throughout. On this basis, cubic indices $(HKL)$ can be converted to hexagonal $(hk \cdot l)$ by the transformation matrix $\frac{1}{2}\frac{\bar{1}}{2}0/0\frac{1}{2}\frac{1}{2}/\frac{1}{3}\frac{1}{3}\frac{1}{3}$. Using the tetrahedral relation between $c$ and $a$, the usual formula for calculating the spacing of hexagonal planes can be converted to

$$d = a \Big/ \sqrt{\frac{8h^2 + 8hk + 8k^2 + 9l^2}{6}}$$

It would be laborious to calculate the relative intensity of $x$-ray diffraction from a large number of planes of all of the possible ZnS polytypes, but sufficiently reliable diffraction data can be built up by analogy, as Ramsdell (1947) and Ramsdell & Mitchell (1953) have indicated. For example, if a $6H$ type gives a fairly strong reflection from 10.1/6, then another polytype with a similar stacking but with a longer $c$-period, such as $51R$, will give two or more reflections at nearly the same spacing (*i.e.* 10.2/17, 01.3/17). This is shown very well in the Laue and rotation $x$-ray diffraction patterns of SiC with a very long $c$ period of 594 layers (Honjo *et al.*, 1950). Also, since the relative reflecting powers of Zn/S are nearly the same as Si/C, the more extensive SiC data can be used without much alteration, especially at small Bragg angles.

Relative intensities of $10.l$, $20.l$, *etc.* can readily be estimated when the atomic positions are shown as a right projection on a plane perpendicular to one of the $a$ directions (Fig. 1). All of the atoms can be shown, and lie at 0, 1/3, 2/3, and 1 of the projected $a$ cell dimension. This projection shows very well the zig-zag sequences of Ramsdell and has the advantage of displaying undistorted $10.l$ and $01.l$ plane spacings. For example, it can be shown in this way that for regular polytypes more than half cubic, the plane 10.0 extinguishes, but $10.l$ reflections persist, but with diminishing total relative intensity, to the cubic limit, except 10.1/3, 10.2/3, 10.4/3, 20.1/3, etc. which become stronger and remain as cubic reflections (111, 200, 220, 311, *etc.*) at the cubic limit.

The two end members of the cubic-hexagonal polytypes have repeat periods of 3 and 2 layers (Fig. 1). In the Ramsdell notation, the zig-zag sequences are ∞ and 1 1, and in other notations *ABCABC*----- and *ABAB*----- , or $3C$ and $2H$, or $k$ and $h$, or 1.0 and 0.0 cubic, respectively. (In cubic packing, any one layer has nearest neighbor layers which are dissimilar, and in hexagonal packing, these are similar.) The simplest regular polytypes have zig-zag sequences of 2 2, 3 3, 4 4, ----- , or $4H$, $6H$, $8H$, ----- , or *hkhk*----- , *hkkhkk*----- , *hkkkhkkk*----- , ----- , or 0.50, 0.67, 0.75----- cubic, respectively, in which groups of cubic layers are separated by hexagonal layers at regular intervals. All of these have hexagonal symmetry and and even number of layers of ZnS in the *c* period. The intermediate simple polytypes have sequences such as 1 2, 2 3, 3 4----- , or 9*R*, 15*R*, 21*R*,----- , or *hhk*----- , *hkhkk*----- , *hkkhkkk*----- , or 0.33, 0.60, 0.71----- cubic, respectively. All of these are rhombohedral and have an odd number of layers of ZnS in the *c* period. A rare type of hexagonal intermediate polytype has sequences such as 2 2 3 3 (10*H*) (Ramsdell & Kohn, 1951*b*). More complex polytypes are possible and many have been described in the case of SiC, such as 51*R*, which may be 3×(3 3 3 3 3 2) (0.647 cubic) or 3×(2 2 2 2 2 2 2 3) (0.529 cubic) (Ramsdell & Kohn, 1952). In addition, polytypes with imperfect regularity or mixed regularities have been reported (Jagodzinski, 1949*a*, *b*, *c*, 1954; Strock & Brophy, 1955). By extension, it appears possible that crystals of ZnS and SiC could have no regular stacking periods at all. These would not be two-dimensional crystals because they lack a point repetition in the *c* direction, since there is a regular layer period. The unit cell, however, would have to be considered to have an infinite extent in the *c* direction.

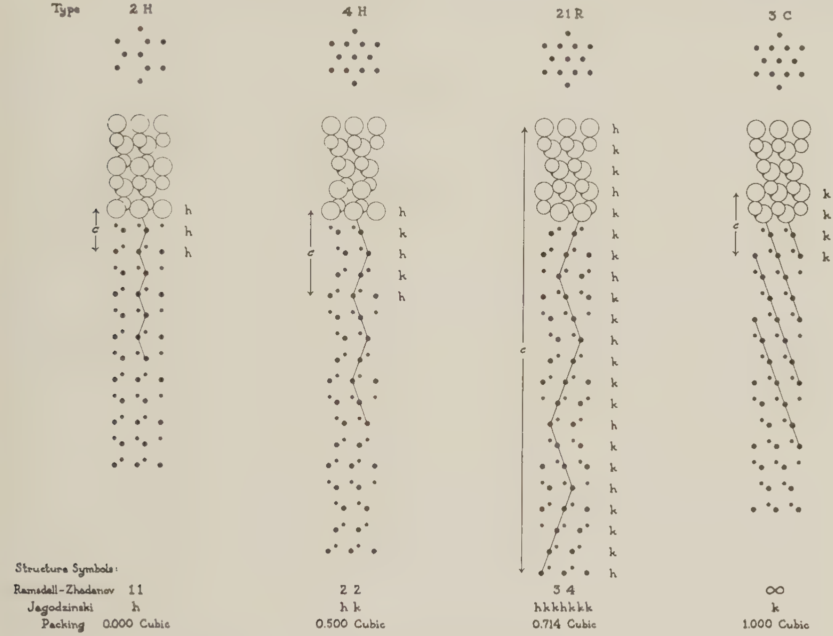
Type
2 H
4 H
21 R
3 C
c
h h h
h k h k h
h k k h k k k h k k h k k k h k k h k k k h
k k k k
Structure Symbols:
Ramsdell-Zhdanov 11 22 34 ∞
Jagodzinski h hk hkkhkkk k
Packing 0.000 Cubic 0.500 Cubic 0.714 Cubic 1.000 Cubic

FIG. 1. Schematic representation of the structure of four ZnS polytypes on a plane perpendicular to *a*.

The number of *x*-ray diffraction spectra increases with the number of layers of the *c*-period, but when this is very large, or infinite, incomplete resolution gives more or less continuous streaks with greater density near 10.1/2, 10.3/2, 10.5/2, 20.1/2, *etc.*, and other spacings depending on the major *k* and *h* sequences. Jagodzinski (1949-*c*, 1954) and Strock & Brophy (1955) have suggested that polytypic crystals may have various degrees of regularity of *c*-period, so that even if a crystal gives reflections which can be indexed for a 6*H* type, it may also give streaks and broadened reflections which indicate longer, or infinite *c*-periods as well.

Proceeding in the manner indicated above, the spacing of most of the reflecting planes of the simpler polytypes of ZnS were calculated and are shown in Table 1. In this table, no distinction is made between 10.*l* and 01.*l*, whereas in the rhombohedral polytypes they are not equivalent. Thibault (1944, pp. 345–346), Ramsdell & Mitchell (1953), and Mitchell (1953) have discussed the extinction conditions of the analogous SiC polytypes.

Considering the hexagonal end member of the ZnS polytypes (2*H*), a calculation of the relative intensity of diffraction by the six 10.0 planes (containing both Zn and S in two planes $\frac{1}{3}$ or $\frac{2}{3}$ phase apart) and by the two 00.1 planes (containing Zn in one plane and S in another, $\frac{1}{4}$ or $\frac{3}{4}$ phase apart) gave

$$I(10.0)/I(00.1) = 2.04 \pm 0.24.$$

This was arrived at by multiplying together the following factors: structure amplitude factor $= 0.500/0.7365 = 0.679$ for an ideally perfect crystal, but $(0.679)^2 = 0.46211$ for an ideally imperfect crystal, and 0.606 for approximately $\frac{2}{3}$ perfection; number of planes factor $= 6/2 = 3$; angle factors $= 1.12$; temperature factor $\times$ absorption factor $= 1$. The calculations and assumptions are based on a discussion by Bunn (1945, pp. 195–209). The relative diffracting powers of Zn and S were taken to be 29 and 17 (*i.e.* two valence electrons are shared equally), but the ratio of intensities is not sensitive to small variation of the ratio of diffracting powers. The greatest uncertainty is the relation between intensity and structure amplitude, with 2.28 and 1.55 as the limiting values of the intensity ratio. The choice of value was influenced by the fact that in the case of diamond, also homopolar and structurally analogous, the intensity of diffraction varies as $F$, not $F^2$. Zinc sulphide, however, is much softer than diamond and probably has a greater amount of mosaic structure. Ulrich & Zacharaisen (1925) calculated the ratio to be $7.0/4.2 = 1.67$, and Fuller (1929) calculated it to be $2.12/1.29 = 1.64$.

The measured intensity ratios, all on synthetic wurtzite, are 3.3 and 2.0 (Fuller, 1929), 2.1 (Hanawalt *et al.*, 1938), and 1.2 (Swanson & Fuyat, 1953). The average of the four available ratios is 2.1, but since no evidence was presented in any of these determinations that the 2*H* structure was the only one present, the calculated value (2.04) is preferred.

TABLE 1. ZnS DIFFRACTION SPECTRA

| Indices | | $\frac{3.822}{b}=d$ | | *Polytype Diffractions in Three Degrees of Intensity* | | | | | | |
|---|---|---|---|---|---|---|---|---|---|---|
| Cubic | Hexag. | | | 2*H* | 9*R* | 4*H* | 15*R* | 6*H* | 21*R* | 3*C* |
| | | | | 1 1 | 1 2 | 2 2 | 2 3 | 3 3 | 3 4 | |
| *hkl* | *hk·l* | *b* | *d*(Å) | .000 | .333 | .500 | .600 | .667 | .714 | 1.00 |
| | 10.0 | 1.155 | 3.309 | — | | — | | | | |
| | 10.1/15 | 1.157 | 3.302 | | | | — | | | |
| | 10.2/21 | 1.161 | 3.293 | | | | | | — | |
| | 10.1/9 | 1.163 | 3.287 | | — | | | | | |
| | 10.2/15 | 1.166 | 3.279 | | | | — | | | |
| | 10.1/6 | 1.172 | 3.261 | | | | | — | | |
| | 10.4/21 | 1.178 | 3.244 | | | | | | — | |
| | 10.2/9 | 1.186 | 3.223 | | — | | | | | |
| | 10.5/21 | 1.190 | 3.210 | | | | | | — | |
| | 10.1/4 | 1.194 | 3.202 | | | — | | | | |
| | 10.4/15 | 1.200 | 3.187 | | | | — | | | |
| 111 | 00.1<br>10.1/3 | 1.225 | 3.121 | — | — | — | — | — | — | — |
| | 10.8/21 | 1.245 | 3.070 | | | | | | — | |
| | 10.4/9 | 1.276 | 2.996 | | — | | | | | |
| | 10.7/15 | 1.288 | 2.968 | | | | — | | | |
| | 10.10/21 | 1.294 | 2.954 | | | | | | — | |
| | 10.1/2 | 1.306 | 2.927 | — | | — | | — | | |
| | 10.11/21 | 1.321 | 2.894 | | | | | | — | |
| | 10.8/15 | 1.326 | 2.882 | | | | — | | | |
| | 10.5/9 | 1.340 | 2.853 | | — | | | | | |
| | 10.13/21 | 1.381 | 2.768 | | | | | | — | |
| 200 | 10.2/3 | 1.414 | 2.703 | | | | - - | - - | — | — |
| | 10.11/15 | 1.462 | 2.614 | | | | — | | | |
| | 10.3/4 | 1.475 | 2.591 | | | — | | | | |
| | 10.1 | 1.683 | 2.271 | — | | — | | | | |
| | 10.11/9 | 1.890 | 2.023 | | — | | | | | |
| | 10.25/21 | 1.905 | 2.006 | | | | | | — | |
| | 10.5/4 | 1.916 | 1.995 | | | — | | | | |
| | 10.19/15 | 1.934 | 1.977 | | | | — | | | |
| 220 | 11.0<br>10.4/3 | 2.000 | 1.911 | — | — | — | — | — | — | — |
| | 11.2/7 | 2.030 | 1.883 | | | | | | — | |
| | 11.1/3 | 2.041 | 1.872 | | — | | | | | |
| | 11.4/7 | 2.119 | 1.803 | | | | | | — | |
| | 11.3/5 | 2.130 | 1.794 | | | | — | | | |
| | 11.2/3 | 2.160 | 1.769 | | — | | | | | |
| | 10.3/2 | 2.170 | 1.762 | — | | — | | — | | |
| | 11.5/7 | 2.183 | 1.751 | | | | | | — | |
| | 11.4/5 | 2.227 | 1.717 | | | | — | | | |
| | 11.6/7 | 2.258 | 1.693 | | | | | | — | |
| | 20.0 | 2.309 | 1.656 | — | | | | | | |
| | 20.1/6 | 2.319 | 1.648 | | | | | — | | |
| | 20.4/15 | 2.332 | 1.638 | | | | — | | | |

TABLE 1. *Continued*

| Indices | | $\frac{3.822}{b}=d$ | | Polytype Diffractions in Three Degrees of Intensity | | | | | | |
|---|---|---|---|---|---|---|---|---|---|---|
| Cubic *hkl* | Hexag. *hk·l* | *b* | *d*(Å) | 2*H* 1 1 .000 | 9*R* 1 2 .333 | 4*H* 2 2 .500 | 15*R* 2 3 .600 | 6*H* 3 3 .667 | 21*R* 3 4 .714 | 3*C* 1.00 |
| 311 | 11.1<br>10.5/3<br>20.1/3 | 2.244 | 1.631 | — | — | — | ━ | ━ | — | ━ |
| | 20.4/9 | 2.371 | 1.612 | | — | | | | | |
| | 20.7/15 | 2.379 | 1.606 | | | | — | | | |
| | 20.1/2 | 2.390 | 1.599 | — | | — | | — | | |
| | 20.8/15 | 2.400 | 1.593 | | | | — | | | |
| | 20.5/9 | 2.407 | 1.588 | | — | | | | | |
| | 10.7/4 | 2.433 | 1.571 | | | — | | | | |
| 222 | 00.2<br>20.2/3 | 2.450 | 1.560 | — | — | - - | — | — | — | — |
| | 20.1 | 2.612 | 1.463 | — | | — | | | | |
| | 20.5/4 | 2.770 | 1.380 | | | — | | | | |
| 400 | 20.4/3 | 2.828 | 1.352 | | | | — | — | — | — |
| | 20.3/2 | 2.950 | 1.296 | — | | — | | — | | |
| | 21.0 | 3.055 | 1.251 | — | - | — | — | — | — | |
| 331 | 10.7/3<br>20.5/3<br>21.1/3 | 3.081 | 1.241 | | | | | — | | — |
| | 21.1/2 | 3.117 | 1.227 | — | | — | | — | | |
| 420 | 11.2<br>21.2/3 | 3.161 | 1.209 | | — | | — | — | — | — |
| | 10.5/2 | 3.273 | 1.168 | — | | — | | | | |
| 422 | 10.8/3<br>21.4/3<br>30.0 | 3.463 | 1.104 | — | — | — | — | ━ | ━ | ━ |
| | 21.3/2 | 3.565 | 1.072 | — | | — | | — | | |
| 333<br>511 | 00.3<br>20.7/3<br>21.5/3<br>30.1 | 3.674 | 1.041 | — | — | — | — | — | — | — |
| | 20.5/2 | 3.835 | 0.997 | — | | — | | | | |
| 440 | 20.8/3<br>22.0 | 4.000 | 0.956 | — | — | — | — | — | — | — |
| 531 | 11.3 | 4.182 | 0.914 | — | — | — | — | — | — | — |
| | 31.1/2 | 4.207 | 0.908 | — | | | | | | |
| | 21.5/2 | 4.324 | 0.884 | — | | — | | | | |
| 620 | 21.8/3 | 4.472 | 0.855 | | — | | — | — | — | — |
| | 31.3/2 | 4.550 | 0.840 | — | | — | | — | | |

Two other measurements, by Aminoff (1923), and Ulrich & Zacharaisen (1925) were on polytypes far from the 2*H* type, or on mixtures of hexagonal and cubic phases (Fuller, 1929).

Noting that in the more cubic polytypes the reflections from the 10.0 planes extinguish but a number of 10.$l$ reflections appear between 10.0 and 10.1/3, an approximate calculation showed that the relative value of $I(10.0+10.(0 \text{ to } \frac{1}{3}))$ shows a linear decrease from 2.04 at the hexagonal limit to zero at the cubic limit. On the other hand $I(00.1+10.1/3)$ increases nearly linearly from 1 at the hexagonal limit to 4 at the cubic limit. Assuming both linearities, the calculated values of the ratio $I$ (10.0 to 10.1/3) /$I$ (00.1+10.1/3) are given in Table 2 and are shown in Fig. 2 plotted against the fraction of cubic packing. By means of this curve, and as a first approximation, the ratio of integrated intensities of all the polytype diffractions at a smaller angle than 00.1, added together, to the integrated intensity of the 00.1−10.1/3 diffraction, gives directly the ratio of hexagonal to cubic packing, whether the mixture is on an atomic scale or in syntaxic intergrowth or even on a macroscopic scale. However, polytypes with small and regular *k-h* periodicities, especially if the *c* periods also are small, give many diffractions impossible from a mechanical mixture of the cubic and hexagonal end members, so that indexing of a number of diffraction lines should accompany relative intensity measurements.

Table 2. ZnS Polytypes

| Packing | | Calculated Ratio of $x$-ray Intensities |
|---|---|---|
| Cubic | Hexagonal | $I(10.0 \text{ to } 10\cdot\frac{1}{3}/I(00.1+10\cdot\frac{1}{3})$ |
| 0.0 | 1.0 | 2.04 |
| 0.1 | 0.9 | 1.42 |
| 0.2 | 0.8 | 1.02 |
| 0.3 | 0.7 | 0.752 |
| 0.4 | 0.6 | 0.556 |
| 0.5 | 0.5 | 0.408 |
| 0.6 | 0.4 | 0.292 |
| 0.7 | 0.3 | 0.197 |
| 0.8 | 0.2 | 0.120 |
| 0.9 | 0.1 | 0.0552 |
| 1.0 | 0.0 | 0.0000 |

Superficial examination of $x$-ray diffraction of minerals identified by other means as wurtzite have led, in the past, to erroneous conclusions that the minerals are mixtures of sphalerite and wurtzite or that they are sphalerite. This is due, obviously, to the fact that the strong spectra of wurtzite polytypes are also those of sphalerite and the weak wurtzite spectra may be too broad to be easily detected. However, since a large amount of work on hexagonal-cubic polytypes has been published since 1920, such cursory treatment should now be considered unsatisfactory.

Edwards & Lipson (1943) used the ratio of intensities of 200 from cubic cobalt and 10.0 from hexagonal cobalt to measure the ratio of abundance in a range of transition. This ratio can be used if it is known that only two phases can be present, the 3*C* and 2*H* types, but in general this cannot be assumed. For example if the 4*H* type is the only phase present, the cubic 200 reflection extinguishes (Table 1) although the packing is half cubic. The ratios of several other reflections were considered for measuring the ratio of cubic to hexagonal packing, but the one outlined above has many practical advantages due to the small Bragg angles.

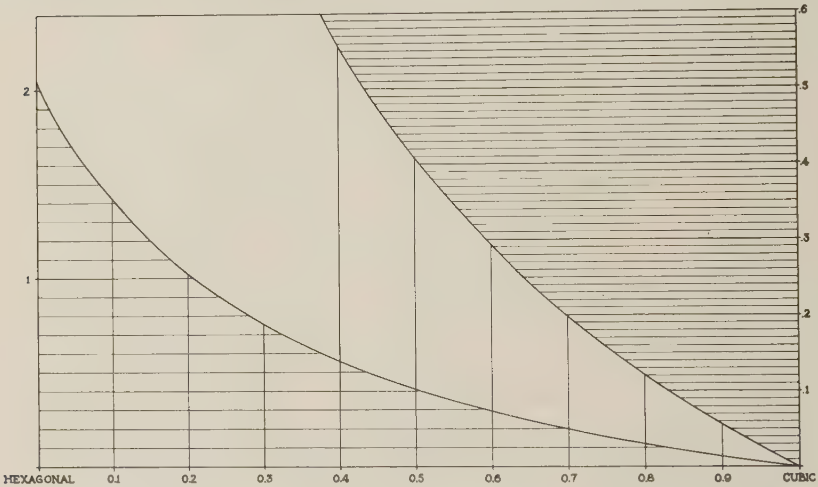

FIG. 2. Graphical representation of Table 2. Calculated ratio of integrated intensities of the low angle diffractions of ZnS polytypes *vs* ratio of cubic to hexagonal packing. The ratio of intensities value (vertical axis) is obtained by dividing 1) the sum of the integrated reflections (resolved or unresolved) from 10.0 to, but not including, 00.1, by 2) the integrated reflection of $00.1+10\frac{1}{3}$. Hexagonal unit layer indices are used as described in the test.

## THERMODYNAMICS

The small differences in energy of the ZnS polytypes (Allen, Crenshaw & Merwin, 1912, 1914) must be due almost entirely to differences in structural entropy analogous to that in order-disorder systems (Edwards & Lipson, 1943), since the coordination and packing density are the same. The cubic end member, stable below 1020° C. (Allen, Crenshaw & Merwin, 1914), or 870° C. (Müller, 1952), has a greater degree of order (higher symmetry) than the hexagonal end member. In the analogous SiC system, the heat content of the cubic polytype is only 27.4 cal/gram less that that of the 6*H* polytype (Humphrey *et al.*, 1952). As a first approximation, it can be assumed that the entropy of intermediate polytypes varies linearly between the two end members according to the ratio of cubic to hexagonal packing, both above and below the inversion temperature.

During crystallization of ZnS, most of the growth is on the hexagonal or trigonal planes, and it is not difficult to visualize the sheet mechanism (Verma, 1953) by which one or more layers of ZnS grow with the same relationship to the prior sheet as the nucleus of the sheet had to the prior sheet. This can be seen to be dependent on the probability of the nucleus starting growth of a sheet which is structurally the same as, or different than, the sheet below the surface sheet. This can be said to be a second layer influence which must be weak, being screened by the first layer. The source of the second layer influence may be a partial interaction of S atoms of one plane with Zn of the second (hexagonal) or third (cubic) plane, these distances being 5/4 and 9/4 of the layer spacing. Below the inversion temperature the second layer influence gives a probability between 0.5 and 1.0 that a nucleus of growth will be in a cubic relation to the first and second layers already formed. If growth is by stacks of layers in spirals around screw dislocations (Verma, 1953) the later growth of a crystal is strongly influenced by its early pattern of stacking, but this does not affect the argument (Jagodzinski, 1954*b*). Disregarding compositional effects, the probability would be near 1.0 immediately below the inversion temperature, but would go toward 0.5 (randomness) as the temperature approaches zero, because the ratio of heat of crystallization of the two end types must go toward unity as these values increase with fall of temperature. In other words, the heat evolved during crystallization increases as the temperature falls, but there is less percentage difference between the two end types. From this, it can be derived that the lower the temperature, below the inversion temperature, the weaker is the cubic second layer influence, and the greater is the randomness. Therefore metastable crystallization of hexagonal polytypes in the stable field of the cubic end member would be expected to vary with the temperature, but even at a very low temperature, the most hexagonal type would be 4*H* (0.5 cubic packing). This entire matter deserves a detailed study and theoretical analysis. As an example of the problems remaining, the inversion temperature of ZnS is really a band with the 3*C* structure at one limit, and 2*H* structure at the other limit. The band has a considerable temperature extent, because Müller (1952) crystallized several ZnS polytypes at 870–905° C. Perhaps a theoretical treatment would lead to a prediction of the most probable polytype to crystallize, given the crystallization conditions.

## ZINC SULPHIDE MINERALS

The latest revision of Dana's System (1944) does not mention the ZnS polytypes. Sphalerite is said to be optically isotropic unless strained, and a variety, schalenblende, is said to be a banded intergrowth with wurtzite. The data on wurtzite indicate only the one (2*H*) type occurs. More recently Frondel & Palache (1950) identified and described crystals of wurtzite, types 4*H*, 6*H*, and 15*R* (in order of abundance), from concretions. They pointed out the absence of exact data on natural wurtzite, and the uncertainty that the 2*H* type occurs as a mineral.

Jagodzinski & Laves (1948) and Jagodzinski (1949*c*) discussed *x*-ray rotation diffraction of wurtzite (from the Kirka mine, near Dedeagatsch in Thrace) which was described by Ramdohr & Websky (1943). Heavy streaks connect 10.*l* spots of 2*H* wurtzite and other spots which can be indexed as cubic, even though they used visibly homogeneous single crystals. However, the 10.*l* reflections and their relative intensities could be due to a syntaxic intergrowth of 4*H* and 6*H* wurtzite. The heavy streak between 10.0 and 10.1/3, and the more or less symmetrical broadening of 10.1/2, 10.1, 10.3/2 show that more complex polytypes with long *c*-periods also are present.

The writer examined the ZnS minerals available at the University of Toronto and the pertinent *x*-ray data on file. It was found that optically isotropic sphalerite is rare, but material from ore deposits usually considered to be formed at high temperature approaches this condition. On the other hand, drusy sphalerite from the Tri-State, Illinois, Wisconsin, and similar deposits in sediments is variably anisotropic, optically positive (as is wurtzite) with the uniaxial optic axes perpendicular to octahedral growth planes. Several specimens labelled as wurtzite, from various sources, apparently are no more anisotropic than sphalerite from low temperature deposits. *X*-ray powder diffraction films of two of these specimens showed that they were of mixed polytypes with a substantial amount of hexagonal packing, but neither had the 2*H* structure, even in part.

Only one *x*-ray powder diffraction film of wurtzite (Llallagua, Bolivia, UT-R595) showed the 10.0 line at least twice as dense as the 00.1+10.1/3 line. This had been measured and indexed for the "Peacock Atlas of *X*-ray Data" by R. M. Thompson. All of the lines were checked against the calculated spacings given in Table 1 and were found to belong to the *2H* type. Thompson calculated the unit cell dimensions to be $a=3.87$, $c=6.31$ Å. These are significantly greater than for ZnS minerals, and a chemical analysis indicated a very high content of iron and manganese. Subsequent investigation showed that this mineral is a manganoan ferroan wurtzite, approximately $Zn(Mn,Fe)S_2$ (this will be reported on later).

It was concluded from this preliminary study of zinc sulphide minerals, and from the data in the literature, that the *2H* or wurtzite structure must be uncommon if not absent but that polytypic structures, intermediate between those of the hexagonal and cubic limits, are well represented. Therefore a more extensive study was made of a variety of zinc sulphide minerals to obtain quantitative data.

A suite of zinc sulphide minerals was selected and prepared for *x*-ray diffraction study, with the object of representing many localities, origins, compositions and crystal habits. Each specimen was cleaned by suitable means and ground in acetone to about 600 mesh. After drying, the powder was mixed with balsam-xylol solution on a plate glass. A number of control tests were made to determine the optimum powder/balsam ratio, the effect of preferred orientation of cleavage surfaces against the bottom and top of the mixture, and reproducibility of quantitative intensity and angular measurements.

The *x*-ray diffraction measurements were made with a Norelco geiger counter scanning apparatus, using CuK$\alpha$ radiation. Angles of resolved $\alpha_1$ peaks were read to 0.001° using a very slow scanning speed. Calibration and control tests indicated that the reproducibility of angle was within $\pm 0.003°$. The silicon diffraction angles ($\alpha_1$) taken as calibration standards were 28.442° (111), 47.302 (220), 56.122 (311), 94.952 (333), 106.708 (440). Diffraction angles were converted to spacings using U. S. Bureau of Standards tables of 1950.

Only a few of the diffraction spectra of each preparation were recorded. A traverse was made across the peaks due to 10.0 and 00.1 in order to determine cubic/hexagonal ratio of packing, and also across the peaks due to 11.0 or 22.0 and 00.3 to obtain the *a* and *c* dimensions. The ratio of integrated intensities was obtained from composite curves 10.0 to 10.1/3 and the single curve due to 00.1+10.1/3. A certain amount of ambiguity in the graphical resolution allows no greater accuracy than about $\pm 3\%$ in the ratios of integrated intensities.

The results, shown in Table 3, indicate a few relationships that may be significant. No specimen of *2H* wurtzite was in the suite, but polytypes with a substantial amount of hexagonal packing were represented, notable specimens from Prizbram (Bohemia), Montserrat (Bolivia) and Moresnet (Belgium). Most of the material has a large proportion

TABLE 3. EXPERIMENTAL RESULTS[1]

| Locality | Color, *etc.* | % Cubic Packing | Lattice Dimensions (Å) Cubic | Hexagonal[2] | |
|---|---|---|---|---|---|
| | | | *a* | *a* | *c* |
| *Low(?) temperature zinc sulphide:* | | | | | |
| Bautch Mine, Wisconsin | White band | 95.8 | 5.4102 | 3.8256 | (3.1236) |
| Bautch Mine, Wisconsin | Brown band | 92.1 | 5.4106 | 3.8259 | (3.1238) |
| Bruce Peninsula, Ontario | Light brown | 89.3 | 5.4106 | 3.8259 | (3.1238) |
| Clay Centre, Ohio | Very light brown | 84.2 | 5.4097 | 3.8252 | (3.1233) |
| De Rocher, Wisconsin | Dark brown | 84.8 | 5.4108 | 3.8260 | (3.1238) |
| El Potosi Mine, Mexico | Black | 89.9 | 5.4232 | (3.8348) | 3.1311 |
| Gibsonberg, Ohio | Light brown | 89.3 | 5.4095 | 3.8251 | (3.1232) |
| Mascot, Tennessee | Light yellow | 91.1 | 5.4101 | 3.8255 | (3.1235) |
| North Hunt Mine, Oklahoma | Very light brown | 91.2 | 5.4108 | 3.8260 | (3.1239) |
| Ottawa Co., Oklahoma | Very light brown | 88.4 | 5.4122 | 3.8270 | (3.1247) |
| Picher, Oklahoma (M Bed) | Very light brown | 78.4 | 5.4101 | 3.8255 | (3.1235) |
| Picher, Oklahoma (J Bed) | Very light orange | 88.5 | 5.4113 | 3.8264 | 3.1239 |
| Pine Point, N.W.T., Canada | Light brown crystals | 94.8 | 5.4106 | 3.8259 | (3.1239) |
| Pine Point, N.W.T., Canada | Brown banded | 86.8 | 5.4105 | 3.8258 | (3.1238) |
| Pine Point, N.W.T., Canada | Brown fossil filling | 91.1 | 5.4102 | 3.8256 | (3.1236) |
| *Intermediate(?) temperature zinc sulphide:* | | | | | |
| Bleisharley Mine, Germany | Brown banded | 90.5 | 5.4106 | 3.8259 | (3.1239) |
| Butte, Montana | White band | 93.0 | 5.4092 | 3.8249 | (3.1230) |
| Butte, Montana | Brown band | 90.2 | 5.4106 | 3.8259 | (3.1239) |
| Darwin Mine, California | Black | 89.3 | 5.4196 | (3.8322) | 3.1290 |
| Freiberg, Saxony | Light brown band | 95.0 | 5.4132 | (3.8270) | 3.1247 |
| Freiberg, Saxony | Light brown band | 93.8 | 5.4128 | (3.8274) | 3.1251 |
| Gaspé, Quebec | Very light yellow | 90.0 | 5.4106 | 3.8259 | (3.1239) |
| Keno Hill, Yukon | Red | 90.3 | 5.4125 | 3.8272 | (3.1249) |
| Leadville, Colorado | Light brown | 90.2 | 5.4111 | 3.8262 | (3.1241) |
| Llallagua, Bolivia | Black | 0.0 | 5.4806 | 3.8754 | 3.1638 |
| Llallagua, Bolivia | Very dark brown | 24.1 | 5.4246 | 3.8358 | 3.1337 |
| Montserrat, Bolivia | Brown | 33.2 | 5.4113 | 3.8264 | (3.1242) |
| Moresnet, Belgium | Light brown band | 86.0 | 5.4073 | 3.8235 | (3.1219) |
| Moresnet, Belgium | Dark brown band | 63.0 | 5.4087 | 3.8245 | (3.1227) |
| Oswaldo Mine, New Mexico | Brown | 92.8 | 5.4138 | 3.8281 | (3.1256) |
| Prizbram, Bohemia | Brown acicular | 92.3 | 5.4133 | (3.8278) | 3.1254 |
| Prizbram, Bohemia | Brown acicular | 60.2 | 5.4138 | (3.8281) | 3.1256 |
| Santander, Spain | Light yellow | 87.3 | 5.4091 | 3.8248 | (3.1229) |
| *High(?) temperature zinc sulphide:* | | | | | |
| Bachelor Lake, Quebec | Light yellow | 96.3 | 5.4111 | 3.8262 | 3.1240 |
| Balmat, New York | Brown | 99.6 | 5.4152 | 3.8291 | (3.1265) |
| Eskaminish, Manitoba | Dark brown | 88.8 | 5.4177 | (3.8309) | 3.1280 |
| Frontenac Mine, Ontario | Brown | 90.6 | 5.4173 | 3.8306 | (3.1277) |
| New Calumet Mine, Ontario | Brown | 91.3 | 5.4172 | 3.8305 | (3.1276) |
| Ogdensburg, New Jersey | Very light yellow | 90.0 | 5.4116 | 3.8266 | 3.1240 |
| Parry Sound, Ontario | Brown | 92.0 | 5.4166 | 3.8301 | (3.1273) |

[1] The last digit of each number is uncertain.

[2] Values in brackets were calculated from $c/a = \sqrt{2/3}$.

of cubic packing, but this appears to be less in the specimens from low temperature deposits. In banded brown and white specimens, the brown bands apparently have more hexagonal packing than the white.

The measurements and the data in the literature appear to be compatible with the following hypotheses: 1) the lower the temperature below some temperature which is below the cubic-hexagonal transition, the more nearly equal are the relative amounts of cubic and hexagonal packing in zinc sulphide; 2) manganese and iron in the zinc sulphide phase reduce the temperature of the cubic-hexagonal transition; 3) below but near the cubic-hexagonal transition temperature, there is a range of existence of various polytypes with mixtures of cubic and hexagonal packing. Stated more definitely, it appears that light-colored zinc sulphide from high temperature deposits has mostly cubic packing, but similar material from low temperature deposits has somewhat larger amount of hexagonal packing. Conversely, it appears that very dark-colored zinc sulphide from high temperature deposits has a large amount of hexagonal packing, but similar material from low temperature deposits has mostly cubic packing. However, when light- and dark-colored zinc sulphide are interbanded, the latter has more hexagonal packing than the former.

The relations between the type of packing, composition, temperature and other conditions of crystallization of (Zn, Fe, Mn, Cd)S compounds are now being investigated, with the hope that a new pressure-insensitive geothermometric relation may be derived.

## Acknowledgements

The *x*-ray diffraction spectrographs were made with apparatus in the Department of Metallurgical Engineering of this University, with the kind permission of L. M. Pidgeon. In developing the theoretical arguments, I was aided by discussions with Ursula M. Martius, E. W. Nuffield, and W. C. Winegard. Many of the mineral specimens were provided by R. M. Thompson.

## References

Allen, E. T., Crenshaw, J. L., & Merwin, H. E. (1912): The sulphides of zinc, cadmium, and mercury; their crystalline forms and genetic conditions. *Amer. Journ. Sci.* (4), **34,** 341–396.

——— (1914): Effect of temperature and acidity in the formation of marcasite ($FeS_2$) and wurtzite (ZnS); a contribution to the genesis of unstable forms. *Amer. Journ. Sci.* (4), **38,** 393–431.

Aminoff, G. (1923): Untersuchungen über die Kristallstrukturen von Wurtzit und Rotnickelkies. *Zeit. Krist.* **58,** 203–219.

Bragg, W. L. (1937): *Atomic Structure of Minerals.* Cornell Univ. Press.

Buck, D. C., & Strock, L. W. (1954): Trimorphism in zinc sulfide. *Am. Mineral.*, **39,** 318 (abs.); **40,** 192–200.

Bunn, C. W. (1945): *Chemical Crystallography,* Oxford.

Corey, A. S. (1953): Note on sphalerite and wurtzite. *Am. Mineral.* **38,** 141–143.

Dana, J. D., & E. S. (1944): *System of Mineralogy,* **1,** ed. 7, by C. Palache, H. Berman & C. Frondel, New York.

Edwards, O. S., & Lipson, H. (1943): An *x*-ray study of the transformation of cobalt. *Jour. Inst. Metals* **69,** 177–188.

Evans, R. C. (1953): *An Introduction to Crystal Chemistry.* Cambridge.

Frondel, C., & Palache, C. (1950): Three new polymorphs of zinc sulphide. *Am. Mineral.* **35,** 29–42.

Fuller, M. L. (1929): The crystal structure of wurtzite. *Phil. Mag.* **8,** 658–664.

Gevers, R. (1952): Desordre unidimensionnel dans SiC et son influence sur les intensités diffractées des rayons X. *Acta Cryst.* **5,** 518–524.

——— (1954*a*): The diffraction of *x*-rays by close-packed crystals containing both 'growth stacking faults' and 'deformation or transformation stacking faults.' *Acta Cryst.* **7,** 337–343.

——— (1954*b*): *X*-ray diffraction by close-packed crystals with 'growth stacking faults' assuming an 'n-layer influence.' *Acta Cryst.* **7,** 492–494.

Hanawalt, J. D., Rinn, H. W., & Frevel, L. K. (1938): Chemical analysis by *x*-ray diffraction. *Ind. Eng. Chem.*, Anal. Ed. **10,** 457–512.

Hendricks, S., & Teller, E. (1942): *X*-ray interference in partially ordered layer lattices. *Jour. Chem. Phys.* **10,** 147–167.

Honjo, G., Miyake, S., & Tomita, T. (1950): Silicon carbide of 594 layers. *Acta Cryst.* **3,** 396–397.

Humphrey, G. L., Todd, S. S., Coughlin, J. P., & King, E. G. (1952): Some thermodynamic properties of silicon carbide. *U. S. Bur. Mines, Rept. Invest.* **4888.**

Jagodzinski, H. (1949*a*, *b*, *c*): Eindimensionale Fehlordnung in Kristallen und ihr Einfluss auf die Röntgeninterferenzen. I. II. III. *Acta Cryst.* **2,** 201–207, 208–214, 298–304.

——— (1954*a*): Der Symmetrieeinfluss auf den allgemeinen Lösungsansatz eindimensionaler Fehlordnungsprobleme. *Acta Cryst.* **7,** 17–25.

——— (1954*b*): Polytypism in SiC crystals. *Acta Cryst.* **7,** 300.

——— & Laves, F. (1948): Eindimensional fehlgeordnete Kristallgitter. *Schweiz. Min. Pet. Mitt.* **28,** 456–467.

Kröger, F. A. (1939): Formation of solid solutions in the system zincsulfide-manganesesulfide. *Zeit. Krist.* **100,** 543–545.

——— (1940): Solid solutions in the ternary system ZnS—CdS—MnS. *Zeit. Krist.* **102,** 132–135.

Méring, J. (1949): L'interférence des rayons X dans les systèmes à stratification désordonnés. *Acta Cryst.* **2,** 371–377.

Mitchell, R. S. (1953): Application of the Laue photograph to the study of polytypism and syntaxic coalescence in silicon carbide. *Am. Mineral.* **38,** 60–67.

——— & Corey, A. S. (1954): The coalescence of hexagonal and cubic polymorphs in tetrahedral structures as illustrated by some wurtzite-sphalerite groups. *Am. Mineral.* **39,** 773–782.

Müller H. (1952): Die eindimensionale Umwandlung Zinkblende-Wurtzit und die dabei auftretenden Anomalien. *Neues Jahrb. Min.* **84,** 43–76.

Paterson, M. S. (1953): *X*-ray diffraction by face-centred cubic crystals with deformation faults. *Jour. Appl. Phys.* **23,** 805–811.

RAMDOHR, P., & VON WEBSKY, C. (1943): Wurtzitkristalle und Zwillinge. *Neues Jahrb. Min.* Mon. A, 1943, 65–71.

RAMSDELL, L. S. (1944): The crystal structure of alpha-SiC, type IV. *Am. Mineral.* **29,** 431–442.

——— (1945): The crystal structure of alpha-SiC, type VI. *Am. Mineral.* **30,** 519–525.

——— (1947): Studies on silicon carbide. *Am. Mineral.* **32,** 64–82.

——— & KOHN, J. A. (1951*a*): Three new polymorphs of silicon carbide, 8*H*, 75*R*, and 84*R*. *Acta Cryst.* **4,** 75.

——— (1951*b*): Disagreement between crystal symmetry and *x*-ray diffraction data as shown by a new type of silicon carbide, 10*H*. *Acta Cryst.* **4,** 111–113.

——— (1952): Developments in silicon carbide research. *Acta Cryst.* **5,** 215–224.

——— & MITCHELL, R. S. (1953): A new hexagonal polymorph of silicon carbide, 19*H*. *Am. Mineral.* **38,** 56–59.

RANDALL, J. T. (1937): The effects of temperature on the intensity of fluorescence of some impurity solids. *Proc. Phys. Soc.* **49,** 46–56.

SCHLEEDE, A. (1935): Über die Zinksulfid- und Zinkcadmiumsulfid-Luminophore und ihre Bedeutung für das Problem des Fernsehens. *Angew. Chemie* **48,** 276–277.

STROCK, L. W., & BROPHY, V. A. (1955): Synthetic zinc sulfide polytype crystals. *Am. Mineral.* **40,** 94–106.

SWANSON, H. E., & FUYAT, R. K. (1953): Standard *x*-ray diffraction powder patterns. *U. S. Bur. Stands.* Circ. **539.**

THIBAULT, N. W. (1944): Morphological and structural crystallography and optical properties of silicon carbide. *Am. Mineral.* **29,** 249–278, 327–362.

——— (1948): Alpha-silicon carbide, type 51*R*. *Am. Mineral.*, **33,** 588–599.

TUCKER, C. W. JR., & SENIO, P. (1954): *X*-ray scattering by lattice defects in neutron-irradiated single crystals of boron carbide. *Acta Cryst.* **7,** 456.

ULRICH, F., & ZACHARAISEN, W. (1925): Über die Kristallstruktur des alpha- und beta-CdS, sowie des Wurtzits. *Zeit. Krist.* **62,** 260–273.

VERMA, A. R. (1953): *Crystal Growth and Dislocations.* London.

WILSON, A. J. C. (1942): Imperfections in the structure of cobalt. II. Mathematical treatment of proposed structure. *Proc. Roy. Soc. London,* **180A,** 277–285.

WYCKOFF, R. W. G. (1951): *Crystal Structures,* **1,** Ch. 3. New York.

ZHDANOV, G. S., & MINERVINA, Z. V. (1947): (Crystal structure of SiC VI and geometrical theory of silicon carbide structures.) *Jour. Exptl. Theor. Phys.* (U.R.S.S.) **17,** 3–6.

# THE MINERALOGY AND GENESIS OF THE BAUXITE DEPOSITS OF JAMAICA, B.W.I.

V. G. Hill, *University of Toronto, Toronto, Canada.*

## Abstract

The principal bauxite deposits of Jamaica are located in the parishes of Manchester, St. Elizabeth and St. Ann. They are surface accumulations, and show a close relationship to the fault pattern of the region. The distance between the top of the White Limestone and the impervous formations below determine the degree of desilication of the deposits. Gibbsite, boehmite, iron oxide, kaolinite and quartz are the most abundant minerals. Field and laboratory evidence indicate that the White Limestone is the source of the ore, and by comparison with other deposits and phase equilibria work on related systems it is deduced that a volcanic ash could not be the source material. This approach further suggests that the deposits are not in equilibrium, because the mineralogy is not consistent.

## Introduction

The bauxite deposits of Jamaica B.W.I. were discovered in 1942, as the result of an investigation into the cause of the lack of fertility of the pasture regions. On the basis of chemical analysis, Mr. R. F. Innes of the Department of Agriculture suggested that these soils might be an aluminium ore, but it was the energy and foresight of Sir Alfred DaCosta that drew the attention of the mining companies to the deposits.

To date, attention has been focused on the location and treatment of the ore. The three interested mining companies have now located the major deposits, and have been able to modify North American extraction processes to handle the ore. However, there is still wide scope for research, and much can be done to improve the methods of evaluating the grade and character of the ore. Schmedeman (1948), Zans (1952), and Hartman (1955), have done some fundamental work on the deposits, but to date there has been no real concerted effort made to elucidate the problem of the genesis of the deposits. Investigators have suggested that it may have been derived from the White Limestone, volcanic ash, or vaguely as a wind blown deposit. The actual mechanism of the process or processes involved has never been clearly defined, and has been a rather controversial subject.

## Geology

The geology of the island has been discussed by Sawkins (1869), Hill (1899), Hose (1950), Zans (1951, 1952), and Hartman (1955). The White Limestone is the only formation in which we will be interested, and the following description of it is given by Zans (1954, pp. 317–318).

"The lower part of the White Limestone Formation is formed by hard compact dolomites and dolomitic limestones with *Dictyoconus*. This horizon is the lowest which is associated in its outcrops with bauxite and terra rossa. The deposits, however, are small owing to the narrowness of the solution hollows excavated in these extremely hard, compacted rocks. The succeeding beds of the White Limestone formation are crystalline or compact limestones of Middle and Upper Eocene age, including the zones of *Lepidocyclina pustulosa H. Douville*, *L. chaperi Lem.* and *R. Douv.* along with *Dictyoconus fontabellensis.* (*Vaughan*) and *D. cookei Mob.* Lithologically this series consists of extremely pure white limestone, often nodular or chalky and brecciated along fault zones. It is this series which carries the rich bauxite deposits in Jamaica, most of them being associated in particular with beds of Upper Eocene age. Recent surveys in the western parts of the island show that these beds are overlain unconformably by less compacted Upper Oligocene Limestone, indicating a break in sedimentation during Lower and Middle Oligocene times, which may have involved the first stage of karstification. The lowest part of the succeeding Upper Oligocene contains a typical Antiguan fauna of *Lepidocyclina undosa Cushman*, *L. favosa Cush.*, etc. and again carries terra rossa and bauxite."

The major structural feature is an anticline with axis of approximately NW–SE trend. The Pre-cretaceous basement complex was part of a stable land mass that suffered subsidence, and on which were deposited unconformably the younger sediments which lap out from the ancient core. A rather complex fault pattern has been superimposed on this during the Miocene deformation. It is this orogeny that determined the present physiographic features of the island. The major faults trend from E–W and from NW–SE. These faults determine the present coastlines of the island. Across the central regions where the accumulation of limestone is thickest there are a series of subsidiary N–S faults. The intense faulting is the result of the adjustments of the limestone covering to the tectonic forces. The uplift and shattering of the rocks resulted in the development of the present karst topography, the fault and fracture zones acting as channels for the subsurface drainage pattern. Only in those regions where the down faulting (probably of the graben type) was sufficient to depress the surface below sea level do we find surface drainage on the Pleistocene rocks.

## Distribution and Morphology of the Ore Bodies

The commercially important bauxite deposits are localized in three areas. The largest accumulation occurs in the Mandeville-Williamsfield-Mile Gully trough. The general trend is roughly NW–SE and is localized by a block fault widening in the SE direction. In close geographic association with these deposits are those controlled by the step faulting of the St. Elizabeth region starting from Spur Tree and extending along the axis of these faults to Alligator Pond and Santa Cruz. The third major belt extends from Mount Brasso through the Clarement-Moneague basin. The deposits in this area tend to be discontinuous and in general patchy. There are minor occurrences of ore in the karst area of Trelawny, and in the limestone area at the foot of Mount Diablo. The former de-

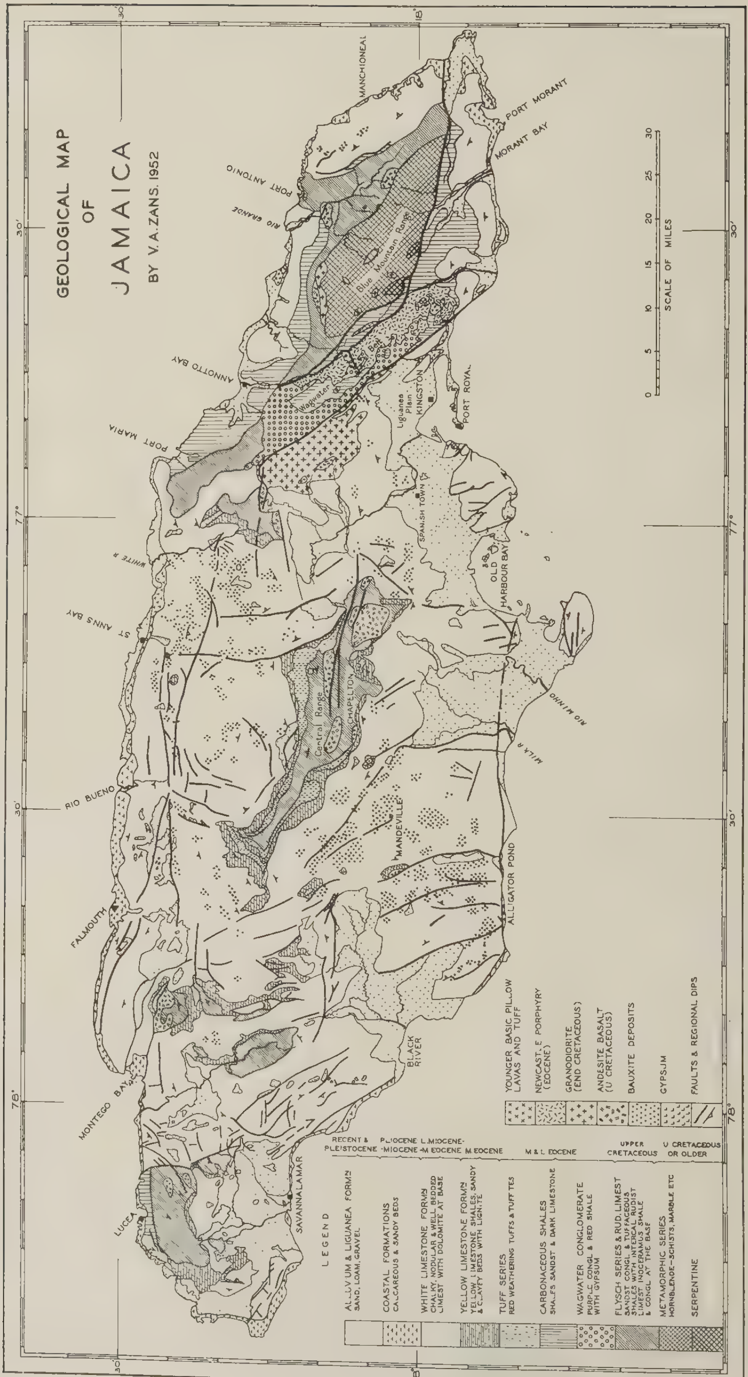
GEOLOGICAL MAP
OF
JAMAICA
BY V. A. ZANS. 1952
MANCHIONEAL
PORT MORANT
MORANT BAY
PORT ANTONIO
RIO GRANDE
Blue Mountain Range
ANNOTTO BAY
Wagwater
Liguanea Plain
KINGSTON
PORT ROYAL
PORT MARIA
SPANISH TOWN
WHITE R.
OLD HARBOUR BAY
ST ANNS BAY
CHAPELTON
Central Range
RIO MINHO
MILK R.
RIO BUENO
MANDEVILLE
ALLIGATOR POND
FALMOUTH
BLACK RIVER
MONTEGO BAY
SAVANNA LA MAR
LUCEA
0 5 10 15 20 25 30
SCALE OF MILES
18°
30'
77°
78°
LEGEND
ALLUVIUM & LIGUANEA FORMN
SAND, LOAM, GRAVEL
COASTAL FORMATIONS
CALCAREOUS & SANDY BEDS
WHITE LIMESTONE FORMN
CHALKY, NODULAR & WELL BEDDED LIMEST WITH DOLOMITE AT BASE
YELLOW LIMESTONE FORMN
YELLOW LIMESTONE SHALES, SANDY & CLAYEY BEDS WITH LIGNITE
TUFF SERIES
RED WEATHERING TUFFS & TUFFITES
CARBONACEOUS SHALES
SHALES SANDST & DARK LIMESTONE
WAGWATER CONGLOMERATE
PURPLE CONGL & RED SHALE WITH GYPSUM
FLYSCH SERIES & RUD. LIMEST
SANDST CONGL & TUFFACEOUS SHALES WITH INTERCAL RUDIST LIMEST INOCERAMUS SHALE & CONGL AT THE BASE
METAMORPHIC SERIES
HORNBLENDE-SCHISTS, MARBLE ETC
SERPENTINE
RECENT & PLEISTOCENE
PLIOCENE-MIOCENE
L. MIOCENE-M. EOCENE
M. EOCENE
M & L EOCENE
UPPER CRETACEOUS
U CRETACEOUS OR OLDER
YOUNGER BASIC PILLOW LAVAS AND TUFF
NEWCASTLE PORPHYRY (EOCENE)
GRANODIORITE (END CRETACEOUS)
ANDESITE BASALT (U CRETACEOUS)
BAUXITE DEPOSITS
GYPSUM
FAULTS & REGIONAL DIPS

posits tend to be small and very erratic, while the latter though somewhat more continuous are of a very low grade. Still other deposits abound in the White Limestone area, but these need not be considered as they are generally low grade and extremely erratic.

The general morphology of the individual ore bodies varies in a continuous trend from pipe-like masses through long tabular shapes to the blanket types in troughs up to twenty miles long and ten miles wide. Many of the transitional forms can be observed on a small scale in the Belmont mining area. The ore occurs at the surface with only a thin mantle of top soil covering it. There is a sharp knife edge contact between the ore and limestone, although the boundary is undulatory. Very often the underlying limestone is a friable powder, but even in this case the purity of the limestone, (in areas where the ore is well developed) differs very little in composition from the rest of the White Limestone formation. In other cases the underlying White Limestone is broken and shattered. This friable nature of the underlying White Limestone is typical of the bauxite deposit.

The surface expression of the deposits is dependent on the size and shape of the ore body, and the enclosing limestone. The larger deposits tend to be undulatory with low mounds of bauxite, and more independent of the structure of the underlying rocks. The smaller ones may be a mere U shaped cover in the valleys, while in a few cases the ore is localized on one side of the valley.

Local and regional faults tend to localize the trend and occurrence of the ore. Superimposed on this is the modification caused by the resulting drainage pattern. Speaking generally, one can say that the commercially important deposits occur at elevations greater than 250 feet above sea level. The important factor is the height of the deposit above the water table, which is controlled by the argillaceous formations. The grade of the ore is related to the distace of separation from the water table. The best deposits occur from 1,000 to 3,000 feet above sea level. A separation of 1,000 to 1,500 feet between the pervious White Limestone and impervious Yellow Limestone formation seems to give the optimum conditions for development of the ore.

There is a complete absence of visible bedding features in the ore bodies, but for a dark zone of enrichment of pyrolusite near the contact of the limestone. The occurrence of vertical areas of a lighter colour material is due to the leaching of iron oxide resulting from the reduction of the ferric iron by decaying roots. Local miniature slip structures in the ore represent possible adjustment features and channel ways for the downward migration of water. The platy morphology of gibbsite and kaolinite readily facilitates the occurrences of these slip planes.

## COMPOSITION OF THE ORE

There is a continuous variation series in the change of composition of the laterites, so there is no sharp compositional boundary between the bauxitic laterities, ferruginous laterites, and lateritic clays. The distinction of good bauxite is simply made on economic considerations. The composition of individual ore bodies is relatively constant when mature, while there are more systematic variations in the more youthful deposits. There are also marked differences between the ore from St. Elizabeth basin as compared with that from either the Claremont-Moneague basin, or the Williamsfield-Mile Gully trough. The ore from the St. Catherine district is very youthful, and so shows differences in composition from the more mature deposits. The composition of the bauxite laterities is:

| | St. Ann | Manchester | St. Elizabeth | Range |
|---|---|---|---|---|
| $Al_2O_3$ | 47.52 | 46.04 | 42.08 | 45.0 –52.0% |
| $H_2O(110°)$ | 27.62 | 27.40 | 26.04 | 18.0 –28.0% |
| $Fe_2O_3$ | 20.33 | 20.51 | 26.66 | 15.0 –25.0% |
| $SiO_2$ | 0.52 | 2.75 | 0.42 | 0.1 –10.0% |
| $TiO_2$ | 2.58 | 2.17 | 2.53 | 2.0 – 2.6% |
| $P_2O_5$ | 0.42 | 0.23 | 0.96 | 0.1 – 5.0% |
| MnO | 0.79 | 0.37 | 0.46 | 0.1 – 3.0% |
| MgO | n.d. | n.d. | n.d. | 0.01– 0.1% |
| CaO | tr. | tr. | tr. | tr. – 1.0% |

The mineral composition of the ore was determined by $x$-ray diffraction, differential thermal analysis, electron microscope, and optical microscope on selected samples. In all other cases the mineralogy was deduced from the results of chemical analysis. All the principal minerals but the iron oxide gave excellent $x$-ray diffraction patterns, and the results show excellent agreement. The samples for the electron micrographs were used without treatment where it was desired to study the bauxitic minerals. However, in the case of the clay minerals, the dilute hydrochloric acid insoluble residue was used.

Gibbsite, $Al(OH)_3$, is the most abundant mineral in the ore, and may account for up to 80% of the mineralogical composition in a few cases. The crystals have an average size of about 0.2 microns, (Fig. 1), but show good crystal outlines and give quite sharp $x$-ray diffraction patterns.

Boehmite, $(AlO \cdot OH)$, generally occurs as a very minor mineral, but may be as abundant as 20%. The crystals have an average size of 0.2 microns, and are quite poorly developed.

Kaolinite and halloysite, $Al_2Si_2O_5(OH)_4$, are the principal clay minerals. These minerals are extremely fine grained with particle size of 0.1 to 0.4 microns, and are rather poorly developed (Figs. 2 & 3). The clay mineral

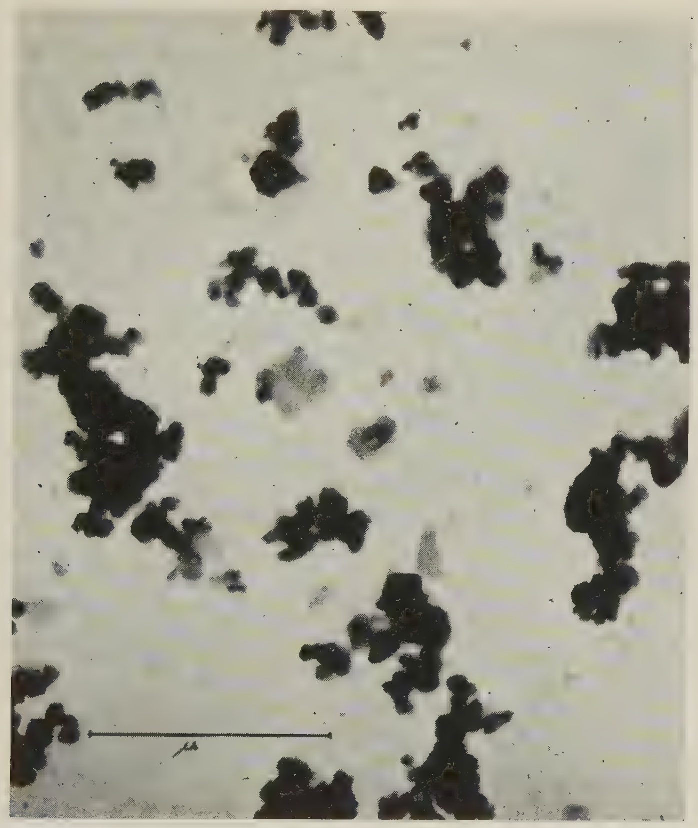

FIG. 1. Electron micrograph of bauxite showing crystals of gibbsite. The fine background particles are believed to be iron oxide.

content shows a roughly inverse relationship to the iron oxide content. The halloysite crystals show the characteristic tubular morphology under the electron microscope, but have poor outlines and frayed edges.

The iron in the ore is believed to be present in the form of a fine gel coating on the other minerals on the basis of the electron microscope studies. *X*-ray work indicates the presence of only small amounts of haematite, and suggests that the majority of the iron is present in the colloidal form. It is this colloidal iron oxide that is responsible for the variation in colour of the bauxite. The colour varies from yellowish brown to red, but minor amounts of pyrolusite may impart a darker tone. Slight valency changes may also affect the colouration of the iron oxide. Differences in particle size of the clay size minerals on which the gel occurs also seem to affect the colour.

The titanium in the ore appears to be present in the cryptocrystalline

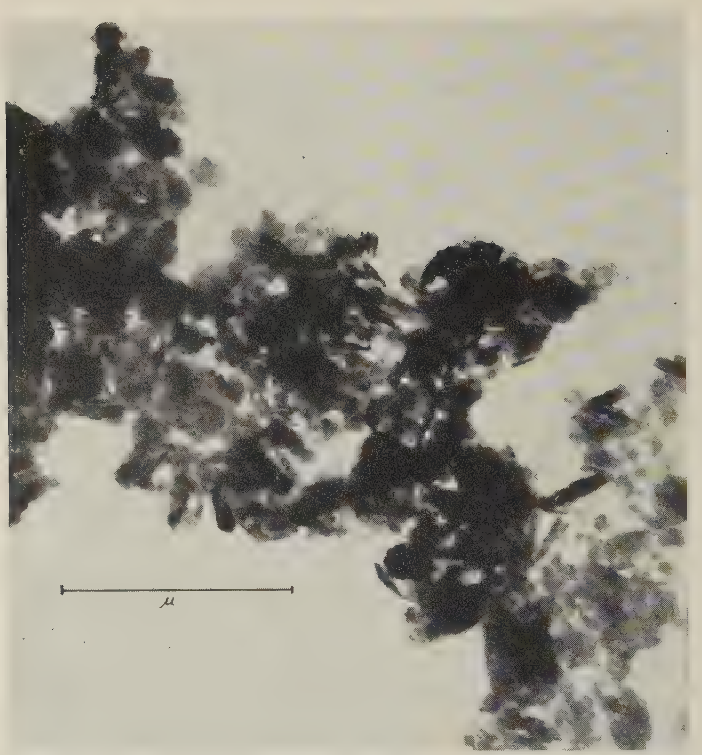

FIG. 2. Electron micrograph of the hydrochloric acid insoluble residue of bauxite showing crystals of kaolinite flakes and tubular endellite.

form. Some of it also is present as minute crystals of rutile and anatase, which may be in a mass of leucoxene. Titanomagnetite and ilmenite are present to a minor extent. The fact that the phosphorous is not 'available' for plant nutrition suggests that it may be present as ferric or aluminium phosphate. However, this is not conclusive evidence, as it could be present as apatite. This idea is supported by the fact that the high phosphorous ore also contains an appreciable amount of calcium. The difficulty in resolving this problem is that the ore in high in iron and so has to be treated with hydrochloric acid before microscopic examination. This treatment could dissolve the tiny apatite crystals if present. Quartz and chert occur in the size range of sand size to clay size. The larger grains are quite erratic, while the finer sizes occur in areas where the clay content is high but variable. Muscovite and orthoclase feldspar have been identified under the petrographic microscope. Minor amounts of tourmaline, garnet, and volcanic glass have been reported (Hartman, 1955, pp. 25–26).

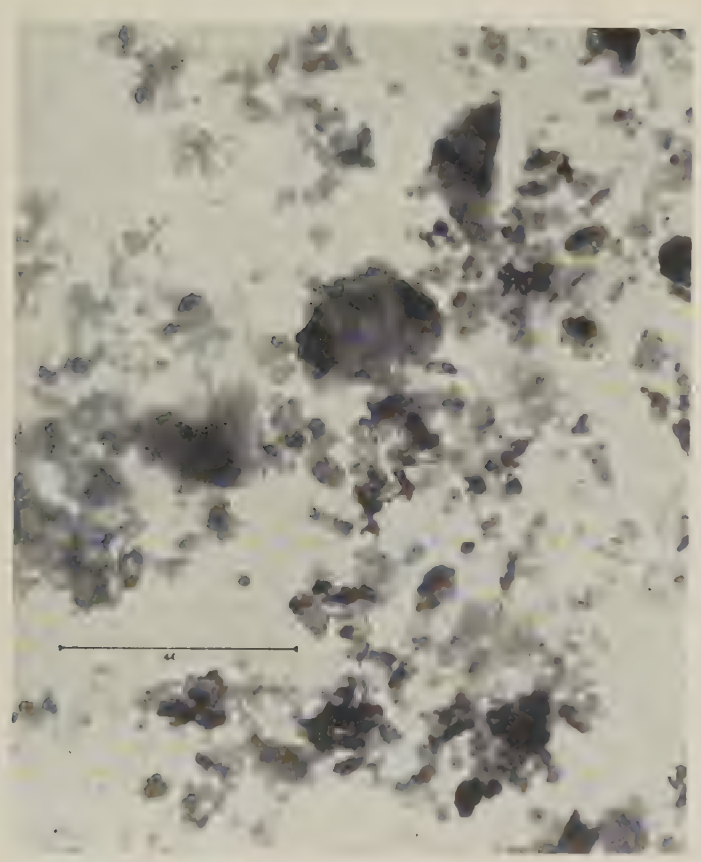

FIG. 3. Electron micrograph of the hydrochloric acid insoluble of bauxite showing kaolin, endellite and mica.

Detailed examination of ore bodies shows that they are zoned both mineralogically and chemically. The top soil of the ore bodies is always higher in silica than the other parts. There is also a silica rich zone situated just below the centre of the ore body, and grades out gradually into zones of lower silica content. Manganese concentrates near the limestone contact as little oolites of wad and finely disseminated manganese dioxide. Phosphorous content is zoned roughly similar to that of manganese. Superimposed on this broad basic zoning is another distribution pattern of small patches of silica-rich ore grading into areas of slightly lower silica content in much the same fashion as xenoliths in a granite. The silicates seem to act as the bonding agent of the ore minerals, because the regions of higher silica content form lumps, while the lower silica areas being more friable, are more readily broken.

## GENESIS OF THE ORE

The simplicity and similarity between the mineralogy of the acid insoluble residue in the White Limestone and the bauxite and their difference from those of other formations would suggest that the White Limestone is the immediate source of the bauxite. This idea is further supported by the fact that the White Limestone contains the same minor elements as the bauxite and in approximately similar ratios. The extreme purity of the White Limestone is the principal objection to the theory that it is the immediate source of the ore. Chemical analysis of the White Limestone shows that it contains about 0.5% acetic acid insoluble residue. This includes the following principal constituents: $Al_2O_3$, $Fe_2O_3$, $SiO_2$, $TiO_2$, $P_2O_5$ and water. The ore occupies only about 15% of the present White Limestone surface, and of an average thickness of about 25 feet. This volume of ore could be obtained from the solution of the limestone to a depth of 750 feet. Even if we assume that the retention was only 50% efficient, the depth of erosion would only be 1,500 feet. On this basis the degree of solution cannot be regarded as excessive or improbable.

It is well known that the rainfall in tropical regions is seasonal. During the rainy season there is solution of the limestone by the surface water. The non-carbonate materials are released and may be dissolved, form a colloidal suspension, or be mechanically transported. These are deposited when the water leaves the surface to enter the subsurface drainage system. The limestone acts as a precipitating agent for many of the substances in true or colloidal solution. The result is a hodge-podge mixture of colloidal hydrous oxides and silica, fine grained clays and bauxitic minerals, with varying amounts of quartz, titanohematite, and ilmenite of sand grain size. During the succeeding dry seasons, there is an upward migration of the enclosed water by capillary action. On reaching the surface the water evaporates, leaving a residue of gelatinous silica and sometimes calcium carbonate. In the next rainy season the carbonate dissolves leaving a residue of partly dehydrated silica, and there is continued deposition of more insoluble residue. This oscillation of wet and dry seasons causes an increase in the size of the deposit, a depletion in the silica content, and a destruction of depositional features. The difference in solubility and ionic potentials cause a separation of the elements. The degree of separation is also dependent on the seasonal variation in rainfall, temperature, and depth of vertical drainage through the limestone. If the silica is removed rapidly then the residue is a bauxite deposit, while a slow desilication process allows enough time for the silica to react with the alumina to form an argillaceous laterite. The latter condition is true of the St. Catherine deposits, and even more

TABLE 1. ANALYSES OF WHITE LIMESTONE

| LOI | $SiO_2$ | $R_2O_3$ | $P_2O_5$ | MnO | $TiO_2$ | CaO | MgO |
|---|---|---|---|---|---|---|---|
| St. Ann | | | | | | | |
| 43.74 | 0.12 | 0.39 | 0.007 | 0.003 | 0.016 | 55.54 | 0.14[1] |
| 43.65 | 0.04 | 0.99 | 0.051 | 0.005 | * | 55.10 | 0.20[1] |
| 43.86 | 0.06 | 0.31 | 0.034 | 0.005 | * | 55.65 | 0.17[1] |
| 42.77 | 0.05 | 0.31 | 0.023 | 0.004 | 0.005 | 56.74 | 0.17[1] |
| 43.80 | 0.03 | 0.26 | 0.021 | 0.004 | 0.004 | 56.33 | 0.24[1] |
| 45.83 | 0.11 | 0.19 | 0.048 | 0.002 | 0.006 | 53.49 | 0.24[1] |
| 43.45 | 0.19 | 4.02 | 0.028 | 0.005 | * | 51.79 | 0.36[1] |
| 43.61 | 0.06 | 0.04 | 0.045 | 0.005 | 0.003 | 56.48 | 0.16[1] |
| 43.01 | 0.04 | 0.02 | 0.042 | 0.005 | 0.003 | 56.70 | 0.15[1] |
| 44.05 | 0.04 | 0.18 | — | — | — | 55.71 | — |
| 44.50 | 0.01 | 0.12 | — | — | — | 55.04 | — |
| 43.92 | 0.05 | 0.24 | — | — | — | 55.89 | — |
| 44.12 | 0.01 | 0.15 | — | — | — | 55.33 | — |
| 44.042 | 0.00 | 0.03 | — | — | — | 55.20 | — |
| 43.96 | 0.03 | 0.18 | — | — | — | 55.18 | — |
| Manchester | | | | | | | |
| 44.19 | 0.02 | 0.15 | — | — | — | 56.05 | — |
| 44.08 | 0.04 | 0.08 | — | — | — | 55.97 | — |
| 44.39 | 0.04 | 0.15 | — | — | — | 54.88 | — |
| 43.28 | 0.00 | 0.31 | — | -- | — | 55.92 | — |
| 43.94 | 0.02 | 0.27 | — | — | — | 56.02 | — |
| St. Elizabeth | | | | | | | |
| 44.01 | | 0.05 | — | — | — | 55.31 | — |

* Less than 0.005% present.

[1] Values from Hartman (1955, p. 20). All other values from Zans (1951, p. 23).

so of the 'Moneague Lake' area, where the water table is almost at the surface. The rapid horizontal change of bauxite to clay as is found in the Carton area of Claremont is related to this difference in the height of the water table, due to vertical displacement of the impervious limestone by faulting.

The gradual increase in the accumulation of the laterite is accommodated by the solution of the limestone tending to give a funnel shape deposit. The degree of shattering and fault patterns control the general solution trends. Gradually adjoining "sinks" coalesce by lateral growth to form larger catchment basins. The general effect can be considered as one of growth, and the various invaginations extending from the ore into the limestone are mere outposts of replacement of the limestone by the bauxite. The occurrence of a column of limestone about 50 feet high in one of the ore bodies mined by Alumina Jamaica Limited, is evidence of an area that was less susceptible to solution than the limestone that once surrounded it.

The distribution of manganese and phosphorous does not seem to fit into this simple scheme. The composition of the White Limestone formation is quite uniform over the entire island, and yet the bauxite deposits show wide variations in the phosphorous and manganese content. For example the ores from St. Elizabeth contain from 0.5–5% $P_2O_5$ and 1–0.5% MnO while those from St. Ann and Manchester contain 1.5 0.2% $P_2O_5$, and 0.5–0.1% MnO. The relative enrichment of these two elements in the ore from St. Elizabeth is related to their geochemistry. The concentration of these elements around the margins of the ore bodies is dependent on their difference in ionic potential from iron, aluminium, and titanium, but it is believed that minor difference in pH and redox potential in the St. Elizabeth deposits may cause the relative enrichment of phosphorous and manganese there. However this subject should be investigated more fully.

The fact that montmorillonite has not been detected in the ore is noteworthy, especially as bits of volcanic glass have been reported. The conclusion is that the intensity of weathering was insufficient to destroy the glass, so were a volcanic ash the original source material, it would be expected that the chemical environment would be quite complex, and result in the crystallisation of such stable minerals as montmorillonite, illites, etc. This is not the case. In fact, by analogy with the weathering of basaltic rocks (Allen, 1948, pp. 632–633), we can deduce that the presence of montmorillonite (nontronite) is a necessary step in the weathering process, and occurs at the expense of the volcanic materials. The inference is that this glass was carried into the forming limestone by streams, and one cannot use it as an index or criterion of volcanic origin of the ore. Again, one would expect a volcanic ash to be quite widespread, especially as there is a definite relationship between the origin of the deposits in Haiti, and the Dominican Republic. The use of beds of bentonite, a weathering product from volcanic ash, as marker horizons over wide areas is well known in stratigraphy. This would lead one to expect a montmorillonite to occur in areas where the drainage is poor. In actual practice, it has only been reported in two localities in Jamaica, and so we can say that the volcanic theory has no real support. This conclusion is further supported by the fact that kaolinite is the stable mineral where the water table is near the surface, a condition that does not allow for the rapid removal of alkali and alkaline earth ions which would affect the pH and stability relationship of the phases. Grim (1953, pp. 321 323) discusses the phase stability relationships among the alumina-silica-water minerals under acid and alkaline conditions, and in the presence of potassium and magnesium ions. His general conclusions agree with those deduced from the mineralogy of the bauxite deposits, suggesting that there was insufficient alkali ions present in the source material of the ore. A volcanic ash would have supplied these ions.

The major components of the ore are alumina, ferric oxide, silica, and water. At the temperatues that have existed in the ore since its formation, ferric oxide does not interfere with the reactions among the other components, except in so far as it may modify the rate of attaining equilibrium, so we may neglect it in considering the phase equilibria. The work of Roy & Osborn (1954), shows that the equilibrium phases in the system $Al_2O_3$—$SiO_2$—$H_2O$ for such compositions at low temperatures are gibbsite, and endellite, or kaolinite. It is believed on the basis of the results obtained by Sand (1954), that the crystallisation of either endellite or kaolinite is related to factors, such as the position of the water table and the structural control exercised by the parent minerals. It is immediately evident that the presence of quartz and boehmite in many ore bodies, and the absence of montmorillonite does not fit into this simple scheme. The evident explanation is that we are dealing with a process that has not attained equilibrium. This hypothesis is supported by the distribution of silica (quartz and kaolin) in the deposits. Boehmite has not been identified in many of the deposits, and its distribution follows a different pattern to the other minerals. It seems to show a general association with the faulting of the region. This suggests that it is a "fossil" mineral derived from the limestone in which it was produced by decomposition of gibbsite during faulting.

Examination of the acetic acid insoluble residue from the White Limestone by *x*-ray diffraction gave inconclusive results because of the complexity of the mineral assemblage, the high iron content, and the presence of some amorphous material. This explanation is supported by the fact that the equilibrium temperature for the transformation of gibbsite to boehmite is 130° and there is no evidence to support the idea that the ore was at these temperatures after deposition.

## Conclusion

On the basis of the results obtained from the study of the bauxite deposits and the White Limestone the conclusion is that this formation is the immediate source of the bauxite. This idea is supported by phase equilibria studies and comparison with other bauxite occurrences, which show that a clay mineral of the montmorillonite group should be present in the low grade bauxitic clays if a volcanic ash was the source material. This mineral (nontronite) has not been identified in any of the clays studied. The boehmite in the ore was produced during faulting of the limestone, and so occurs in the ore as a "fossil" mineral.

## ACKNOWLEDGEMENTS

The author wishes to express his thanks to Dr. F. G. Smith of the University of Toronto, and Dr. Rustum Roy of the Pennsylvania State University for critically reading the manuscript. The electron microscope work was done at the Pennsylvania State Univesity, and the x-ray studies at the above institution and the University of Toronto. Mr. James A. Hartman, former geologist of the Reynolds Jamaica Mines, Ltd., and the author did the field work. The laboratory work was done while the author was a member of the staff of Reynolds Jamaica Mines, Ltd. The geological map of Jamaica is published with the kind permission of Dr. V. A. Zans, Director of the Geological Survey Department, Jamaica B.W.I. This report is published with the permission of Mr. William S. Cole, Jr., Manager of Reynolds Jamaica Mines, Ltd.

## REFERENCES

ALLEN, V. T. (1948), Formation of bauxite from basaltic rocks of Oregon: *Econ. Geol.* **48,** 619–626.

ERVIN, G. JR., & OSBORN, E. F. (1951), The system $Al_2O_3$-$H_2O$: *Jour. Geol.*, **59,** 381–394.

GOLDRICH, S. S., & BERQUEST, H. R. (1947), Aluminous lateric soil of the Sierra de Bahoruco area. Dominican Republic, W.I. *U.S.G.S. Bull.* 953-C, 53–84.

GOLDRICH, S. S., (1948), Aluminous lateritic soil of the Republic of Haiti, W.I., *U.S.G.S. Bull.* 954-C, 63–109.

GRIM, R. E. (1953), *Clay Mineralogy,* New York.

HARDER, E. C. (1949), Stratigraphy and origin of bauxite deposits: *Bull. Geol. Soc. Am.*, **60,** 887–908.

——— (1949), Bauxite, *Industrial minerals and rocks*, 2nd edition, *A.I.M.E.* 95–118.

——— (1952), Examples of bauxite deposits illustrating variations in origin. Problems of clay and laterite genesis symposium, *Am. Inst. Min. Metal. Eng.* 35–64.

HARTMAN, J. A. (1955), The heavy minerals in the bauxite deposits of Jamaica: *M.S. thesis, University of Wisconsin.*

HILL, R. T. (1899), The geology and physical geography of Jamaica: *Bull. Mus. of Comp. Zoo. of Harvard.*

HOSE, H. R. (1950), The geology and mineral resources of Jamaica: *Colon. Geol. Min. Resour.* **1,** (11–36).

ROY, R. & OSBORN, E. F., (1954), The system, $Al_2O_3$-$SiO_2$-$H_2O$: *Am. Mineral.*, **39,** 853–885.

SAND, L. B. (1952), Mineralogy and petrology of the residual kaolin of the Southern Appalachian region: *Ph.D. Dissertation, Pennsylvania State University.*

SAWKINS, J. G. *et al.* (1869), Report on the geology of Jamaica: *Mem. Geol. Surv.* 1–340.

SCHMEDEMAN, O. C. (1948), Caribbean aluminum ores: *Eng. Min. Jour.* **149,** 78–82,

——— (1950), First Caribbean bauxite development: Reynolds Jamaica Mines, Ltd., *Eng. Min. Jour.*, **151,** 98–100.

ZANS, V. A. (1951), Economic geology and mineral resources of Jamaica: *Geol. Surv. Jam. Bull. No. 1*, 1–61.

——— (1952), Bauxite resources of Jamaica and their development: *Colon. Geol. and Min. Resour.* **3,** 307–333.

# NOTES AND NEWS

## "HEWETTITE" AND "METAHEWETTITE"

W. H. Barnes, *Division of Physics, National Research Council, Ottawa, Canada.*

The investigation of the structures of "hewettite" and "metahewettite" (Barnes & Qurashi, *Am. Mineral.*, **37**, 409, 1952) has been hampered, not only by the poor quality of single crystals of these minerals, but also by their hydration characteristics. In an attempt to establish reference standards for "wet" and "dry" material, a systematic *x*-ray diffraction powder investigation has been undertaken. Briefly the procedure has been to take up crushed specimens in capillary tubes (Matthews, *Anal. Chem.*, **26**, 619, 1954; Barnes & Sheppard, *Bull. on Narcotics, U. N. Dept. Social Affairs*, **6** (2), 27, 1954) and then (*a*) fill with distilled water, seal with Household (Duco) Cement or collodion, and take photographs at intervals until no change in the powder pattern was observed, on (*b*) store over $P_2O_5$ in a desiccator, remove at intervals, seal, photograph, open the seal, restore to the desiccator, and repeat until a constant pattern was obtained. Similar tests have been made starting with "wet" samples from (*a*) and drying as in (*b*), and commencing with dry samples from (*b*) and saturating with water as in (*a*). Individual samples also have been subjected to repeated cycles of hydration and dehydration.

The following specimens[1] have been employed:

1. Metahewettite, in conglomerate, Cactus Rat mine, Yellow Cat district, Grand Co., Utah (Harvard 98019).
2. Hewettite, Yellow Cat (Webber. U.S.G.S.).
3. Hewettite, Jo Dandy mine, Montrose Co., Colorado (MNG/4/49, U.S.G.S.; Sherwood-analyzed material).
4. Metahewettite, Montrose Co., Colorado (Harvard 95445).
5. Metahewettite, East Paradox Valley, Montrose Co., Colorado (Harvard 93306; type material from Dr. W. F. Foshag, U. S. National Museum).
6. Metahewettite, on gypsum with carnotite, Hummer mine, East Paradox Valley, Montrose Co., Colorado.
7. Hewettite, with pascoite in patronite, Minasragra, Cerro de Pasco, Peru (Harvard 96258; type locality).
8. Synthetic sodium vanadate (Marvin, U.S.G.S.; Magin-analyzed material).

The following results have been obtained:

*A*. The powder patterns of specimens 2, 3, 5, 6, and 7 vary with the degree of hydration of the material. Identical patterns, however, are obtained from all of these specimens (including the typical "hewettite" and the typical "metahewettite") after dehydrating "to constant pattern" over $P_2O_5$; this "dry" phase undoubtedly is the trihydrate, $CaO \cdot 3V_2O_5 \cdot 3H_2O$ (Hillebrand, Merwin & Wright, *Proc. Am. Phil. Soc.*, **53**, 31, 1914). On the addition of water to the samples, the powder pattern changes but the final "constant" pattern frequently is not precisely the same (especially in the region of small $2\theta$ values) for samples from different specimens, and even for the same sample after repetition of the dehydration-hydration cycle; no regularities, however, have been observed to suggest any basis for distinction between the behaviour of "hewettite" and "metahewettite." In all cases the pattern of the hydrated samples returns to the standard one for "dry" material after dehydration over $P_2O_5$. The fully-hydrated phase presumably is $CaO \cdot 3V_2O_5 \cdot 9H_2O$ (Hillebrand, Merwin & Wright, *loc. cit.*) and the small differences among the spacings and relative intensities observed in different patterns for the "wet" samples may result from the manner in which water molecules enter the lattice. Although little attention so far has been directed to possible intermediate stages of hydration in the present investigation, the patterns obtained during hydration and dehydration of the samples are not composed simply of those given by the "dry" and "wet" phases; there is no doubt that at least one intermediate hydrate exists. Hillebrand, Merwin & Wright (*loc. cit.*), largely on the basis of hydration-dehydration characteristics, came to the conclusion that hewettite and metahewettite are specifically distinct isomers. The present results, however, indicate that they are structurally identical. It seems unnecessary, therefore, to retain the name "metahewettite" unless it is employed to designate one of the hydrate phases, as in the case of rossite ($CaO \cdot V_2O_5 \cdot 4H_2O$) and metarossite ($CaO \cdot V_2O_5 \cdot 2H_2O$) (Foshag & Hess, *Proc. U. S. Nat. Museum*, **72,** art. 11, 1927).

---

[1] I am indebted to Professor Clifford Frondel for specimens 1, 4, 5, and 7, and to Mrs Alice D. Weeks for specimens 2, 3, and 8. Specimen 6 was obtained from Minerals Unlimited; it is completely different in general appearance from specimen 5.

*B.* Specimen 1 (Harvard 98019) from the Cactus Rat mine was the source of the crystals from which preliminary structural data for "metahewettite" were obtained (Barnes & Qurashi, *loc. cit.*). The structure, however, is *not* water-sensitive, and one of the "vanadium" peaks on the ($h0l$) electron-density map ($\frac{1}{2}$ cell) is rather low for V but of about the appropriate height for Na, while the peak tentatively identified as Ca could be V, at least insofar as height is concerned. Recently a sodium analogue of hewettite, $Na_2O \cdot 3V_2O_5 \cdot 3H_2O$, has been found in the Cactus Rat mine by Mrs. A. D. Weeks (Weeks & Thompson, U. S. Geol. Survey, Bull. **1009-B**, 1954, summarized by Fleischer, *Am. Mineral.*, **39,** 1038, 1954), and a sodium vanadate of this composition has been synthesized at the U. S. Geological Survey. The synthetic material gives the same powder pattern as the natural (Na) specimen except for slight differences in intensity (private communication from Mrs. A. D. Weeks). The powder pattern of the synthetic sodium vanadate (specimen 8 of the present study) is identical with that of specimen 1, except for a diffuse band (not present in photographs of the latter) along the small-$2\theta$ edge of the strongest line, and it is not affected by drying the sample or saturating it with water. Finally, a Beckmann flamephotometer determination, kindly made by Mr. J. C. Bartlet, Food and Drug Laboratories, Ottawa, on $\sim 2$ mg. hand-picked blades of specimen 1 showed 6.5% Na; this is in very good agreement with the theoretical value of 6.95% Na for $Na_2O \cdot 3V_2O_5 \cdot 3H_2O$, particularly in view of the small size of the sample and the difficulty of ensuring complete removal of adhering fragments of other minerals. For comparison it may be noted that a similar measurement on blades from specimen 3 (Jo Dandy, water-sensitive $CaO \cdot 3V_2O_5 \cdot nH_2O$) was negative ($<0.2\%$ Na). There is little doubt, therefore, that specimen 1 (Harvard 98019) is, in fact, identical with Mrs. Weeks' sodium analogue of hewettite.

*C*. The status of specimen 4 (Harvard 95445) is not yet clear. The exact locality in Montrose County, Colorado, from which it was obtained is unknown (private communication from Prof. C. Frondel). It consists of long, red blades closely resembling the Jo Dandy material (specimen 3) in appearance, together with very finely-divided red powder, on, and impregnating, sepiolite and quartz. On the basis of powder photographs of wet and dry samples, however, the structure is not water-sensitive and, in this respect, it resembles specimen 1, but the powder pattern is markedly different from that of specimen 1. A flamephotometer measurement by Mr. J. C. Bartlet on $<1$ mg. of hand-picked blades showed 3.7% Na. It is possible, therefore, that it is a mixed (Ca, Na)-analogue of hewettite.

Thus at present there appear to be three types of material variously labelled "hewettite" or "metahewettite," namely, (I) hewettite, $CaO \cdot 3V_2O_5 \cdot nH_2O$ (comprising both the "hewettite" and the "metahewettite" of Hillebrand, Merwin & Wright), which exists in at least three hydrate forms with $n=3$, 6 (probably), and 9, (II) the unnamed sodium analogue of hewettite in the trihydrate form, $Na_2O \cdot 3V_2O_5 \cdot 3H_2O$, reported by Mrs. Weeks, the structure of which is not water-sensitive, and (III) the material, also insensitive to hydration and dehydration, and possibily a mixed sodium-calcium variety of the sodium analogue, represented by specimen 4 (Harvard 95445).

Mrs. H. M. Sheppard and Mr. B. J. Cowick have assisted in taking the powder photographs and measuring many of the patterns.

## HEAZLEWOODITE FROM MILES RIDGE, YUKON TERRITORY

Vladimir S. Papezik, *University of British Columbia, Vancouver, B.C.*

The mineral heazlewoodite, $Ni_3S_2$, has been found, so far, in a very few localities. Specimens from the type locality in Tasmania have been described by Peacock (1947) and Ramdohr (1950). Ramdohr (1950) also mentions traces of a mineral which he considers to be heazlewoodite in josephinite from Oregon. No description of this mineral from a Canadian locality could be found in the literature.

During summer work in 1953, the writer collected a small specimen of a mineral, then considered to be pentlandite, near the top of Miles Ridge, about 10 miles east of the Alaska-Yukon boundary and 2 miles west of the Alaska Highway bridge across the White River. Mr. W. G. Smitheringale, who studied a polished section of the specimen, drew his attention to an unknown mineral with a peculiar anisotropism, which the writer tentatively identified as heazlewoodite on the basis of its polarization colors and associations. The identification was checked by etching and microchemical tests with later *x*-ray confirmation by Dr. R. M. Thompson.

Heazlewoodite, in polished section, is pale yellow with a granular texture. Individual grains reach usually $\frac{1}{2}$ mm. or less, the largest one being about 2 mm. long. It has a good polish, a hardness of C, and is strongly anistropic with typical polarization colors lilac to green.

The mineral gave the following etch reactions: $HgCl_2$ stains brown; $FeCl_3$, KOH stain faintly brown, some grains negative; HCl stains slightly brown; KCN negative; $HNO_3$ stains greyish brown without effervescence; Aqua Regia stains brown with slow effervescence. This corresponds closely to the reactions of heazlewoodite from Tasmania given by Peacock (1947). The *x*-ray pattern of the mineral is identical with the pattern of heazlewoodite from the type locality.

Heazlewoodite in the section is associated with granular pentlandite which can be distinguished from the rarer mineral by its higher relief, more fractured appearance (due perhaps to better cleavage), its color which looks slightly brownish yellow in contrast, and by its isotropism. Both minerals are embedded in a spongy mass of magnetite. In the section, the metallic minerals form a split veinlet $\frac{1}{2}$ to $\frac{1}{4}$ inch wide in green serpentine-like gangue with disseminated magnetite.

In the field, the minerals occur in a short, 1 inch wide stringer of sulphides on the lower contact of a serpentinized peridotite dyke, about 200 feet wide and several miles long, which cuts a series of silicified tuffs and limestones of probably Carboniferous age. The rocks near the veinlet are brecciated and strongly altered to serpentine and carbonates.

A stringer of massive maucherite ($Ni_{12\ x}As_8$) with minor magnetite and millerite (NiS), about five feet long and two inches wide, lies in a similar position one mile to the northwest. Other sulphide stringers in the area contain pyrrhotite and chalcopyrite. Scattered grains of native copper are found in limestone pebbles in some of the creeks.

The locality at Miles Ridge is part of the nickel-bearing belt extending from the Yukon-Alaska boundary southeast through the White River pyrrhotite showing to the Hudson Bay nickel-copper property at Quill Creek, and possibly farther. The area is readily accessible from the Alaska Highway and may prove to be an interesting locality for nickel minerals.

The writer wishes to thank Dr. R. M. Thompson of the University of British Columbia for his advice and encouragement, and Mr. W. G. Smitheringale, who first noticed this mineral in polished section.

## REFERENCES

PEACOCK, M. A. (1947): On Heazlewoodite and the Artificial Compound $Ni_3S_2$, *Univ. Toronto Studies, Geol. Series*, **51**, 59–68.

RAMDOHR, P. (1950): Ueber das Vorkommen von Heazlewoodit und . . . Shandit, *Sitz. Ber. Deutsch. Akad. Wiss.*, **6** Berlin, 1950.

——— (1950): Ueber Josephinit, Awaruit, Souesit, ihre Eigenschaften, Entstehung und Paragensis, *Min. Mag.*, **29**, 374–394.

## NIGGLIITE, A MONOTELLURIDE OF PLATINUM?

W. O. J. GROENEVELD MEIJER,[1] *Queen's University, Kingston, Ontario, Canada.*

Niggliite, named by Scholtz (1936) after the late Professor Paul Niggli, was found in a concentrate which was obtained by panning large amounts of oxidized sulphide ore from Waterfall Gorge, Insizwa, South Africa. Microchemical tests showed the presence of tellurium and platinum and a chemical analysis, performed on a fraction of a milligram, yielded 34.8 per cent platinum. The formula $PtTe_3$ was assigned to the mineral.

The author is not aware of any $AX_3$ compounds of platinum and B-subgroup elements. $PtTe_2$, with a cadmium iodide structure, is the only platinum telluride which has been synthesised (Thomassen, 1929 and Groeneveld Meijer, 1955). Neither optical characteristics, nor interplanar spacings and intensities of diffraction lines on $x$-ray powder photographs of $PtTe_2$, check with the data given by Scholtz (1936) for niggliite. With the exception of seven weak and very weak lines, which according to Niggli (in Scholtz, 1936, p. 185) might be due to impurities, the author has been able to index the powder diagram from the original data. On this basis, the unit cell is hexagonal with $a_0=4.111$ Å, $c_0=5.446$ Å; $c=1.325$ (Table 1).

---

[1] Now with McPhar Geophysics Limited, 36 Cranfield Road, Toronto, Canada.

It is of interest to note how closely the optical characteristics of niggliite check with those obtained on synthetic PdTe. Specifically the remarks of Scholtz (1936) on cleavage, colour in hand specimen and

TABLE 1. COMPARISON OF CALCULATED AND OBSERVED INTERPLANAR SPACINGS OF NIGGLIITE

| | Scholtz (1936) | | Calculated | |
|---|---|---|---|---|
| | θ (Cu) | d (meas) | d (calc) | *hk.l* |
| mw* | 12° 33′ | 3.54 | 3.56 | 10.0 |
| w | 13 27 | 3.31 | — | — |
| w | 14 45 | 3.03 | — | — |
| mw | 15 05 | 2.96 | 2.98 | 10.1 |
| mw | 15 49 | 2.83 | 2.72 | 00.2? |
| w? | 19 18 | 2.33 | — | — |
| w? | 19 48 | 2.27 | — | — |
| st | 20 59 | 2.15 | 2.16 | 10.2 |
| st | 22 03 | 2.05 | 2.06 | 11.0 |
| mw | 25 45 | 1.773 | 1.780 | 20.0 |
| mw | 27 12 | 1.685 | 1.692 | 20.1 |
| w | 28 03 | 1.638 | 1.641 | 11.2 |
| w | 28 36 | 1.609 | 1.583 | 10.3 |
| st | 31 14 | 1.486 | 1.490 | 20.2 |
| w | 32 39 | 1.438 | — | - |
| w | 33 03 | 1.412 | — | — |
| mw | 34 13 | 1.358 | 1.361 | 11.3, 00.4 |
| mw | 35 00 | 1.343 | 1.346 | 20.1 |
| w | 35 30 | 1.326 | — | — |
| m | 36 12 | 1.304 | 1.306 | 21.1 |
| m | 37 24 | 1.268 | 1.271 | 20.3, 10.4 |
| st | 39 45 | 1.205 | 1.206 | 21.2 |
| m | 40 30 | 1.186 | 1.187 | 30.0 |
| mw | 42 48 | 1.134 | 1.135 | 11.4 |
| ww | 45 00 | 1.089 | 1.088 | 30.2, 00.5 |
| mw | 45 27 | 1.081 | 1.081 | 21.3, 20.4 |
| w | 47 45 | 1.041 | 1.042 | 10.5 |
| m | 48 30 | 1.028 | 1.028 | 22.0 |

* m = medium, w = weak, st = strong.

d (meas): interplanar spacings as calculated from Scholtz' (1936) θ values ($CuK\alpha_1 = 1.5405$ Å).

d (calc): interplanar spacings as calculated from the determined lattice dimensions $a_0=4.111$ Å, $c_0=5.446$ Å; $c=1.325$.

polished section, polish, hardness, reflectivity, and anisotropism of niggliite find their equal in PdTe. PdTe reacts strongly with $HNO_3$; niggliite, according to Scholtz (1936), behaves inertly toward all standard etch reagents. The etch reactions of PdTe and $PdTe_2$ are quite similar and distinct from those of niggliite and $PtTe_2$ which are likewise related to each other. We believe on this basis that niggliite is likely the monotelluride of platinum.

Platinum monotelluride could not be synthesized by Thomassen (1929). The compound $PtTe_2$ does not melt under the conditions of fusion and the failure to obtain PtTe is understandable. However, failure to obtain a compound by a certain procedure of synthesis does not preclude the possibility of its existence as a mineral.

The unit cell of niggliite compares favourably with that of PdTe and IrTe. Thomassen (1929) gives for PdTe: $a_0 = 4.127$ Å, $c_0 = 5.663$ Å; $c = 1.372$ and the present author (1955) obtained for IrTe: $a_0 = 3.930$ Å, $c_0 = 5.386$ Å; $c = 1.371$. As with all platinum and palladium compounds, the palladium homologue has the smaller unit cell volume.

On the basis of the above observations we are inclined to favour PtTe as the formula for niggliite. In short these are:

1) Presence of platinum and tellurium as indicated by the original microchemical and chemical work.

2) No $AX_3$ compounds of platinum and palladium have been found reported upon in the literature.

3) $X$-ray pattern, optical, and physical characteristics of niggliite are unlike those of $PtTe_2$.

4) Physical and optical properties of niggliite compare closely with those of PdTe; $x$-ray data indicate a similar unit cell with a smaller volume for that of the mineral.

5) Etch reactions on PdTe and $PdTe_2$ are similar; also those of niggliite and $PtTe_2$. Etch reactions on $PdTe_2$ and $PtTe_2$ are dissimilar; it is suggested, therefore, that niggliite is PtTe.

6) Indexing of the powder pattern of niggliite is possible on a unit cell of the niccolite type, similar to that of PdTe and IrTe, and of plausible dimensions.

A remark of Scholtz in Ramdohr (1950) to the effect that niggliite is the monostannide of platinum, cannot be commented upon without further chemical data on the original material. The unit cell of PtSn, as determined by Oftedal (1928), is of the niccolite type with $a_0 = 4.103$ Å, $c_0 = 5.428$ Å; $c = 1.323$.[1]

---

[1] *Editor's note.* Unpublished $x$-ray powder data by R. M. Thompson for synthetic PtSn, also compare closely with Scholtz data. This would be expected from the similarity of the lattice dimensions for PtSn and those derived here for niggliite, PtTe.

## REFERENCES

GROENEVELD MEIJER, W. O. J. (1955): Synthesis, structures, and properties of platinum metal tellurides. *Am. Mineral.*, **40,** 646–657.

OFTEDAL, I. (1928): Röntgenographische Untersuchungen von Manganarsenid, Eisentellurid, Nickelstannid und Platinstannid. *Z. phys. Chem.*, **132,** 208–216.

RAMDOHR, P. (1950): *Die Erzmineralien und ihre Verwachsungen.* Berlin, Akademie Verlag.

SCHOLTZ, D. L. (1936): The magmatic nickeliferous ore deposits of East Griqualand and Pondoland. *Publ. Univ. Pretoria; Series II: Nat. Sc.* No. **1,** 81–210.

THOMASSEN, L. (1929): Über Kristallstrukturtypen einiger binärer Verbindugen der Platinmetalle. *Z. phys. Chem.*, **48,** 277–287.

# LATTICE DIMENSIONS OF CADMIUM SULPHIDE

F. G. SMITH, *University of Toronto, Toronto, Canada.*

There appears to be a discrepancy between the structure assigned to certain tetrahedral compounds and the measured lattice dimensions. In wurtzite-type structures, if the coordination is tetrahedral, the ratio $c/a=\sqrt{2/3}\times Z=0.81650\ Z$. However, in the case of hexagonal cadmium sulphide, the following lattice dimensions and ratios have been reported:

| | $c$ | $a$ | $Z$ | $c/a\ Z$ |
|---|---|---|---|---|
| Ulrich and Zacharaisen (1925)[1] | 6.724 | 4.142 | 2 | 0.8115 |
| Schnaase (1933)[2] | 6.691 | 4.131 | 2 | 0.8099 |

These values agree fairly well, but the mean ratio, 0.8107, is significantly smaller than the theoretical vaue, 0.8165.

Pure cadmium sulphide was precipitated, dried, mixed with about 10 per cent by weight of $Na_2S_x$ in evacuated vycor tubes, and heated in a controlled furnace for several hours. The chilled crystalline products were ground, washed free from alkali, and mounted on glass plates with balsam. After curing, the specimens were ground flat. Analysis of several $x$-ray diffractions was carried out with a Norelco geiger counter diffractometer. Instrumental calibration for angle was by the direct comparison method using a Norelco silicon standard. Diffraction angles of $CuK\alpha_1$ radiation were converted to spacings using U. S. Bureau of Standards tables (1950). The $a$ dimension (=tetrahedral edge) was obtained from twice the spacing of the 11.0 plane, and the $c$ dimension (=tetrahedral height) was obtained from three times the spacing of the third order of the basal plane. From calibration and reproducibility tests, both values are probably accurate to ±0.0005 Å. The experimental conditions and results are given below:

---

[1] *Zeit. Krist.* **62,** 260–270 (1925).

[2] *Zeit. phys. Chemie* **20B,** 89–117 (1933).

| Temperature | Time Hours | $c/Z$ | $a$ | $c/a\,Z$ |
|---|---|---|---|---|
| 586±5° C. | 15 | 3.3747 | 4.1360 | 0.81593 |
| 832 | 65 | 3.3747 | 4.1350 | 0.81613 |
| 957 | 62 | 3.3741 | 4.1334 | 0.81630 |

The mean of the above ratios, 0.8161, is much nearer the theoretical value of 0.8165 than the earlier values. Whether the small difference remaining is real or not was not determined. However, the $c/a$ ratio is less than 0.1% from the tetrahedral value.

In order to test whether the kind of flux used for crystallizing had a significant effect, a run at 515° C. for 237 hours was made with a flux consisting of a low melting temperature mixture of NaCl, KCl, and LiCl. The measured values, as in the above table, were 3.3747, 4.1356, 0.81601. One run at 900° C. for 3 hours with no flux gave 3.3750, 4.1356, 0.81608. These data are very similar to those of the first set.

The above results for hexagonal CdS crystallized at 550–950° C. in the presence of excess sulphur are:

$$a=4.1348\pm0.0015\ \text{Å},$$
$$c=6.7490\pm0.0010\ \text{Å},$$

when $Z=2$, and

$$c/aZ=0.8161\pm0.0002.$$

## A NEW CENTRIFUGE TUBE FOR MINERAL SEPARATION[1]

E. H. Nickel,[2] *Mines Branch, Ottawa, Canada.*

### Abstract

A centrifuge tube consisting of three components is described, which permits the efficient separation and removal of the sink and float fractions in heavy liquid separation.

### Introduction

In the gravity separation of minerals using heavy liquids, centrifuging is frequently desirable and sometimes necessary. This procedure is particularly effective in the separation of minerals whose specific gravities are very similar, or with mineral powders which are very fine grained. A difficulty frequently encountered in work of this type is the efficient recovery of the sink and float fractions after centrifuging. The device described below permits the rapid separation of the two fractions with very little contamination.

---

[1] Published by permission of the Deputy Minister, Department of Mines and Technical Surveys, Ottawa, Canada.

[2] Mineralogist, Mineragraphic Laboratory, Department of Mines and Technical Surveys, Ottawa, Canada.

### Description and Use of the Device

The device, shown in Figure 1, consists of three parts, the outer tube (A) which may be a test-tube, an inner collar (B), and a plunger (C).

The inner collar fits loosely into the outer tube and is supported by a lip at the upper end. Near the lower end there is a constriction with a ground surface to match that of the plunger. It is useful to flare the bottom of the collar almost to the outer tube so that if particles sink partly down and then rise again, they are funnelled back into the collar instead of into the space between collar and tube.

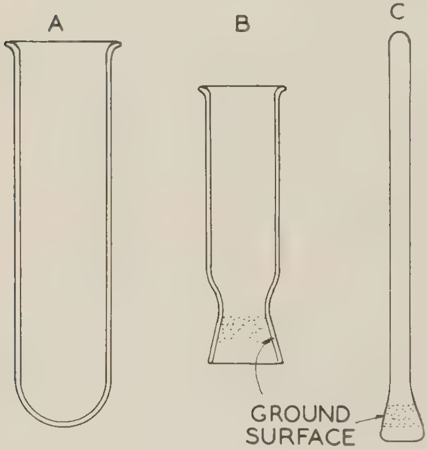

Fig. 1

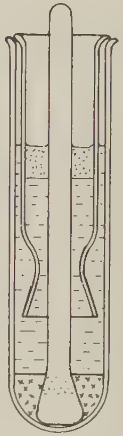

Fig. 2

The plunger should be somewhat longer than the outer tube and have a bulb at the lower end, somewhat wider than the constriction in the collar, and with a ground surface to match that in the collar.

In making this device it is important to have the sloping sides of the collar and plunger quite steep, to prevent mineral particles from adhering there.

The components are assembled as shown in Figure 2, and the liquid poured in. The mineral powder is then poured into the collar. If it is desired to stir the powder to separate the particles, this can be done by agitating a wire inserted from the top while keeping the plunger pulled up into the constriction; after stirring, the plunger can be lowered gently to the bottom of the tube.

The entire device is then centrifuged for an appropriate length of time. When removed from the centrifuge, the float portion is in the collar and the sink portion at the bottom of the test-tube. If the plunger is then grasped at its upper end and pulled upward it will close the collar and lift collar and contents out of the test-tube, leaving the sink portion at the bottom.

The components are preferably made of glass and the over-all size can be made to fit the tube-holder in use. The length of the collar relative to the tube may be varied depending on the amount of the sink fraction expected. Incidentally, the inner collar may be made from a test-tube having a smaller diameter than the outer one.

## THE DISTRIBUTION OF MAJOR AND MINOR ELEMENTS AMONG SOME CO-EXISTING FERROMAGNESIAN SILICATES

E. H. Nickel, *Mines Branch, Ottawa, Canada.*

In a recent paper[1] the author discussed the distribution of some elements in co-existing biotite, hornblende and chlorite. Due to space considerations, the average values for each element were given, rather than the results of the separate spectrographic analyses. It has since been requested that the individual analyses be published to permit other workers to reanalyze the data for their own purposes.

In the following tables the atomic fractions of the elements in their sites in the mineral structures are given for each of the minerals analyzed. These have been recalculated from the weight percentages determined spectrographically. For the minor elements, below each table are given their minimum, maximum, and average amounts, in parts per million.

---

[1] Nickel, E. H., *Am. Mineral.*, **39,** 486–493 (1954).

TABLE 1. THE ATOMIC FRACTIONS OF ALUMINUM IN TETRAHEDRAL POSITIONS
Total Al/Al & Si is given in brackets

| Sample No. | Al in Hornblende | Al in Biotite | Al in Chlorite |
|---|---|---|---|
| S-133-35 | 0.130 | — | 0.290 (.429) |
| S-133-37 | .105 | — | .350 (.460) |
| S-133-42 | .101 | 0.413 | .325 (.464) |
| S-133-99 | .113 | .377 | — |
| S-133-102 | .098 | .412 | — |
| S-133-121 | — | .390 | .270 (.438) |
| S-133-142 | .088 | .341 | — |
| T1-50W | .101 | .384 | — |
| T1-40W | .087 | .394 | — |
| T1-10W | .091 | .326 | — |
| T1-0 | .091 | .326 | — |
| T1-30E | — | .422 | .265 (.451) |
| T1-40E | — | .382 | .295 (.480) |
| T1-50E | .112 | .409 | — |
| T4-43W | .139 | — | .285 (.464) |
| T4-50W | .131 | .433 | .290 (.481) |

TABLE 2. THE ATOMIC FRACTIONS OF IRON AND MAGNESIUM IN OCTAHEDRAL POSITIONS

| Sample No. | Fe in Hornblende | Fe in Biotite | Fe in Chlorite | Mg in Hornblende | Mg in Biotite | Mg in Chlorite |
|---|---|---|---|---|---|---|
| S-133-35 | 0.197 | — | 0.218 | 0.684 | — | 0.576 |
| S-133-37 | .195 | — | .203 | .760 | — | .606 |
| S-133-42 | .180 | 0.312 | .208 | .712 | .616 | .592 |
| S-133-99 | .200 | .330 | — | .708 | .563 | — |
| S-133-102 | .184 | .350 | — | .710 | .622 | — |
| S-133-121 | — | .269 | .204 | — | .579 | .569 |
| S-133-142 | .193 | .256 | — | .772 | .626 | — |
| T1-50W | .208 | .319 | — | .748 | .636 | — |
| T1-40W | .200 | .298 | — | .706 | .616 | — |
| T1-10W | .204 | .336 | — | .698 | .649 | — |
| T1-0 | .199 | .301 | — | .736 | .589 | — |
| T1-30E | — | .291 | .206 | — | .699 | .552 |
| T1-40E | — | .220 | .181 | — | .693 | .469 |
| T1-50E | .214 | .298 | — | .700 | .689 | — |
| T4-43W | .218 | — | .210 | .782 | — | .542 |
| T4-50W | .218 | .290 | .216 | .798 | .636 | .516 |

TABLE 3. THE ATOMIC FRACTIONS OF COBALT, NICKEL AND CHROMIUM IN OCTAHEDRAL POSITIONS

| Sample No. | $Co \times 10^{-4}$ in Hornblende | $Co \times 10^{-4}$ in Biotite | $Co \times 10^{-4}$ in Chlorite | $Ni \times 10^{-3}$ in Hornblende | $Ni \times 10^{-3}$ in Biotite | $Ni \times 10^{-3}$ in Chlorite | $Cr \times 10^{-3}$ in Hornblende | $Cr \times 10^{-3}$ in Biotite | $Cr \times 10^{-3}$ in Chlorite |
|---|---|---|---|---|---|---|---|---|---|
| S-133-35 | 1.02 | — | 1.27 | 1.34 | — | 1.79 | 1.10 | — | 1.74 |
| S-133-37 | 1.03 | — | 0.840 | 1.51 | — | 2.21 | 1.26 | — | 2.80 |
| S-133-42 | 0.636 | 0.687 | 0.793 | 0.87 | 2.09 | 1.96 | 0.76 | 4.47 | 1.42 |
| S-133-99 | 1.35 | 1.93 | — | 1.25 | 2.18 | — | 1.05 | 4.10 | — |
| S-133-102 | 1.25 | 1.63 | — | 1.15 | 2.03 | — | .990 | 4.40 | — |
| S-133-121 | — | 1.90 | 1.74 | — | 1.76 | 1.83 | — | 3.14 | 1.38 |
| S-133-142 | 1.27 | 1.68 | — | 1.34 | 2.48 | — | 1.25 | 5.70 | — |
| T1-50W | 1.14 | 1.84 | — | 1.21 | 2.25 | — | 0.796 | 3.04 | — |
| T1-40W | 0.776 | 1.84 | — | 0.794 | 2.31 | — | 0.491 | 5.17 | — |
| T1-10W | 0.958 | 2.39 | — | 0.978 | 2.60 | — | 0.604 | 4.53 | — |
| T1-0 | 1.10 | 1.72 | — | 1.09 | 2.22 | — | 0.630 | 3.24 | — |
| T1-30E | — | 1.94 | 1.26 | — | 2.18 | 1.73 | — | 3.29 | 1.17 |
| T1-40E | — | 1.65 | 0.866 | — | 2.08 | 1.15 | — | 3.00 | 0.99 |
| T1-50E | 1.21 | 2.04 | — | 1.92 | 2.27 | — | 0.806 | 2.30 | — |
| T4-43W | 1.87 | — | 2.11 | 1.87 | — | 2.50 | 1.80 | — | 4.00 |
| T4-50W | 1.60 | 1.96 | 1.57 | 1.69 | 2.21 | 2.17 | 1.72 | 6.10 | 7.00 |

|  | Cobalt Content (p.p.m.) |  |  | Nickel Content (p.p.m.) |  |  | Chromium Content (p.p.m.) |  |  |
|---|---|---|---|---|---|---|---|---|---|
|  | Minimum | Maximum | Average | Minimum | Maximum | Average | Minimum | Maximum | Average |
| Hornblende | 22 | 64 | 41 | 280 | 640 | 440 | 150 | 550 | 310 |
| Biotite | 26 | 90 | 69 | 660 | 980 | 830 | 770 | 2040 | 1350 |
| Chlorite | 48 | 126 | 79 | 690 | 1490 | 1150 | 530 | 3700 | 1360 |

TABLE 4. THE ATOMIC FRACTIONS OF TITANIUM, VANADIUM AND MANGANESE IN OCTAHEDRAL POSITIONS

| Sample No. | Ti×$10^{-2}$ in Hornblende | Ti×$10^{-2}$ in Biotite | Ti×$10^{-2}$ in Chlorite | V×$10^{-4}$ in Hornblende | V×$10^{-4}$ in Biotite | V×$10^{-4}$ in Chlorite | Mn×$10^{-3}$ in Hornblende | Mn×$10^{-3}$ in Biotite | Mn×$10^{-3}$ in Chlorite |
|---|---|---|---|---|---|---|---|---|---|
| S-133-35 | 1.22 | — | 0.982 | 5.88 | — | 3.90 | 4.38 | — | 2.94 |
| S-133-37 | 1.02 | — | .809 | 5.36 | — | 3.87 | 4.32 | — | 2.99 |
| S-133-42 | 1.10 | 2.46 | .466 | 4.52 | 6.64 | 3.07 | 4.72 | 4.49 | 3.30 |
| S-133-99 | 0.973 | 1.99 | — | 5.32 | 6.80 | — | 4.60 | 3.66 | — |
| S-133-102 | 0.765 | 2.19 | — | 4.58 | 7.20 | — | 4.58 | 4.23 | — |
| S-133-121 | — | 2.51 | .286 | — | 9.44 | 2.61 | — | 3.50 | 3.46 |
| S-133-142 | 0.983 | 2.64 | — | 4.90 | 7.87 | — | 4.62 | 3.31 | — |
| T1-50W | 0.666 | 2.11 | — | 4.36 | 9.60 | — | 5.12 | 3.60 | — |
| T1-40W | 0.812 | 2.23 | — | 3.18 | 9.53 | — | 4.48 | 3.28 | — |
| T1-10W | 0.815 | 1.92 | — | 3.84 | 12.1 | — | 4.42 | 3.48 | — |
| T1-0 | 0.760 | 2.00 | — | 3.82 | 8.33 | — | 4.62 | 3.96 | — |
| T1-30E | — | 1.76 | .433 | — | 9.07 | 2.60 | — | 3.53 | 3.24 |
| T1-40E | — | 1.68 | .244 | — | 8.77 | 1.58 | — | 3.63 | 3.23 |
| T1-50E | 0.888 | 2.12 | — | 4.08 | 6.67 | — | 4.74 | 3.73 | — |
| T4-43W | 0.795 | — | .536 | 7.54 | — | 3.67 | 5.56 | — | 3.24 |
| T4-50W | 0.788 | 2.17 | .307 | 6.62 | 8.13 | 2.30 | 5.58 | 3.93 | 3.02 |
|  | Titanium Content (p.p.m.) |  |  | Vanadium Content (p.p.m.) |  |  | Manganese Content (p.p.m.) |  |  |
|  | Minimum | Maximum | Average | Minimum | Maximum | Average | Minimum | Maximum | Average |
| Hornblende | 1900 | 3500 | 2500 | 83 | 196 | 130 | 1420 | 1780 | 1550 |
| Biotite | 5300 | 8200 | 6600 | 190 | 276 | 233 | 1150 | 1480 | 1290 |
| Chlorite | 1200 | 4800 | 2500 | 72 | 181 | 135 | 1590 | 1930 | 1770 |

Table 5. The Atomic Fractions of Zirconium and Scandium in Octahedral Positions

| Sample No. | $Zr\times10^{-4}$ in Hornblende | $Zr\times10^{-4}$ in Biotite | $Zr\times10^{-4}$ in Chlorite | $Sc\times10^{-4}$ in Hornblende | $Sc\times10^{-4}$ in Biotite | $Sc\times10^{-4}$ in Chlorite |
|---|---|---|---|---|---|---|
| S-133-35 | 3.30 | — | 1.40 | 2.05 | — | 0.157 |
| S-133-37 | 2.50 | — | 1.19 | 1.34 | — | .140 |
| S-133-42 | 2.60 | 1.82 | 1.18 | 1.66 | 0.380 | $<.1$ |
| S-133-99 | 3.36 | 1.62 | — | 1.50 | $<.1$ | — |
| S-133-102 | 3.22 | 1.78 | — | 1.63 | .149 | — |
| S-133-121 | - | 2.09 | 1.18 | — | .483 | .141 |
| S-133-142 | 2.58 | 1.91 | — | 1.57 | .344 | — |
| T1-50W | 3.18 | 1.57 | — | 1.42 | .240 | — |
| T1-40W | 2.10 | 1.70 | — | 0.942 | .318 | — |
| T1-10W | 2.52 | 1.47 | — | 1.76 | .270 | — |
| T1-0 | 2.68 | 1.97 | — | 0.993 | .272 | — |
| T1-30E | — | 2.05 | 1.14 | — | .680 | .241 |
| T1-40E | — | 2.15 | 0.816 | — | .740 | .185 |
| T1-50E | 2.48 | 2.16 | — | 0.946 | .250 | — |
| T4-43W | 1.80 | — | 0.633 | 1.45 | — | $<.1$ |
| T4-50W | 1.34 | 0.824 | 0.406 | 1.30 | .173 | $<.1$ |
|  | Zirconium Content (p.p.m.) |  |  | Scandium Content (p.p.m.) |  |  |
|  | Minimum | Maximum | Average | Minimum | Maximum | Average |
| Hornblende | 71 | 183 | 141 | 25 | 55 | 38 |
| Biotite | 48 | 132 | 104 | n.d. | 22 | 10 |
| Chlorite | 38 | 129 | 93 | n.d. | 10 | 5 |

# WALKER MINERALOGICAL CLUB*

## OFFICERS 1954

*Honorary President*, A. L. Parsons; *President*, R. Ford; *Secretary*, Mrs. W. H. Bush; *Treasurer*, Mrs. M. H. Frohberg; *Editor*, Dr. L. G. Berry; *Councillors*, L. G. Smith, D. H. Gorman, C. V. G. Phipps, Dr. V. B. Meen.

## ABSTRACT OF PROCEEDINGS, 1954

*January 21, 1954*. The financial report for the year 1953 was presented by the Secretary—Balance on hand in Ordinary Account—$781.99; balance on hand in Prize Fund Account—$4.01; Bonds for Prize Fund Account held in safekeeping—$2700. Dr. Wm. Gross, lecturer in the Department of Geological Sciences, University of Toronto, spoke on "Some Geological Aspects of Africa" and illustrated his talk with colour slides.

*February 18*. Three graduate students from the Department of Geological Sciences, University of Toronto addressed the Club. R. Arnold spoke on "Remarks on the Mineralogy and Origin of Blind River Conglomerates"; G. Perrault, "Minerals of the Proterozoic Rocks of the Labrador Trough"; G. Harper, "Distribution of Radioactive Minerals in Rocks of the Athabaska Area."

*March 11*. Members inspected their display of minerals and lapidary work on exhibit in the rotunda of the Royal Ontario Museum for the month of March. C. V. G. Phipps was speaker of the evening, his topic being "Mineral Collecting in Eastern United States." Colour slides and mineral specimens were shown.

*April 14*. In preparation for the annual Spring Field Trip to the Niagara Falls area, M. Seward spoke on the minerals to be found there and exhibited specimens; W. A. Tovell explained the "Geology of the Niagara Escarpment"; P. A. Peach discussed "The Minerals of the Niagara Area and their Origin"; D. H. Gorman spoke on "Field Identification of Minerals, Based on their Simple Physical Characteristics." Members then withdrew to a laboratory where they were able to carry out tests on various minerals.

*May 15*. Members gathered at the rock dumps near Niagara Falls for their annual Spring Field Trip. Calcite, gypsum, fluorite and dolomite were collected.

*October 8 to 11*. The eighth annual Fall Field Trip was held north of Kingston with headquarters at Westport. Quartz, calcite and graphite were collected at the Lyndhurst Quartz Crystal Mine; blue calcite, apatite and biotite at the Silver Queen Mine; tourmaline at Verona, peristerite near Holleford and tremolite and feldspar at the Richardson Mine.

*November 18*. This was Auction Night, with minerals sold both by auction and sale. Lucky draws were held and door prizes were given out. An on-the-spot identification service was also featured. Refreshments were served.

*December 16*. Dr. W. W. Moorhouse, Associate Professor of Geology, Department of Geological Sciences, University of Toronto, spoke on "A Busman's Holiday in Britain and Scandinavia" and illustrated his talk with colour slides. Minerals and rocks collected on his trip were also shown.

The Council of the Walker Mineralogical Club wishes to acknowledge the courtesy of the Council of the Mineralogical Society of America in again making possible the publication of a Canadian number of *The American Mineralogist*.

MRS. HELEN BUSH, *Secretary*

---

* Founded in 1938 and named in honour of the late Professor T. L. Walker (1867–1942), then Professor Emeritus of Mineralogy and Petrography in the University of Toronto and Director of the Royal Ontario Museum of Mineralogy. The by-laws of the Club were published in *Am. Mineral.* **34,** 469, 1949.

# PEACOCK MEMORIAL PRIZE, 1955

The Walker Mineralogical Club offers The Peacock Memorial Prize of One Hundred Dollars ($100.00) for the best scientific paper on pure or applied mineralogy (including crystallography, mineralography, petrology, ore genesis, and geochemistry) submitted by any graduate student enrolled in a Canadian university, by a Canadian graduate student enrolled in any university, or by any graduate student on a Canadian subject. The paper will be accepted for competition up to two years after completion of the work even though the author may be no longer enrolled as a graduate student.

Full information on the conditions governing the presentation of this prize may be had by writing: The Secretary, Walker Mineralogical Club, 100 Queen's Park, Toronto 5.

All papers for this year's competition must be in the Secretary's hands by October 31, 1955.

# THE ALKALI FELDSPARS: I. ORTHOCLASE-MICROPERTHITES

W. S. MacKenzie and J. V. Smith, *Geophysical Laboratory, Carnegie Institution of Washington, Washington, D. C.*

## Abstract

A study of the lamellar structure of a number of analyzed feldspars belonging to the orthoclase-microperthite series has been made using $x$-ray oscillation photographs. Differences in the $x$-ray diffraction patterns have been correlated with the bulk composition of the feldspars. Measurements of the reciprocal lattice angles $\alpha^*$ and $\gamma^*$ of the soda phase give results which indicate that the composition of the soda phase may be determinable from these angles.

The variations in optic axial angle for a known chemical composition have also been correlated with differences in the $x$-ray diffraction patterns.

## Introduction

The importance of the soda-lime or plagioclase feldspars in the classification of igneous rocks has been recognized for a long time, but the alkali feldspars, probably because of their more limited distribution in igneous rocks, have not received the same detailed attention until very recently.

In 1950 Bowen and Tuttle made the most significant advance in our knowledge of the alkali feldspar series by their determination of liquidus, solidus, and sub-solidus relations in the system $KAlSi_3O_8 - NaAlSi_3O_8 - H_2O$. It had long been suspected that at high temperatures the alkali feldspars formed a complete series of solid solutions, whereas, in rocks thought to have been formed at low temperatures or slowly cooled from high temperatures, two feldspars were found either intimately intergrown or as separate crystals. Bowen and Tuttle were able to demonstrate that complete solid solution did pertain at high temperatures, but that at low temperatures there was only limited miscibility between the two end members of the series. These writers made it clear, however, that the optical properties of the synthetic feldspars were similar to those of some natural high-temperature forms, and that in no case were they able to synthesize material similar to the natural low-temperature feldspars. The sub-solidus relations are thus still only imperfectly known, and it is only by detailed study of natural minerals that we can hope to obtain a clearer understanding of these relations.

Tuttle (1952*b*) divided the alkali feldspars into four series on the basis of the value of the optic axial angle and orientation of the optic plane for a known chemical composition. A slightly modified form of the diagram given by Tuttle to show these relations is reproduced in Fig. 1 and the curves on this diagram have been adopted to define the four series of feldspars. The intermediate members of each series are frequently unmixed and consist of intimate intergrowths of a potash- and a soda-rich phase. These intimate intergrowths are referred to as perthites. For the high-temperature feldspars (high sanidines, sanidines, and anorthoclases) the two phases can rarely be detected optically and the term cryptoperthite is suitable.[1] The term microperthite is generally applicable to the low-temperature feldspars orthoclase and microcline.

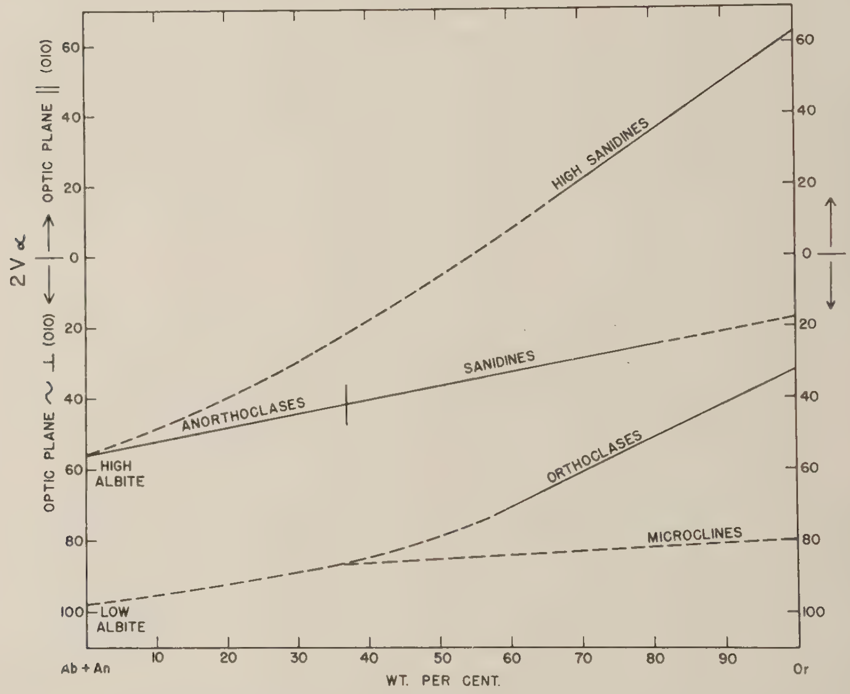

FIG. 1. Diagram showing the relation between optic axial angle and chemical composition in the alkali feldspars (after Tuttle, 1952*b*). The curves are used to define four series of alkali feldspars: microcline-low albite, orthoclase-low albite, sanidine-anorthoclase-high albite, high sanidine-high albite. The dashed portions of the curves indicate where the data are limited or absent.

To name a particular alkali feldspar using the curves in Fig. 1, it is not necessary to know whether or not the feldspar is unmixed, the optic axial angle being that of either a homogeneous crystal or the aggregate effect produced by the intergrowth of the separate phases. Thus a feldspar of composition $Or_{45}Ab_{55}$ with a mean optic axial angle of 40° will be either a sanidine or a sanidine-cryptoperthite; in some cases only by *x*-ray methods can one decide whether or not the feldspar is unmixed. Specimens which fall between two of the curves (Fig. 1) are considered as intermediate between the two series defined by the curves. Examples of such feldspars are described by Tuttle and Keith (1954).

---

[1] The term cryptoperthite is used here to include perthites which appear optically homogeneous under the highest magnification although $x$-ray studies show them to be unmixed (Tuttle, 1952*a*), and to include perthites in which optical examination suggests unmixing although the boundaries of each phase cannot be accurately delineated by optical methods.

This is the first of a series of papers devoted to a systematic study of the alkali feldspars. This study consists of two parts—first a purely mineralogical investigation of selected specimens, and second a petrologic investigation of the alkali feldspars from granites and related rocks belonging to the same suite. The present paper is an investigation by single-crystal *x*-ray methods of a number of feldspars belonging to the orthoclase-microperthite series. The second paper (Smith and MacKenzie) describes a simple but accurate *x*-ray technique developed in the course of this work for the study of the triclinic phases in perthites. The third paper will be devoted to an optical and *x*-ray study of sanidine- and anorthoclase-cryptoperthites. A paper on the relation between orthoclase and microcline has already been published (MacKenzie, 1954), so the mineralogical aspects of the alkali feldspars have been treated in some detail.[2]

With the data obtained from the purely mineralogical study of the alkali feldspars a detailed petrologic study of the alkali feldspars in a few selected granites and related minor intrusions has been undertaken. It is believed that this study will provide further information as to the changes which take place in the alkali feldspars in the solid state.

## Previous Studies of Micro- and Cryptoperthites

The existence of micro- and cryptoperthitic intergrowths of a soda- and a potash-rich feldspar has long been interpreted as the result of unmixing of an originally homogeneous feldspar. Kôzu and Endô (1921) were the first to study perthites by *x*-ray methods and they found that the two phases could be homogenized and partially unmixed again by suitable heat treatment. Spencer (1930, 1937) made very careful optical, chemical, and thermal studies of a number of alkali feldspars, and he observed that in many cases the microperthitic structure could be made to disappear by heat treatment. Chao, Smare, and Taylor (1939) found from a single-crystal *x*-ray study of some of Spencer's specimens that in many cases the two phases in microperthites had lattice parameters which corresponded with nearly pure potash feldspar and soda feldspar.

---

[2] Alkali feldspars in which the optic plane is parallel to the symmetry plane, defined by Tuttle (1952*b*) as high sanidines, are much rarer in occurrence than most mineralogy textbooks indicate. Such feldspars have not yet been studied in detail.

In 1940 Chao and Taylor classified Spencer's specimens into two groups: those having an albite-twinned soda phase whose lattice angles were close to those of low-temperature albite, and those having a pericline-twinned soda phase whose lattice angles did not agree with low-temperature albite. At the time this work was done the existence of a high-temperature form of albite had not been clearly established, although Spencer (1937) had found an appreciable change in the optical properties of a specimen of albite from Amelia, Va., as a result of prolonged heating at 1080° C. Tuttle and Bowen (1950) proved without doubt that a high-temperature form of albite did exist. They showed that synthetic albite crystallized at about 800° C. had optical properties similar to those of the material produced by prolonged heating of natural low-temperature albite and to those of the natural sodic plagioclase phenocrysts from lavas. Laves and Chaisson (1950) determined the lattice angles of high-temperature albite, and Taylor (personal communication, 1951) suggested that the soda phase of some perthites corresponded to the high-temperature form of albite. Laves (1951) reported that the soda phase of a sanidine cryptoperthite had lattice angles close to those of high-temperature albite.

Ito and Sadanaga (1952) did not distinguish between high- and low-temperature albite in perthites but concluded that the type of twinning shown by the soda phase was dependent on the bulk chemical composition of the feldspar. Their conclusion that potash-rich perthites showed an albite-twinned soda phase and soda-rich perthites showed a pericline-twinned soda phase was directly contrary to the observations of Chao and Taylor (1940) in their study of low-temperature feldspars.

Laves (1952) thought that the different lattice parameters of high- and low-temperature albite controlled the type of twinning shown by the soda phase of perthites so that high-temperature albite showed pericline twinning and low-temperature albite showed albite twinning. Smith and MacKenzie (1954) have since shown that the soda phase of perthites may be albite twinned, pericline twinned, or both albite and pericline twinned, whether it is near high- or low-temperature albite.

Tuttle and Keith (1954) have described feldspars which contain, in addition to a monoclinic potash phase, two soda phases, one near low-temperature albite and the other near high-temperature albite. Smith and MacKenzie (1954) have briefly described an additional complexity in the structure of perthites by noting a specimen consisting of two potash phases, one monoclinic and the other triclinic, with a soda phase close to low-temperature albite.

From this brief review of the status of knowledge of the structure of perthites it is clear that only by examination of a large number of specimens of known chemical composition and from all manner of geological environments will the full story of the development of the different types of structure be unravelled. When this has been done the information obtainable from a study of the alkali feldspars will be of considerable value in any petrologic study.

## PRESENT INVESTIGATION

This paper deals with a series of optically monoclinic perthites from presumed low-temperature geologic environments and for such specimens the term orthoclase-microperthite is generally applicable. Spencer (1937) and subsequently Tuttle (1952*b*), using most of the specimens which are studied here, constructed curves relating the variation in optic axial angle to chemical composition in the alkali feldspars. The curve drawn by Tuttle (1952*b*) for the orthoclase—low-temperature albite series is here considered as a definition of this series, since it is not always possible on geologic grounds to distinguish between a high-temperature and a low-temperature environment. It has been suggested (MacKenzie in Tuttle and Keith, 1954) that perthites be subdivided on the basis of the nature of the soda phase; thus an orthoclase-perthite has a soda phase near low-temperature albite and a sanidine-perthite has a soda phase near high-temperature albite.[3]

Twelve of the specimens used here are from Dr. Edmondson Spencer's series of alkali feldspars on which he did much careful work (Spencer, 1930, 1937). These specimens were received from Drs. Bowen and Tuttle and the writers are much indebted to Drs. Spencer, Bowen, and Tuttle for the opportunity to use these specimens. Many of them have already been studied by *x*-ray single-crystal techniques by Chao, Smare, and Taylor (1939) and by Chao and Taylor (1940), but some of the samples not available to these investigators have been studied. The two soda-rich specimens were received from Professor C. E. Tilley, whose kindness is gratefully acknowledged.

It was found that the simplest method of studying a large number of alkali feldspars by single-crystal *x*-ray methods was to use *b*-axis oscillation photographs. In each case the (001) plane was made parallel to the *x*-ray beam in the center of the 15° oscillation arc. Figure 2 shows a *b*-axis oscillation photograph of a homogeneous feldspar crystal taken in this orientation.[4] For each crystal investigated a photograph taken in identical orientation was obtained and they could be readily compared. Albite and pericline twinning of the soda phase can be distinguished at a glance and in almost every case there are slight differences which can be found after careful examination of the photographs. The reciprocal lattice parameters $\alpha^*$ and $\gamma^*$ can be readily measured if albite- or pericline-twinned reflections occur (see following paper).

---

[3] A division of perthites based on the size of the optic angle may be preferable since it is not dependent on the unmixing of the specimen. It will be seen (p. 724), however, that these two alternative definitions are not always complementary for specimens in the compositional range $Or_{90}Ab_{10}$—$Or_{75}Ab_{25}$.

[4] The completely indexed photograph is reproduced in the following paper by Smith and MacKenzie.

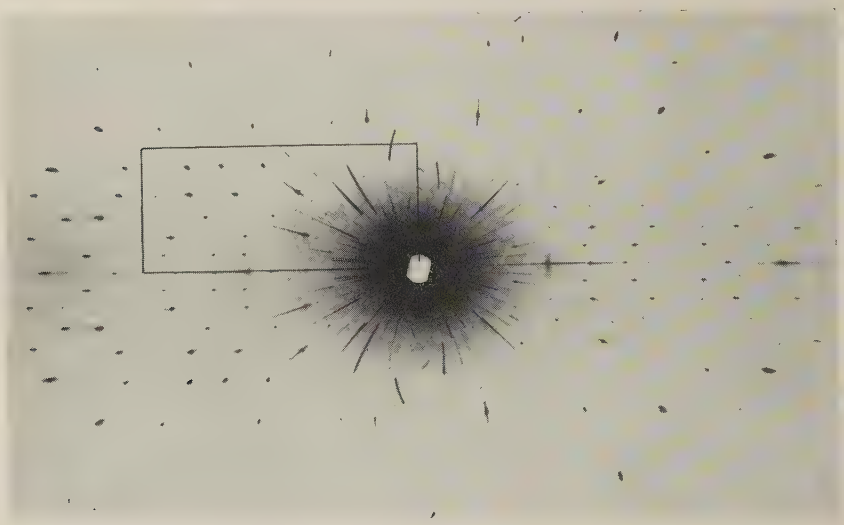

FIG. 2. $b$-axis oscillation photograph of a crystal of specimen $F$ previously heated until homogeneous. The $x$-ray beam was set parallel to (001) in the center of a 15° oscillation arc. The rectangular area shows the reflections which appear in the small parts of the $x$-ray photographs in Fig. 3.

A small part of the $x$-ray photograph of each of the 14 specimens studied is reproduced in Fig. 3. The area of the photograph selected is marked on Fig. 2. The photographs are arranged in order of increasing soda content of the feldspars, and the letters used to designate the specimens are those used by Spencer (1937); the specimens numbered 1 and 2 are those received from Professor Tilley.

Table 1 gives the chemical composition and optic axial angle for each specimen, together with the values of the reciprocal lattice angles $\alpha^*$ and $\gamma^*$ of the soda phase where these could be measured. To compare these values with each other and with the values of low- and high-temperature albite and adjacent feldspars the method selected has been to plot the value of $\alpha^*$ against $\gamma^*$.

Figure 4 shows a plot of $\alpha^*$ against $\gamma^*$ for the following feldspars:

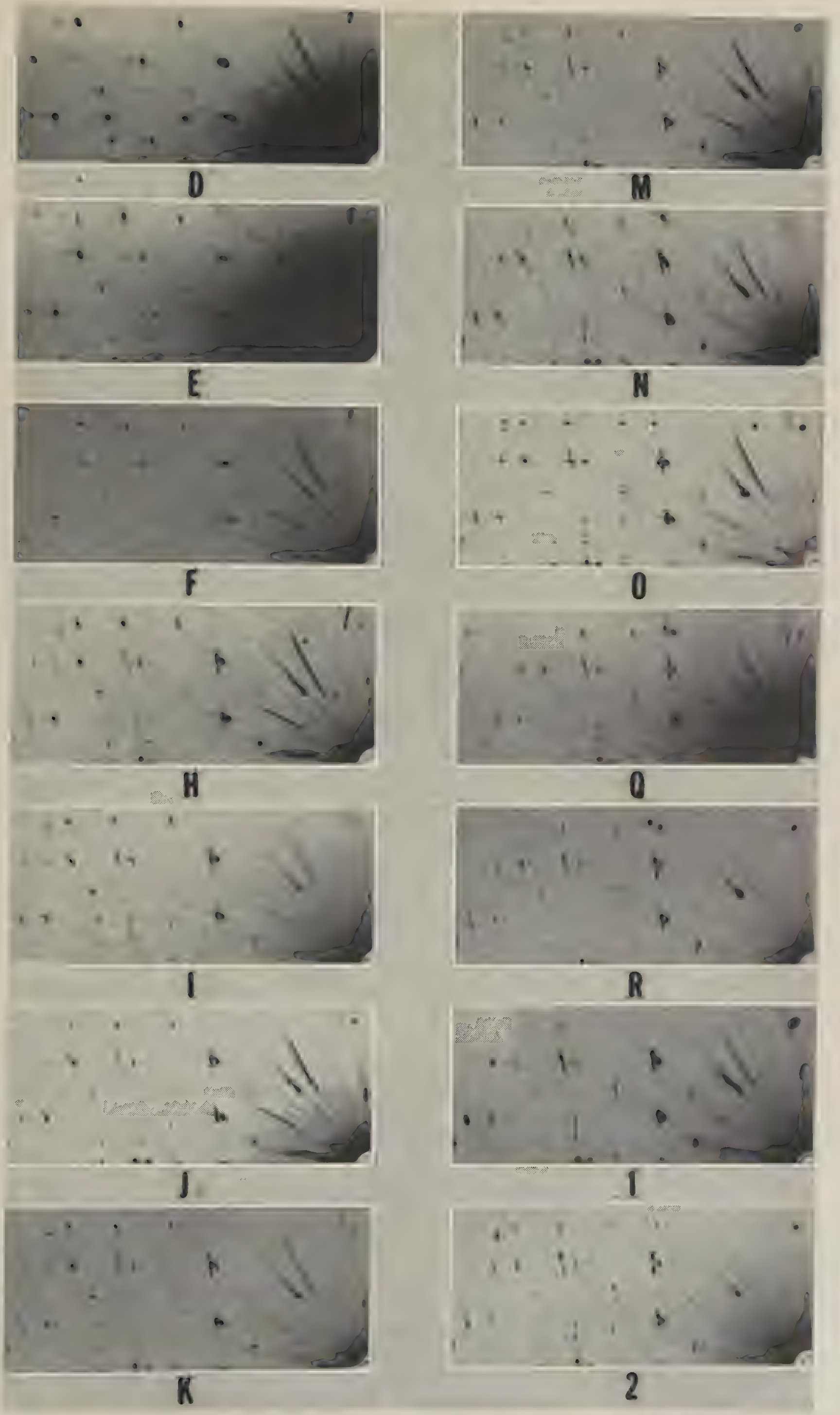

FIG. 3. Small parts of the *b*-axis x-ray oscillation photographs of 14 low-temperature feldspars. The letters and numbers refer to the specimens described in the text.

TABLE 1. DATA ON ORTHOCLASE-MICROPERTHITES

| Specimen | Chemical composition weight % | | | $2V_\alpha$ | Reciprocal lattice angles of soda phases | | Type of twinning of soda phase |
|---|---|---|---|---|---|---|---|
| | Or | Ab | An | | $\alpha^*$ | $\gamma^*$ | |
| *D* | 84.5 | 13.8 | 1.7 | 46.2 | not measured | | (pericline type superstructure) |
| *E* | 83.3 | 14.9 | 1.8 | 57.6 | 87° 58′ | 89° 05′ | pericline |
| *F* | 78.8 | 18.9 | 2.3 | 52.9 | not measured | | (pericline type superstructure) |
| *H* | 72.5 | 25.8 | 1.7 | 61.5 | not measured | | (albite-twin type superstructure) |
| *I* | 69.4 | 28.9 | 1.7 | 69.1 | not measured | | (albite-twin type superstructure) |
| *J* | 66.6 | 32.5 | 0.9 | 75.0 | not measured | | (albite-twin type superstructure) |
| *K* | 64.4 | 33.8 | 1.8 | 61.4 | not measured | | (albite-twin type superstructure) |
| *M* | 57.3 | 40.3 | 2.4 | 73.7 | 87° 00′ | 90° 32′ | albite |
| *N* | 53.7 | 45.6 | 0.7 | 83.5 | 86° 48′ | 90° 33′ | albite |
| *O* | 48.5 | 47.3 | 4.2 | 82.8 | 86° 45′<br>86° 43′ | 90° 15′<br>90° 15′ | pericline<br>albite |
| *Q* | 45.6 | 50.2 | 4.2 | 81.7 | 86° 52′ | 90° 17′ | albite |
| *R* | 44.1 | 51.6 | 4.3 | 71.3 | 86° 55′ | 90° 08′ | albite |
| 1 | 31.5 | 68.3 | 0.2 | 82.0 | 86° 39′ | 90° 34′ | albite |
| 2 | 19.8 | 72.7 | 7.5* | 78.5 | 86° 13′<br>86° 29′ | 89° 30′<br>89° 58′ | pericline<br>albite |

* Includes 1.5% Cs.

orthoclase; maximum microcline;[5] two intermediate microclines; high-temperature albite and synthetic feldspars, $Or_{10}Ab_{90}$, $Or_{20}Ab_{80}$, $Or_{30}Ab_{70}$; low-temperature albite and three natural low-temperature plagioclase feldspars of composition near $Ab_{89}An_{11}$, $Ab_{80}An_{20}$, and $Ab_{70}An_{30}$. The angles $\alpha^*$ and $\gamma^*$ for these feldspars are given in Table 2. The values of the reciprocal lattice angles of the soda phase of the orthoclase-perthites are also plotted. This diagram shows that some of the specimens have a soda phase which corresponds fairly closely with low-temperature albite but others show considerable departure from the lattice angles of low-temperature albite. One specimen (*E*) has a soda phase corresponding to a high-temperature feldspar of composition near $Or_{25}Ab_{75}$. This will be discussed more fully after the specimens used in this study are described.

---

[5] A microcline with maximum deviation from monoclinic symmetry has been described as a maximum microcline (MacKenzie, 1954) and it is proposed that any triclinic potash feldspar having less than the maximum deviation from monoclinic symmetry should be described as an intermediate microcline.

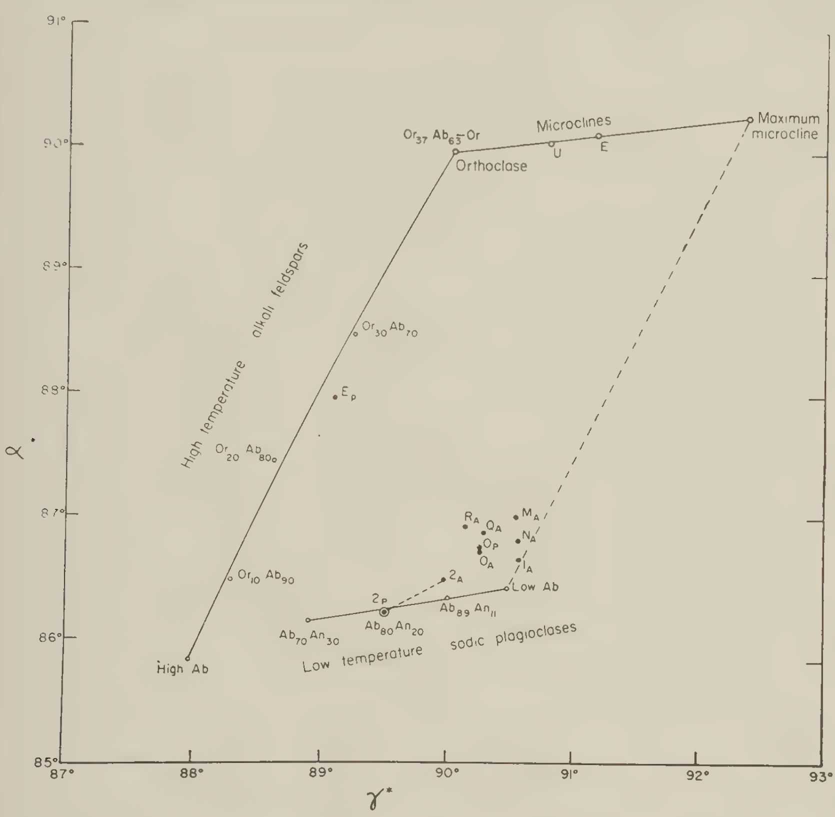

FIG. 4. Plot of the reciprocal lattice angles $\alpha^*$ against $\gamma^*$ for triclinic alkali feldspars and three low-temperature sodic plagioclases. The point marked "orthoclase" at $\alpha^* = \gamma^* = 90°$ includes all homogeneous monoclinic feldspars. The value of $\alpha^*$ is plotted against $\gamma^*$ for the soda phase or phases of eight low-temperature feldspars. The suffixes *A* and *P* denote the type of twinning (albite or pericline) from which the measurements were made. Specimen *2* has two soda phases, one albite twinned and the other pericline twinned. Specimen *O* has one soda phase twinned according to both the albite and pericline laws.

Certain differences in the small parts of the *x*-ray patterns shown in Fig. 3 suggest a subdivision of the 14 specimens based on their bulk chemical composition. The groups are as follows: (i) *D*, *E*, and *F*, (ii) *H*, *I*, *J*, and *K*, (iii) *M*, *N*, *O*, *Q*, *R*, *1* and *2*.

*Specimens D, E, and F.* These specimens were grouped together by Chao and Taylor (1940) as representing one type of structure, and specimen *F* was described in some detail. The small parts of the $x$-ray photographs in Fig. 3 show that these specimens are distinct from the remaining specimens, in that reflections representing the soda phase lie only on the main layer lines of the photograph.

TABLE 2. RECIPROCAL LATTICE ANGLES $\alpha^*$ AND $\gamma^*$ FOR SELECTED FELDSPARS

| | $\alpha^*$ | $\gamma^*$ | Reference |
|---|---|---|---|
| *Microclines* | | | |
| Blue Mountain, Ontario (maximum microcline) | 90° 18′ | 92° 22′ | MacKenzie (1954) |
| Specimen *E* (Spencer, 1937) | 90° 09′ | 91° 09′ | |
| Specimen *U* (Spencer, 1937) | 90° 05′ | 90° 46′ | |
| *Synthetic high-temperature alkali feldspars* (crystallized hydrothermally) | | | |
| Or$_{30}$Ab$_{70}$ | 88° 29′ | 89° 14′ | Donnay and Donnay (1952) |
| Or$_{20}$Ab$_{80}$ | 87° 27′ | 88° 37′ | |
| Or$_{10}$Ab$_{90}$ | 86° 29′ | 88° 17′ | |
| Ab | 85° 50′ | 87° 58′ | |
| * *Synthetic high-temperature plagioclasses* | | | |
| Ab (crystallized hydrothermally) | 85° 58′ | 87° 54′ | Smith (in preparation) |
| Ab$_{90}$An$_{10}$ (crystallized dry) | 85° 57′ | 87° 59′ | |
| Ab$_{70}$An$_{30}$ (crystallized dry) | 86° 04′ | 88° 00′ | |
| Ab$_{50}$An$_{50}$ (crystallized dry) | 86° 04′ | 87° 54′ | |
| *Natural low-temperature plagioclases* | | | |
| Ab | 86° 24′ | 90° 29′ | |
| Ab$_{89}$An$_{11}$ | 86° 18′ | 89° 59′ | |
| Ab$_{80}$An$_{20}$ | 86° 14′ | 89° 27′ | |
| Ab$_{70}$An$_{30}$ | 86° 11′ | 89° 00′ | |

* These values are included to show the very slight differences in the angles $\alpha^*$ and $\gamma^*$ of high-temp. plagioclases.

Specimens *D* and *F* were found by Spencer in the gem-washing residues of the Mogok Ruby Mines, Burma (Spencer, 1930). Specimen *E* was obtained from a garnetiferous granite-gneiss in the railway cutting near Ombadowla, Kalahandi State, Orissa, India (Spencer, 1937). Although specimen *E* was classified by Spencer as an orthoclase-microperthite and the crystal used to make the $b$-axis $x$-ray photograph, part of which is shown in Fig. 3, was optically monoclinic and has a monoclinic potash phase, it has been found that much of this sample should be described as an intermediate microcline with somewhat variable lattice angles (MacKenzie, 1954). A crystal of specimen *E* with a 7½° extinction angle on an (001) cleavage fragment gave the *x*-ray pattern of an untwinned microcline with diffuse streaks indicating only very slight unmixing.

The *b*-axis oscillation photograph of specimen *E* shows, in addition to the monoclinic potash phase, two sets of two closely spaced reflections lying on the layer lines of the monoclinic potash host. If the two closely spaced reflections are considered as a single reflection then the soda phase can be interpreted as twinned on the pericline law. The reciprocal lattice angles $\alpha^*$ and $\gamma^*$ measured on this assumption are set down in Table 1, and from Fig. 4 it can be seen that these correspond closely to a high-temperature feldspar of composition near $Or_{25}Ab_{75}$.

The oscillation photographs of specimens *D* and *F* are very similar to each other and have, in addition to a monoclinic potash phase, a soda phase represented by three diffuse reflections. These cannot be interpreted as due to pericline twinning. In the crystal of specimen *F* studied by Chao and Taylor (1940) the soda phase was pericline twinned and the lattice angles corresponded more nearly with a high-temperature soda feldspar than with low-temperature albite (Taylor, personal communication). The type of structure shown by specimens *D* and *F* will be described as a pericline type superstructure, since the reflections are aligned in the direction given by pericline-twinned reflections. It is believed that this is an intermediate stage in the development of pericline twinning of the soda phase. The fine structure noted in the soda phase of specimen *E* may be a further stage in this process.

*Specimens H, I, J, and K*. The *x*-ray patterns of these specimens have one feature in common which distinguishes them from the remaining specimens. In each case the soda phase is represented by an odd number of reflections usually connected by diffuse streaks, the center reflection lying on the layer lines of the monoclinic potash phase. This structure is described as an albite-twin type superstructure for the reflections are aligned in the direction given by albite-twinned reflections. It is probably somewhat analogous to the pericline type superstructure already mentioned. Previous writers have noted the presence of a fine structure in the soda phase of some perthites. Laves (1952) has explained this as a result of the strain produced in the triclinic soda feldspar by the monoclinic potash structure. The strain is reduced by the growth of twin lamellae only a few unit cells across; this produces a superstructure which results in the complex pattern of reflections. The lattice angles of the soda phase cannot be measured by the simple method devised for twinned crystals (see following paper).

Specimen *H* is from the gem-washing residues of the Mogok Ruby

Mines, as are specimens *D* and *F*. Spencer (1930) noted that the extinction on (001) is sometimes oblique and may be as much as 4° from straight extinction but that there is no sign of microcline twinning.

Specimens *I* and *J*, two moonstones from Ambalangoda, Ceylon, are of very similar chemical composition. They occur in pegmatites within a region of feldspathic gneisses which appear to have been decomposed by hydrothermal solutions (Spencer, 1930).

Specimen *K* is from the contact of a pegmatite with a limestone at Myo Taung, $3\frac{1}{4}$ miles northeast of Mogok, Burma.

A careful examination of the *x*-ray photographs of specimens *I* and *J* reveals that the reflection representing the potash phase is not sharp but shows a diffuse streak at about 45° to the main layer lines. This will be discussed in detail in a following section.

*Specimens M, N, O, Q, R, 1,* and *2.* These specimens show either albite twinning or, in some cases, both albite and pericline twinning of the soda phase. Specimens *M* and *Q* show a fine structure of the albite-twinned soda phase but, if the centers of the two groups of reflections are measured, the reciprocal lattice angles are very similar to those of low-temperature albite.

Specimen *M* is from Ambalangoda, the same locality as that of specimens *I* and *J*. This sample was used by Chao and Taylor (1940) as an example of a perthite with an albite-twinned soda phase with lattice angles similar to those of low-temperature albite. The reciprocal lattice angles of the soda phase are given in Table 1 and plotted in Fig. 4, and their similarity to those of low-temperature albite can be readily seen.

Specimen *N* is from a locality $3\frac{1}{4}$ miles east-northeast of Mogok, Burma. The small part of the *x*-ray photograph (Fig. 3) shows that the potash phase is represented by three reflections; the relations in this specimen have already been briefly described (Smith and MacKenzie, 1954) and further details are given below.

Specimen *O* is described by Spencer (1930) as *Burma Black I*, but no locality is given for this specimen. The reciprocal lattice angles $\alpha^*$ and $\gamma^*$ were measured for both the pericline-twinned reflections and the albite-twinned reflections. The results obtained were almost identical and are close to those of low-temperature albite.

Specimen *Q* is described by Spencer (1930) as *Burma Black II* and shows a blue schiller. In the single-crystal photograph a fine structure of the soda phase is present; the reciprocal lattice angles were measured by considering the centers of the two groups of reflections.

Specimen *R* is from Fredricksvärn, Norway.[6] Spencer (1937) noted that in thin section this material has an appearance similar to that described by Alling (1921) as incipient microcline twinning. The $x$-ray photograph shows that the $b$-axis of the potash phase is not exactly normal to the twin plane of the albite-twinned soda phase.

---

[6] One pegmatite in the Langesundsfjord area provides most of the specimens of microperthite from this region. Oftedahl (1948) gives a sketch-map showing the location of the pegmatite.

Specimen *1* was separated from the lestiwarite from north of Kvelle church, Laagendal, Norway. Brögger (1898, p. 216) gave a chemical analysis of this rock from which he calculated the mineral content as 91% microperthite, $7\frac{1}{2}$% aegirine and $1\frac{1}{2}$% sphene, and derived the composition of the feldspar from this mode as $Or_{35.8}Ab_{64.2}$. The analysis of the rock shows 0.85% CaO and thus the anorthite content of the feldspar is less than 4%.[6a] In thin section the feldspar is cryptoperthitic except for a narrow zone of microperthite at the grain boundaries where the two phases are distinctly visible and give a serrated border to most of the crystals. Brögger (1898) gives a drawing of this type of structure as it appears in a lestiwarite from Lyseböfjord. In the single-crystal $x$-ray photograph the reflections due to the potash phase show diffuse streaks in a direction at about 45° to the main layer lines (cf. specimens *I*, *J*, and *N*). The soda phase is albite twinned and has lattice angles very close to those of low-temperature albite.

Specimen *2* is an unusually soda-rich feldspar from a nepheline syenite in Mogok, Burma, recently studied by Tilley (1954). The feldspar has been described by Tilley as an orthoclase-microperthite, since most of the crystals are optically monoclinic despite the high soda content. A few crystals have been found showing albite twinning and others showing albite and pericline twinning when examined under the petrographic microscope. Single-crystal $x$-ray photographs show a monoclinic potash phase and a soda phase which is albite twinned or both pericline and albite twinned. One crystal which was albite twinned as observed under the microscope gave a single-crystal $x$-ray pattern having a monoclinic potash phase and an albite-twinned soda phase, i.e. the $x$-ray pattern was identical with that produced by an optically untwinned crystal.

A powdered sample of this feldspar was heated at 1050° C. for 65 hours and then $x$-rayed at elevated temperatures on the Philips high-angle spectrometer. Although the preliminary heat treatment had not completely homogenized the sample, only one triclinic phase could be detected in the $x$-ray powder patterns and this became monoclinic at elevated temperature. When homogeneous, this feldspar would be described as an anorthoclase (MacKenzie, 1952).

The reciprocal lattice angles $\alpha^*$ and $\gamma^*$ (of the soda phase) were measured from an $x$-ray photograph which showed both albite- and pericline-twinned reflections. The values differ by an amount greater than the error in measurement and the difference is sufficient to warrant describing these as two distinct phases. It can be seen also, from Fig. 4, that the angles measured from the pericline-twinned phase depart further from the values of low-temperature albite than any of the other specimens studied.

---

[6a] Through the courtesy of Professor Tilley, a chemical analysis of this mineral was made by Mr. J. H. Scoon, after completion of the manuscript. Its composition is calculated as $Or_{31.5}Ab_{68.3}An_{0.2}$.

Comparison of the relative intensities of the soda and potash reflections in the *x*-ray photographs made from different crystals of this specimen indicates that the chemical compositions of the individual crystals differ. This difference has been neglected in the present study, but an *x*-ray method of determining the composition of individual crystals is being investigated.

## RELATION BETWEEN CHEMICAL COMPOSITION AND THE NATURE OF THE SODA PHASE

From examination of the single-crystal photographs (Fig. 3) a division of these feldspars into three groups on the basis of the arrangement of the reflections representing the soda phase has been suggested. In the first group, only in the case of specimen *E* have the reciprocal lattice angles been measured, and these correspond to a high-temperature soda-rich feldspar. Specimen *F* was found by Taylor (personal communication) to have lattice angles close to a high-temperature soda-rich feldspar. It is believed that specimen *D* has a soda phase with similar lattice angles. The existence of a high-temperature soda phase in these specimens, which are presumed to be from low-temperature environments, presents a problem for which no completely satisfactory explanation is at present available. This difficulty might, of course, be overcome in the case of specimens *D* and *F* by describing them as sanidine-microperthites, since the optic axial angles of sanidines in the compositional range $Or_{100}$ to $Or_{75}Ab_{25}$ are not known and the curve for orthoclases and orthoclase-microperthites in this compositional range is based partly on specimens *D* and *F* (Tuttle, 1952*b*). It has already been noted, however, that specimen *E* partly consists of an intermediate microcline, and the term sanidine has invariably been used to denote a high-temperature feldspar. Although the lattice angles of the soda phase were not determined on the crystal having a triclinic potash phase, this does necessitate a fairly close association of the assumed lowest temperature modification of potash feldspar with the high-temperature form of soda feldspar.

The lattice angles of the soda phase of specimen *E* are close to those of a high-temperature feldspar of composition about $Or_{25}Ab_{75}$. *If this represents the true composition of the soda phase, it may be impossible for it to invert to the low-temperature form if the structure of low-temperature albite* *cannot accommodate more than a very limited amount of potash.*[7] Low-temperature alkali feldspars having less than about 25% soda feldspar in their bulk composition might be expected in many cases to have a soda phase which is not pure $NaAlSi_3O_8$ and so would not invert to the low-temperature form. This does not exclude the possibility of specimens in this compositional range being completely unmixed to almost pure potash feldspar and pure soda feldspar, in which case the soda phase would be expected to be low-temperature albite if the specimen occurred in a low-temperature environment. Specimens of this type have been found.

Specimens in the composition range $Or_{75}$–$Or_{60}$ (approx.) are characterized by the albite-twin type superstructure. If this type of structure is due to a periodicity of the albite cells reducing the strain caused by the presence of triclinic cells in a monoclinic host structure, it is to be expected that the existence of the superstructure will be dependent on the bulk composition of the sample, since the greater the potash content the greater will be the strain on the soda phase. The appearance of the albite-twin type superstructure in only the four specimens in this composition range gives further support to this explanation of the superstructure.

Specimens having less than 60% potash feldspar in their bulk composition have a soda phase which is albite twinned or albite and pericline twinned. Specimens *M* and *Q*, instead of having single spots representing the albite-twinned reflections, have groups of two spots. This may be a relict of the superstructure formed during the exsolution process. Since the proportion of soda feldspar in the remaining specimens is almost equal to or greater than the potash feldspar content, the soda phase should be considered as the host structure. The strain in the soda phase should therefore be small and the tendency to form a superstructure correspondingly less.

The tendency to form a superstructure is probably highest at the beginning of the unmixing process. As the unmixing proceeds, the size of the lamellae of the soda phase should increase, thus reducing the value of the strain per unit volume. It is thus reasonable to suppose that the formation of a superstructure is an intermediate step in the formation of a twinned crystal. We have, however, no evidence to prove this hypothesis.

It should be made clear at this point that the subdivision of these low-temperature perthites suggested here is based on only a limited number of specimens and may have to be modified as other samples of known composition are investigated.

---

[7] Low-temperature alkali feldspars of composition near $Or_{25}Ab_{75}$ are comparatively rare and those that do exist are almost certainly unmixed.

Chao and Taylor (1940) gave a tentative explanation of the difference in the twinning and in the lattice angles of the soda phase in low-temperature perthites with relation to the bulk chemical composition. On the basis of the change in length of the *a*-axis they concluded that when the soda feldspar content is between 10 and 30%, only the soda feldspar in excess of the 10%, which might be held in solid solution in the potash phase, is exsolved. When the soda feldspar is in excess of 30% in the bulk composition they considered that all of it was exsolved and formed a separate soda phase with lattice angles close to those of low-temperature albite. In an attempt to determine the composition of the unmixed phases in the present investigation, using the change in spacing of the $20\bar{1}$ reflection in an *x*-ray powder pattern (Bowen and Tuttle, 1950), it was found that some specimens gave impossible results for the composition of the potash phase. A similar effect has been noted by Laves (1952) and explained by him as resulting from the unmixed phases not showing the same lattice parameters as they would if crystallized independently. Since the lattice edges of the unmixed phases do not give the values which would be expected if the phases had crystallized independently, it may be argued that the lattice angles also give incorrect values. From the present study, taken in conjunction with a study of high-temperature cryptoperthites, it is believed that a closer approximation to the composition of the soda phase is given by the lattice angles than by the lattice edges.

## ORTHOCLASE-MICROPERTHITES WITH A TRICLINIC POTASH PHASE

Previous studies of orthoclase-microperthites have all indicated that the potash phase in such specimens is monoclinic. Four[8] of the specimens described here have a triclinic potash phase in addition to a monoclinic potash phase. It must be emphasized that these specimens would not be described as microcline-microperthites by the petrologist since the triclinic potash phase cannot be detected optically either by twinning or by oblique extinction. Even from *x*-ray powder patterns is it not possible to detect with certainty the existence of two potash phases.

Specimens *I*, *J*, and *1* show diffuseness of the reflections representing the potash phase, causing an elongation of the spots in a direction at about 45° to the main layer lines. In specimen *N* the potash phase is represented by three distinct spots and this material has been studied in detail. The reciprocal lattice angles $\alpha^*$ and $\gamma^*$ of the triclinic potash phase are given in Table 3 and plotted in Fig. 5 along with the values for the

---

[8] Specimen *E* will be excluded from this discussion since the optically monoclinic crystals examined have a monoclinic potash phase and optically triclinic crystals have a triclinic potash phase.

TABLE 3. EFFECT OF HEAT TREATMENT ON RECIPROCAL LATTICE ANGLES OF SPECIMENS *N*, *O* AND *R*

| Specimen | Heat treatment | Soda phase | | Potash phase | |
|---|---|---|---|---|---|
| | | $\alpha^*$ | $\gamma^*$ | $\alpha^*$ | $\gamma^*$ |
| *N* | unheated | 86° 52′ | 90° 35′ | 90° 50′ | 92° 35′ |
| | heated at 800° C. for 6 hrs. | 87° 31′ | 90° 45′ | 90° 48′ | 92° 16′ |
| | then heated at 950° for 6 hrs. | 88° 09′ | 91° 12′ | 90° 39′ | 92° 06′ |
| | then heated at 1025° for 5 hrs. | 88° 27′ | 91° 16′ | 90° 21′ | 91° 51′ |
| | then heated at 800° for 24 hrs. | 87° 41′ | 90° 49′ | — | |
| | then heated at 600° for 48 hrs. | 87° 21′ | 90° 42′ | 90° 48′ | 92° 17′ |
| *O* | unheated | 86° 45′ | 90° 15′ | | |
| | heated at 900° C. for 1½ hrs. | 88° 11′ | 90° 47′ | | |
| *R* | unheated | 86° 55′ | 90° 08′ | | |
| | heated at 900° C. for 240 hrs. | 87° 46′ | 90° 23′ | | |

soda phase. The values of $\alpha^*$ and $\gamma^*$ are comparable with those of a maximum microcline, but both $\alpha^*$ and $\gamma^*$ depart further from 90° than do those of any microcline so far reported. This may result from the intimate intergrowth of the three phases affecting the true values of the lattice parameters.

From Laue, precession and Weissenberg $x$-ray photographs the following relations were found between the three phases of specimen *N*. The triclinic potash phase and the soda phase are oriented so that the $b^*$-axes of the potash phase are symmetrical about the common $b^*$-axis of the albite-twinned soda phase and make angles of 1° 24′ with it. The $a^*$-axes of the triclinic potash phase are also symmetrical about the two $a^*$-axes of the soda phase and are at angles of 48′ to the $a^*$-axes of the soda phase. The monoclinic potash phase has no simple crystallographic relation to either the triclinic potash phase or the soda phase.

Specimen *N* has been shown to consist of three phases, and it is of interest to determine the possible sequence of events in the exsolution process. With this in view the crystal, whose lattice angles had been carefully determined, was heated for 6 hours at 800° C., 6 hours at 950° C., and 5 hours at 1025° C. After each period of heating, the lattice angles of the two triclinic phases were measured. The values are given in Table 3 and plotted in Fig. 5. In this diagram the solid circles represent the plot of $\alpha^*$ against $\gamma^*$ after heating at the temperature indicated beside the circles. In the case of the soda phase the triangles represent the plot of $\alpha^*$ against $\gamma^*$ after heating the same crystal at progressively lower temperatures, i.e. at 800°C. for 24 hours and 600° C. for 48 hours. The triangle in the top right-hand corner of the diagram represents the plot of $\alpha^*$ against $\gamma^*$ for the triclinic potash phase after heating at 600° C. for 48 hours. From Fig. 5 it can be seen that the change in the reciprocal lattice angles of the soda phase with heating is in the direction of a maximum microcline. The angles of the triclinic potash phase do not change directly toward low-temperature albite as would be expected if complete solid solution exists between microcline and low-temperature albite (Laves, 1952). After heating at 1025° C. measurement of the reciprocal lattice angles became difficult, and it was judged that further heating would make it impossible to measure the angles without introducing considerable error.

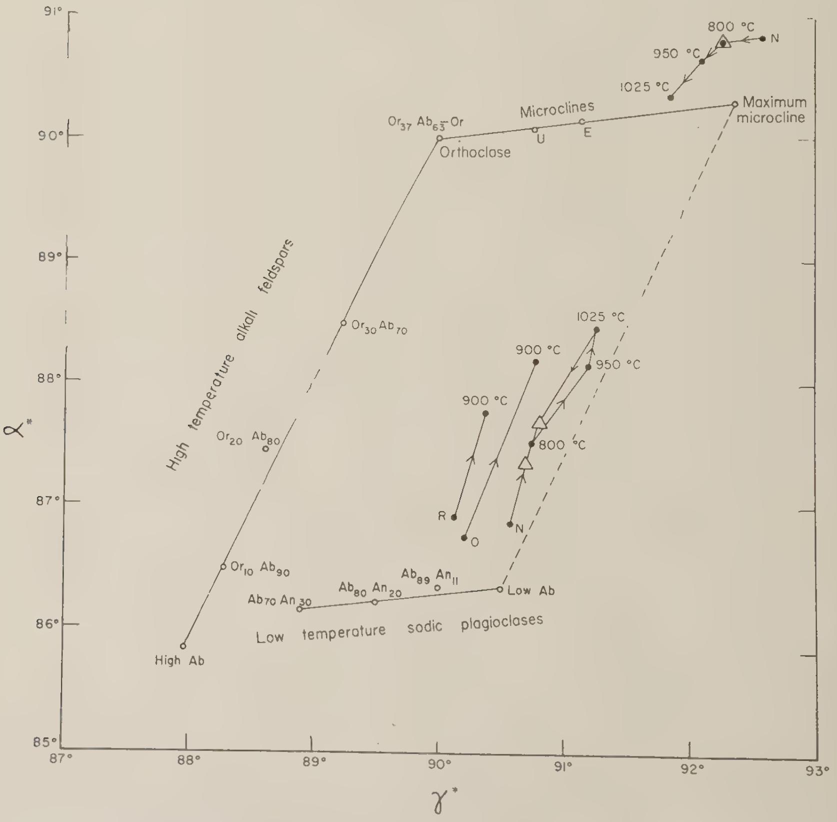

FIG. 5. Diagram to show the effect of heating at progressively higher temperatures on the values of $\alpha^*$ and $\gamma^*$ of the soda phase in specimens *N*, *O*, and *R* and of the triclinic potash phase of specimen *N*. The triangles represent the points obtained by reversal of this process in specimen *N* by heating the same crystal at 800° C. for 24 hours and then at 600° C. for 48 hours.

To determine whether these changes were reversible the same crystal which had been heated at 1025° for 5 hours was heated at 800° for 24 hours and 600° for 48 hours. The results given in Table 3 and Fig. 5 indicate that the changes produced in both the soda and potash phases are reversible, although heating at 600° did not restore the angles to their original values; prolonged heating at lower temperature might have this effect since this is undoubtedly a rate process.

Two other specimens were heated for varying lengths of time, and from the figures given in Table 3 and plotted in Fig. 5 it can be seen that the angles of the soda phase of these specimens also change in the direction of those of microclines.

In the case of the soda phase of specimen *N* it is certain that the changes in the lattice as a result of heat treatment are due to the solid solution of potash in the soda phase, and it is assumed that the changes in the lattice of the potash phase result from the solid solution of soda.[9] It is now fairly well known that prolonged heating of a microcline at a temperature fairly near its melting point produces a change in the lattice, the final product being a monoclinic feldspar. The heat treatment to which specimen *N* was subjected was insufficient to cause any change in the lattice unless it be due to the solid solution of soda feldspar.

In the single-crystal $x$-ray photographs the appearance of streaks, or two sharp spots lying at the extremities of the streaks, making an angle of approximately 45° with the main layer lines is the characteristic feature of these four specimens. This is to be contrasted with the development of microcline from a potash-rich orthoclase where the first sign of a departure from monoclinic symmetry is indicated in the $x$-ray oscillation photographs by the appearance of diffuse streaks lying on curves of constant $\zeta$ or curves of constant $\xi$ representing pericline or albite twinning, respectively, or in many cases both types of twinning appear together. The association of orthoclase and microcline in a feldspar from the Bear Paw Mountains, Montana, has already been described (MacKenzie, 1954) and it has been shown that there is a simple crystallographic relationship between the two potash phases. The evidence that the triclinic form was derived from the monoclinic form is fairly conclusive.

In the case of specimen *N* the crystallographic relationship between the triclinic potash phase and the triclinic soda phase suggests that these two phases are the result of the same period of exsolution but that the monoclinic potash phase was probably exsolved at an earlier stage. If the temperature of the final period of exsolution is within the stability field of microcline and the composition of the potash phase is nearly pure $KAlSi_3O_8$, then the potash phase would be expected to be a microcline (MacKenzie, 1954).

---

[9] The monoclinic potash phase also takes some soda feldspar into solid solution with heat treatment.

These small differences found in the single-crystal $x$-ray patterns of specimens *I*, *J*, *N*, and *1* almost certainly have some petrologic significance which is not yet fully understood. Further work on specimens of this type from carefully investigated geologic environments may help to solve this problem and enable future investigators to make use of these small differences which are easily detected on an $x$-ray oscillation photograph.

## RECIPROCAL LATTICE ANGLES OF THE SODA PHASE

In a study of a series of high-temperature sanidine-cryptoperthites (to be described in paper III of this series) it has been found that the reciprocal lattice angles of the soda phase of these specimens correspond closely with the values expected from high-temperature soda-rich feldspars, and it is believed that from these angles the amount of potash feldspar in the soda phase may be determined. In the case of perthites whose soda phase corresponds approximately with low-temperature albite the points representing $\alpha^*$ plotted against $\gamma^*$ are distributed in an apparently random manner near the point representing low-temperature albite (Fig. 4). The values of $\alpha^*$ and $\gamma^*$ of the soda phase of a perthite will permit making a distinction between a high- and a low-temperature soda phase, but it would be desirable to have an explanation for the cause of the spread of values near low-temperature albite.

Consideration of the reciprocal lattice angles of the soda phase of these low-temperature feldspars with respect to those of low-temperature albite (Table 1) along with the total anorthite content of the samples, suggests that the value of $\gamma^*$ of the soda phase decreases with an increase in the total anorthite content. That the effect of solid solution of potash feldspar in the soda phase is to increase the value of $\alpha^*$ has been shown by the heating experiments already described. Thus the values of $\alpha^*$ and $\gamma^*$ of the soda phase may give an indication of its chemical composition.

The measurements made from both the albite-twinned and pericline-twinned phases of specimen *2* are very different from those of low-temperature albite, and it is seen (Fig. 4) that the plot of the pericline-twinned phase falls approximately halfway between high- and low-temperature albite with reciprocal lattice angles equivalent to those of a low-temperature plagioclase of composition $Ab_{80}An_{20}$. From the values of $\alpha^*$ plotted against $\gamma^*$ for soda-rich low-temperature plagioclases it may be seen that the anorthite molecule has an effect on low-temperature albite very similar to that which would be expected from materials transitional between the two forms of albite. The lattice angles of the soda phases of specimen *2* may therefore deviate from those of low-temperature albite, either because these phases are transitional to the high-temperature form or because they have a high content of anorthite.[10] The total anorthite content of specimen *2* is 6% and is greater than that of any of the other specimens studied.

It is almost certain that the deviations of $\gamma^*$ of both the albite- and pericline-twinned phases from $\gamma^*$ of low-temperature albite are due to the high anorthite content of this specimen and not to a transition to the high-temperature forms. The soda-rich part of this specimen may thus be considered as a plagioclase of bulk composition near $Ab_{85}An_{15}$ which consists of two phases of approximate composition $Ab_{90}An_{10}$ and $Ab_{80}An_{20}$ (see Fig. 4). It is interesting to note that, although the temperature of final crystallization of this feldspar has been low enough to form two low-temperature plagioclase phases (peristerite), there is no evidence of the development of a triclinic potash phase. Laves (1952) has briefly noted the existence of three-phase feldspars of this type.

Specimens *O*, *Q*, and *R* each have about 4% of the anorthite molecule in their bulk composition (Table 1). These are represented in Fig. 4 by points lying considerably to the left of a line joining low-temperature albite to maximum microcline. The remaining specimens *M*, *N* and *1* (see footnote 6*a*) have much smaller anorthite contents and are represented by points lying fairly close to the line joining low-temperature albite to maximum microcline. This suggests that increase in the bulk anorthite content of the feldspar does reduce the value of $\gamma^*$ of the soda phase.

Because of the very limited solid solution between lime feldspar and potash feldspar (Schairer and Bowen, 1947) it may be assumed that in a perthite almost all the lime feldspar is held in the soda phase. Unfortunately, the proportion of lime feldspar to soda feldspar in this phase cannot be determined since it will depend on the amount of soda in the potash phase, and at present we have no means of determining this amount accurately.[11]

Specimens *M*, *N*, *O*, *Q*, and *R* have values of $\alpha^*$ differing from that of low-temperature albite by amounts greater than the error in measurement, whereas specimens *1* and *2* have values close to that of low-temperature albite. The heating experiments on specimens *N*, *O*, and *R* indicate that the effect of solid solution of potash in the soda phase is to increase the value of $\alpha^*$, and so it is believed that specimens *M*, *N*, *O*, *Q*, and *R* have soda phases which are not pure NaAlSi$_3$O$_8$ but contain small amounts of potash in solid solution. From what has already been stated in discussing the soda phase of specimen *E* (page 724) is it assumed that the amount of potash which can be held in solid solution in a low-temperature albite is rather small. The solid solution of potash in the soda phase of specimens *N*, *O*, and *R* as a result of heat treatment probably represents metastable equilibrium.

---

[10] These two alternatives are not mutually exclusive since the effect of lime on the values of $\alpha^*$ and $\gamma^*$ of high-temperature albite is negligible (see Table 3). Thus the soda phases might have a high lime content and also be transitional to the high-temperature form.

[11] It has been noted on a previous page that the $20\bar{1}$ spacing cannot be used to determine the composition of the potash phase in many perthites.

If the deviations in the values of $\gamma^*$ and $\alpha^*$ in the soda phases of low-temperature perthites are due, as has been proposed above, to the lime and potash feldspar contents respectively, it may eventually be possible to determine accurately the composition of the soda phase and so calculate the composition of the potash phase of a specimen of known bulk composition.

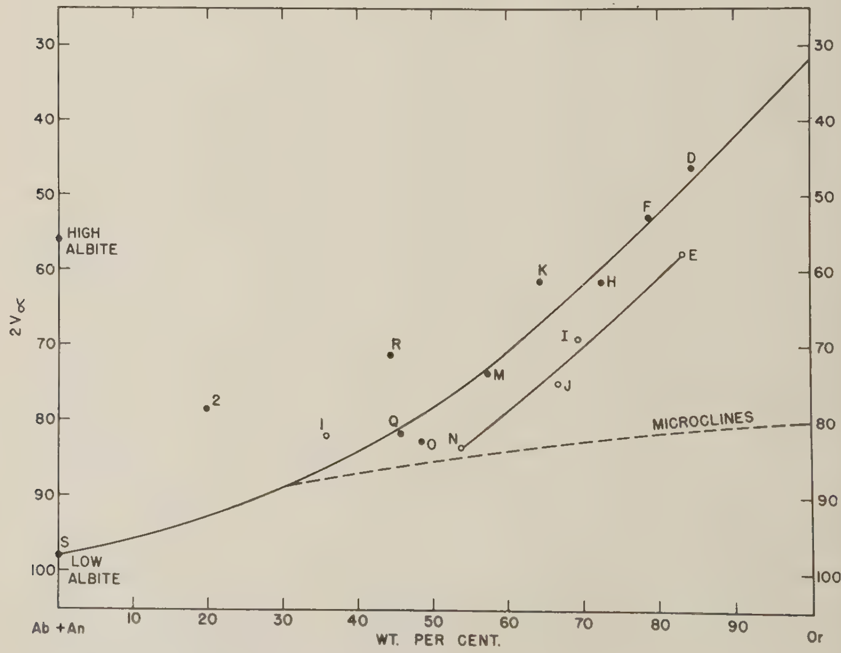

FIG. 6. Plot of the optic axial angle against chemical composition for the orthoclase-microperthites investigated. The closed circles denote specimens having a monoclinic potash phase and the open circles denote specimens having a triclinic potash phase in addition to a monoclinic potash phase. The point indicated by the letter *S* is the value of 2V for Amelia albite given by Spencer (1937). A point for high-temperature albite is given for comparison.

## THE OPTIC AXIAL ANGLE OF ORTHOCLASE-MICROPERTHITES

In Fig. 6 the values of the optic axial angle of each of 14 specimens investigated have been plotted against their orthoclase content as obtained from chemical analyses. The points representing specimens which have a monoclinic potash phase are represented by closed circles and those which have a triclinic potash phase in addition to a monoclinic phase are represented by open circles. The curves relating the optic axial angle with chemical composition for the "orthoclases" and "microclines" are reproduced from Fig. 1 and a separate curve has been drawn through the points marked by open circles, representing specimens *E*, *I*, *J*, and *N*. Specimens whose bulk compositions lie in the range $Or_{84.5}$–$Or_{45.6}$ fall fairly close to the curve for orthoclases if they have only a monoclinic potash phase. Specimens in this range which have a triclinic potash phase in addition to the monoclinic potash phase have values of optic angle greater than would be expected.

The three specimens more soda-rich than $Or_{45.6}$ show a rather large scatter of the values for their optic axial angles. Specimen *2* is very much displaced from the curve, and it has already been noted that the reciprocal lattice angles of the soda phase of this specimen deviate considerably from those of low-temperature albite. Specimen *1* falls above the orthoclase curve although it has a triclinic potash phase and is similar to specimens *E*, *I*, *J*, and *N* in this respect. The scatter of the values of optic axial angle in this compositional range cannot be accounted for by any one variable.

Tuttle and Keith (1954) have shown that the optic axial angle of some alkali feldspars may be intermediate between the expected value for an orthoclase-microperthite and a sanidine-cryptoperthite of corresponding composition and have attributed this to the soda phase having partly inverted to the low-temperature modification, with part remaining as high-temperature albite. Further investigation of the specimens studied by Tuttle and Keith has shown that the value of the optic angle of an alkali feldspar for a known composition is a function of the ratio of high- to low-temperature albite. From the data given here it is suggested that the optic axial angle of low-temperature perthites may also be affected by the nature of the potash phase. Thus the value of the optic angle will be greater in a feldspar which has a triclinic potash phase than it will be if no triclinic potash phase is present.

In specimen *E* the soda phase is near a high-temperature soda-rich feldspar and the potash phase is sometimes triclinic. These two factors should have the opposite effect on the value of the optic angle. It appears that the number of variables affecting the value of the optic axial angle is too great to permit using the 2V as an indication of the nature of the potash phase. A single-crystal *x*-ray oscillation photograph will give important information as to the nature of both the potash and the soda phase.

## SUMMARY AND CONCLUSIONS

To describe the feldspar specimens studied, the subdivision of the alkali feldspars into four series as proposed by Tuttle (1952*b*) has been adopted and the curves relating optic axial angle with chemical composition have been used to define members of these series. Single-crystal *x*-ray studies of a number of chemically analyzed orthoclase-microperthites have shown that the reciprocal lattice angles of the soda phase can be used to indicate whether the soda phase is a high- or low-temperature form. In addition, an approximation to the chemical composition of the soda phase may be determinable from these angles.

Most of the orthoclase-microperthites, in which the nature of the soda phase could be determined, have a soda phase with lattice parameters close to those of low-temperature albite.[12] Studies of sanidine-cryptoperthites, to be reported in paper III of this series, reveal that these have soda phases comparable with high-temperature soda feldspar. Tuttle and Keith (1954) have shown that specimens which fall intermediate between the orthoclase-microperthite series and the sanidine-cryptoperthite series have two soda phases, one a high-temperature form and the other a low-temperature form. Thus the subdivision of the alkali feldspars into the orthoclase-microperthites and sanidine-cryptoperthites based on the value of the optic angle for a known chemical composition is not merely an arbitrary subdivision, but has a genetic significance, particularly relative to the temperature of final crystallization.

No perthites have been found having a soda phase which gives conclusive evidence of stable states transitional between high- and low-temperature soda feldspar, although such transitional forms have been postulated by other workers from both optical and *x*-ray studies for single-phase soda feldspars.

Many of the specimens which have been classed as orthoclase-microperthites do not always show straight extinction on (001) cleavage fragments. In addition, some specimens have a triclinic potash phase as well as a monoclinic potash phase and the term orthoclase has generally been understood to apply to monoclinic potash feldspar. It is thought that, until the significance of these slight differences in orthoclase-microperthite specimens can be elucidated, no useful purpose can be served by giving special names to such specimens.

---

[12] The exceptions have been discussed on a previous page.

A mineralogical study of this type can merely indicate a possible sequence of events in the crystallization history of the alkali feldspars. It is hoped, however, that by using the *x*-ray technique, adopted here and described in detail in the following paper, the petrologist investigating alkali feldspar-bearing rocks will obtain considerable help in deducing the history of the rocks. Conversely the detailed study of the alkali feldspars from a carefully investigated geologic environment will give a more accurate picture of the sub-solidus equilibria in this series.

## Acknowledgments

The writers are indebted to Professors O. F. Tuttle and C. E. Tilley and Dr. W. H. Taylor for the interest which they have shown and the advice which they have given in the course of this work. Dr. H. S. Yoder kindly read and commented on the manuscript of this paper.

## References

Alling, H. L. (1921): The mineralogy of the feldspars. Part I: *Jour. Geol.*, **29,** 193–294.

Bowen, N. L., & Tuttle, O. F. (1950): The system $NaAlSi_3O_8$—$KAlSi_3O_8$—$H_2O$: *Jour. Geol.*, **58,** 489–511.

Brögger, W. C. (1898): Die Eruptivgesteine des Kristianiagebietes. III. Das Ganggefolge des Laurdalits. Oslo.

Chao, S. H., Smare, D. L., & Taylor, W. H. (1939): An *x*-ray examination of some potash-soda felspars: *Mineral. Mag.*, **25,** 338–350.

———, & Taylor, W. H. (1940): The lamellar structure of potash-soda felspars: *Proc. Roy. Soc.*, ser. A, **174,** 57–72.

Donnay, G., & Donnay, J. D. H. (1952): The symmetry change in the high-temperature alkali-feldspar series: *Am. Jour. Sci.*, Bowen volume, 115–132.

Ito, T., & Sadanaga, R. (1952): The lamellar structure of certain microcline and anorthoclase: *Acta Cryst.*, **5,** 441–449.

Kôzu, S., & Endô, Y. (1921): *X*-ray analysis of adularia and moonstone, and the influence of temperature of the atomic arrangement of these minerals: *Sci. Rept. Tohoku Univ.*, ser. 3, **1,** 1–17.

Laves, F. (1951): Relationship between exsolved plagioclase and its host: Abstract of paper to the American Crystallographic Association, Washington, D. C.

——— (1952): Phase relations of the alkali feldspars: *Jour. Geol.*, **60,** 436–450, 549–574.

———, & Chaisson, U. (1950): An *x*-ray investigation of the "high"-"low" albite relations: *Jour. Geol.*, **58,** 584–592.

MacKenzie, W. S. (1952): The effect of temperature on the symmetry of high-temperature soda-rich feldspars: *Am. Jour. Sci.*, Bowen volume, 319–342.

——— (1954): The orthoclase-microcline inversion: *Mineral. Mag.*, **30,** 354–366.

Oftedahl, C. (1948): Studies on the igneous rock complex of the Oslo region. IX. The feldspars: *Norsk vidensk.-acad. Oslo Skr. 1 Math.-natur. Kl.*, no. 3, 63–133.

Schairer, J. F., & Bowen, N. L. (1947): The system anorthite—leucite—silica: *Bull. Soc. Géol. de Finlande*, **20,** 67–87.

SMITH, J. V., & MACKENZIE, W. S. (1954): Further complexities in the lamellar structure of the alkali felspars: *Acta Cryst.*, **7**, 380.

SPENCER, E. (1930): A contribution to the study of moonstone from Ceylon and other areas and of the stability relations of the alkali felspars: *Mineral. Mag.*, **22**, 291–367.

——— (1937): The potash-soda-felspars. I. Thermal stability: *Mineral. Mag.*, **24**, 453–494.

TILLEY, C. E. (1954): Nepheline-alkali feldspar parageneses: *Am. Jour. Sci.*, **252**, 65–75.

TUTTLE, O. F. (1952*a*): Origin of the contrasting mineralogy of extrusive and plutonic salic rocks: *Jour. Geol.*, **60**, 107–124.

——— (1952*b*): Optical studies on alkali feldspars: *Am. Jour. Sci.*, Bowen volume, 553–567.

———, & BOWEN, N. L. (1950): High-temperature albite and contiguous feldspars: *Jour. Geol.*, **58**, 572–583.

———, & KEITH, M. L. (1954): The granite problem: Evidence from the quartz and feldspar of a Tertiary granite: *Geol. Mag.*, **91**, 61–72.

*Manuscript received July 22, 1954*

# THE ALKALI FELDSPARS: II A SIMPLE *X*-RAY TECHNIQUE FOR THE STUDY OF ALKALI FELDSPARS

J. V. Smith and W. S. MacKenzie, *Geophysical Laboratory, Carnegie Institution of Washington, Washington, D.C.*

## Abstract

A routine $x$-ray method has been developed for the study of alkali feldspars. From a single-crystal $x$-ray oscillation photograph the symmetry, twinning and unmixing may be seen at a glance. The reciprocal lattice angles $\alpha^*$ and $\gamma^*$ of triclinic phases, twinned on either the albite or pericline law, can be readily measured from the oscillation photograph by a new precision method.

## Introduction

$X$-ray powder methods are now in general use by mineralogists and petrologists for routine work of identification and determination of lattice parameters of known and unknown materials. Single-crystal techniques, however, are rarely used in routine work, and this is unfortunate because a wealth of information not accessible by powder methods can be obtained with little difficulty. This paper presents a single-crystal $x$-ray method for studying the lamellar structure of the alkali feldspars and for determining the reciprocal lattice angles $\alpha^*$ and $\gamma^*$ of a triclinic feldspar if it is twinned on either the albite or pericline law. The procedure for obtaining the $x$-ray photograph is hardly more difficult than the operation of the universal stage on a petrographic microscope, and the photograph may be interpreted at a glance. The reciprocal lattice angles $\alpha^*$ and $\gamma^*$ may be determined in 30 minutes with an accuracy of 3′–10′ of arc. This $x$-ray method is thus ideally suited for a routine investigation of a large number of crystals. In order to encourage the use of this method by those mineralogists and petrologists whose knowledge of single-crystal work is elementary, the techniques will be described in some detail. Readers not familar with single-crystal $x$-ray methods should consult a textbook such as Buerger (1942) or Henry, Lipson, and Wooster (1951).

Alkali feldspars are generally unmixed to two or more phases. The soda-rich phase or phases are triclinic and may have lattice angles similar to those of a low-temperature albite-oligoclase or to those of an anorthoclase (a high-temperature alkali feldspar of composition between $Or_{37}Ab_{63}$ and $Or_0Ab_{100}$). The potash-rich phase or phases may be monoclinic (sanidine or orthoclase) or triclinic (microcline).* However, most of the microperthites and cryptoperthites retain the morphology of a monoclinic feldspar from which they unmixed and often have optically monoclinic symmetry also. This pseudo-monoclinic symmetry may be used in the alignment of the crystals in the *x*-ray camera. From examination of various types of *x*-ray photographs of alkali feldspars we have found that a *b*-axis oscillation photograph with an oscillation angle of 15° is most suitable. A standard orientation has been adopted for each photograph, the crystal being set with the (001) cleavage parallel to the *x*-ray beam in the center of the oscillation.

---

* Laves (1952) has noted that a soda-rich high-temperature cryptoperthite may have a triclinic potash phase which is not microcline but potash feldspar forced to be triclinic by the predominant triclinic soda phase.

Most alkali feldspar crystals have the (010) and (001) cleavages well developed. By use of the tele-microscope, fitted to some single-crystal *x*-ray cameras, or an auxiliary single-circle goniometer, the crystal may be set with an accuracy of 1° 2°. If the (010) and (001) cleavages are not visible, one of the standard *x*-ray setting techniques has to be used. With an orientation error of 1° -2° the resulting photograph is readily interpretable; however, if measurements are to be made from the photograph it is advisable to reduce the setting error below 1° using an *x*-ray setting technique.

The crystal setting is more difficult when the crystal consists solely of an albite twinned triclinic phase, as this gives two sets of layer lines at an angle of about 4°. The crystal may be set approximately by optical means, and after a preliminary *x*-ray photograph has been taken it may be adjusted on the arcs so that the two sets of layer lines are symmetrical about the equator of the photograph. A pericline twinned triclinic phase presents no difficulty since the *b*-axis is common to the twinned parts and there is only one set of layer lines.

A cylindrical camera has been used in preference to a flat plate camera because of the greater range in $\theta$ and because it is an advantage to have straight layer lines. Filtered copper radiation was found to be the most convenient.

## Interpretation of the Photograph

In 1940, Chao and Taylor demonstrated that a simple crystallographic relationship exists between the differently oriented units of a microperthite. Others have confirmed the findings of Chao and Taylor and have amplified their results. The angular relations may be stated briefly as follows. A microperthite generally has a monoclinic potash phase whose orientation corresponds to the morphology of the crystal; thus the *b*-axis of the potash phase is coincident with the morphological *b*-axis of the crystal. The soda-rich phase or phases are triclinic and are twinned on the albite or pericline law. For the albite law the $b^*$-axis is common to the twinned individuals and almost always coincides with the morphological *b*-axis; only two crystals have been found which violate this rule. For the pericline law the *b*-axis is common to the twinned individuals and coincides with the morphological *b*-axis. Sometimes albite and pericline twinning occur together and this may represent a single soda phase or two soda phases, one pericline twinned and the other albite twinned. Some low-temperature perthites have a triclinic potash phase twinned on the albite law or on both the albite and pericline law. In other cases the angular relations between the two triclinic units do not correspond with twinning on either the albite or pericline law.

In the *x*-ray oscillation photographs the potash-rich phases may be distinguished from the soda-rich phases since their reflections are generally nearer to the center of the photographs because of the differences between the lattice parameters of the two phases.

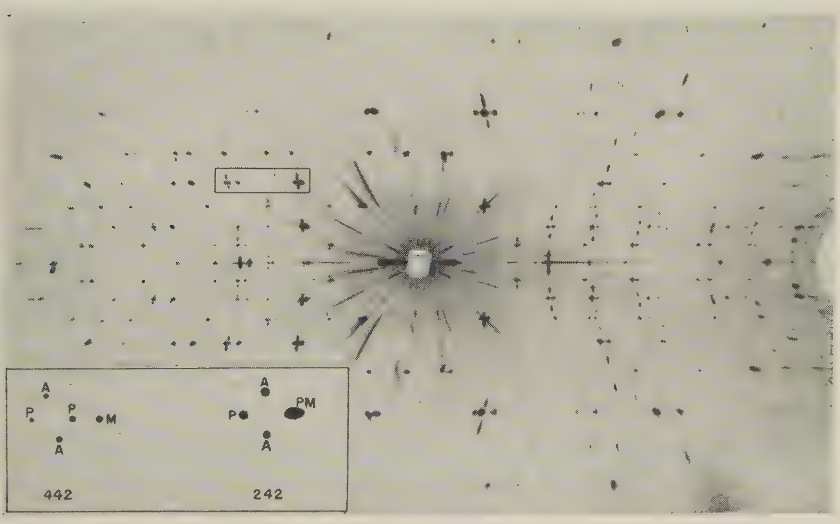

FIG. 1. Specimen *O*, *b*-axis oscillation photograph with the *x*-ray beam parallel to (001) in the center of a 15° oscillation. The inset diagram in the bottom left-hand corner provides a key for the interpretation of the reflections enclosed in the small rectangle in the top left-hand corner. *A* and *P* denote the reflections from the albite- and pericline-twinned soda phase, respectively; *M* denotes the reflection from the potash phase.

Figure 1 is a *b*-axis oscillation photograph of specimen *O*† which has a monoclinic potash phase together with a triclinic soda phase twinned according to the albite and pericline laws. It will be noticed that the potash reflections are usually closer to the center of the photograph and that they are symmetrical about the zero layer line. The albite twinned soda reflections lie symmetrically above and below each layer line on curves of constant $\xi$, whereas the pericline twinned reflections lie on the layer lines (constant $\zeta$). The separation of the pericline twinned reflections is zero on the equatorial layer line and increases with the order of the layer line. The common $b^*$-axis of the albite twinned reflections is coincident with the common $b$-axis of the pericline twinned reflections and with the $b$-axis of the monoclinic potash phase.

---

† The three specimens mentioned in this paper are from a series of feldspars described by Spencer (1937). The letters *O*, *N* and *F* used to denote these specimens are in accordance with the list in Spencer's paper.

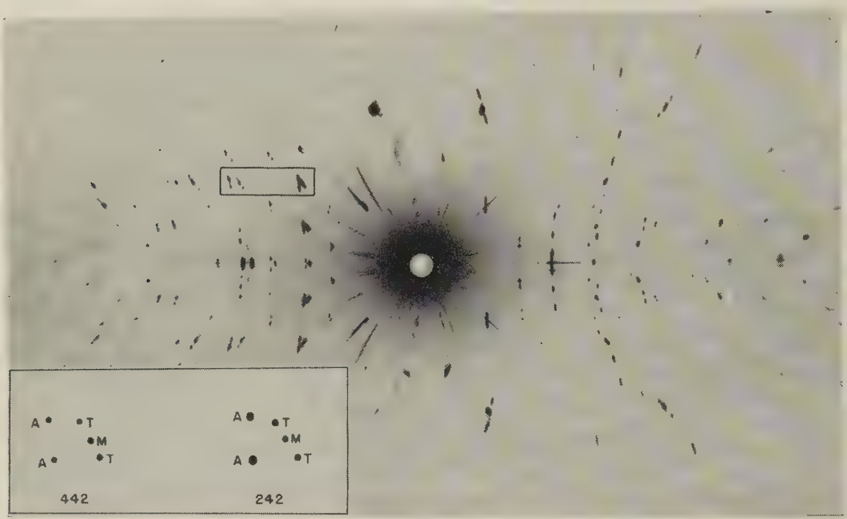

FIG. 2. Specimen *N*, $b$-axis oscillation photograph with the *x*-ray beam parallel to (001) in the center of a 15° oscillation. The inset diagram in the bottom left-hand corner provides a key for the interpretation of the reflections enclosed in the small rectangle in the top left-hand corner. *A* denotes the reflections from the albite-twinned soda phase; *M* and *T* denote the monoclinic and triclinic components of the potash phase, respectively.

Figure 2 is an *x*-ray photograph of specimen *N*. The soda phase is albite twinned. The potash phase is represented by three reflections—the central spot is from a monoclinic component and the two outer reflections are from two triclinic components—which are angularly related in a complex manner. They are not twinned according to either the albite law or the pericline law, for the reflections lie neither on curves of constant $\xi$ nor on curves of constant $\zeta$. The angular relations are given in the accompanying paper (MacKenzie and Smith).

Figure 3 is an *x*-ray photograph of a crystal of specimen *F* which was heated for 17 minutes at 700° C. to homogenize the soda and potash phases. It consists of a single monoclinic phase. The reflections in the upper half of the photograph have been indexed and, since all photographs have been taken in the same orientation, the indices for the potash-rich phase in a perthitic feldspar may be obtained by comparison with this photograph. The indices of a soda-rich phase may also be obtained by comparison, but care is required in the high-angle regions because of the difference in lattice parameters between the soda and potash phases.

Untwinned homogeneous triclinic alkali feldspars are found and their *x*-ray photographs are very similar to those of monoclinic crystals so that great care must be taken before concluding that a feldspar is monoclinic. No confusion should arise for anorthoclase because there are large intensity differences between equivalent reflections above and below the zero layer line. For microclines, however, the intensity deviations are small, especially for the intermediate microclines. However, by careful comparison of intensities above and below the zero layer line (especially for reflections (71$\bar{7}$) and (7$\bar{1}\bar{7}$), (82$\bar{7}$) and (8$\bar{2}\bar{7}$)) microcline can be distinguished from a monoclinic potash phase.

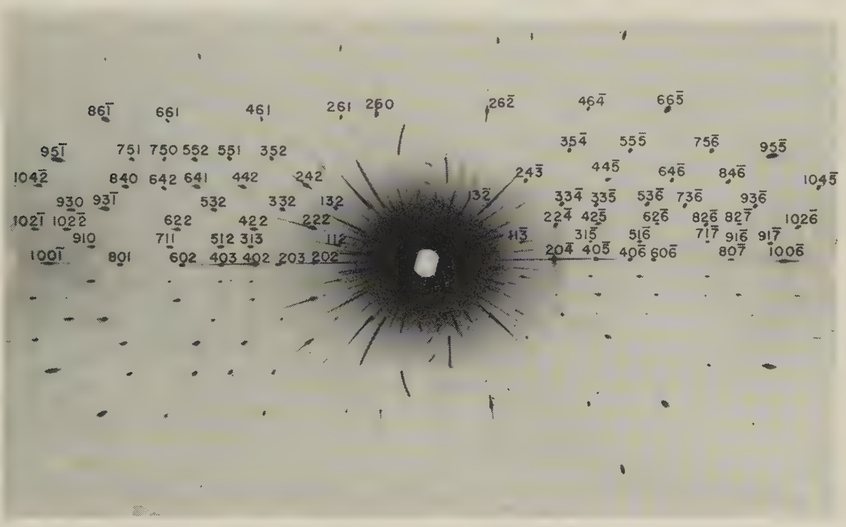

FIG. 3. Specimen *F*, heated 17 minutes at 700° C. to homogenize the soda and potash phases; *b*-axis oscillation photograph with the *x*-ray beam parallel to (001) in the center of a 15° oscillation. The reflections in the upper half of the photograph have been indexed, and for clarity these reflections have been replaced by small solid circles. The intensities of the reflections may be obtained from the lower half of the photograph. The composition of this specimen is $Or_{78.8}Ab_{18.9}An_{2.3}$ (Spencer, 1937).

The reflections from alkali feldspars are often diffuse and are sometimes accompanied by diffuse streaks which join the sharp spots. The diffuse streaks are caused by material whose structure is either strained or transitional between the structures which give the sharp reflections. Diffuse spots are caused by material which either is disordered or consists of very small blocks. These effects may be seen in Fig. 3 of the accompanying paper (MacKenzie and Smith).

As shown in the previous paper, knowledge of the angles $\alpha^*$ and $\gamma^*$ enables one to distinguish high-temperature from low-temperature soda-rich phases and also to distinguish a maximum from an intermediate microcline. The following section is devoted to a method for measuring the angles $\alpha^*$ and $\gamma^*$ from the standard *b*-axis oscillation photographs.

Bowen and Tuttle (1950) showed that the composition of a homogeneous high-temperature alkali feldspar can be determined from the spacing of the $\bar{2}01$ reflection in a powder diffraction pattern. A simple method, based on the same principle, for determining the bulk composition of a single alkali feldspar crystal from a standard *b*-axis oscillation photograph will be described at a later date.

## DETERMINATION OF $\alpha^*$ AND $\gamma^*$ FOR TWINNED TRICLINIC PHASES

Figure 4 shows the angular relations for albite and pericline twinning. In albite twinning the twin axis is normal to (010), i.e., the $b^*$-axis; in pericline twinning the twin axis is $b$ and the $b^*$-axes do not coincide. In either case the reflections occur in pairs such that the twinned $\underline{\bar{h}k\bar{l}})$‡ reflection is adjacent to the untwinned ($hkl$) reflection.

Using the formula which relates film coordinates $\zeta$ and $\xi$, with the reciprocal lattice constants (Buerger, 1942),

$$\zeta^2 + \xi^2 = \frac{\lambda^2}{d^2_{hkl}} = h^2a^{*2} + k^2b^{*2} + l^2c^{*2} + 2klb^*c^* \cos\alpha^*$$
$$+ 2lhc^*a^* \cos\beta^*$$
$$+ 2hka^*b^* \cos\gamma^*$$

where

$$a^* = \frac{\lambda}{d_{100}}, \qquad b^* = \frac{\lambda}{d_{010}}, \quad \text{and} \quad c^* = \frac{\lambda}{d_{001}}$$

the following equation is obtained

$$\zeta^2_{hkl} + \xi^2_{hkl} - \zeta^2_{\bar{h}k\bar{l}} - \xi^2_{\bar{h}k\bar{l}} = 4kb^*[lc \cos\alpha^* + ha^* \cos\gamma^*]$$

For albite twinning $\xi_{hkl} = \xi_{\underline{\bar{h}k\bar{l}}}$ and for pericline twinning $\zeta_{hkl} = \zeta_{\underline{\bar{h}k\bar{l}}}$. Therefore

$$4kb^*[lc^* \cos\alpha^* + ha^* \cos\gamma^*] = \zeta^2_{hkl} - \zeta^2_{\underline{\bar{h}k\bar{l}}} \text{ (albite twinning)}$$
$$= \xi^2_{hkl} - \xi^2_{\underline{\bar{h}k\bar{l}}} \text{ (pericline twinning).}$$

---

‡ Indices of faces in the twinned position are underlined.

ALBITE TWINNING

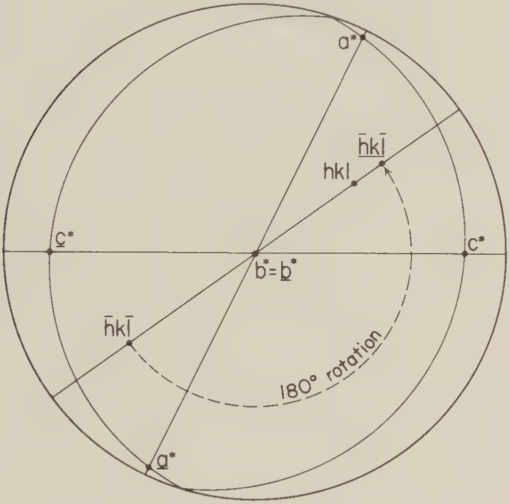

PERICLINE TWINNING

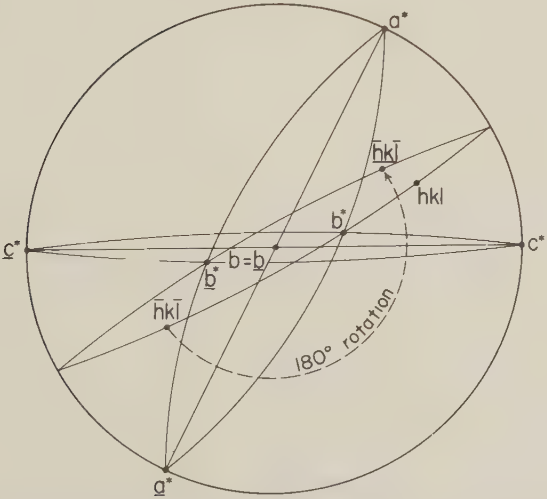

FIG. 4. The angular relations for albite and pericline twinning shown on stereographic projections. The angles $\alpha^*$ and $\gamma^*$ have been exaggerated.

By determining the values of

$$(\zeta^2_{hkl} - \zeta^2_{\underline{\bar{h}k\bar{l}}}) \quad \text{or} \quad (\xi^2_{hkl} - \xi^2_{\underline{\bar{h}k\bar{l}}})$$

for several sets of the paired reflections the values of $c^*$ cos $\alpha^*$ and $a^*$ cos $\gamma^*$ may be determined and hence $\alpha^*$ and $\gamma^*$ may be found.

The determination of $\zeta$ and $\xi$ from a Bernal chart is not sufficiently accurate for the present purpose, and the best method is to measure the displacement between the paired reflections using a viewing screen equipped with a vernier scale.

The equation for the albite twinning may be rewritten as

$$\begin{aligned} lc^* \cos\alpha^* + ha^* \cos\gamma^* &= \frac{1}{4kb^*}(\zeta_{hkl} + \zeta_{\underline{\bar{h}k\bar{l}}})(\zeta_{hkl} - \zeta_{\underline{\bar{h}k\bar{l}}}) \\ &= \frac{1}{2}(\zeta_{hkl} - \zeta_{\underline{\bar{h}k\bar{l}}})\text{§} \quad \text{for} \quad \zeta_{hkl} + \zeta_{\underline{\bar{h}k\bar{l}}} = 2kb^*. \end{aligned}$$

If a layer line $\zeta$ in a cylindrical camera is displaced $y$ mm. from the zero layer and

$$A = \frac{1}{2}\left(\frac{d\zeta}{dy}\right) \quad \text{at} \quad \zeta = \frac{1}{2}(\zeta_{hkl} + \zeta_{\underline{\bar{h}k\bar{l}}})$$

then if $\Delta y_{hkl}$ is the separation of $(hkl)$ and $(\underline{\bar{h}k\bar{l}})$ measured *perpendicular* to the layer lines,

$$lc^* \cos\alpha^* + ha^* \cos\gamma^* \simeq A\Delta y_{hkl}\| \quad \text{for} \quad \Delta y \ \text{small.}$$

The value of $A$ may be calculated from the equation

$$y = r\zeta/\sqrt{1 - \zeta^2}$$

which expresses the relation between $y$ and $\zeta$ for a cylindrical camera of radius $r$ (Buerger, 1942, p. 141).

The equation for pericline twinning may be rewritten as

$$lc^* \cos\alpha^* + ha^* \cos\gamma^* = \frac{1}{4kb^*}(\xi_{hkl} + \xi_{\underline{\bar{h}k\bar{l}}})(\xi_{hkl} - \xi_{\underline{\bar{h}k\bar{l}}}).$$

If $\Delta x$ is the displacement between the positions of $(hkl)$ and $(\underline{\bar{h}k\bar{l}})$ and

$$\frac{1}{B} = \frac{1}{4kb^*}(\xi_{hkl} + \xi_{\underline{\bar{h}k\bar{l}}})\left(\frac{dx}{d\xi}\right) \quad \text{at} \quad \xi = \frac{1}{2}(\xi_{hkl} + \xi_{\underline{\bar{h}k\bar{l}}}) \quad \text{and} \quad \zeta = \zeta_{hkl}$$

then

$$lc^* \cos\alpha^* + ha^* \cos\gamma^* \simeq \frac{1}{B}\cdot \Delta x_{hkl} \ \text{for} \ \Delta x \ \text{small.}$$

---

[§] It may be shown that this equation is valid for $k=0$ even though the derivation is not valid.

[||] All approximation signs imply a possible error of about 1% which may be neglected in view of the required accuracy of the method.

$(dx/d\xi)$ may be calculated from the equation

$$x = \frac{2\pi r}{360^\circ} \cos^{-1}\left(\frac{2 - \zeta^2 - \xi^2}{2\sqrt{1 - \zeta^2}}\right)$$

(Buerger, 1942, p. 141).

For both albite and pericline twinning, values of $lc^* \cos \alpha^* + ha^* \cos \gamma^*$ may be obtained. In order to determine $c^* \cos \alpha^*$ and $a^* \cos \gamma^*$ the measured values of $lc^* \cos \alpha^* + ha^* \cos \gamma^*$ are divided by $h$ and plotted against $l/h$. The values should fall on a straight line whose gradient is $c^* \cos \alpha^*$ and whose intercept at $l/h = 0$ is $a^* \cos \gamma^*$.

Tables 1 and 2 and Fig. 5 contain data from which the values of $A$ and $B$ may be determined. As $b^* \simeq 0.120$ throughout the alkali feldspar series the values of $A$ are approximately the same for all the alkali feldspars. The values of $A$ in Table 1 have been calculated for $b^* = 0.120$ and for cameras of radius 3 and $9/\pi$ cm. Figure 6 contains graphs of $B$ as a function of $(\xi_{hkl} + \xi_{\underline{\bar{h}k}\bar{l}})$ for the layer lines 3, 4, 5, and 6. The value 0.120 for $b^*$ has again been used. Curves for the layer lines 1 and 2 are not given because the accuracy of measurement of these layer lines is insufficient.

TABLE 1. VALUES OF $A$

| Layer line | $\zeta$ | $A$ for 3 cm. camera | $A$ for $9/\pi$ cm. camera |
|---|---|---|---|
| 0 | 0.00 | 0.01667 | 0.01745 |
| 1 | 0.12 | 0.01650 | 0.01727 |
| 2 | 0.24 | 0.01525 | 0.01596 |
| 3 | 0.36 | 0.01354 | 0.01417 |
| 4 | 0.46 | 0.01125 | 0.01178 |
| 5 | 0.60 | 0.00853 | 0.00893 |
| 6 | 0.72 | 0.00587 | 0.00583 |

The procedure for albite twinning is as follows:

(1) Measure $\Delta y$ (in mm.) perpendicular to the layer lines for the sets of $(hkl)$ and $(\underline{\bar{h}k\bar{l}})$ reflections. Take the average of the two values of $\Delta y$ obtained for the positive and negative layer lines. The reflections may be indexed by comparison with Fig. 3.

(2) Multiply $\Delta y$ by $A$ and divide by the appropriate value of $h$. $A$ may be found from Table 1. If a soda phase is being measured, values of $A/h$ may be found in Table 3.

(3) Plot the values of $A\Delta y/h$ against $l/h$. Measure the gradient and the intercept at $l/h = 0$. Cos $\alpha^*$ = gradient$/c^*$ and cos $\gamma^*$ = intercept$/a^*$.

A set of values of $\Delta y$ for specimen $O$ is given in Table 3 and has been plotted in Fig. 6. The value of $A\Delta y/h$ may be either positive or

TABLE 2. DATA FOR THE CONSTRUCTION OF FIGURE 5

| $\xi(hkl)+\xi(\bar{h}\bar{k}\bar{l})$ | Values of *B* | | | |
|---|---|---|---|---|
| | 6th layer | 5th layer | 4th layer | 3rd layer |
| 0.25 | | | | 215.5 |
| 0.35 | | | | 139.1 |
| 0.45 | | | 164.5 | 104.3 |
| 0.55 | | | 126.1 | 84.7 |
| 0.65 | | 159.2 | 103.6 | 71.5 |
| 0.75 | 244.6 | 129.0 | | |
| 0.85 | 179.4 | 110.0 | 77.4 | 54.5 |
| 0.95 | 146.7 | 96.3 | 69.2 | 49.0 |
| 1.05 | 125.8 | 86.1 | 62.6 | 44.7 |
| 1.15 | | 78.2 | 57.3 | |
| 1.25 | 100.6 | 72.0 | 53.1 | 38.0 |
| 1.65 | 76.4 | 56.2 | 41.9 | 30.1 |
| 2.05 | 65.3 | 48.4 | 36.1 | 25.8 |
| 2.45 | 62.3 | 45.2 | 33.2 | 23.6 |
| 2.85 | 67.8 | 46.4 | 33.2 | 23.2 |
| 3.05 | 78.7 | | | |
| 3.25 | 115.2 | 57.9 | 37.9 | 25.4 |
| 3.35 | | 66.1 | | |
| 3.45 | | 82.9 | 45.3 | 28.8 |
| 3.55 | | | 53.6 | |
| 3.65 | | | 74.2 | 35.6 |
| 3.75 | | | | 50.2 |

negative, for no attempt has been made to determine the sign. It is obvious in this case, that to obtain a linear relation the values of $A\Delta y/h$ for $l/h$ negative must have an opposite sign from those with $l/h$ positive. In triclinic crystals the interaxial angles may be taken arbitrarily as greater or less than 90°. For albite it is customary to take $\alpha^*$ less than 90° and for microcline it is customary to take $\alpha^*$ greater than 90°, which relations may be obtained by taking $A\Delta y/h$ negative for negative values of $l/h$. The values $a^*=0.211$ and $c^*=0.242$ may be used for the soda phase of an alkali feldspar, since low-albite (composition $AB_{100}$) has values of 0.2109 and 0.2413, high-albite ($Ab_{100}$) has 0.2109 and 0.2424 and a high-temperature feldspar of composition $Or_{10}Ab_{90}$ has 0.2100 and 0.2418, which values do not deviate by more than 1% from the chosen values. The values $a^*=0.200$ and $c^*=0.238$ may be used for microcline. For specimen *O*, $\alpha^*=86°\ 43'$, $\gamma^*=90°\ 15'$ from the gradient and intercept of Fig. 7.

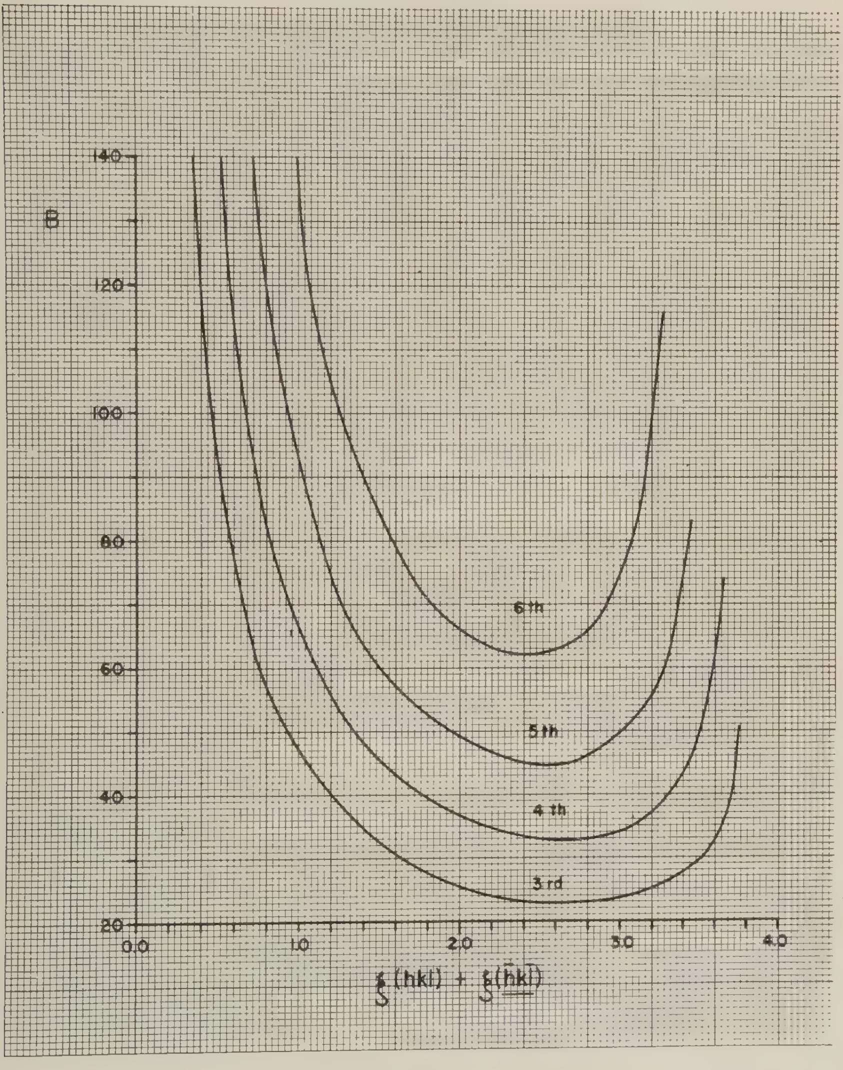

FIG. 5. $B$ as a function of $(\xi_{hkl}+\xi_{\bar{h}\bar{k}\bar{l}})$ for the 3rd, 4th, 5th and 6th layer lines with $b^*=0.120$. The values have been calculated for a cylindrical camera of radius 3 cm. To obtain values of $B$ for a camera of radius $9/\pi$ cm. multiply the value of $B$ obtained from the diagram by $3/\pi$. The data for construction of the diagram are set down in Table 2.

The procedure for pericline twinning is as follows:

(1) Measure $\Delta x$ in mm. Take the average of the two values of $\Delta x$ obtained for the positive and negative layer lines. The reflections may be indexed by comparison with Fig. 3.

TABLE 3. ALBITE TWINNING OF SPECIMEN *O*

| *hkl* | *l/h* | $\Delta y$ (mm.) | $A\Delta y/h$ | $A/h$ 3 cm. camera | $A/h$ $9/\pi$ cm. camera |
|---|---|---|---|---|---|
| $66\bar{5}$* | −0.833 | 14.3 | 0.01327 | .000928 | .000972 |
| $46\bar{4}$ | −1.0 | 10.9 | 0.01517 | .001392 | .001457 |
| $26\bar{2}$* | −1.0 | 5.25 | 0.01462 | .002785 | .002915 |
| $55\bar{5}$ | −1.0 | 8.95 | 0.01527 | .001706 | .001786 |
| $35\bar{4}$ | −1.333 | 7.0 | 0.01990 | .002843 | .002977 |
| $44\bar{5}$* | −1.25 | 6.65 | 0.01870 | .002812 | .002945 |
| $24\bar{3}$ | −1.5 | 3.9 | 0.02194 | .005625 | .005890 |
| 242* | 1.0 | 2.25 | 0.01266 | .005625 | .005890 |
| 442* | 0.5 | 2.10 | 0.00590 | .002812 | .002945 |
| $33\bar{5}$ | −1.667 | 5.15 | 0.02324 | .004513 | .004723 |
| $13\bar{2}$ | −2.0 | 2.00 | 0.02708 | .01354 | .01417 |
| 132* | 2.0 | 1.95 | 0.02640 | .01354 | .01417 |
| 332* | 0.667 | 1.80 | 0.00812 | .004513 | .004723 |
| $42\bar{5}$ | −1.25 | 4.8 | 0.01830 | .003812 | .003990 |
| $22\bar{4}$* | −2.0 | 3.7 | 0.02821 | .007625 | .007980 |
| 222* | 1.0 | 1.55 | 0.01182 | .007625 | .007980 |
| $40\bar{6}$ | −1.5 | 5.25 | 0.02188 | .004167 | .004362 |
| $20\bar{4}$* | −2.0 | 3.6 | 0.03000 | .008333 | .008725 |
| 202 | 1.0 | 1.55 | 0.01292 | .008333 | .008725 |
| 203* | 1.5 | 2.4 | 0.02000 | .008333 | .008725 |
| 402 | 0.5 | 1.6 | 0.00667 | .004167 | .004362 |

Measurements were made on a camera of radius 3 cm.
* Most suitable reflections.

TABLE 4. PERICLINE TWINNING OF SPECIMEN *O*

| *hkl* | *l/h* | $\xi hkl+\xi\bar{h}\bar{k}\bar{l}$ | $\Delta x$ (mm). | $\Delta x/Bh$ | $Bh$ 3 cm. camera | $Bh$ $9/\pi$ cm. camera |
|---|---|---|---|---|---|---|
| 461 | 0.25 | 1.96 | — |  | 271 | 249 |
| 262 | −1.0 | 0.95 | 4.1 | 0.01385 | 296 | 283 |
| $46\bar{4}$ | −1.0 | 1.91 | 3.9 | 0.01444 | 270 | 258 |
| $66\bar{5}$ | −0.833 | 2.60 | — |  | 380 | 363 |
| 352 | 0.667 | 1.93 | — |  | 154 | 147 |
| $35\bar{4}$ | −1.333 | 1.91 | 2.97 | 0.01967 | 151 | 144 |
| $55\bar{5}$ | −1.0 | 2.395 | 3.27 | 0.01441 | 227 | 217 |
| 641 | 0.167 | 2.79 | — |  | 198 | 189 |
| $24\bar{3}$ | −1.5 | 1.305 | 2.27 | 0.02204 | 103 | 98 |
| 242 | 1.0 | 1.55 | 1.07 | 0.01216 | 88 | 84 |
| 442 | 0.5 | 2.31 | 0.87 | 0.00640 | 136 | 130 |
| 132 | −2.0 | 0.86 | 1.55 | 0.02844 | 54.5 | 52 |
| $33\bar{5}$ | −1.667 | 2.16 | 1.8 | 0.02432 | 74 | 70.7 |
| 132 | 2.0 | 1.22 | — |  | 38.7 | 37 |
| 332 | 0.667 | 1.93 | 0.65 | 0.00788 | 82.5 | 78.8 |

Measurements were made on a 3 cm. camera. The reflections for which $\Delta x$ is not recorded will be found useful if a high-temperature feldspar is measured.

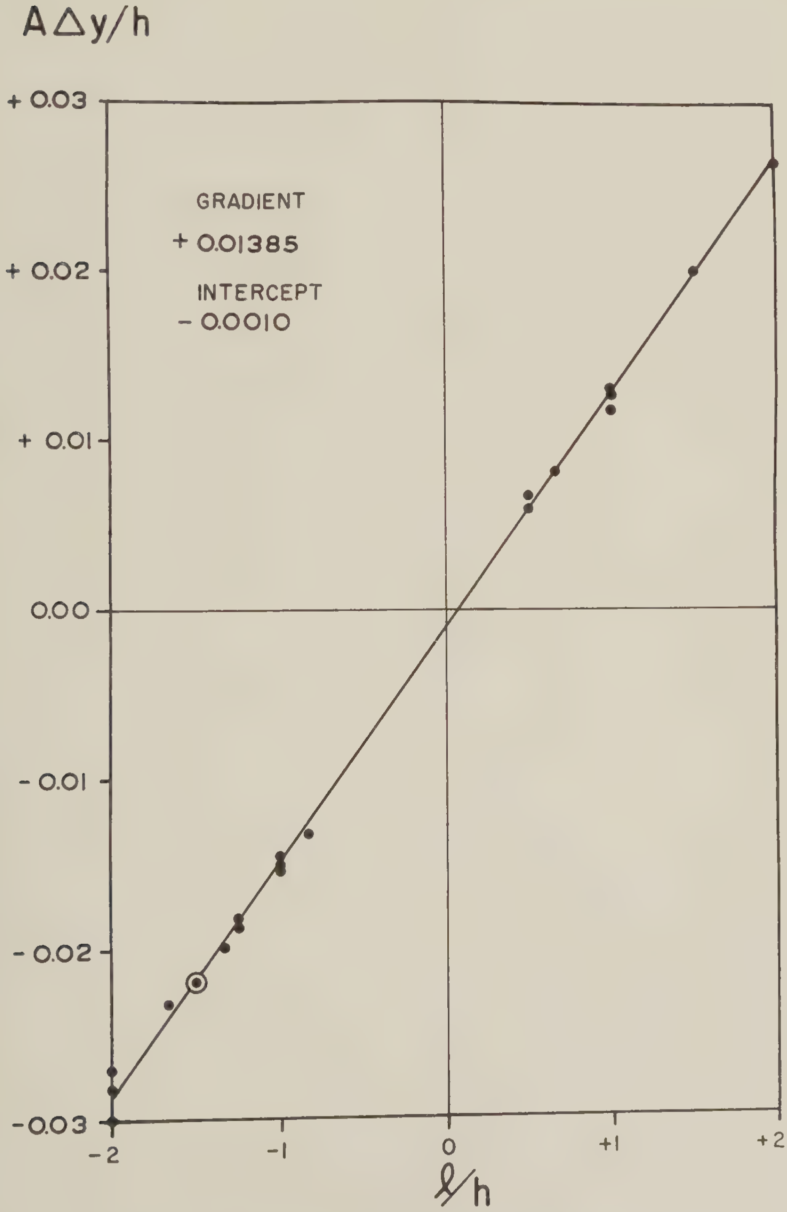

FIG. 6. A graph of $A\Delta y/h$ versus $l/h$ for values of $\Delta y$ taken from the albite-twinned soda phase of specimen *O*. The data are set out in Table 3.

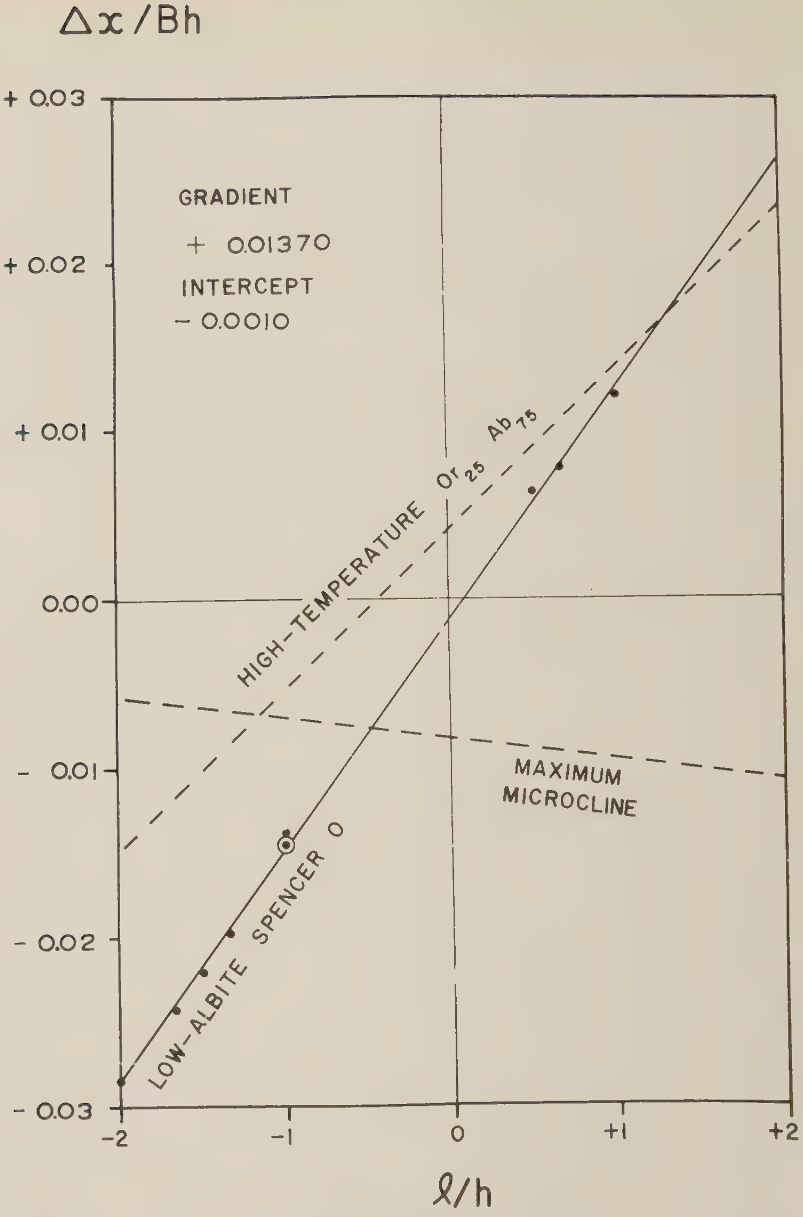

FIG. 7. A graph of $\Delta x/Bh$ versus $l/h$ for values of $\Delta x$ taken from the pericline-twinned soda phase of specimen $O$. The data are set out in Table 4. All low-albite phases will give values close to those for specimen $O$. For comparison the lines relating $(c^* \cos \alpha^* + a^* \cos \gamma^*)$ with $l/h$ for a maximum microcline and for a high-temperature alkali feldspar of composition near $Or_{25}Ab_{75}$ are also shown. The lattice angles of the microcline have been taken as $\alpha^* = 90° \ 18'$, $\gamma^* = 92° \ 22'$, and for the high-temperature alkali feldspar the values $\alpha^* = 87° \ 44'$, $\gamma^* = 88° \ 52'$ have been used.

Steps 2 and 3 may be omitted if a soda phase is being measured, since values of $Bh$ for the most suitable reflections are given in Table 4. If a potash phase is being measured the procedure is:

(2) Measure $\xi_{hkl}$ and $\xi_{\underline{\bar{h}k\bar{l}}}$ using a Bernal chart.

(3) From the appropriate curve in Fig. 5 determine the value of B for $\xi=(\xi_{hkl}+\xi_{\underline{\bar{h}k\bar{l}}})$.

(4) Divide $\Delta x$ by $Bh$.

(5) Plot the values of $\Delta x/Bh$ against $l/h$. Further steps are identical with those for the albite twinning.

A set of values of $\Delta x$ for specimen $O$ is given in Table 4 and plotted in Fig. 7. They give $\alpha^*=86° 45'$ and $\gamma^*=90° 15'$.

The accuracy obtainable from the method depends, of course, on the quality of the $x$-ray reflections and the number of measurements. In general, it has been found that an accuracy between 3′ and 10′ of arc is obtainable from most photographs. The measurement and calculation of $\alpha^*$ and $\gamma^*$ for one pair of twinned individuals takes about 30 minutes.

We are indebted to Drs. Spencer, Bowen, and Tuttle for the opportunity to use the three specimens for which $x$-ray photographs are given in this paper. Drs. J. D. H. and G. Donnay critically reviewed the manuscript and we are grateful to them for their suggestions.

## REFERENCES

BOWEN, N. L., & TUTTLE, O. F. (1950): The system $NaAlSi_3O_8$—$KAlSi_3O_8$—$H_2O$: *Jour. Geol.*, **58**, 489–511.

BUERGER, M. J. (1942): X-ray Crystallography, John Wiley & Sons, Inc., New York.

CHAO, S. H., & TAYLOR, W. H. (1940): The lamellar structure of potash-soda felspars: *Proc. Roy. Soc.*, Ser. A, **174**, 57–72.

HENRY, N. F. M., LIPSON, H., & WOOSTER, W. A. (1951): The Interpretation of X-ray Diffraction Photographs, Macmillan & Co., London.

LAVES, F. (1952): Phase relations of the alkali feldspars: *Jour. Geol.*, **60**, 436–450, 549–574.

SPENCER, E. (1937): The potash-soda-felspars. I. Thermal stability: *Mineral. Mag.*, **24**, 453–494.

*Manuscript received July 22, 1954*

# KUTNAHORITE: A MANGANESE DOLOMITE, $CaMn(CO_3)_2$*

CLIFFORD FRONDEL AND L. H. BAUER,† *Department of Mineralogy, Harvard University, Cambridge, Mass., and New Jersey Zinc Company, Franklin, N. J.*

## KUTNAHORITE FROM CZECHOSLOVAKIA

The name kutnahorite was proposed by Bukowsky (1901) for a supposed manganese member of the dolomite group, ideally $CaMn(CO_3)_2$. One of his analyses of pale rose cleavable aggregates from Kutnahora, Czechoslovakia, corresponded approximately to $Ca(Mn,Mg,Fe)(CO_3)_2$, with $Mn:Mg:Fe \sim 6:2:1$. Rigorous proof has been lacking that his mineral belonged in the dolomite structure-type, $AB(CO_3)_2$, and was not merely a calcite-type solid solution, with the formula $(Ca,Mn,Mg,Fe)(CO_3)_2$, that fortuitously approached the dolomite ratios.

Through the kind effort of Dr. Jan Kutina of the Department of Mineralogy of the Charles University, Prague, a type specimen of kutnahorite was obtained from the museum of the school in Kutná Hora where Professor Bukowsky taught. The label glued on the specimen reads (translation by Dr. Kutina): "*Kutnohorite (ferroan mangandolomite with cleavage). Kutná Hora, from a stony fencing of a field above the Vašata's quarries. Ant. Bukovský, 1900.*" An analysis also is given, which is stated in recast form in Table 1, column 5. A differential thermal analysis and $x$-ray study of this specimen has now shown that the mineral is in fact of the dolomite-type. In addition, Dr. Kutina sent us a specimen of a carbonate from Chvaletice, Czechoslovakia, described by Žák (1949), that has a composition very close to that of the original kutnahorite. The analysis of this material is repeated in Table 1, column 6. Žák states that the mineral gives an $x$-ray pattern similar to that of ankerite (in the old sense of ferroan dolomite), and we have confirmed this identification as a member of the dolomite group by both $x$-ray and differential thermal analysis. The existence of kutnahorite[1] as a valid member of the dolomite group thus is established.

---

* Contribution from the Department of Mineralogy and Petrography, Harvard University, No. 353.

† Deceased, January, 1954.

[1] The name mangandolomite has been employed by some authors for the theoretical "molecule" $CaMn(CO_3)_2$ in the dolomite group. It is objectionable because it has been used with other meanings: by Eisenhuth (1901) for a mineral that may be ideally $MgMn(CO_3)_2$, by Doelter (1912) for ordinary dolomite containing small amounts of Mn in solid solution, and by Naumann (cited by Hey (1950)) for rhodochrosite with $Mn \sim Ca$. The name greinerite of Boldyrev (1928) also has been applied to manganoan varieties of dolomite.

Table 1. Analyses of Kutnahorite and of Minerals Possibly Identical Therewith

|  | 1 | 2 | 3 | 4 | 5 | 6 |
|---|---|---|---|---|---|---|
| CaO | 27.44 | 28.24 | 26.71 | 28.83 | 24.66 | 24.43 |
| MgO | 2.21 | 2.72 |  | 6.88 | 5.18 | 5.16 |
| MnO | 28.31 | 26.87 | 24.61 | 11.43 | 23.76 | 23.39 |
| FeO | 0.50 | 0.47 | 6.95 | 8.58 | 4.27 | 4.79 |
| $CO_2$ | 41.80 | 42.09 | 40.58 | 43.28 | 42.62 | 42.17 |
| Rem. |  | 0.08 | 1.15 |  |  | 0.17 |
| Total | 100.26 | 100.47 | 100.00 | 100.00 | 100.49 | 100.11 |
|  |  |  | *Molecular Percentages* |  |  |  |
| $CaCO_3$ | 51.50 | 52.65 | 51.77 | 54.10 | 45.69 | 45.38 |
| $MgCO_3$ | 5.77 | 7.05 |  | 17.36 | 13.34 | 13.33 |
| $MnCO_3$ | 42.00 | 39.61 | 37.71 | 16.39 | 34.79 | 34.35 |
| $FeCO_3$ | 0.73 | 0.69 | 10.52 | 12.15 | 6.18 | 6.94 |
| Total | 100.00 | 100.00 | 100.00 | 100.00 | 100.00 | 100.00 |
| S.G. | 3.12 | 3.052 |  | 3.01 | 3.06 | 3.09 |

1. Kutnahorite, Franklin, N. J. C. M. Smink *analyst*, N. J. Zinc Company, 1953 Harvard specimen 85670.
2. Kutnahorite? Franklin, N. J. The "manganesian dolomite" of Roepper (1870). Rem. is insol.
3. Kutnahorite? Vester Silfberg, Dalecarlia, Sweden. The "manganocalcite" of Weibull (1885). Average of two analyses. Rem. is insol.
4. Kutnahorite, Kutnahora, Czechoslovakia. The original material of Bukowsky (1901).
5. Kutnahorite, Kutnahora, Czechoslovakia. The original material of Bukowsky (1901).
6. Kutnahorite, Chvaletice, Czechoslovakia. Called ankerite by Źák (1949) and compared by him to the kutnahorite of Bukowsky (1901). Rem. is insol. 0.14, $H_2O$ 0.03.

## Kutnahorite from Franklin, New Jersey

The writers surveyed a small collection of pink, manganese-containing carbonates from Franklin and Sterling Hill, New Jersey, and found four specimens that gave an $x$-ray powder pattern resembling that of dolomite. One of these specimens, No. 85670, was found on chemical analysis and differential thermal analysis to be a member of the dolomite group with almost the ideal composition $CaMn(CO_3)_2$. Small amounts of Mg and Fe are present in substitution for the Mn (analysis 1, Table 1). The grouping of the Mg and Fe with Mn rather than with Ca, here required to make the analysis conform to the dolomite type of formula, is consistent with the closer approach of Mg and Fe in ionic size to Mn than to Ca. There is also a small excess of Ca over the requirement of the *A* position of the formula. This presumably is in substitution for Mn in the *B* position, analogous to calcian dolomite, $Ca(Mg,Ca)(CO_3)_2$, and the complete formula may be written $Ca(Mn,Mg,Ca,Fe)(CO_3)_2$.

The differential thermal analysis curve of the material is shown in Fig. 1. It closely resembles the *DTA* curve of ankerite, and to a less extent the curve of dolomite proper (which lacks oxidizable cations).

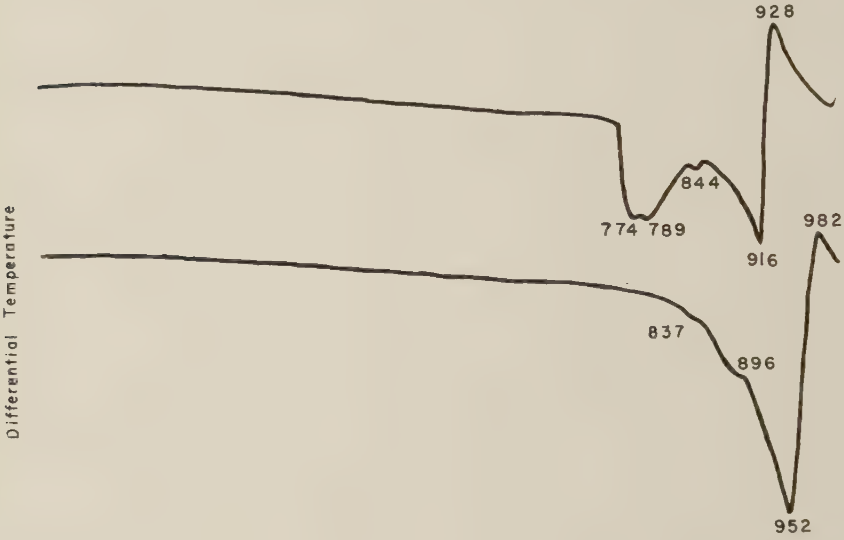

Fig. 1. Top curve, kutnahorite from Franklin, N. J. (no. 85670), analysis 1, Table 1. Bottom curve, rhodochrosite from Franklin, N. J., analysis 9, Table 2.

It differs completely from the *DTA* curves of calcite and rhodochrosite, which show a single endothermic break marking dissociation into oxide and $CO_2$. In dolomite, two endothermic breaks are obtained corresponding to the stepwise dissociation of the two structurally non-equivalent cations. In ankerite and kutnahorite the curves are further complicated by oxidation of the FeO or MnO and reaction with the CaO. Thermal curves for the rhodochrosite-calcite series have been described by Kulp, Wright and Holmes (1949), for ankerite by Kulp, Kent and Kerr (1951) and Beck (1950), for dolomite by Faust (1944, 1949, 1953), Bradley et al. (1953), Graf (1952), Haul and Heystek (1952) and others. The indices of refraction of kutnahorite, *n*O 1.727, *n*E 1.535, agree exactly with the values calculated from the indices of refraction of the $CaCO_3$, $MgCO_3$ and $FeCO_3$ end-members taken in the ratio of the analysis. The specific gravity, 3.12, is slightly lower than the value 3.15 similarly calculated from the end-members. The indexed $x$-ray powder spacing data are given in Table 2. The unit cell dimensions obtained are $a_0$ 4.85 Å, $c_0$ 16.34. The pattern contains several of the lines diagnostic of dolomite-type structures. The kutnahorite from Chvaletice analyzed by Žák (analysis 6, Table 1) has the cell dimensions $a_0$ 4.83 Å, $c_0$ 16.18.

Kutnahorite occurs at Franklin as anhedral masses with curved cleavage surfaces up to three centimeters in size in a small veinlet cutting the normal franklinite ore. It is translucent, with a pale pink color. The vein is bordered by a thin layer of dark pink rhodochrosite; this has $n$O 1.792, corresponding to a content of 85 per cent $MnCO_2$ according to the data of Wayland (1942).

TABLE 2. $X$-RAY POWDER SPACING DATA FOR KUTNAHORITE

Material of analysis 1, Table 1, from Franklin, N. J.
Iron radiation, manganese filter, in Ångstroms.
Relative intensities from spectrometer chart.

| *I* | *d* | *Indices* | | *I* | *d* | *Indices* | |
|---|---|---|---|---|---|---|---|
| 5 | 4.268 | $10\bar{1}1$ | 100 | 3 | 1.540 | 2132 | 211 |
| 20 | 3.753 | $01\bar{1}2$ | 110 | 7 | 1.486 | $21\bar{3}4$ | 310 |
| 100 | 2.935 | $10\bar{1}4$ | 211 | 3 | 1.469 | $02\bar{2}8$ | 224 |
| 5 | 2.730 | 0006 | 222 | 3 | 1.465 | $11\bar{2}9$ | 432 |
| 4 | 2.593 | $01\bar{1}5$ | 221 | 5 | 1.409 | $12\bar{3}5$ | 320 |
| 14 | 2.437 | $11\bar{2}0$ | $10\bar{1}$ | 5 | 1.363 | 000.12 | 444 |
| 19 | 2.225 | $11\bar{2}3$ | 210 | 3 | 1.294 | $20\bar{2}.10$ | 442 |
| 4 | 2.095 | $02\bar{2}1$ | $11\bar{1}$ | 4 | 1.258 | $12\bar{3}8$ | 431 |
| 19 | 2.043 | $10\bar{1}7$ | 322 | 4 | 1.189 | $20\bar{2}.11$ | 533 |
| 9 | 1.876 | $02\bar{2}4$ | 220 | 4 | 1.145 | $21\bar{3}.10$ | 532 |
| 27 | 1.837 | $01\bar{1}8$ | 332 | 4 | 1.141 | | |
| 31 | 1.814 | 0009 | 333 | 5 | 1.126 | $13\bar{4}4$ | $32\bar{1}$ |
| 6 | 1.588 | $21\bar{3}1$ | $20\bar{1}$ | 4 | 1.089 | 000.15 | 555 |
| 4 | 1.566 | $12\bar{3}2$ | 211 | 5 | 1.022 | $20\bar{2}.14$ | 644 |
| | | | | 5 | 0.9763 | $11\bar{2}.15$ | 654 |

The other three specimens examined appeared on optical, $x$-ray and thermal analysis to be mechanical mixtures of kutnahorite with a calcite-type carbonate. It is hoped to give a fuller description of this material at a later time.

A few analyses of minerals that may be identical with kutnahorite have been found in the literature. These analyses are listed in Table 1. Crystallographic or other data that would identify the material as belonging to the dolomite structure-type are lacking, and the assigning of these minerals to kutnahorite rests entirely on the closeness to which the analyses approach the ratio Ca:(Mn, Mg, Fe) = 1:1. The material of Roepper (1870) from Franklin (analysis 2) is very close in composition to the kutnahorite specimen here described. The material of Weibull (1885) from Sweden (analysis 3) appears to be a ferroan variety of kutnahorite. If this mineral actually belongs to the dolomite-type, it is the only member of the dolomite-ankerite-kutnahorite group so far analyzed that does not contain over about 5 mol per cent $MgCO_3$. The kutnahorite of analyses 5 and 6 requires a substitution of Fe for Ca, or a distribution of both Fe and Mn between the *A* and *B* positions, in order to make the analyses conform to the requirements of the dolomite formula-type. Analysis 4 requires the entrance of Ca into the *B* position; this material has not been shown directly to belong in the dolomite group.

Table 3. New Analysis of Calcite and Rhodocrosite from Franklin and Sterling Hill, N. J.

(all analyses in weight percentages)

| | 1 | 2 | 3 | 4 | 5 | 6 | 7 | 8 |
|---|---|---|---|---|---|---|---|---|
| $CaCO_3$ | 98.41 | | 56.44 | 56.57 | | | | 3.71 |
| $MgCO_3$ | | | 6.58 | 2.93 | | | | 1.44 |
| $MnCO_3$ | 0.90 | 33.38 | 36.14 | 40.35 | 81.47 | 82.5 | 83.5 | 94.93 |
| $FeCO_3$ | 0.86 | | 0.93 | | | | | 0.44 |
| $PbCO_3$ | | 0.07 | | 0.22 | | | | |
| Total | 100.17 | | 100.09 | 100.07 | | | | 100.02 |
| S.G. | 2.73 | 3.04 | 3.06 | 3.06 | 3.53 | 3.55 | 3.50 | ~3.6 |
| *n*O | 1.658 | 1.712 | 1.716 | 1.716 | 1.791 | 1.792 | 1.792 | 1.806 |

1. Calcite, orange brown color. Franklin, N. J. L. H. Bauer, *analyst.*
2, 3, 4. Manganoan calcite, Franklin, N. J. L. H. Bauer, *analyst.*
5, 7. Calcian rhodochrosite, Franklin, N. J. L. H. Bauer, *analyst.*
6. Calcian rhodochrosite, Sterling Hill, N. J. L. H. Bauer, *analyst.*
8. Rhodochrosite, Franklin, N. J. C. M. Smink, *analyst.*

Eight new analyses, four complete and four partial, on members of the calcite-rhodochrosite series from Franklin and Sterling Hill are reported in Table 3. The nine analyses of calcite-rhodochrosite that have been reported in the literature from these localities are summarized in Table 4. The material of analyses 3, 4, 5, and 8 of Table 3 and of analysis 8 of Table 4 was verified as of the calcite-type by differential thermal analysis. The curve of the material of analysis 8 of Table 3 is reproduced in Fig. 1.

The analytical data of Tables 3 and 4 are plotted in Fig. 2 in order

TABLE 4. PUBLISHED ANALYSES OF CALCITE AND RHODOCHROSITE FROM FRANKLIN AND STERLING HILL, N. J.

|  | 1 | 2 | 3 | 4 | 5 | 6 | 7 | 8 | 9 |
|---|---|---|---|---|---|---|---|---|---|
| $CaCO_3$ | 85.96 | 79.96 | 85.57 |  | 82.33 | 63.90 | 77.94 | 65.98 | 20.59 |
| $MgCO_3$ | 0.59 | 1.94 | 2.54 |  |  | 11.05 |  | n.d. | 3.80 |
| $MnCO_3$ | 2.98 | 11.09 | 11.55 | 15.40 | 16.57 | 17.43 | 22.35 | 32.34 | 74.99 |
| $FeCO_3$ |  | 0.60 |  |  | 0.50 | 0.30 |  | n.d. | 0.36 |
| $ZnCO_3$ | 2.88 | 0.58 |  |  |  | 0.32 |  | 0.69 | 0.26 |
| Rem. | 7.70 | 5.67 |  |  | 1.20 | 7.00 |  |  |  |
| Total | 100.11 | 99.84 | 99.66 |  | 100.50 | 100.00 | 100.29 | 99.01 | 100.00 |
| S.G. |  |  |  | 2.856 |  |  |  | 3.021 | 3.47 |
| $nO$ |  |  |  | 1.680 |  |  |  | 1.713 |  |
| $nE$ |  |  |  | 1.503 |  |  |  | 1.519 |  |

1. Calcite, black color. Franklin, N. J. Jenkins and Bauer analysis cited by Palache (1935). Rem. is $SiO_2$ 0.50, ZnO 1.86, $Fe_2O_3$ 0.17, $Al_2O_3$ 0.24, $Mn_2O_3$ 4.93, due to inclusions.
2. Manganoan calcite ("spartaite"), Sterling Hill, N. J. Jenszch (1855). Rem. is $CaF_2$ 5.35, $H_2O$ 0.32.
3. Manganoan calcite ("spartaite"), Sterling Hill, N. J. Richter analysis cited by Rammelsberg (1860).
4. Manganoan calcite, Franklin, N. J. Bauer analysis cited by Krieger (1930).
5. Manganoan calcite, Sterling Hill, N. J. Van Dyke analysis cited by Cook (1868). Rem. is $H_2O$ 1.00, insol. 0.20.
6. Manganoan calcite, Franklin, N. J. Levison (1916). Rem. is insol.
7. Manganoan calcite, Sterling Hill, N. J. Shepard and Tyler (1865).
8. Manganoan calcite, Franklin, N. J. Bauer analysis cited by Krieger (1930). Mg and Fe present but not determined.
9. Calcian rhodochrosite, Franklin, N. J. Bright pink color. Browning (1890). Recalculated after deducting $SiO_2$ 0.32 as willemite, $Fe_2O_3$ 0.16, and excess ZnO as zincite.

of increasing weight per cent of $MnCO_3$. The figure also contains new data on the $MnCO_3$ content of 29 specimens of calcite-rhodochrosite from Franklin. These were determined from the indices of refraction using the graph of Wayland (1942), with a supplementary linear graph for the region from 50 per cent $MnCO_3$ to pure $CaCO_3$. The values for the $MnCO_3$ content thus obtained are not very precise because the content of Fe, Zn and, in particular, Mg is not known. Figure 2 indicates that the calcite-rhodochrosite series is incomplete under the particular genetic conditions obtaining at Franklin. At this locality a solid solution series apparently extends from the end-composition $CaCO_3$ up to manganoan calcite containing about 40 weight per cent $MnCO_3$, with a gap then extending up to calcian rhodochrosite containing about 75 weight

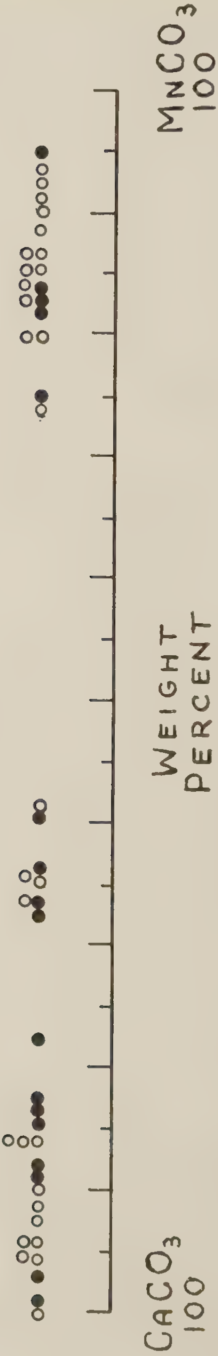

Fig. 2. Graph showing the content in weight per cent of MnCO$_3$ of 46 specimens of the calcite-rhodochrosite series from Franklin, New Jersey. Solid circles are the analyzed samples of Tables 2 and 3. Open circles based on optical determination of specimens in the Harvard collection.

per cent $MnCO_3$, and a continuous series extending from there to the end-composition $MnCO_3$. Vegard (1947) found in material synthesized at room temperature that the gap was larger, extending from 12.5 mol per cent $MnCO_3$ up to 75 mol per cent $MnCO_3$. Under some geologic conditions the series may be complete. A study of synthetic material to determine the temperature dependency of the solid solubility would be highly desirable.

## ORDERED PHASES IN THE CALCITE AND OLIVINE GROUPS

The extent of solid solution in binary disordered solid solutions involving Ca, Mn, Fe or Mg ions and the occurrence of ordered phases in these systems appears to be controlled principally by the relative size of the cations involved. The term ordering is here used to mean the two cations that are structurally equivalent in the disordered phase become structurally non-equivalent in the ordered phase, without implying that the overall crystal structures of the ordered and disordered phases are closely related. With increasing closeness in ionic size, the olivine-type nesosilicates and the NaCl-type oxides of the four cations mentioned in general show: (1) increasing solid solubility in the disordered binary series; (2) decreasing tendency to form ordered phases. The observations are summarized[2] in Table 5.

Further more or less complete examples of the relations described are shown by other minerals. Thus in the idealized $A_3''Al_2(SiO_4)_3$ members of the garnet group complete series apparently exist between Mg-Fe and Mn-Fe, partial series between Mg-Mn and Ca-Mn, and very small series between Ca-Mg and Ca-Fe, in natural material.

The reciprocal relation between extent of solid solution in the binary disordered series and the occurrence of ordered phases is primarily a matter of structural strain. Ordering relieves the strain caused by the random fitting together of ions of different sizes, and the ordering potential should increase as the strain or difference in size increases. The ordered phases listed in Table 5 have crystallized directly from solution, and not in the solid state from a parent solid solution, but this does not alter the general reasoning. The geometry of the ordering is facilitated at or near simple whole number ratios of the ion species involved; the most common ratios observed are 1:1, 1:2 and 1:3. With increasing similarity in ionic size, the ordering potential decreases and the formation of random substitutional solid solutions is favored.

---

[2] Data on the extent of solid solubility in the binary systems cited were obtained from Hall and Insley (1947); Dana's System of Mineralogy (1951); Ford (1917); Kulp, Kent, and Kerr (1951); Greer (1932); Passerini (1930); Natta and Passerini (1929); Petterson (1946); Jay and Andrews (1944, 1946).

TABLE 5. RELATION OF IONIC SIZE TO SOLID SOLUBILITY AND ORDERING IN SOME IONIC COMPOUNDS OF Ca, Fe, Mn AND Mg

(Ionic radii: Ca 1.06, Mn 0.91, Fe 0.83, Mg 0.78 kX)

| Difference in ionic size | Extent of solubility in binary disordered systems | Occurrence of 1:1 ordered phases | Occurrence of other ordered phases |
|---|---|---|---|
| **Large**<br>Ca—Mg (26.5%) | **Very small solubility**<br>$CaCO_3$—$MgCO_3$, small solubility<br>$Ca_2SiO_4$—$Mg_2SiO_4$, no solubility?<br>CaO—MgO, very small solubility | **Common**<br>$CaMg(CO_3)_2$, dolomite<br>$CaMg(SiO_4)$, monticellite | $CaMg_3(CO_3)_4$, huntite<br>$Ca_3Mg(SiO_4)_2$, merwinite |
| **Moderate**<br>Ca—Fe (21.7%) | **Moderate solubility**<br>$CaCO_3$—$FeCO_3$, extensive solubility<br>$Ca_2SiO_4$—$Fe_2SiO_4$, moderate solubility<br>CaO—FeO, moderate solubility | **Less common**<br>$Ca(Fe, Mg)(CO_3)_2$, ankerite<br>$CaFe(SiO_4)$, (synthetic) | **None** |
| **Small**<br>Ca—Mn (14.3%) | **Large or complete solubility**<br>$CaCO_3$—$MnCO_3$, large or complete solubility<br>$Ca_2SiO_4$—$Mn_2SiO_4$, extensive solubility<br>CaO—MnO, extensive solubility | **Rare**<br>$CaMn(CO_3)_2$, kutnahorite<br>$CaMn(SiO_4)$, glaucochroite | **None** |
| Mg—Mn (14.3%) | $MgCO_3$—$MnCO_3$, large solubility<br>$MgSiO_4$—$MnSiO_4$, complete solubility?<br>MgO—MnO, extensive solubility | **None?** | **None** |
| Fe—Mn (8.8%) | $FeCO_3$—$MnCO_3$, complete solubility<br>$FeSiO_4$—$MnSiO_4$, nearly complete solubility?<br>FeO—MnO, large or complete solubility | **None** | **None** |
| **Very Small**<br>Mg—Fe (6.0%) | **Complete solubility**<br>$MgCO_3$—$FeCO_3$, complete solubility<br>$Mg_2SiO_4$—$Fe_2SiO_4$, complete solubility<br>MgO—FeO, complete solubility | **None** | **None** |

One may also expect that in two isostructural binary series separated by a gap, $(A, B)X$—$(B, A)X$, that the smaller ion $B$ will substitute to a larger extent for $A$ in $(A, B)X$ than the larger ion $A$ will substitute for $B$ in $(B, A)X$, since the strain introduced by the substitution should be less. This follows since the introduction of a large ion in place of a smaller one at constant $A$—$X$ distance involves work against a high-power exponential repulsive force arising in the overlap of the electron clouds about the nuclei, while the introduction of a smaller ion involves work against the weaker, inverse square attractive force between oppositely charged ions. The series $CaCO_3$—$MgCO_3$ appears to illustrate the rule, with Mg present in (Ca, Mg)$CO_3$ up to about 29 mol per cent and Ca present in (Mg, Ca)$CO_3$ only up to about 7 mol per cent, according to the data of Ford (1917) and Chave (1952). The solubility of Mg in (Ca, Mg)O also is greater than that of Ca in (Mg, Ca)O according to Petterson (1946). The partial series between $MgCO_3$—$MnCO_3$ and $CaCO_3$—$CdCO_3$ also show the expected relation, as do the partial series between CaO—FeO, MnO—CaO, MnO—MgO, MnO—CdO and CaO—SrO from the data of Passerini (1930), Natta and Passerini (1929), Petterson (1946) and Primak et al. (1948). Under other conditions the series CaO—MnO and MgO—MnO may be complete (Jay and Andrews (1944, 1946) and Petterson (1946)). In the partial binary series between ZnO and NiO, MgO, MnO and CdO the greater solubility is of the larger ion substituting for the smaller, as shown by Rigamonti (1946), but in this case the structure-type and the bond-type is different at opposite ends of the series.

One might also expect that the solvus curves in continuous high-temperature random solid solution series would tend to be asymmetrically displaced toward the end-component with the smaller ionic radius.

Ordered phases with ratios other than 1:1 are found in the calcite and olivine groups only with the ion pair Ca-Mg, in which the difference in ionic size is a maximum. The cation ratios in these instances appears to be related to the asymmetry in the central gap between the two partial disordered solid solution series. Thus $CaMg_3(CO_3)_4$, huntite, apparently is more stable than $Ca_3Mg(CO_3)_4$ because the ordering potential is greater towards the Mg end of the binary series, as indicated by the greater extent of solid solubility towards the Ca end of the series. The compound $Ca_3Mg(CO_3)_4$ was described as a mineral, conite, by Retzius in 1795, but his material was shown to be a mixture. A highly calcian dolomite Ca(Mg, Ca)$(CO_3)_2$ in which the actual ratios are close to the the formula $Ca_3Mg(CO_3)_4$ was analyzed by Strobentz (1926), indicating that the magnesian calcite and calcian dolomite series virtually overlap in this region of composition. The supposed mineral $CaMg_2(CO_3)_3$, leesbergite, of Blum (1907) also was shown to be a mixture.

An ordered compound of the dolomite-type between Mg and Mn appears to be as likely as that between Ca and Mn, since the difference in ionic size in the two cases is the same. A possible example may be a mineral from Greiner, Switzerland, called mangandolomite by Eisenhuth (1901). If his analysis, cited below, is accepted as of a dolomite-type compound, and no evidence was given to justify this, the interpretation suggested by the relative sizes of the ions involved is (Mg, Fe, Mn)(Mn, Ca)$(CO_3)_2$. Mn is then distributed between the *A* and *B* positions to fit the requirements of the formula, somewhat analogous to the dolomite solid solutions Ca(Mg, Ca)$(CO_3)_2$ and (Ca, Mg)Mg$(CO_3)_2$ described by Foote and Bradley (1914) and Ford (1917). Ankerite with Fe in both the *A* and *B* positions was analyzed by Strobentz (1926).

| *Eisenhuth* (1901) | |
|---|---|
| CaO | 10.48 |
| MnO | 23.41 |
| FeO | 6.59 |
| MgO | 14.58 |
| $CO_2$ | 45.59 |
| Insol. | 0.16 |
| | 100.81 |

| *Molecular Percentages* | | |
|---|---|---|
| $CaCO_3$ | 19.25 | 53.28 |
| $MnCO_3$ | 34.03 | |
| $FeCO_3$ | 9.45 | 46.72 |
| $MgCO_3$ | 37.27 | |
| | 100.00 | |

An ordered compound of the formula $MgFe(CO_3)_2$ seems to be the least likely for the four cations under consideration. Nevertheless, two analyses of material from Thurnberg, Germany, by Fritzsche (1847) and Ettling (1853), and analyses of material from Traversella, Italy, by Stromeyer (1875) and Saarbruecken, Germany, by Weiss (1885) approach the ratio Mg:Fe=1:1 closely. Stromeyer's analysis has Fe:Mg=1:1.02. Crystallographic or other evidence (aside from the analytical ratios) which definitely place any of these four samples in either the dolomite or calcite groups is lacking. The name pistomesite was proposed by Breithaupt (1847) for the material from Thurnberg. We have examined two specimens from Traversella and a third specimen from Brozzothal, Italy, containing Fe and Mg in almost equal proportions, as indicated by the indices of refraction. These specimens proved on differential thermal analysis to belong in the calcite structure-type.

## ACKNOWLEDGMENTS

We wish to express our thanks to Mr. Brian Skinner, Department of Mineralogy, Harvard, for making numerous differential thermal analysis runs, and to Dr. George T. Faust, U. S. Geological Survey, for inde-

pendently verifying the *DTA* curves on three of our samples. Dr. Faust's thermal curves are used in the present report.

## References

Beck, C. W., Differential thermal analysis curves of carbonate minerals: *Am. Mineral.*, **35,** 985 (1950).

Blum, L., Leesbergite, un nouveau carbonate calcaréo-magnésique: *Ann. géol. Belg., Bull.* **34,** 118 (1908).

Boldyrev, A. K., Kurs opisatelnoi min., Leningrad, Pt. 2, 162 (1928).

Bradley, W. F., Burst, J. F., & Graf, D. L., Crystal chemistry differential and thermal curves of dolomite: *Am. Mineral.*, **38,** 207 (1953).

Breithaupt, J., Carbonites Pistomesites, etc.: *Ann. Phys.* **70,** 147 (1847).

Browning, P. E., Analysis of rhodochrosite from Franklin Furnace, N. J.: *Am. J. Sci.*, **40,** 375 (1890).

Bukowsky, A., Kuttenberger manganmineralien. Anz. der III Congr. Böhm. Naturforsch. und Ärzte. Prague, 293 (1901). Abstracted in *Jb. Min.*, **II,** 338 (1903), and *Zeits. Krist.*, **39,** 400 (1903).

Chave, K. E., A solid solution between calcite and dolomite: *J. Geol.*, **60,** 190 (1952).

Cook, G. H., Geology of New Jersey. 69 (1868).

Doelter, C., Handbuch der Mineralchemie, Leipzig, **I,** 360, 376 (1912).

Dana's System of Mineralogy by C. Palache, H. Berman and C. Frondel, New York, 7th ed., 141 (1951).

Eisenhuth, K., Beiträge zur kenntnis der bitterspäthe: *Zeits. Kryst.*, **35,** 582 (1901).

Ettling, C., Untersuchung einiger rhomboedrischen Karbonspathe: *Ann. Chem.* **99,** 203 (1853).

Faust, G. T., Differentiation of magnesite from dolomite in concentrates and tailings: *Econ. Geol.*, **39,** 192 (1944).

——— Dedolomitization, and its relation to a possible derivation of a magnesium-rich hydrothermal solution: *Am. Mineral.*, **34,** 789 (1949).

Foote, H. W., & Bradley, W. M., On solid solution in minerals. V. The isomorphism between calcite and dolomite: *Am. J. Sci.*, **37,** 339 (1914).

Ford, W. E., Studies in the calcite group: *Trans. Conn. Acad. Arts Sci.*, **22,** 211 (1917).

Fritzsche, J., cited in Breithaupt (1847).

Graf, D. L., Preliminary report on the variations in differential thermal curves of low-iron dolomite: *Am. Mineral.*, **37,** 1 (1952).

Greer, W. L. C., Mix-Crystals of $CaMnSiO_4$ and $Mn_2SiO_4$: *Am. Mineral.*, **17,** 135 (1932).

Hall, F. P., & Insley, H., Phase diagrams for ceramists: *J. Am. Ceram. Soc.*, Pt. **II,** Bov. (1947).

Haul, R. A. W., & Heystek, H., Differential thermal analysis of the dolomite decomposition: *Am. Mineral.*, **37,** 166 (1952).

Jay, A. H., & Andrews, K. W., Composition of some binary oxide systems: *J. Iron Steel Inst.*, **152,** 15 (1946), *Nature*, **154,** 116 (1944).

Jenzsch, G., Fluor im Kalkspath und Aragonit: *Ann. Phys.*, **96,** 145 (1855).

Krieger, P., Notes on an *x*-ray diffraction study of the series calcite-rhodochrosite: *Am. Mineral.*, **15,** 23 (1930).

Kulp, J. L., Kent, P., & Kerr, P. F., Thermal study of the Ca-Mg-Fe carbonate minerals: *Am. Mineral.*, **36,** 643 (1951).

Kulp, J. L., Wright, H. D., & Holmes, R. J., Thermal study of rhodochrosite: *Am. Mineral.*, **34,** 195 (1949).

Levison, W. G., Columnar manganocalcite from New Jersey: *Am. Mineral.*, **1**, 5 (1916).

Natta, G., & Passerini, L., Soluzioni solide—I sistemi CaO-MnO, CaO-MgO, etc.: *Gazz. chim Ital.*, **59**, 129 (1929).

Naumann, C. F., Cited by Hey, M. L., An index of mineral species and varieties, London, 76, 1950.

Palache, C., The minerals of Franklin and Sterling Hill, Sussex County, New Jersey: *U. S. Geol. Surv., Prof. Paper* **180** (1935).

Passerini, L., Soluzioni solids III—I sistemi MnO-CdO, MnO-MgO: *Gazz. chim. Ital.*, **60**, 535 (1930).

Petterson, H., Investigation of the solubility in the solid state in the binary systems of the oxides, CaO, MnO, MgO and FeO: *Jernkont. Ann.*, **130**, 653 (1946).

Primak, W., Kaufman, H., & Ward, R., *X*-ray diffraction studies of systems in the preparation of alkaline earth sulfide and selenide phosphors: *J. Am. Chem. Soc.*, **70**, 2043 (1948).

Rammelsberg, C. F., Handbuch der Mineralchemie, 209 (1860); **II**, 231 (1875).

Retzius, A. J., Försök till mineralrikets uppställn., etc.: *Lund*, **136** (1795).

Rigamonti, R., Soluzioni solide tra ossido di zinco ed ossido di metalli bivalenti: *Gazz. chim. Ital.*, **76**, 474 (1946).

Roepper, W. T., Notice of some minerals from New Jersey: *Am. J. Sci.*, **50**, 35 (1870).

Rozsa, M., Die enstehung des dolomites, etc.: *Zbl. Min.*, 229, (1926).

Shepard, C. U., & Tyler, S. W., Analysis of a carbonate of lime and manganese from Sterling, Sussex County, N. J.: *Am. J. Sci.*, **39**, 174 (1865).

Strobentz, H., Analysen von ungarischen dolomitkrystallen: *Föld Közl.*, **55**, 49 (1926).

Stromeyer, H., Analysis cited in Rammelsberg (1875).

Vegard, L., Mixed crystals of carbonates of the calcite group: *Norske Vid.-Akad. Skrifter, Oslo, Nat.-Nat. Kl., No.* **2**, 6 (1947).

Wayland, R. G., Composition, specific gravity and refractive indices of rhodochrosite: *Am. Mineral.*, **27**, 614 (1942).

Weibull, M., Untersuchung schwedischer minerale: *Min. Mitth.*, **7**, 108 (1885).

Weiss, C. E., Einige carbonate aus der steinkohlenformation: *Jb. preuss. geol. Landesanst.*, 113 (1885).

Žák, L., Paragenesis of the manganese carbonates of the ore deposit of Chvaletice in Železné Hory, East Bohemia: *Bull. Int. Acad. Czech. Sci.* (1949); *Rozpravy tř. České Akad.*, **59**, No. 25 (1950).

*Manuscript received July 20, 1954*

# NOTES AND NEWS

## A NEW METHOD FOR MOUNTING SAMPLES FOR POWDER X-RAY SPECTROMETRY*

H. D. Holland, W. B. Head III, G. G. Witter, Jr.,
and G. B. Hess

During the course of an investigation of the effect of nuclear radiation on the structure of zircon, it became necessary to determine accurately the unit cell dimensions of crystals by means of a Norelco High Angle X-ray Spectrometer. Various smear techniques were tried, but it was found that errors in the measurement of $2\,\theta$ usually were on the order of 0.01 to 0.02°. The same conclusion was reached by Adams and Rowe (1954) in their survey of the sample mounting techniques available at present. These authors also discuss a pressed-sample mounting technique developed by them but do not state in their paper the reproducibility attainable thereby. The method finally adopted in this laboratory has been used successfully during the past year; the average difference in $2\,\theta$ between the values measured on two sample slides of the same material is 0.003°. It appears unlikely that additional refinements of the technique will decrease this error appreciably.

### Sample Preparation

The samples of zircon were crushed and then ground in a Fisher Scientific Co. automatic grinder equipped with tungsten carbide mortar and pestle, using methyl alcohol as a grinding medium. The resultant slurry was pipetted into a vial, and the volume brought up to 35 cc. with additional methyl alcohol. The suspension was then poured into a 250 ml. beaker and permitted to stand for five minutes. After this length of time the supernatant liquid was pipetted into a second 250 ml. beaker and permitted to stand for 25 minutes. The sample still remaining in suspension was discarded or saved for other purposes and the material which had accumulated in the bottom of the beaker mixed with a small amount of methyl alcohol, was transferred to a glass vial. The concentration of zircon in this suspension was determined by evaporating 1 cc. on a watch glass and weighing the residue after heating at approximately 100° C.

The same procedure was followed in the preparation of a suspension of silicon metal (silicon metal powder, Fairmount Chemical Co. Inc., 600 Ferry Street, Newark, N. J.). Thus the settling velocity distribution

---

* The work reported in this paper was supported by the office of Naval Research under contract number *Nonr 250(00)*.

of the grains in the sample and reference suspensions was approximately the same. The desired volume of the two suspensions was then pipetted into the sedimentation cell shown in Fig. 1. The cell was made of brass and consisted of a base plate, *A*, ring, *B*, half-cylinder, *C*, and set screws, *D*. A brass planchet, *E*, whose surface had been polished on a diamond lap, was introduced between the base plate and the ring and half-cylinder and clamped tightly by means of the set screws. After the two suspensions had been introduced, the holder was placed on a level shelf and covered with a 250 ml. beaker. At normal room temperatures the zircon and silicon powders settle out of the suspension in about 6 hours, and evaporation of the methyl alcohol is usually complete in 36 hours. The evaporation can be speeded up considerably by removing the beaker

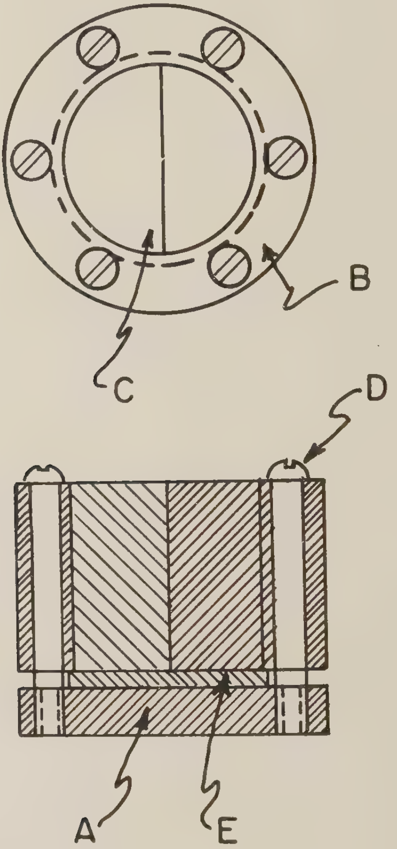

FIG. 1

after the first 6 hours of settling, but care should be taken to prevent the formation of convection currents, particularly near the end of the period of evaporation. After the methyl alcohol has evaporated completely, the sample planchet is removed from the holder and is then ready for introduction into the Norelco Spectrometer.

Recently a holder of the type shown in Fig. 2 has been put into use. The principle of operation is the same as that of the holder described above; however, two improvements have been made. The shape of the sample well approximates more closely that of the $x$-ray beam, and glass slides can be used as mounting planchets. This saves the expense of machining and polishing, permits one to observe the underside of the sample mount, and eliminates interference from $x$-ray reflections from the brass planchet itself.

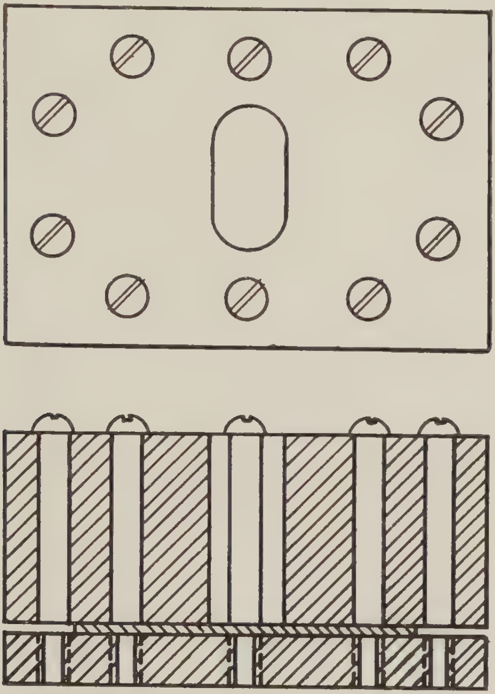

FIG. 2

The quantity of silicon and sample used in the preparation of the slides varies somewhat with the problem at hand. In the present work approximately 5 mg. of silicon and 10 mg. of zircon were used. It was found that the difference in 2 $\theta$ values between the zircon peaks and the reference silicon peaks was insensitive to the ratio of the two components and to the total weight of material used, which indicates that the mixing of the two components was adequate and that the silicon acted as a true internal standard.

## MEASUREMENT OF 2 $\theta$ VALUES

The sample was mounted in the head of the Norelco Spectrometer. The following program is typical of that used in the determination of the unit cell dimensions of the zircon samples:

1. The recorder pen was drawn across the strip chart at right angles to the long direction of the chart by means of the manual control in the rear of the recorder.
2. The spectrometer was set so that 2 $\theta$ was slightly less than 28.000°.
3. The switch controlling the scanning motor on the spectrometer was turned on, and the clutch connecting the spectrometer with the scanning motor was thrown in.
4. The motion of the spectrometer was watched with a hand lens, and, as 2 $\theta$ reached 28.000° the strip chart recorder switch was turned to the on position, starting the motion of the strip chart.
5. The (111) peak of silicon at approximately 28.45° was then scanned. After passage of the peak, the recorder chart switch was turned off at an accurately determined value of 2 $\theta$, usually 28.700°, and the 2 $\theta$ value at this final point marked on the chart.
6. The pen was then drawn across the recorder strip chart as before.
7. The motion of the scanning motor and of the spectrometer were disconnected by releasing the clutch, and the spectrometer was set at 2 $\theta$ slightly less than 19.700°.
8. The clutch was again thrown in, and the strip chart recorder switch turned on when 2 $\theta$ was just equal to 19.700°. The (101) peak of zircon at approximately 20.00° was then scanned.
9. At an accurately determined value of 2 $\theta$ near 20.300° the strip chart recorder switch was turned off, and the pen drawn across the paper as before.
10. The above procedure, steps 2 through 9, was carried out four more times so that the (111) peak of silicon and the (101) peak of zircon were each scanned five times.
11. The same scanning procedure was then used for obtaining reflections from the (200), (112) and sometimes the (312) peaks of zircon. A complete run of this type therefore consisted of twenty Si (111) peaks and five peaks each of the (101), (200), (112), and (312) reflections of zircon. On the strip chart zircon and silicon peaks thus alternate. A scanning speed of $\frac{1}{8}^\circ$ per minute and a chart speed of $\frac{1}{4}''$ per minute were used throughout. It was found that the measured 2 $\theta$ values were

insensitive to changes in the scale factor setting, but that the time constant and multiplier settings should not be changed during a run.

After completion of the scanning program the strip chart was removed from the recorder. The height of each peak was measured from the base of the peak, and a point 15% from the top of the peak was marked off. The midpoint of the peak at this point was measured and the distance from the midpoint to the reference line drawn across the chart at the conclusion of the peak was determined to the nearest 0.001° with an engineer's rule and hand lens. It is preferable to use the line drawn at the conclusion of the scanning of each peak rather than at the beginning of the scan since errors are sometimes incurred due to lags in the motion of the strip chart motion just after the strip chart switch has been turned on.

From these measurements the $2\theta$ values at the midpoints of the peaks are calculated. The five values thus obtained for each zircon are then averaged and a probable error is assigned to this average such that at least three of the five measured values fall within the average plus and the average minus, the assigned probable error. The same procedure is carried out for the Si (111) peaks associated with each of the zircon peaks. A probable error is assigned to this average in the same manner as to the average for each of the zircon peaks. The average for each zircon peak is then corrected by subtracting the difference between the measured average value for Si (111) and the standard value of 28.447° accepted for this angle. The probable error of the corrected value of $2\theta$ for the zircon peaks is the sum of the probable error for the uncorrected average of the zircon peak, and the probable error for the average $2\theta$ value for the Si (111) peak. A sample determination of the corrected value of a $ZrSiO_4$ (101) peak is shown in Table 1. The combined error in the two readings is usually between 0.002 and 0.004°. That this procedure is justified is shown by the fact that for a given zircon sample the four averages for the Si (111) peak determined in the manner shown above [one average each is determined in conjunction with the calculation of the corrected $2\theta$ values of the $ZrSiO_4$ (101), (200), (112), and (312) peaks] rarely fall outside the limits determined by any one of the averages plus and minus, the assigned probable error.

## RESULTS

In Table 2 the data on the reproducibility of duplicate sample slides studied during the past year have been summarized. This includes some data on slides which looked rather poor, having been disturbed by convection currents during the evaporation process. It can be seen that in most cases the difference $(2\theta_{ZrSiO_4}-2\theta_{Si})$ between duplicate sample slides

TABLE 1. SAMPLE CALCULATION OF 2 $\theta$ VALUE OF A $ZrSiO_4$ (101) PEAK

Sample: Zr 4-42H2

| Peak No. | Si (111) | $ZrSiO_4$ (101) |
|---|---|---|
| 1 | 28.452 | |
| 2 | | 20.004 |
| 3 | 28.450 | |
| 4 | | 20.003 |
| 5 | 28.449 | |
| 6 | | 20.000 |
| 7 | 28.451 | |
| 8 | | 20.001 |
| 9 | 28.451 | |
| 10 | | 19.998 |
| average | 28.451±0.001 | 19.999±0.002 |

$$\begin{array}{r} 28.451\pm0.001 \\ -28.447 \\ \hline \end{array}$$

correction factor: 0.004±0.001

corrected value of $2\theta$ for $ZrSiO_4$ (101)

$$\begin{array}{r} 19.999\pm0.002 \\ -\ 0.004\pm0.001 \\ \hline 19.995\pm0.003 \end{array}$$

TABLE 2. DIFFERENCES IN MEASURED VALUES OF $(2\theta_{ZrSiO_4}-2\theta_{Si})$ FOR DUPLICATE SLIDES*

| $(2\theta_{ZrSiO_4}-2\theta_{Si})$ | Number of cases in which this difference was found |
|---|---|
| 0.000° | 4 |
| 0.001 | 14 |
| 0.002 | 8 |
| 0.003 | 19 |
| 0.004 | 5 |
| 0.005 | 6 |
| 0.006 | 1 |
| 0.007 | 2 |
| 0.008 | 3 |
| 0.009 | 0 |

* In all of these measurements Si (111) was used as the reference peak; the zircon peaks most commonly measured were (101), (200), (112), and (312).

is less than 0.005°. In the present work this permitted the determination of the unit cell dimensions of zircon to approximately 1.5 parts in 10,000.

At the moment it appears doubtful that this technique can be improved appreciably. The main residual error now lies in the measurement of the 2 $\theta$ values on the strip chart. This in turn is probably controlled mainly by fluctuations in the count rate of the spectrometer. The present technique therefore probably represents the extreme of accuracy to which *x*-ray powder spectrometry can be carried with the Norelco instrument.

## REFERENCE

Adams, L. H., and Rowe, F. A. (1954), The preparation of specimens for the focusing-type *x*-ray spectrometer: *Am. Mineral.*, **39**, 215–221.

## BEYRICHITE, A DISCREDITED SPECIES*

Charles Milton and Joseph M. Axelrod, *U. S. Geological Survey, Washington 25, D.C.*

Inasmuch as many museums and private collections possess specimens labeled beyrichite and there seems to have been no unambiguous statement in the literature concerning its status, it is hoped that this note may remove whatever uncertainty or confusion may exist in regard to beyrichite. To summarize the following data, the original description probably referred to what we now term violarite, and all specimens of so-called beyrichite which we have been able to examine have been shown to be well-known minerals or artificial substances.

Beyrichite was first described by K. Th. Liebe (1871) from "Lammrichs Kaul Fdgrb," Westerwald, Germany. Its specific gravity was 4.7 (millerite sp. gr. 5.9), color lead gray, and composition determined as $3NiS \cdot 2NiS_2$ or $2NiS \cdot NiS_2$. A loss of sulfur on heating was construed by Liebe as indicating change of beyrichite into millerite; he also held that beyrichite, by addition of nickel from solution, forms millerite. Liebe's views were adopted by Laspeyres (1892), who went so far as to assert that all millerite is an alteration product of beyrichite and that the change involves only the physical properties—color and density—with no chemical or cystallographic change. Hintze (1904) summarizes the early literature, and accepts beyrichite as a dimorph of millerite. He notes that unchanged beyrichite is known from only one locality—Altenburg near Oberlahr (Grube Lammerichskaule) in Rhenish Prussia.

---

* Publication authorized by the Director, U. S. Geological Survey.

We have tried to obtain all specimens labeled beyrichite and have examined six such specimens. *X*-ray and other studies of these six specimens have given the results tabulated below.

Composition of "Beyrichites"

| Source | Locality | Found |
|---|---|---|
| Brush Collection, Yale University, Brush Collection 5330 | Dillenburg, Germany | Millerite (and a very little unidentified material) |
| U. S. Geological Survey | Etna mine, Napa County, Calif. | Violarite (on cinnabar) |
| U. S. National Museum | Roebling Collection 617, Westerwald, Germany | Iron carbide with iron |
| | Canfield Collection 520, Eisleben, Saxony | Bismuth, bismuthinite, and niccolite, etc. |
| Harvard Museum | Holden Collection 82029, Eisleben, Saxony | Goethite |
| | Holden Collection 82030, Lammerichskaule mine, Westphalia, Germany | Emplectite |

In answer to an inquiry, G. F. Claringbull, Acting Keeper of Mineralogy, The British Museum, wrote as follows " . . . B. M. 1913348 was originally labeled millerite with beyrichite, linnaeite and copper pyrites . . . locality . . . Victoria Mine, Littfeld, Westphalia. The specimen consists of an intergrowth of chalcopyrite, galena, and linnaeite shot through with needles of millerite. . . . "

H. Strunz (personal communication) has written that having been for some years dubious as to the nature of beyrichite, he had sought specimens in the Humboldt University of Berlin, and on receiving our request for the loan of material had further gone through the collection of the Technische Hochschule in Berlin and the Hochschule at Regensburg, without finding any. A similar reply was received from H. Schneiderhöhn of the Mineralogisches Institute of the University of Freiburg. Other attempts to obtain specimens, as by a notice in this journal (vol. 39, p. 151, 1954), were also unsuccessful.

In a study, now in progress, of the mineralogy of the nickel mineralization in southwestern Wisconsin, we have noted extensive replacement of millerite, NiS, by violarite $(Ni, Fe)_3S_4$, also perhaps by bravoite $(Fe, Ni)S_2$, and, rarely, by chalcopyrite. The properties of violarite (including specific gravity, 4.79) agree reasonably well with those reported by Liebe, Laspeyres, and others for beyrichite. Where a nickel sulfide is actually in question, it is probable that, in most instances, violarite is present replacing millerite. Violarite, it may be noted, was not established as a species until 1924, when it was described by Lindgren and Davy; although it had been noted by Calkins (1916) and by Hudson (1922) as "polydymite," by Tolman and Rogers (1916) as "pentlandite," and by Buddington (1924) as an unknown "not pentlandite-bravoite?." Short and Shannon (1930) identified it correctly as violarite; but shortly thereafter Schneiderhöhn and Ramdohr (1931, p. 173) confused violarite with bravoite. Although Schneiderhöhn and Ramdohr (1931, p. 177–178) rejected Short and Shannon's correct confirmation of Lindgren and Davy's violarite and proposed that the name violarite be dropped, they nevertheless in a discussion of millerite (Schneiderhöhn and Ramdohr, 1931, p. 145–146) were undoubtedly referring to violarite, as follows (in translation): "Formerly it was generally believed that millerite formed by replacement of a mineral 'beyrichite,' of similar or identical composition. No support for this is found by microscopic study. But several specimens of millerite are crusted with an extremely delicate coating of a soft, gray-white, strongly pleochroic mineral, which appears quite different from the millerite needles in the same specimen." Unquestionably Schneiderhöhn and Ramdohr are describing violarite. In view of this history of violarite, it is not surprising that as "beyrichite" it was so misunderstood by the early workers.

It might be suggested that the name beyrichite should have priority over violarite, and this suggestion is made specifically with the idea of discouraging it. After many vicissitudes, the name violarite is now in good standing for a well-defined mineral species, and beyrichite is not.

## References

Buddington, A. F. (1924), Alaskan nickel minerals: *Econ. Geology*, **19**, 521–541.

Calkins, F. C. (1916), An occurrence of nickel ore in San Diego County, California: *U. S. Geol. Survey, Bull.* **640**, 77–82.

Hintze, C. (1904), Handbuch der Mineralogie, **I**, 606–615.

Hudson, F. S. (1922), Geology of the Cuyamaca region of California, with special reference to the origin of the nickeliferous pyrrhotite: *California Univ., Dept. Geol. Sci., Bull.* **13**, 175–252.

Laspeyres, A. (1892), Beyrichit von der Grube Lammerichskaule bei Altenkirchen im Siegen'schen: *Zeits. Krist.*, **20**, 535–550.

Liebe, K. Th., (1871), Beyrichite and millerite: *Neues Jahrb.*, 843, **1871**.

Lindgren, W., & Davy, W. M. (1924), Nickel ores from Key West mine, Nevada: *Econ. Geology*, **19**, 309–319.

Schneiderhöhn, H., & Ramdohr, P. (1931), Lehrbuch der Erzmikroskopie.

Short, M. N., & Shannon, E. V. (1930), Violarite and other rare nickel sulfides: *Am. Mineral.*, **15,** 1–17.

Tolman, C. F., Jr., & Rogers, A. F. (1916), A study of the magmatic sulfide ores: *Leland Stanford Junior Univ. Pub.*, 76 p.

## LLAMA BONES WITH LEAD-COPPER MINERALIZATION FROM BOLIVIA*

Charles Milton, *U. S. Geological Surevy, Washington 25, D. C.*

In assembling materials for a paper dealing with the preservation of fossils being prepared by a member of the U. S. Geological Survey, it was learned that there were some mineralized and supposedly fossil bones in the paleontological collections at Harvard College. The bones were reported to be replaced by copper or copper compounds. Through the kindness of Dr. Alfred S. Romer of the Museum of Comparative Zoology, the bones (Fig. 1) were borrowed for examination. They are labeled in German: "Vertebrae impregnated with copper—mineral collection of Friedrich Ahlfeld."

The bones are notably heavy and show perfectly preserved bone structure. They consist of calcium phosphate largely replaced by green and red oxides (massicot and litharge) and also probably by lead phosphate, with metallic lead, copper, and probably traces of silver. Figure 2 shows a polished section of the bone. Figure 3 is of another polished section showing replacement of bone by lead oxide.

The observed relations of the metallic lead and copper are in all respects those that would follow from the cooling of a melt consisting of lead with some copper, as may be seen from consideration of the equilibrium diagram for the Pb-Cu system (Fig. 4). It is possible that in a cupellation process bones were used for some reason, instead of the customary bone ash. Molten lead then would seep down, with its dissolved copper (and perhaps silver), to lodge eventually in the bone pores and there crystallize. At the same time oxide compounds of these metals would crystallize as illustrated.

To confirm or disprove this hypothesis of the mineralization of the bones, inquiry was made of Señor Ahlfeld, who, under date of May 4, 1954, stated that "the bones were those of the modern llama collected from the surface near an old copper smelter in the Corocoro district."

---

* Publication authorized by the Director, U. S. Geological Survey.

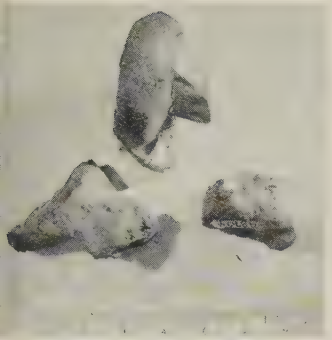

. 1. Llama bones with copper-lead-
silver(?) replacement.

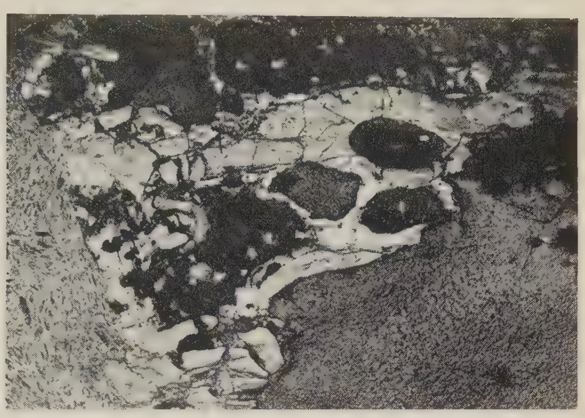

FIG. 2. Polished section (×25) showing bone structure with lead (gray in lower right and center) and copper crystals in the lead.

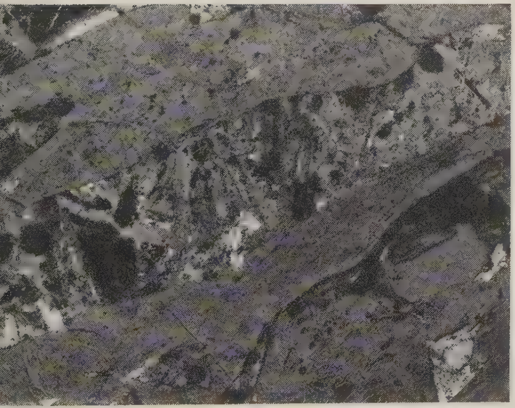

. 3. Polished section (×50). The diagonal, large, gray,
ly smooth areas are essentially unmineralized bone.
lized lead oxide is in the bones pores across the middle
upper left. The light-gray area in the lower right is
e, the embedding medium.

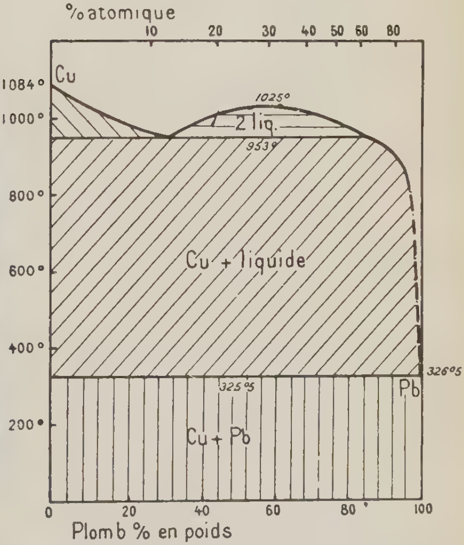

FIG. 4. Equilibrium diagram of copper-lead system (after Pascal, Paul, *Traite de Chimie Minerale*, **12**, 429, 1934).

### BIBLIOGRAPHY ON URANIUM IN ARKANSAS, IOWA, KANSAS, LOUISIANA, MINNESOTA, NEBRASKA, NORTH DAKOTA, OKLAHOMA, SOUTH DAKOTA AND TEXAS

The Geological Society of America published the following article in the March, 1955, issue of its *Bulletin:* "Bibliography and Index of Literature on Uranium and Thorium and Radioactive Occurrences in the United States. Part 4: Arkansas, Iowa, Kansas, Louisiana, Minnesota, Missouri, Nebraska, North Dakota, Oklahoma, South Dakota and Texas," by Margaret Cooper for the Division of Raw Materials, U. S. Atomic Energy Commission Since this 70-page bibliography may prove helpful to both geologists and laymen interested in uranium prospecting, the Society has prepared reprints for public sale at 50 cents per copy. Remittance must accompany orders, which should be sent to:

*The Geological Society of America,*
*419 West 117 Street,*
*New York 27, New York.*

---

*One Hundred Arizona Minerals* is the title of a small Bulletin (No. 165) of the Arizona Bureau of Mines (Mineral Technology Series No. 49) recently issued by the University of Arizona, Tucson, Arizona. The author is Richard T. Moore. The price of this Bulletin is thirty cents, but may be obtained free if a resident of Arizona.

---

The fifth issue of the second series of the French Bibliographical Digest, devoted to all branches of crystallography and mineralogy, is now ready for distribution. It is published as a sequel to the volume dealing with geology which appeared in October 1954. The present bibliography lists publications for the years 1949–1954 and contains author's name, title of article, translation of the title into English, with volume, year and page references (with short abstracts). There are 582 entries of papers published by 433 authors. The preparation of the manuscript is largely the labor of Professor J. Wyart of the University of Paris.

---

The French Bibliographical Digest is intended primarily to make French scientific work better known in the United States. It is edited and published by the Cultural Division of the French Embassy, 972 Fifth Ave., New York 21, N. Y. Libraries, university departments and scientists will, upon request, be placed on the mailing list and receive the publications without charge.

---

Dr. Robert A. Hatch since 1947 associated with the Electro-Technical Laboratory of the U. S. Bureau of Mines at Norris, Tenn., where he directed research on synthetic mica, synthetic asbestos, industrial diamond substitutes and other synthetic mineral and ceramic materials has joined the ceramics section of the Electrical Products Laboratory of the Minnesota Mining & Manufacturing Co., St. Paul, Minnesota.

---

# MINERALOGICAL SOCIETY (LONDON)

A meeting of the Society was held on Thursday, January 27th, 1955, at 5 P.M., in the apartments of the Geological Society of London, Burlington House, Piccadilly, W.1 (by kind permission).

The following papers were read:

## (1) SPACE LATTICES OF THE CRYSTALLINE ELEMENTS IN RELATION TO THE PERIODIC TABLE

By Dr. S. I. Tomkeieff

By combining the space lattices of the crystalline elements into four groups it is possible to map them over the spiral periodic table. The field of high-symmetry lattices covers the region of metals and inert gases, while the field of low-symmetry lattices covers the region of non-metals. The transition zone between the two fields includes the diamond type structure. Packing density, symmetry, and coordination number, like the lattices themselves, show a regular distribution over the field of the periodic spiral and are shown to have a direct relation to the electronic structure of the elements.

A new arrangement of the fourteen Bravais space lattices is also proposed, and a comparison is made of a statistical distribution of crystalline elements, minerals and other compounds among the seven crystal systems.

## (2) AN ACCURATE DETERMINATION OF THE CELL DIMENSIONS OF BULTFONTEINITE, $Ca_4Si_2O_{10}H_6F_2$

By Dr. H. D. Megaw and Miss C. H. Kelsey

The cell dimensions and interaxial angles of bultfonteinite, $Ca_4Si_2O_{10}H_6F_2$, which is triclinic but markedly pseudo-orthorhombic, have been determined with fairly high accuracy from $x$-ray photographs with an oscillation camera. The values are: $a = 10.992 \pm 0.004$ Å, $b = 8.183 \pm 0.002$ Å, $c = 5.671 \pm 0.001$ Å, $\alpha = 93°57'$, $\beta = 91°19'$, $\gamma = 89°51'$. The method is outlined. Some tentative suggestions about the structure of the crystal are put forward; it is related to afwillite, $Ca_3Si_2O_{10}H_6$, as originally suggested by Parry, Williams & Wright (1932).

## (3) THE PHASE RELATIONS IN SANIDINE- AND ORTHOCLASE-PERTHITES

By Dr. J. V. Smith and Mr. W. S. MacKenzie

A routine $x$-ray method for studying perthitic feldspars has been developed. From a single-crystal oscillation photograph the symmetry, twinning and unmixing can be seen at a glance. The lattice angles $\alpha^*$ and $\gamma^*$ of twinned triclinic phases can be accurately determined from the photograph. Using this method the lamellar structure of a number of sanidine- and orthoclase-perthites has been investigated in detail. The angles $\alpha^*$ and $\gamma^*$ determined for the soda phases provide information on their composition.

Sanidine-cryptoperthites have a monoclinic potash phase and a soda phase with lattice angles equal to those of anorthoclases of composition near $Or_{20}Ab_{80}$.

Orthoclase-microperthites always contain a soda phase whose lattice angles correspond to low-temperature albite or oligoclase. The potash phase may be either monoclinic or triclinic (microcline).

Specimens from the Beinn an Dubhaich granite of Skye consist of a monoclinic potash phase together with an anorthoclase and a low-temperature albite-oligoclase. The evidence clearly demonstrates that orthoclase-perthites may be derived from sanidine-perthites by slow cooling.

### (4) THE STRUCTURES OF THE PLAGIOCLASE FELDSPARS. VI. NATURAL INTERMEDIATE PLAGIOCLASES

By Dr. P. Gay

Specimens from some 40 different localities over the composition range from about 20% An to about 70% An have been examined by *x*-ray single-crystal methods. The majority of these specimens show the normal intermediate plagioclase pattern characterized by weak pairs of subsidiary layer lines of variable separation. It has been found that the separation of these layer lines is a linear function of composition over the *whole* composition range. Further, this range is found to extend to more soda-rich compositions than was formerly believed, whilst the limits of the range are approximately defined by the compositions at which the separations of the subsidiary layer lines about either the *a* or *b* axes become zero.

The anomalous patterns shown by some specimens are discussed, and it is shown that most of these may be interpreted in terms of the previous geological history of the specimens.

A comparison of the present results with those obtained by previous workers in this field is made, and it is shown how the principal points of difference may be resolved. An account of the phase relationships of the low-temperature plagioclase series is given, and the problems arising from the present work are discussed.

### (5) THE STRUCTURAL FORMULA OF A HYDROUS AMPHIBOLE

By Dr. G. D. Nicholls and Dr. J. Zussman

The analysis of a hornblende presented by Buddington and Leonard has been re-examined using the direct method of formula derivation described by Hey in 1939. The mineral is seen to contain hydrogen in excess of that needed to make (OH, F, Cl) = 2, unaccompanied by excess oxygen, so that neither (OH) ions nor water molecules can be occupying the normally vacant "A" sites in the structure.

Some aspects of the method are discussed and its possible application to incomplete and partial analyses is noted.

### (6) THE VARYING ROLE OF WATER IN SILICATES AS ILLUSTRATED BY HYDROUS ANTHOPHYLLITE; AND ON THE CORRELATION OF PHYSICAL PROPERTIES AND COMPOSITION IN MULTIVARIATE SYSTEMS AS ILLUSTRATED BY ANTHOPHYLLITE

By Mr. G. H. Francis and Dr. M. H. Hey

A gedrite from Glen Urquhart contains nearly 99 oxygen atoms per unit cell instead of the normal 96, and is highly hydrous; methods of establishing the true unit-cell contents are discussed, and all the available data on the unit-cell contents of anthophyllite are reviewed. A procedure for deriving equations correlating physical data with composition where the composition involves several variables is described, and applied to the *b*-axis cell-dimension and the refractive indices of anthophyllite and gedrite.

The following papers were taken as read:

### (1) DEHYDRATION OF THE MONTMORILLONITE MINERALS

By Dr. R. Greene-Kelly

Neither of the two closely related systems, Li-montmorillonite-beidellite and Li-Na-montmorillonite is a uniform one. In the former it seems that there must be differences in composition between silicate sheets bound in the same crystallite, and in the latter the majority of the sodium ions aggregate to form a sodium-rich "phase." The effect of heating on the internal surface available to glycerol of the Li-saturated montmorillonite-beidellite is shown to be correlated with the amount of octahedral substitution, less than 70% leading to some glycerol penetration. In the Li-Na-montmorillonite system, if there is less than 70% Li ions in the interlamellar spaces, expansion also occurred after heating. No evidence was found of an intermediate state of expansion at 14 Å.

### (2) The Structure of Wadeite

By Mr. D. E. Henshaw

The complete structure of wadeite has been determined by *x*-ray methods. It has the space group, $P6_3/m$, unit cell dimensions $a=6.893\pm0.004$ Å, $c=10.172\pm0.002$ Å, and may be represented ideally by the formula $Zr_2K_4Si_6O_{18}$.

The fundamental structural unit is the $(Si_3O_9)^{6-}$silicon-oxygen ring. The only previously known silicate mineral to be built up on this unit is benitoite from St. Benito, California, having the formula Ba Ti $Si_3O_9$ and space group $P\bar{6}c2$ ($D^2_{3h}$).

There is evidence of some distortion in the individual silica tetrahedra. This distortion causes two-thirds of the oxygen atoms in wadeite to be closer to the positively charged zirconium and potassium ions than would be the case for regular tetrahedra, and it does not alter the Si-O distances or the average O-O distances in each tetrahedron.

### (3) Australites from Harrow, Victoria

By Mr. George Baker

Description of a collection of 34 specimens from the north bank of the Glenelg river, of various types (buttons, lenses, boats, dumb-bells, cores), giving weights (2–29 grams), specific gravity (2.39 2.47, mean 2.42), dimensions in different directions, and radii of curvature of surfaces. Radii of curvature are related to ablation during flight. Specimens from more easterly areas in S.W. Victoria have on the average a slightly lower specific gravity.

### (4) The Thermal Reactions of Nacrite and the Formation of Metakaolin, $\gamma$-Alumina, amd Mullite

By Dr. G. W. Brindley and Mr. K. Hunter

The thermal transformation of single crystals of nacrite heated progressively to 1250° C. are followed by *x*-ray single-crystal techniques. Persistance of residual crystalline order in the metakaolin phase up to 880° C. is established. After heating to 950° C., an oriented diagram of $\gamma$-alumina superposed on a random powder diagram of mullite is obtained; silica occurs as cristobalite. The $\gamma$-alumina has (110) parallel to the *a*-axis of nacrite. A second recrystalliaztion occurs at about 1150° C. when the $\gamma$-alumina reacts with silica to yield more mullite. The present results are discussed in relation to those obtained for kaolinite and kaolin clays. The formation of $\gamma$-alumina is considered to be a significant stage in the reaction series but not an intermediate stage for mullite formation at 950° C. The exothermic reaction at 950° C. is considered to arise from mullite formation and the fact that mullite is not always observed in *x*-ray diagrams is attributed to slow growth of the mullite nuclei.

(*Titles and abstracts kindly submitted by G. F. Claringbull, General Secretary*)

---

A meeting of the Society was held on Thursday, March 24th, 1955, at 5 P.M. in the apartments of the Geological Society of London, Burlington House, Piccadilly, W.1 (by kind permission).

The following papers were read:

### (1) *Isokite, $CaMgPO_4F$, a new mineral from Northern Rhodesia*

By Mr. T. Deans and Mr. J. D. C. McConnell, with a chemical analysis by Mr. R. Pickup

Small white spherulites of this new mineral occur in the ankeritic dolomite rocks which form the carbonatite plug of Nkumbwa Hill, near Isoka, Northern Rhodesia. The radiating platy crystals are monoclinic, biaxial positive with $Bx_a$ normal to the one very good cleavage. $\alpha=1.590$, $\beta=1.595$, $\gamma=1.615$ (all $\pm0.002$), $2V=51°$, dispersion $r>v$. G.=3.27, H. =roughly 5, soluble in acids. The chemical analysis conforms closely to $CaMgPO_4F$, with only minor substitution of Sr for Ca and OH for F.

The mineral is not pyroelectric. *X*-ray single crystal photographs indicate monoclinic symmetry, cleavage (010), $a=6.52\pm.05$ Å, $b=8.75\pm.05$ Å, $c=7.51\pm.05$ Å, $\beta=121°28' \pm12'$, space group $C2/c$. Unit cell contains $4CaMgPO_4F$, calculated density 3.29. Optical orientation $\gamma=b$, $\alpha{:}c=+32°$. *X*-ray powder data are presented. The mineral belongs to the tilasite group. Strunz has suggested that cryphiolite from Vesuvius has this composition and is isostructural with tilasite, but *x*-ray investigations in the British Museum, Department of Mineraolgy, do not support this view.

The associated minerals are dolomite and strontian fluorapatite, with minor amounts of monazite, pyrochlore, barite, and rare sellaite. Conditions of formation are discussed.

### (2) *Grovesite, the manganese-rich analogue of berthierine*

By Dr. F. A. Bannister, Dr. M. H. Hey, and Dr. W. Campbell Smith

A dark brown micaceous mineral from the Benallt mine, Rhiw, Carnarvonshire, with the same chemical composition as pennantite, gives an *x*-ray powder photograph closely resembling those of berthierine and cronstedtite. It is evidently related to pennantite as berthierine is to chamosite. The optical properties are very near to those of pennantite.

### (3) *Additional notes on rhodonite deposits in Devonshire*

By Sir Arthur Russell

### (4) *The powder patterns and lattice parameters of soda-rich plagioclases*

By Dr. J. V. Smith

Geiger-counter powder records of soda-rich plagioclases have been carefully measured and indexed. The lattice parameters of the synthetic specimens are almost independent of the lime content; the largest variation (that in $\beta^*$) amounting to only 0.2°. After strong heating the powder patterns of the natural specimens closely approached those of the synthetic specimens.

Eight out of the nine natural plagioclases gave lattice parameters which fall within experimental error on a continuous line. There is a fairly large variation in lattice parameters especially for $\gamma^*$ which changes by 2°. As the lime content increases the lattice parameters of the natural plagioclases approach those for the high-temperature synthetic and heated natural specimens until at $An_{50}$ the separation is only one-fifth of that at $An_0$. The ninth specimen (from a dacite) gives parameters midway between the curves, thus exhibiting a state of partial inversion.

The partially-heated natural plagioclases and the dacite give parameters indistinguishable within experimental error from the parameters of unheated plagioclases containing a higher lime content. There is, therefore, no reliable powder *x*-ray method for the determination of composition in the region $An_0$–$An_{50}$. If the composition is known, the powder method may be used for the determination of the thermal state. If the plagioclase can be judged to be in the low temperature state from geological evidence the powder method can be used to estimate the composition with an accuracy of 2% An.

### (5) *A first attempt at a determination of feldspars by activation analysis*

By Dr. J. E. S. Bradley and Dr. Olive Bradley

Small crystals (2 mg) of plagioclase and potassium feldspar were irradiated for four weeks in an atomic pile. Subsequent analysis of the radiation for sodium and potassium content gave promising results, and the method would appear capable of further development in this direction. It has not been possible to obtain satisfactory values for the calcium content.

The following papers were taken as read:

### (1) *Wairakite, the calcium analogue of analcime, a new zeolite mineral*

By Mr. A. Steiner (communicated by Dr. D. S. Coombs)

A new zeolite mineral having the formula $CaAl_2Si_4O_{12} \cdot 2H_2O$, the calcium analogue of analcime, has been named wairakite after the locality Wairakei in the North Island, New Zealand. Wairakite has been discovered in hydrothermally altered cores from holes drilled during exploration for geothermal steam, and in rocks ejected by steam from some of these drill holes. Indices of refraction, optical character, dispersion, and specific gravity of wairakite are given and its diagnostic lamellar twinning is described. The temperature at which wairakite forms in nature has been measured and the prevailing hydrostatic pressure calculated. The conditions of formation of the new mineral are discussed and compared with the attempted syntheses of calcium analcime. The possible existence of an isomorphous series analcime-wairakite is examined.

### (2) *X-ray observations on wairakite and non-cubic analcime*

By Dr. D. S. Coombs

Wairakite is monoclinic and pseudo-cubic with cell dimensions and optical orientation as follows: $a$ (near optical $\beta$) 13.69 Å, $b$ (optical $\alpha$) 13.68 Å, $c$ (near optical $\gamma$) 13.56 Å, $\beta=90.5°$, $8CaAl_2Si_4O_{12} \cdot 2H_2O$, probable space group I$a$ or I2/$a$. The powder pattern confirms that the mineral is structurally related to analcime ($a_0$ 13.72 Å). The complex lamellar twinning can be explained on the assumption that wairakite crystallized in the cubic system, but subsequently inverted to the lower-symmetry modification with secondary twinning on the cubic dodecahedral planes. On the basis of powder data and optical properties, at least two modifications of analcime are recognized and a third inferred (*a*) inferred strictly cubic and isotropic, space group I*a*3*d*; (*b*) birefringent and biaxial, departures from cubic lattice dimensions not detectable although weak anomalous reflections may appear, e.g. Flinders, Australia; (*c*) trigonal or nearly trigonal, the body-centered rhombohedral cell having a 13.71 Å, $\alpha=90°31'$, e.g. Laven, Norway.

### (3) *The effect of isomorphous substitutions on the intensities of (001) reflections of mica- and chlorite-type structures*

By Mr. G. Brown

The effect of isomorphous substitutions on the structure factors of the 001 reflections has been calculated for mica type and chlorite type structures. In the micas (including illites) variations in diffracted *x*-ray intensities occur due to variations in the composition of the octahedral cation sheet and the interlayer cation sheet. The calculations for dioctahedral micas deal with compositions which lie within the field whose corner members are

$K_2\ (Al, Si)_8\ Al_4\ O_{20}\ (OH)_4$
$K_2\ (Al, Si)_8\ Fe_4\ O_{20}\ (OH)_4$
$(H_2O)_2(Al, Si)_8\ Al_4\ O_{20}\ (OH)_4$
$(H_2O)_2(Al, Si)_8\ Fe_4\ O_{20}\ (OH)_4$

and similar calculations have been made for trioctahedral micas. In the chlorite structure there are two kinds of sites for octahedrally co-ordinated cations, and both the kind of octahedral cations and their distribution between the two types of site affects the 001 intensities. The structure factors for 001 reflections of chlorite type structures with compositions between

$$\{(Mg, Al)_{12}\}\{(Si, Al)_8\}\ O_{20}\ (OH)_{16} \text{ and}$$
$$\{(Mg, Al)_4Fe_8\}\{(Si, Al)_8\}\ O_{20}\ (OH)_{16}$$

have been calculated for both symmetrical and asymmetrical distributions of the octahedrally co-ordinated cations between the two types of octaheral sites. The effect of variations in intensities due to isomorphous substitution on the standard mineral method of quantitative mineralogical analysis is pointed out and an alternative method is suggested.

### (4) *Projector for interference figures and for direct measurement of 2V*

By Mr. H. C. G. Vincent (communicated by the Editor)

A simple instrument for the demonstration and study of the optical properties of crystals is described. Without microscope or lens system, the interference figure is displayed in focus over the surface of a ground glass hemispherical screen with both optic axes in view for an angular separation of 120 degrees. The spherical surface of convergent interference phenomena surrounding the whole of the crystal may be explored while the specimen is revolved in its mount, giving, in effect, a working model of the crystal with its indicatrix. The parts of the figure retain their true relationship; 2V may be directly measured and a reverse set of readings is available. The instrument may also be used for orthoscopic studies, and its simplicity renders it suitable for individual student operation.

### (5) *The constitution of voltzite*

By Dr. A. A. Moss

A re-examination of voltzite shows that it contains arsenic, but no oxygen; the unit-cell contents are approximately $Zn_3As_{\frac{1}{2}}S_3$. The *x*-ray powder photograph closely resembles that of blende, but the mineral is strongly birefringent.

(*Titles and abstracts kindly submitted by G. F. Claringbull, General Secretary*)

## SUMMARIES OF PAPERS GIVEN BEFORE THE CLAY MINERALS GROUP OF THE MINERALOGICAL SOCIETY (LONDON)—APRIL 15 AND 16 (1955)

### S. J. Gregg: *Some observations on the aggregation of kaolinite*

The specific area ($S_A$) determined by sorption of nitrogen at −183° C. has been compared with the specific area ($S_D$) calculated from the equivalent spherical diameter as determined by sedimentation, for a series of six fractions prepared from each of four different kaolins. For each series $S_A$ agrees reasonably with $S_D$ for the finer fractions but considerably exceeds it for the coarser fractions on account of the presence in these of vermicules. Bulk densities indicate the presence, particularly in the finer fractions, of temporary aggregates due to inter-particulate adhesion. Since this adhesion is weakened by adsorption, the bulk density is greater in presence of water vapor than in vacuum, whilst the modulus of rupture of kaolin compacts is less. The aggregation of kaolin at elevated temperature, i.e. sintering, is only important at temperatures above about 800° C., $S_A$ being surprisingly little affected by the loss of structural water at 400–500° C.

### A. Auskern and R. W. Grimshaw: *The hydroxyl region of the infra-red spectrum of kaolin minerals*

Absorption bands in the hydroxyl region of the infra-red spectra of kaolin minerals are quite distinctive and can be correlated with those of other hydroxide minerals, where the nature of the hydroxyl groups has been definitely established. Two regions of hydroxy absorption can be established and controlled dehydration experiments have shown that these can be assigned to surface and to internal groups. There is no evidence of hydrogen bonding between the surface layers.

### G. Brown and F. Smithson: *The dickite in certain sandstones in North Wales and Northern England*

The present authors have previously reported the occurrence of dickite in sandstones of the Lower Carboniferous Series, the Millstone Grit and the Middle Jurassic. In view of the comparative paucity of data on this mineral, six samples were selected, purified, and examined by *x*-ray diffraction methods; a dehydration curve, a partial *d.t.a.* curve, and a partial chemical analysis were also obtained for the purest sample (about 97% dickite). The *x*-ray data agree with those of previous investigators but are more extensive; the dehydration curve is similar to that of Ross and Kerr, and the *d.t.a.* curve shows what may be a partially resolved double endothermic peak in the region 470°-700° C., the individual peaks being at 590° C. and 660° C. The optical properties of the mineral were studied, and other minerals observed during the microscopical examination were recorded.

### R. J. W. McLaughlin: *The effect of grinding on dickite*

Data are presented for the effect of wet and dry grinding on dickite from Ouray, Colorado. With increase in time of dry grinding the endothermic *d.t.a.* peak becomes broader and is moved towards a lower temperature, while the exothermic reaction is greatly sharpened. Weight-loss data show a greater water loss over a wider temperature range for ground material. *X*-ray powder photographs show little change after a relatively short period of grinding; destruction of the lattice appears only to proceed to a certain stage, high order (*hkl*) spacings being very persistent.

### R. Greene-Kelly: *Ion fixation by kaolinite*

The effect of drying kaolinite at temperatures up to 300° C. upon the availability of cations introduced by exchange is described. Fixation effects similar to those found for montmorillonite are shown to occur, and the influence upon water sorption measurements is discussed.

### G. Nagelschmidt: *Kaolinite in human lungs*

Rare cases of pneumoconiosis after exposure to kaolinite dust have been described in the literature. Results are given of mineralogical analyses of two such lung residues in which kaolinite was found to be the chief constituent.

### C. Lippi-Boncambi, R. C. Mackenzie and W. A. Mitchell: *The mineralogy of some Italian soil clays*

A set of seven soil clays from Central Italy recently examined provided some interesting results, the clays from a Mediterranean *terra rossa* and a rendzina showing features of particular interest. The mineralogical analyses are briefly described and discussed.

G. Brown: *The report of the Nomenclature Sub-Committee of the Clay Minerals Group*

What appears to be a reasonably logical classification of the various types of minerals likely to be found in clays is described. Introduction of new names has been cut to a minimum, existing names being adopted for minerals, possible minerals, or groups of minerals, wherever names are extant. Suggestions are made as to when minerals should, and should not, be given specific names, and also as to the naming of mixed-layer minerals.

R. L. Stone and E. J. Weiss: *Examination of four coarsely-crystalline chlorites by x-ray and variable-pressure d.t.a. techniques*

In variable-pressure *d.t.a.* gases of known composition (here water vapor) are forced through the specimen during the *d.t.a.* determination; variation of pressure causes some simple peaks to develop into multiple ones, some multiple ones to coalesce, and some thermal reactions to be suppressed completely (e.g. the chlorite exothermic peak at about 870° C.). The results are interpreted in the basis of Pauling's structure of chlorite, and the chemical identities of the minerals concerned.

R. C. Mackenzie, *Secretary*

---

Dr. John Putnam Marble, geochemist, died June 6, 1955, at the age of 58 years, following a heart attack. He was chairman of the Committee on Geological Time of the National Research Council, secretary of the Geophysical Association at the National Museum and a member of numerous scientific organizations.

# BOOK REVIEWS

MINERALS FOR ATOMIC ENERGY, by ROBERT D. NININGER. xii+367 pages, black and white and color plates; charts. D. Van Nostrand Company, New York, 1954. Price, $7.50.

The scope of this book is much broader than is indicated by its title, or even the subtitle, "A Guide to Exploration for Uranium, Thorium, and Beryllium." Nininger is currently Acting Assistant Director, Division of Raw Materials, United States Atomic Energy Commission. He has been associated with the Division of Raw Materials for years and can write with authority on the subjects treated.

Part I (110 pages) is a description of the important minerals and significant deposits of uranium, thorium, and beryllium. Part II (50 pages) is a world-wide geologic and geographic evaluation of potential areas of production of "atomic minerals." Part III (63 pages) tells one how to prepare for prospecting, describes equipment and its use, calls attention to certain regulations, and tells how to evaluate a claim in terms of current prices and market conditions.

Much additional information is given in 16 well chosen appendices (126 pages). The first five give more data on minerals and ore deposits, including tables for identification of the former and a classification of the latter. Instructions for obtaining analyses or assays are also included. The other appendices provide information about manufacturers of equipment, mining laws and prospecting conditions in the United States, Canada, Australia, and the United Kingdom and British Colonial Territories. Sources where additional information can be obtained are also listed.

The author makes no claim of originality for any of the subjects treated. He has drawn information from a wide variety of sources including text-books of mineralogy, circulars and other publications of the U. S. Geological Survey, the U. S. Bureau of Mines, and the Atomic Energy Commission, mining laws of nine western states and various federal agencies, and publications of the Canadian, British, and Australian Governments. Where these sources are not quoted directly the information is summarized succinctly, so the volume is about as authoritative and up-to-date as such a work can be made.

It is inevitable in a compilation from so many sources that some usages and interpretations should creep in that are out-of-date, in error, or at least open to serious question. For example, the definition of an element in footnote 1 on page 11 no longer holds; elements with more than one isotope may be composed of atoms with quite different physical properties.

Throughout the book *niobium* is referred to as *columbium*. The American Chemical Society has adopted *niobium* and the usage should be made uniform.

On page 40 it is stated that, "The uranium (in the Chattanooga shale) is believed to be associated with the clay minerals." Breger, Bates, and others have shown recently that there is a positive correlation between uranium and organic material, but a *negative* correlation with clay minerals.

Uranium minerals formed at the same time as the enclosing sedimentary rocks are referred to as *secondary* (pages 42 and 59). This is not in accord with accepted usage; secondary minerals are formed *in situ* by alteration or replacement of pre-existing ones.

On page 73 the Wind River Basin is said to be "bounded by (the towns of) Lander, Thermopolis, and Casper." This is an unusual method of giving the boundaries of a basin; moreover, Casper is some 40 miles east of the limits of the basin; Thermopolis, more than 10 miles north.

If uranium has a "steady rate of precipitation from sea water" (p. 75) then the red muds of the deep ocean basins should be the most highly radioactive marine sediments. Such is not the case.

The maps on pages 78–79 give an exaggerated idea of the uranium deposits in the United States; many occurrences of uranium minerals are shown in the U. S. that are not workable deposits. The locality shown in North Dakota as *Slim Battes* should be *Slim Buttes*.

The deposits of the Colorado Plateau are said to be of Mesozoic age (p. 114). They are in Mesozoic sedimentary rocks, but the best radioactive age determinations indicate that the uranium deposits were formed during the Tertiary. A notable exception to the statement that nearly all uranium deposits are Precambrian, Mesozoic, or Tertiary in age is the classic occurrence at Joachimsthal, Czechoslovakia, which is late Paleozoic.

On page 145 the impression is created that nitrate and borate deposits occur together on the west flank of the Andes in northern Chile. Actually, the nitrate deposits occur on the east flank of the coast range and the borates extend through to the east flank of the Andes in southern Bolivia and northwestern Argentina.

Gummite is said (p. 223) to be composed of uranium, lead, barium, calcium, etc.; the *oxides* of these metals are its components, of course.

Typographical errors are fairly abundant throughout the book but for the most part they are quite evident and not important enough to require mention in a review.

The five colored pictures of uranium minerals are fairly true and representative, but the one of bead tests (opposite p. 236) has such poor registry, at least in the copy sent to the reviewer, and most of the colors are so far from the real ones that it would have been better to omit the plate and rely on the descriptions of the colors in the tables that precede the plate.

There are books that give much more detailed information on uranium minerals, others on counting methods, still others on mining laws, but Nininger's *Minerals for Atomic Energy* gives better coverage of more different kinds of information on searching for these minerals than any other single volume. For this reason it is useful for reference to the professional geologist as well as to the prospector or interested layman.

Earl Ingerson,
*U. S. Geological Survey, Washington 25, D. C.*

## THE USE OF STEREOGRAPHIC PROJECTION IN STRUCTURAL GEOLOGY,

By F. C. Phillips. Edward Arnold, Ltd., London, 1954, vii+86 pages. Price, $3.00.

In the last two decades structural geologists have turned more and more to stereographic projection for the solution of problems involving directions of intersecting lines and planes. Although this method cannot determine distances, such as the throw of a fault or the magnitude of a stratigraphic interval, it solves in a matter of minutes problems involving only angles and directions that would take hours by the classical approach of descriptive geometry.

There are many examples in earth science journals of the solution of individual problems by stereographic projection, but most textbooks of structural geology mention it only casually, if at all. Bucher (*Jour. Geol.*, **52**, pp. 191–212, 1944) in a "study for students" outlined the methods of stereographic projection and the solution of 13 typical problems. Phillips discusses more than twice as many problems and several kinds not mentioned by Bucher.

Phillips' book is thus the most complete and detailed account yet written of the application of stereographic projection to structural and tectonic solutions and interpretations. There is an introductory chapter on the principle of stereographic projection, one each on true and apparent dip and intersecting oblique planes, two on rotation, one on stereographic projection as an auxiliary and one on tectonic syntheses. In this final chapter the elements of preparation and use of statistical (petrofabric) diagrams are treated very briefly. There is a 10 page appendix on calculations by spherical trigonometry, followed by a list of suggested exercises and answers.

The style is clear and straightforward and it is easy for one who is experienced in these techniques to follow the constructions and solutions. Not all of the steps (positions of the projection with respect to the net) are shown, however, so a beginner is likely to experience some difficulty in following parts of the discussion. It would have been well to have included all of the steps, at least through Chapter III, or to have admonished the novice to use a piece of tracing paper to follow the steps omitted.

There are other evidences of saving space at the expense of clarity. For example, Figures 17 and 42 are geometrical constructions to illustrate the complexity of the classical solution for two of the problems. There are no letters or figures to indicate what the lines mean and no hint of the method used or steps required. The figures might as well have been omitted with the statement "a minimum of $x$ lines would be required to solve the same problem geometrically."

The book is remarkably free of typographical and other errors. Only one requiring mention was noticed: on pp. 15 and 16 the dips of the planes plotted in Fig. 24 are given in the text as 64° to the east and 58° to the south, but on the projection these values are reversed. If the values given in the text are used then the values at the top of p. 16 are "trending E *52*° S and plunging *52*° southeasterly."—While perhaps not actually an error it seems peculiar to speak of projecting the *poles* of lineations (pp. 61–62), meaning the directions of the lineations themselves.

This book will be very useful to practicing structural geologists as well as to students, although nowhere in the book is the use of small "notebook" nets for solutions of problems in the field mentioned. It is unfortunate that so important a subject had to be so compressed; at least twice as many pages could have been used to advantage in expanding the scope of the treatment and in giving more detailed discussions of some of the material included.

Earl Ingerson,
*U. S. Geological Survey, Washington 25, D. C.*

## EINFÜHRUNG IN DIE UNTERSUCHUNG DER KRISTALLGITTER MIT RÖNTGENSTRAHLEN, by Friedrich Trey and Wilhelm Legat. Vienna, Springer-Verlag, 1954, ii+112 pp., 56 figs. and 1 nomogram, 14×21 cm. Paper-bound. Price $3.00.

In writing this short text the authors have set themselves the task of presenting, in an elementary way, the geometrical theory of the diffraction of $x$-rays by a "lattice." Thus, they intend the book to serve as an introduction to the more advanced treatments on the theory of the diffraction of $x$-rays by crystals.

The one-dimensional, two-dimensional, and three-dimensional cases are treated in that order. First, the interaction of $x$-rays with a row ("eindimensionale Punktgitter" or "Liniengitter") is considered; this is followed by a discussion of the diffraction by a net ("zweidimensionale Punktgitter" or "Kreuzgitter"); finally, the case of the lattice ("dreidimensionale Punktgitter" or "Raumgitter") is treated. Laudably, the concept of the Ewald reciprocal lattice (in appropriate dimensions) is introduced early in the text and is used extensively in developing the theory. This reviewer has never been able to understand why the very powerful reciprocal lattice concept is usually so studiously avoided in elementary texts of the present kind.

Following the general development of the geometrical theory of diffraction, several specific techniques for studying crystals are described. These are the Laue, powder, and rotating crystal methods. No moving-film methods are considered. As part of the discussion of the powder method various techniques (all photographic) are described, including the Straumanis asymmetric film technique, and various back-reflection methods.

One of the interesting and useful features of the book is the use throughout of problems and their solutions. These problems vary from the most elementary and self-evident types to those of greater complexity and should be of immense help to anyone attempting to use the book for self-study. The general format of the book is excellent: the type is pleasing to the eye, and the line-drawings and photographs are numerous and of very high quality.

On the other hand this book has its faults. A very serious one is the fallacy of identifying lattice points with atoms, apparently in an attempt to achieve simplicity of development of the diffraction theory. To coin a phrase "a lattice is a lattice is a lattice" (and not a structure). In a similar manner the unit cell is defined in a completely misleading way. The authors also run into rough going when they discuss centered lattices, falling back on the obscure device of defining these in terms of interpenetrating primitive lattices. Again, KCl is used as an example of a substance having a primitive cell. It is mostly in the superposition of the necessary physical concepts on the purely geometrical ones that the book is deficient.

Aside from the language barrier this book would be useful to the student providing that supplemental help is available in the form of personal guidance or some text which presents the necessary physical concepts more adequately.

C. L. CHRIST,
*U. S. Geological Survey, Washington 25, D. C.*

CRYSTAL DATA. CLASSIFICATION OF SUBSTANCES BY SPACE GROUPS AND THEIR IDENTIFICATION FROM CELL DIMENSIONS. By J. D. H. DONNAY AND WERNER NOWACKI with the collaboration of Gabrielle Donnay and many assistants. Pp. ix+719. Memoir 60 of The Geological Society of America, 419 West 117th St., New York 27, N. Y. (1954), Price $5.00.

This important book is divided into two parts which were prepared independently of each other. Part I, by Professor Nowacki of Berne, is an expansion and revision of earlier publications. It consists mainly of a table of 76 pages in which 3,800 substances, grouped in 6 inorganic and 6 organic chemical categories, are listed by space groups. This is based on the literature to 1948 and references are given. A ten page statistical table records the number of substances in each of the chemical categories in every space group. The distribution is most uneven. For 41 space groups there are no representatives. $C_{2h}^5$ is the most favored space group for organic compounds (265) but also harbors 90 inorganic substances. $O_h^5$ is the most favored space group of inorganic materials (289) but also includes 24 "organic compounds" all but one of which are "inorganic compounds with organic radicals." Shorter tables summarize the distribution of crystalline substances among the systems, classes and translation groups and the percentage distribution among the "most frequent" space groups.

Part II, Determinative Tables for Identification of Crystalline Substances from Cell Dimensions, by the Donnays, fills four-fifths of the volume. Any scheme for the systematic identification of crystalline materials depends upon the compilation of data in suitable form. The data in Groth's 5 volume *Chemische Krystallographie* were in a form not convenient for the identification of crystals from morphology. *The Barker Index of Crystals*, when completed, will give these data for non-cubic crystals in suitable form. Mineralogists have long enjoyed the advantages of the Larsen and Larsen-Berman tables for identification of "non opaque" minerals by means of their optical properties. In recent years the identification of crystalline materials by means of *x*-ray powder diffraction patterns has been much in vogue. It is full of pitfalls for the unwary. In the introduction to Part II Donnay says "Since identification by powder diffraction data cannot, in all rigor, be considered reliable until all the lines have been indexed, or matched with those of a previously indexed standard, the knowledge of the cell dimensions and diffraction aspect actually is a prerequisite to a safe application of the powder method. Although single-crystal data obtained by $x$-rays are given in several compendia, they are not listed in such a manner as to be useful for determinative purposes."

Part II contains A. Introduction, B. Determinative Tables, C. Appendix—Tables of Space Group Criteria, followed by name and formula indexes that serve both parts. The introduction is devoted largely to "choice and orientation of the cell." This must be carried out according to conventions which have been followed in preparing data for the tables. Six general rules are followed by an explanation of their application in each of the systems. Following a brief statement of the use of the Delaunay reduction, monoclinic reorientations, orthorhombic transformation and the rhombohedral to hexagonal transformation are explained, each with the aid of a numerical example worked out in detail. The tables give data on about 6000 substances, covering the literature through 1951. Cubic materials are listed in order of increasing $a$, others in order of increasing axial ratios within each system. The data in the tables are partly arranged in columns. For monoclinic crystals these have the headings *a/b, c/b, beta, a, b, c, Space group, Z, Struct. type, Spec. grav. meas., Spec. grav. calc.* Other information given includes name and synonyms, chemical formula, literature references, notes on pseudosymmetry and pseudocells, on original cell constants where these had to be transformed to obtain the conventional setting, on cleavage, color, crystal habit, polymorphs, errors in the literature, cross references, and much other useful material. The data on minerals have been recorded with understanding as shown by the mention of localities and the treatment of members of mix-crystal series.

A puzzling point is the listing of several space-group possibilities for substances with well-established structure. For cubic sodium perchlorate, for instance, the space group is given on page 523 as "$F\bar{4}3m$ or F23" with reference to "SB II, 411." The space group is, to be sure, given in this fashion in *Strukturbericht* **II,** page 411, but two pages farther on in the same work, based on another source, it is given as $F\bar{4}3m$ and this is recorded on page 522 in Part II. The description of the structure as type $HO_5$ (SB II, 84) leaves no doubt that it has this symmetry. Cubic sodium perchlorate and the many other perchlorates of like structure are not listed in Part I. Though the citation of multiple choices for space groups in such cases may be evidence of commendable caution it seems to this reviewer that it can be misleading. It gives the impression that doubt remains concerning the symmetry of a structure even though it is fully established.

The tables in the appendix are a revision of similar tables published by Donnay and Harker under the title *Nouvelles Tables d'Extinctions pour les 230 Groupes de Recouvrements Cristallographiques*, Naturaliste Canadien, **67**: 33–69, 1940. They have been brought into conformity with usage in the *International Tables for X-ray Crystallography*, 1951. This results in differences in space group designations between the appendix and other parts of the work. For instance, the Schoenflies group $D_{6h}^1$ is designated $P6/mmm$ in the appendix and the table of Part II, but $C6/mmm$ on page 584 in the "Concordance of Space Group Notations" and in Part I. The treatment of the monoclinic space groups in the appendix (table 15, page 587) provides for three (or four) orientations but leaves out the orientations which would involve $n$ glides. Thus the space group symbol $P2_1/n$, which is appropriate for monazite and scores of other substances in $C_{2h}^5$, is not found in table 15. Since these orientations would involve "criteria" and "aspects" different from those given for the orientations included in the table, the basis for the exclusion is not apparent to this reviewer.

The technical points just raised are mentioned only because it seems that they are connected with fundamentals. Not even a slight derogation of the work under review is intended. The volume has been put together almost faultlessly. Misprints are few when one considers the magnitude of the task that has been performed. All crystallographers should be grateful to the authors and to the Geological Society of America for making so much valuable information available in such attractive, convenient and inexpensive form. This reviewer has spent pleasant hours just browsing through the tables enjoying the bits of intriguing information. But the volume can be put to much more solid uses and not only in the identification of crystalline substances. In its pages can be found suggestions for many problems in crystal chemistry and the solutions of others. This book is highly recommended to all mineralogists and crystallographers and it is hoped that it may lead some to realize the advantages of single crystal $x$-ray examination for purposes of identification.

A. Pabst,
*University of California, Berkeley 4, Calif.*

## FOURTH NATIONAL CLAY MINERALS CONFERENCE

The Conference will be held at The Pennsylvania State University Monday through Thursday, October 10–13, 1955. Field trips and laboratory visits will take place Monday, and papers will be presented Tuesday, Wednesday, and Thursday. The program will include a number of special sessions in addition to those of general interest. The following topics will be given particular emphasis: mixed-layer clays; thermal transformations; and clay water systems. A number of prominent scientists from abroad have been invited to attend and will present reports on the status of clay mineral investigation in their respective countries.

# NEW MINERAL NAMES

## Indialite

Akiho Miyashiro and Toshimichi Iiyama, A preliminary note on a new mineral, indialite, polymorphic with cordierite. *Proc. Japan Acad.*, **30**, 746–751 (1954).

*X*-ray spectrograms of natural cordierite differ, especially in the range of $2\theta$ between 29° and 30° for Cu $K\alpha$ radiation from those of synthetic $\alpha$—$Mg_2Al_4Si_5O_{18}$ and $\beta$—$Mg_2Al_4Si_5O_{18}$. Alpha—$Mg_2Al_4Si_5O_{18}$ is hexagonal with $a$ 9.782 Å, $c$ 9.365 Å. The so-called "synthetic iron cordierite" (Schairer and Yagi, *Am. J. Sci.*, *Bowen Vol.*, 471–512 (1952)) is the corresponding hexagonal $\alpha$—$Fe_2Al_4Si_5O_{18}$, with $a$ 9.860 Å, $c$ 9.285 Å. Beta—$Mg_2Al_4Si_5O_{18}$, synthesized by F. R. Boyd of the Geophysical Laboratory, is also hexagonal with $a$ 9.792 Å, $c$ 9.349 Å. Both of these give patterns similar to, but distinctly differing from those of the two naturally occurring polymorphs of cordierite which are orthorhombic (or possibly monoclinic), pseudohexagonal.

It has now been found that the "cordierite" described by Venkatesh, *Am. Mineral.*, **37**, 831–948 (1952), **39**, 636–646 (1954) is actually the alpha-form, which is now named indialite. *X*-ray powder data are given; they are indexed and lead to a hexagonal cell with $a$ 9.812 Å, $c$ 9.351 Å, indicating a ratio of Mg: $Fe^{+2}$ of 7:3. The mineral occurs in sedimentary rocks fused by the burning of a coal seam in the Bokaro coalfield, India. The burning was due to some natural cause.

The name is for India.

Michael Fleischer

## Pavonite

E. W. Nuffield, *Am. Mineral.*, **39**, 409–415 (1954).

## Unnamed Magnesium Borate

R. M. Thompson and J. A. Gower, *Am. Mineral.*, **39**, 522–524 (1954).

## Callaghanite

C. W. Beck and J. H. Burns, *Am. Mineral.*, **39**, 630–635 (1954).

## Ortho-antigorite

G. W. Brindley and O. von Knorring, *Am. Mineral.*, **39**, 794–804 (1954).

M. F.

## Berillite

M. V. Kuzmenko, Berillite—a new mineral. *Doklady Acad. Nauk. S.S.S.R.*, **99**, 451–454 (1954) (in Russian).

Berillite occurs as fine spherulites 2–3 mm. in diameter or as crusts up to 2 mm. thick in cavities. Color white, luster silky. Soft. Berillite is optically biaxial, negative, with *n*s, $\alpha = 1.541 \pm 0.003$, $\beta = 1.553 \pm 0.002$, $\gamma = 1.560 \pm 0.002$, 2V small, less than 45°. Extinction parallel, elongation positive. G. = 2.196.

Analysis on 250 mg. by M. E. Kazakova gave $SiO_2$ 34.10, $TiO_2$ tr., $Al_2O_3$ 1.63, $Fe_2O_3$ 0.12, MgO tr., BeO 40.00, CaO 0.50, $Na_2O$ 2.42, $H_2O^+$ 18.95, $H_2O^-$ 3.25; sum 100.97%. (Sum given as 100.47 in original. M.F.). This corresponds closely to $Be_3SiO_4(OH)_2 \cdot H_2O$ (neglecting the $Al_2O_3$, CaO, $Na_2O$, and $H_2O^-$. M.F.). Spectrographic study showed moderate lines of Ba and Mn and weak lines of P and Cu. A dehydration curve is given; about 12% $H_2O$ is lost up to 350°.

$X$-ray powder data are given. The strongest lines have spacings (Å? Kx?) and intensities: 4.10 10, 2.34 10, 3.64 9, 1.351 8, 3.39 7, (3.19, 2.90) 7, 2.12 7, 2.03 7, 1.937 7, 2.703 6.

Berillite occurs in the center of a zoned pegmatite that cuts aegirine lujavrite. The border zone consists mainly (70–80%) of aegirine and arfvedsonite; these decrease in amount towards the center and microcline and natrolite increase. The center zone consists mainly of natrolite with relicts of very coarse sodalite (hackmannite) and with fine-grained albite. Berillite occurs rarely in cavities and coating albite and epididymite. The locality is not stated (could be Kola Peninsula? M.F.)

DISCUSSION: The name as given is a direct transliteration, but perhaps the spelling beryllite would be preferable.

M. F.

## Shcherbakovite

E. M. ES'KOVA AND M. E. KAZAKOVA, Shcherbakovite—a new mineral. *Doklady Akad. Nauk. S.S.S.R.*, **99**, 837–841 (1954) (in Russian).

Analysis (by M.E.K.) gave $SiO_2$ 40.61, $Al_2O_3$ 0.76. $(Nb, Ta)_2O_5$ 10.44, rare earths none, $TiO_2$ 17.91, $ZrO_2$ 1.23, $Fe_2O_3$ 1.080, FeO 0.47, MnO 0.04, MgO 0.26, CaO 0.82, $Na_2O$ 5.82, BaO 6.22, $K_2O$ 12.29, Cl 0.30, $H_2O^+$ 0.54, $H_2O^-$ 0.10, F none; sum 99.61%. Check determinations by O. P. Ostrogorskaya gave $Na_2O$ 5.69, $K_2O$ 12.64%. This corresponds to $(K, Na, Ba)_3 (Ti, Nb)_2(Si_2O_7)_2$, with K+Ba:Na nearly 2:1. Spectroscopic study by L. N. Indichenko showed also moderate V and Sr, weak Sn, and traces of Pb and Cu. The mineral is insoluble in $HNO_3$ and HCl, partly soluble in $H_2SO_4$ on heating.

Shcherbakovite occurs in monoclinic crystals, elongated prismatic, length up to 1.5–2 cm., width 0.3–0.8 cm., and thickness 0.05–0.2 cm. Two-circle goniometric measurements are given for forms $a(100)$, $b(010)$, $c(001)$, $m(110)$, $S(\bar{1}01)$, and $n$ ($hk0$, uncertain, nearest to (310)). Only a few terminated crystals were observed. The measurements give $a:b:c = 0.70:1:?$, beta 126° 33″. Two cleavages were observed under the microscope. $X$-ray powder data are given; the strongest lines in Å were: 2.90 10, 1.081 10, 2.64 7, 1.688 7 1.576 6.

The mineral is dark brown with luster vitreous, greasy on fracture surface. Brittle. H.$=6\frac{1}{2}$, G.=(pycnometer) 2.968. It is biaxial, negative, with $ns$, $\alpha=1.707$, $\beta=1.745$, $\gamma=1.776$, 2V 82°. Elongation positive. Distinctly pleochroic, Z brownish-yellow, Y yellow, X pale yellow. Opaque in hand specimen to translucent on thin edges.

The mineral occurs in a pegmatite in alkalic rocks (rischorrite), associated with and including natrolite–pectolite aggregates. Other minerals present include albite, K feldspar, astrophyllite, apatite, galena, sphalerite, and molybdenite. The locality is not given specifically, but one table is headed "Shcherbakovite from Khibina Tundra." The name is for D. I. Shcherbakov, Russian mineralogist and geochemist.

M. F.